Extended Brueckner Hartree-Fock theory for nuclear matter with realistic nucleon-nucleon interaction

Jinniu Hu

Research Center for Nuclear Physics (RCNP), Osaka University, Ibaraki,

Osaka 567-0047, Japan

September 29, 2011

Doctor of Science Thesis

現実的な核力を用いた拡張ブルックナーハートリーフォック理論による核物質の研究

胡 金牛

大阪大学核物理研究センター

理学博士論文

Abstract

We construct some new theoretical frameworks to describe the properties of nuclear matter with a realistic nucleon-nucleon (NN) interaction in this thesis. It is important to treat the short range repulsion and strong tensor interaction in the intermediate distance of the realistic NN interaction properly in many-body theory. To achieve this goal, we study first the role of form factors, which is an indispensable quantity in the realistic NN interaction, in nuclear matter with relativistic Hartree-Fock (RHF) model. For a quantitative account of nuclear matter, we adopt a phenomenological one-boson-exchange interaction to study the effect of the form factor. We find that the NN interactions are suppressed largely at high momentum region by the form factor.

Next, we study neutron-rich matter in the RHF model with a realistic nucleon-nucleon interaction. It is well known that the tensor interaction contributes very little to neutron-rich matter. Hence, we take into account only the short range correlation in terms of two powerful tools, the unitary correlation operator method (UCOM) and the Jastrow function method. We find that the equations of state (EOS) of neutron-rich matter in our calculations are consistent with those given by a microscopic model, relativistic Brueckner-Hartree-Fock (RBHF) model. However, the case in symmetric nuclear matter is largely different from the results given by the RBHF model particularly in the low density region. This is caused by the lack of the tensor interaction in the Hartree-Fock approximation, which plays an important role in the saturation mechanism of symmetric nuclear matter.

Finally, we compose of traditional Hartree-Fock states and 2-particle-2-hole (2p-2h) states as the nuclear wave function. The strong tensor force and short range correlation of central force can be properly treated by including the 2p-2h states. The content of the 2p-2h states and the wave function of the single particle states are determined by the variational principle for the total energy. We can then extract an effective NN interaction from the equation of motion for the single particle state. This effective interaction has a similar structure to that of the G-matrix interaction in the Brueckner-Hartree-Fock theory, and the above two important characters are properly taken into account. We call our new theoretical framework as an extended Brueckner-Hartree-Fock (EBHF) theory. Using this new framework, we first work out the EOS of the symmetric nuclear matter with the Bonn potential as a realistic NN interaction in a non-relativistic framework. In low density region, the binding energies of the nuclear matter are very similar to those given by the Brueckner-Hartree-Fock theory. As the density increases, more repulsion is obtained due to the 2p-2h correlation in the kinetic energy. It turns out that this additional repulsive energy can improve the saturation properties of nuclear matter significantly, which has never been achieved previously. Next we apply the EBHF theory in a relativistic framework, where we find that the saturation properties are nicely reproduced consistently with the empirical data. The neutron matter

is also calculated with different Bonn potentials. We discuss the role of the tensor force in those nuclear matter properties.

Acknowledgements

First of all, I would like to thank Professor H. Toki and Professor A. Hosaka, my supervisors at Research Center for Nuclear Physics (RCNP) of Osaka University. Without their constant and illuminating guidance and support, I could not finish these materials in this thesis. They supply also extremely a good study place for me to concentrate on my research project. Every small progress I make means a lot of efforts from them during my Ph.D. study. I am also thankful to Professor H. Shen at Nankai University for her recommendation so that I can start my Ph. D. study at RCNP and many helpful discussions during the course of this work.

I would like to express my gratitude to my collaborators, Y. Ogawa, W. Wen, B. Sun and Y.N. Wang for their stimulating discussions on various aspects of the present subject. Special thanks also go to the secretary of RCNP theory group, Ms. M. Yamakami, who has given me a lot of help. With her help, I can live in Japan comfortably and conveniently in the past four years.

I spent about four years for living and studying in Osaka. The kindness of Japanese people gives me a very deep impression, especially all the persons in RCNP. They are all very intelligent and their supports make this research possible. In particular, I want to thank T. Myo, M. Valverde, K. Nawa, S. Uechi for many helpful discussions and conversations.

I wish to thank all the following people for their friendship and all the good times we had together: K. Horii, S. Imai, H. Kaneko, H. Ryu, S. Ohkoda, Y. Yamaguti, T. Shibata, L. Zhu in RCNP, H. Nagahiro in Nara Women U., P. Yue and F. Yang in Nankai University and other friends in my life.

Finally, I am grateful to my girlfriend Y. Zhang in RIKEN whose patient love enabled me to complete this thesis. She also helped me by carefully reading my thesis and gave me many helpful suggestions to improve the presentation of this thesis, many of which have appeared in this final version. I also should express my great gratitude to my parents. They brought me to this world, raised me up and loved me throughout. I dedicate this thesis to my parents.

Contents

List of Figures

List of Tables

Chapter 1

Introduction

1.1 Nuclear matter

Nuclear matter is an infinite uniform system of nucleons interacting through the strong interaction without electromagnetic force. This many-body system is characterized by its energy per nucleon as a function of the nucleon density and temperatures. In this thesis, we concentrate the zero temperature case. The nuclear matter system was often called 'hypothetical', because any real nucleus has far from infinite matter with infinite radius. Where can we find a sample of infinite nuclear matter to obtain experimental values for its energy density and other properties? One possibility is to look at the so-called neutron stars, which are in all likelihood candidates for a physical realization of nuclear matter. But very little information are available about the microscopic properties at individual nucleon level from the bulk properties of neutron stars. The hypothetical system is also supposed to approximate the interior of heavy nuclei. We can extract some properties of infinite nuclear matter from the large real nuclei, for instance, the saturation properties of infinite nuclear matter with the same neutron and proton densities, which is called 'symmetric nuclear matter'.

The semi-empirical Bethe-Weizäcker mass formula of finite nuclei provides a value on the minimum of binding energy, the saturation point of nuclear matter via its volume term [1]. According to the liquid drop model, the Bethe-Weizäcker mass formula for nucleus including A nucleons with Z protons and N neutrons reproduces quite well the experimental binding energies, which can be written as an expansion in N, Z and a asymmetry factor $I = (N - Z)/A$,

$$\frac{E}{A} = a_v + a_s A^{-1/3} + a_{coul} Z^2 A^{-4/3} + a_I I^2 + \delta(A, Z). \tag{1.1}$$

The first term on the r.h.s is known as the volume term, which is the largest one in the expansion and represents the energy in the bulk limit of symmetric nuclear matter ($I = 0$).

The second term, $a_s A^{-1/3}$ is associated with the surface effect, which is negligible in nuclear matter. Next, $a_{coul} Z^2 A^{-4/3}$ is caused by the electrostatic repulsion between protons. The term $a_I I^2$ is related with the asymmetric factor I and tends to reduce the binding energy because the like-nucleon interactions are less attractive than the neutron-proton (unlike) interactions. The a_I is also named as symmetric energy, a_{asy} in nuclear matter. The last term $\delta(A, Z)$ is known as caused by the pairing effect. The energy per particle at saturation density corresponds the volume term, a_v, of the semi-empirical mass formula. Hence, we get

$$\frac{E}{A} = -16 \pm 1 \text{ MeV},\tag{1.2}$$

by using binding energies of about 3100 ($A > 10$) nuclei [3].

There is a minimal energy at the equilibrium density for nuclear matter, which is also called as the saturation density, ρ_0. It is related with the nuclear radius constant r_0, defined as $\rho_0 = 3/(4\pi r_0^3)$. This quantity can be extracted from the measured nuclear central density ρ_c. In the case of muonic atom spectroscopy, the measured nuclear charge distribution is parameterized by [2],

$$\rho_c(r) = \frac{\rho_A}{1 + \rho^{(r-C)/a}},\tag{1.3}$$

for spherical nuclei, where C is the model parameters, ρ_A is the normalization constant, and a is the nuclear surface diffuseness. Furthermore, the nuclear half density radius C, in the Fermi distribution, can be written by the nuclear equivalent sharp radius R as,

$$C = R \left[1 - \frac{1}{3} \left(\frac{\pi a}{R} \right)^2 \right],\tag{1.4}$$

and the equivalent sharp radius can be expressed as

$$R = r_0 A^{1/3}.\tag{1.5}$$

Through the above equations, we can relate the nuclear radius constant r_0 with charge density distribution ρ_c. The fitted r_0 is

$$r_0 = 1.14 \pm 0.02 \text{fm}^{-1} .\tag{1.6}$$

Hence, the saturation density is

$$\rho_0 = 0.16 \pm 0.01 \text{fm}^{-3}.\tag{1.7}$$

Another frequently used parameter related with the particle density is the Fermi momentum k_F which is defined by

$$\rho = \lambda \frac{k_F^3}{3\pi^2},\tag{1.8}$$

where λ is the isospin factor. $\lambda = 2$ represents the symmetric nuclear matter, while $\lambda = 1$ for pure neutron matter. The equilibrium value of Fermi momentum corresponding to the above given ρ_0 is

$$k_F^0 = 1.35 \pm 0.05 \text{ fm}^{-1} = 265 \pm 10 \text{ MeV}. \tag{1.9}$$

for symmetric nuclear matter.

The nuclear matter also can be considered as a fluid. Two thermodynamical quantities are very important in the properties of nuclear matter. One is the pressure, which is defined as,

$$P = -\frac{\partial E}{\partial V}\bigg|_A = \rho^2 \frac{\partial \frac{E}{A}(\rho)}{\partial \rho}\bigg|_A \tag{1.10}$$

This pressure must be equal to zero at the saturation point to satisfy the following equation for the equilibrium density ρ_0:

$$P = \rho_0^2 \left[\frac{\partial \frac{E}{A}(\rho)}{\partial \rho}\right]_{\rho=\rho_0} = 0. \tag{1.11}$$

The other one is the incompressibility or compression modulus K, which is written as,

$$K = 9\frac{\partial P}{\partial \rho} = \frac{18P}{\rho} + 9\rho^2 \frac{\partial^2 \frac{E}{A}(\rho)}{\partial \rho^2}. \tag{1.12}$$

At the equilibrium density ρ_0, i.e. at zero pressure, the first term on the r.h.s vanishes and this incompressibility becomes,

$$K = 9\rho_0^2 \frac{\partial^2 \frac{E}{A}(\rho)}{\partial \rho^2}\bigg|_{\rho=\rho_0} = k_F^2 \frac{\partial^2 \frac{E}{A}(k_F)}{\partial k_F^2} \tag{1.13}$$

The best way to estimate this quantity from experiment comes from the analysis of isoscalar giant monopole resonance (ISGMR) in heavy nuclei [4]. However, the value of incompressibility is strongly dependent on models. The results from the non-relativistic models, such as Skyrme and Gogny calculations about ^{208}Pb [5] tend to provide a value of K around

$$K = 220 - 235 \text{ MeV}. \tag{1.14}$$

However, the results from relativistic mean field calculations about ^{208}Pb [6] tend to provide a larger value of K,

$$K = 250 - 270 \text{ MeV}. \tag{1.15}$$

We would like to show Fig.1 of Ref.[5] to explain this situation more explicitly in Fig.1.1. The monopole energy and incompressibility satisfy a linear relation [4]. The ordinate of this

figure is the monopole energy of ^{208}Pb, while the abscissa is the incompressibility. The two inclined lines are numerical interpolations about the monopole energy and incompressibility from Skyrme and RMF models. The horizontal line is the experimental data on the monopole energy which is about 14.2 MeV. Then, we see in this figure that the incompressibility extracted from the RMF model is larger than the one from Skyrm model.
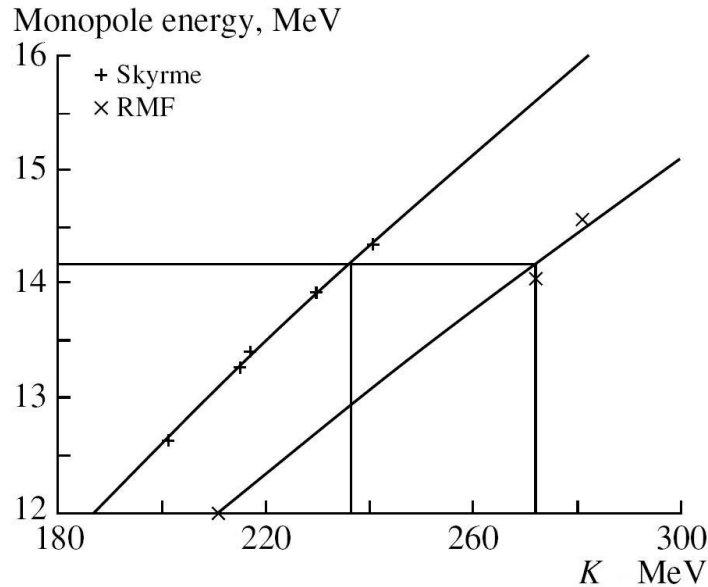
Figure 1.1: The monopole energies in ^{208}Pb calculated with the Skyrme and RMF models as a function of K of these models. The lines denote interpolations of the results of various models. The values of K deduced from the experimental monopole energy are also displayed. The copyright of this figure belongs Ref.[5].

The study of asymmetric matter($N \neq Z$) gives some information about the symmetric energy, a_{asy}, as mentioned above. The coefficient is given by Möller *et al.* from their analysis of experimental data [7],

$$a_{asy} = 32.5 \pm 0.5 \text{ MeV}. \tag{1.16}$$

Therefore, to derive the energy per nucleon as a function of nucleon density for nuclear matter, which is also called as equation of state (EOS), five constraints should be taken into account:

1. The equilibrium density ρ_0;

2. The energy per nucleon at equilibrium density $E/A(\rho_0)$;

3. The incompressibility at equilibrium density K ;

4. The symmetry energy at equilibrium density a_{asy};

5. The effective nucleon mass at equilibrium density M_N^*.

The last constraint is caused by the medium effect of many-body system. The effective mass for nucleon, M_N^*, is about $0.6M_N \sim 0.7M_N$, where M_N is the free nucleon mass. The aim of nuclear matter theory is to give the explanation of these empirical properties microscopically.

Historically, Hans Euler calculated the EOS of nuclear matter with an attractive potential of Gaussian shape in second-order perturbation theory [8]. Modern studies started in the early 1950's after a strong repulsive core in the short range region for the nucleon-nucleon (NN) interaction had been studies by Jastrow [9]. These realistic singular NN interactions could not be described by a perturbation theory any more. Therefore, the special microscopic methods had to be developed with realistic NN interaction, which was obtained by fitting the NN scattering phase shift. From the mid-1950's, Brueckner *et al.* began to introduce the hole-line expansion method and used the G-matrix instead of the bare NN interaction to treat the short range correlation [10]. This method is extended to the relativistic Brueckner Hartree-Fock (RBHF) theory by Brockmann and Machleidt for nuclear matter with Bonn potential [11]. It was the first time to give reasonable saturation properties of symmetric nuclear matter from the microscopic approach. This result illuminates that the relativistic effect is very important in the many-body calculation which provides the repulsive contribution in nuclear matter at high density.

Almost at the same time, another method was formulated to treat the short range correlation through the correlated wave function with variational approach by Jastrow [12]. However, the complexity of this problem that exists, when spin, isospin, tensor, and spin-orbit correlation are included, was considered difficult for nuclear physicists in the 1950's. Then Pandharipande *et al.* pursued this method as a variational chain summation (VCS) approach, based on hyper-netted chain-summation techniques in nuclear matter system in 1970's [13]. Recently, Akmal *et al.* used this method and a realistic NN interaction as the Argonne V18 potential, which excellently fits the NN scattering data, to obtain the EOS of symmetric nuclear matter and neutron matter [14]. These EOSs are in accordance with the constraint by the experimental data of heavy ion collision [15].

On the other hand, at the beginning of 1970's, phenomenological models with a parameterized effective interaction were applied to describe the nuclear matter system. In non-relativistic approach, the most famous effective nucleon-nucleon interaction is the Skyrme type which was performed by Vautherin and Brink [16]. The parameters of Skyrme NN interaction are obtained by fitting the self-consistent mean-field Hartree-Fock results to the experimental data on the ground state properties, such as charge radii and binding energies of a few closed shell nuclei. Now, many different parameterizations of the Skyrme interaction have been proposed to better reproduce data on nuclear masses, radii and other quantities [17]. The advantage of effective Skyrme interaction is due to its simple expression in terms of the $\delta(\vec{r}_1 - \vec{r}_2)$ interaction, which makes the calculations in the Hartree-Fock mean-filed much

simpler. However, Skyrme Hartree-Fock theory can not explain some relativistic phenomena, such as the pseudospin symmetry in finite nuclei [18].

These problems can be explained very well in the relativistic mean field (RMF) model, which uses an effective NN interaction through the exchange of mesons. The proposal of RMF model was made by Johnson and Teller [19], and Duerr [20] in 1950's. It was calculated self-consistently by Walecka [21]. Its original version is just based on the nucleons, scalar and vector mesons. These two mesons provide attractive and repulsive interactions. Furthermore, to take the isospin effect into account, an isovector meson was introduced in the form of the rho meson exchange. Later Boguta and Bodmer proposed self-interaction terms of scalar meson field [22]. The properties of nuclear matter in RMF model were largely improved. In order to reproduce the density dependence of the vector and scalar potential of the RBHF calculations, the nonlinear self-coupling of the vector meson was found to be necessary [23]. With various versions of the nonlinear self-couplings of meson fields, the RMF theory has been used to describe the nuclear matter in the low density and lots of nuclear phenomena of finite nuclei during the past years with great success.

Although these effective NN interaction can give very good saturation properties of nuclear matter, their behaviors of symmetric nuclear matter at high density and neutron matter are completely different [24]. This arbitrary result does not benefit of the prediction about the neutron star which corresponds the extreme case of nuclear matter with very high density and in a neutron-rich environment. It is better to deal with nuclear matter from the microscopic method with realistic NN interaction to reduce uncertainties in the calculation process.

1.2 Nucleon-Nucleon interaction

The interaction between two nucleons is fundamental for all of nuclear physics. One of purposes of nuclear physics is to reproduce the properties of nuclear matter and finite nuclei in terms of the realistic nucleon-nucleon (NN) interaction. With the appearance of quantum chromodynamics (QCD), we are aware of the fact that the NN interaction is not fundamental. However, due to the non-perturbation character of QCD in the low-energy regime, we are still far from a quantitative description of the NN interaction from QCD.

The theoretical description of the NN interaction was first attempted by Yukawa in 1935 [25]. He made the hypothesis that nucleons interact through the exchange of a massive particle in analogy to the photon in QED (quantum electrodynamics). Yukawa's idea has been successfully implemented by identifying the exchanged particle with pion discovered in 1947, whose mass is about 140 MeV. Whereafter, Taketani *et al.* proposed to separate the range of NN interaction into three regions [26]. They distinguished a long-range ($r \geq 2$ fm; r is the distance between the center of two nucleons), an intermediate range (1 fm $\leq r \leq 2$

fm) and a core ($r \leq 1$ fm) region. The long range region is dominated by one-pion exchange. The two-pion exchange is most important, although heavier meson exchange (like ω) also becomes relevant in the intermediate range. Finally, the quark dynamics will influence the core region [27, 28].

However the multi-pion exchange theory of NN interaction could not do well in comparison with experimental data. In particular, it is impossible to derive a sufficiently strong spin-obit force from 2π exchange [29]. The one-boson-exchange (OBE) model was advanced in 1960's with the experimental discovery of heavy mesons [30]. The basic assumption of the OBE model was that multi-pion exchange could be denoted by the exchange of appropriate multi-pion resonances. Today, this model is still an economical and quantitative phenomenology for describing the NN interaction, such as the Bonn potential [31].

Recently, these successful descriptions of the NN interaction encouraged a birth of a new generation of realistic semi-phenomenological NN models, so called high-precision potentials, which fit NN scattering data (4000 data points corresponding to energies up to 350 MeV in the lab frame) with $\chi^2/N_{\text{data}} \sim 1$, such as Reid93 potential [32], Argonne V18 potential [33] and CD-Bonn potential [34]. All these potentials are proposed by the meson-exchange picture, in particular, all of them include the one-pion-exchange. They are also all charge-dependent, as required by deviations of the pp and np data. The Reid93 and Argonne V18 (AV18) potentials do not use meson exchanges for the intermediate and short-range parts and describe them purely phenomenologically. The Reid93 uses local Yukawa functions of multiples of the pion mass, while the AV18 potential employs the functions of the Wood-Saxon type. Unlike other models, the CD-Bonn potential adopts the full nonlocal Feymann amplitudes for the OBE potential.

Now we would like to introduce the Bonn potential and AV18 potential briefly. In the Bonn potential, the nucleon-nucleon (NN) interaction is constructed as the one-boson exchange-potential (OBEP). In low energy region, there are essentially only three boson fields that are of relevance,

1. The pseudoscalar (ps) field;

2. The scalar (s) field;

3. The vector (v) field.

Guided by symmetry principles, simplicity, and physical intuition, the most commonly used interaction Lagrangian that couple these fields to the nucleon are

$$
\begin{aligned}
\mathcal{L}_{ps} &= -g_{ps}\overline{\psi}i\gamma_5\psi\varphi^{(ps)}, \\
\mathcal{L}_s &= +g_s\overline{\psi}\psi\varphi^{(s)}, \\
\mathcal{L}_v &= -g_v\overline{\psi}\gamma^\mu\psi\varphi_\mu^{(v)} - \frac{f_v}{4M}\overline{\psi}\sigma^{\mu\nu}\psi(\partial_\mu\varphi_\nu^{(v)} - \partial_\nu\varphi_\mu^{(v)}),
\end{aligned}
\tag{1.17}
$$

where ψ denotes the nucleon Dirac ⸨⸩ $\varphi_\mu^{(v)}$ are the pseudoscalar,
scalar and vector boson fileds, resp⸨⸩ss. In the last interaction
Lagrangian, the first term is called ⸨⸩·m the tensor (t) coupling.

For the ps field, there is also th⸨⸩r gradient coupling to the
nucleon, which is suggested as an ⸨⸩metry,

$$\mathcal{L}_{pv} = -\frac{f_{ps}}{m_{ps}}\overline{\psi}\gamma_5\gamma^\mu\psi\partial_\mu\varphi^{(ps)} \tag{1.18}$$

The ps and pv couplings are equivalent for on-mass shell nucleons, if the coupling constants are related by $f_{ps} = (m_{ps}/2M)g_{ps}$. In actually calculations, we would like to use the pv coupling which suppresses the antiparticle contribution.

With these interactions, we can plot the Feynman diagram representing a one-boson exchange contribution to NN scattering in the c.m. frame as the lowest-order.
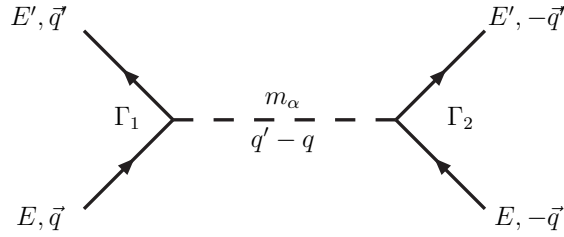
Figure 1.2: Feynman diagram of one boson exchange potential contribution to NN scattering in the c.m frame. Solid line is nucleon and the dashed line is a boson with mass m_α

.

According to Feynman rules, the amplitude of NN scattering can be written in an analytical form,

$$\mathcal{M}_\alpha = \frac{\bar{u}_1(\vec{q}')\Gamma_1 u_1(\vec{q})i\bar{u}_2(-\vec{q}')\Gamma_2 u_2(-\vec{q})}{(q'-q)^2 - m_\alpha^2}, \tag{1.19}$$

where Γ_i are the vertices between the meson-nucleon interaction and u_i is the Dirac spinor,

$$u(\vec{q}, s) = \left(\frac{M+E}{2E}\right)^{1/2}\begin{bmatrix} 1 \\ \dfrac{\vec{\sigma}\cdot\vec{q}}{E+M} \end{bmatrix}\chi(s). \tag{1.20}$$

Here $\chi(s)$ is the Pauli spinor. E is the energy of particle $E = \sqrt{\vec{q}^2 + M^2}$. For a real scattering process, the nucleons are "on their mass shell", which means

$$E = E' = \sqrt{\vec{q}^2 + M^2} = \sqrt{\vec{q}'^2 + M^2}. \tag{1.21}$$

Furthermore, to obtain the analytical form of Bonn potential in coordinate space, we should make a non relativistic expansion for the energy E,

$$E \sim \frac{\vec{q}^2}{2M} + M. \tag{1.22}$$

The detailed expression will be shown in Appendix A. Finally we can write the Bonn interaction in r space as,

$$V(r) = \sum_{S,T} V_c^{ST}(r) + \sum_T V_t^{1T}(r)\hat{S}_{12}(\hat{r}) + \sum_T V_b^T(r)\vec{L}\cdot\vec{S} + \sum_{S,T} \frac{1}{2}\left(\vec{p}^2 V_{\vec{p}^2}^{ST}(r) + V_{\vec{p}^2}^{ST}(r)\vec{p}^2\right) \tag{1.23}$$

Here, the subscripts c, t, b, p^2 of V represent central, tensor, spin-obit and moment square, respectively. In the second term, the operator $\hat{S}_{12}(\hat{r})$ is the spin tensor operator defined by,

$$\hat{S}_{12}(\hat{r}) = 3\frac{(\boldsymbol{\sigma}_1 \cdot \mathbf{r})(\boldsymbol{\sigma}_2 \cdot \mathbf{r})}{r^2} - \boldsymbol{\sigma}_1 \cdot \boldsymbol{\sigma}_2. \tag{1.24}$$

In the third term, $\vec{S} = \frac{1}{2}(\boldsymbol{\sigma}_1 + \boldsymbol{\sigma}_2)$ is the total spin of the two-nucleon system and $\vec{L} = -i\boldsymbol{r}\times\boldsymbol{\nabla}$ the orbital angular momentum operator in r space.

Now we turn to the Argonne potential. It is designed to be useful for practical calculations and is made to be as local as possible. It includes the electro-magnetic interaction beyond the static approximation and contains charge symmetric terms and charge symmetry breaking terms. The strong interaction part of this potential is projected into an operator format with 18 terms [33]:

$$V_{18}(r) = \sum_{p=1}^{18} v^p(r)O_p, \tag{1.25}$$

where 14 components of O_p are charge symmetric part,

$$1, \quad \boldsymbol{\sigma}_i \cdot \boldsymbol{\sigma}_j, \quad \boldsymbol{\tau}_i \cdot \boldsymbol{\tau}_j, \quad (\boldsymbol{\sigma}_i \cdot \boldsymbol{\sigma}_j)(\boldsymbol{\tau}_i \cdot \boldsymbol{\tau}_j), \quad S_{ij}, \quad S_{ij}(\boldsymbol{\tau}_i \cdot \boldsymbol{\tau}_j), \quad \boldsymbol{L} \cdot \boldsymbol{S}, \quad \boldsymbol{L} \cdot \boldsymbol{S}(\boldsymbol{\tau}_i \cdot \boldsymbol{\tau}_j), \tag{1.26}$$
$$L^2, \quad L^2\boldsymbol{\sigma}_i \cdot \boldsymbol{\sigma}_j, \quad L^2(\boldsymbol{\tau}_i \cdot \boldsymbol{\tau}_j), \quad L^2(\boldsymbol{\sigma}_i \cdot \boldsymbol{\sigma}_j)(\boldsymbol{\tau}_i \cdot \boldsymbol{\tau}_j), \quad (\boldsymbol{L} \cdot \boldsymbol{S})^2, \quad (\boldsymbol{L} \cdot \boldsymbol{S})^2(\boldsymbol{\tau}_i \cdot \boldsymbol{\tau}_j).$$

There are three charge-dependent operators,

$$T_{ij}, \quad T_{ij}\boldsymbol{\sigma}_i \cdot \boldsymbol{\sigma}_j, \quad T_{ij}S_{ij}, \tag{1.27}$$

where $T_{ij} = 3\tau_{zi}\tau_{zi} - \boldsymbol{\tau}_i \cdot \boldsymbol{\tau}_j$ is the isotensor operator, defined in analogy to the S_{ij} operator. The last one is the charge-asymmetric operator

$$\tau_{zi} + \tau_{zj} \tag{1.28}$$

The central components of Bonn and AV18 potentials at $S = 0, T = 1$ channel in coordinate space are plotted in Fig.1.3. We can find that there is a very strong repulsion at the short range region ($r \leq 0.5$ fm) in the central force of these two realistic NN interactions.
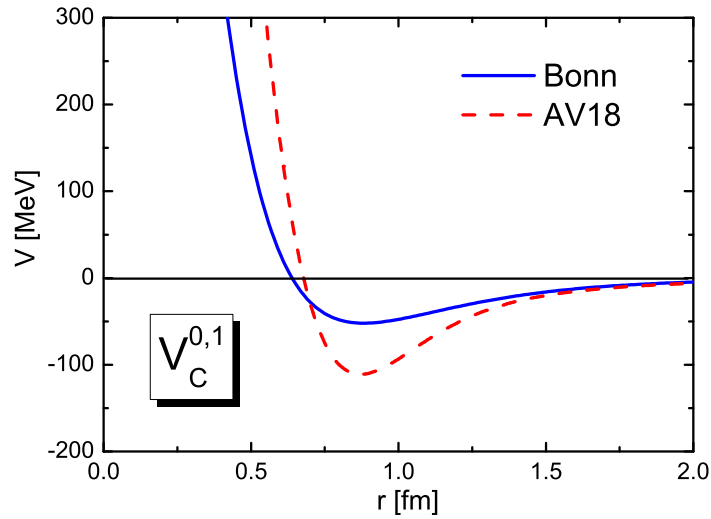
Figure 1.3: The central components of Bonn and AV18 potentials at $S = 0, T = 1$ channel in coordinate space. The solid curve denotes the Bonn potential. The dashed curve is the AV18 potential.

Although they are constructed differently, their divergent behaviors in the core region are very similar.

Analogously we also show the tensor components of Bonn and AV18 potentials at $S = 1, T = 0$ channel in Fig. 1.4. It reveals that the realistic NN contains very strong attractive tensor components which should be treated correctly.
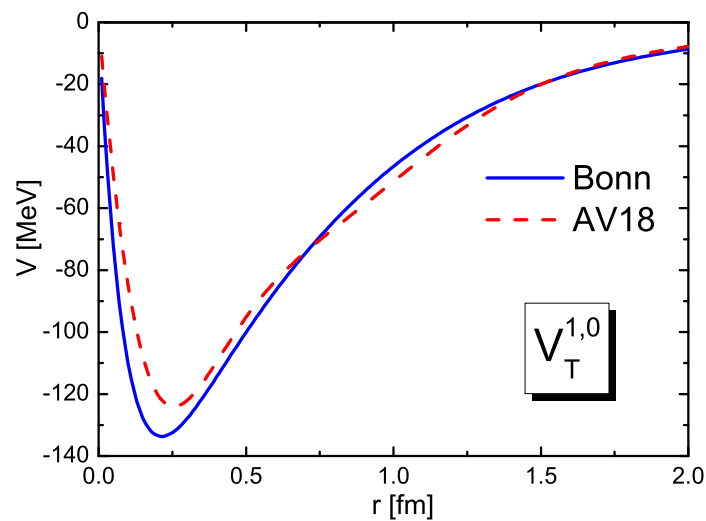
Figure 1.4: The tensor components of Bonn and AV18 potentials in the $S = 1, T = 0$ channel in coordinate space. The solid curve denotes the Bonn potential. The dashed curve is the AV18 potential.

Therefore, we can give a summary about the characteristics of realistic NN interaction from the above two figures:

1. There is a very strong repulsion in the short range region;

2. A strong attractive tensor interaction exists in the intermediate region.

Therefore, the purpose of this thesis is to develop some new microscopic many-body theories to investigate the nuclear matter properties with realistic nucleon-nucleon interaction. This new theory can properly deal with the tensor interaction and short range correlation of realistic NN interaction.

The thesis is arranged as follows. In chapter 2, an introduction to the relativistic Hartree-Fock model with effective nucleon-nucleon interaction and form factor effect is given. In chapter 3, we discuss the short range correlation about the realistic NN interaction, Bonn potential in nuclear matter. In chapter 4, we extend the Brueckner Hartree-Fock model to study the properties of nuclear matter with Bonn potential. A few useful derivations are provided in the appendix part.

Chapter 2

The relativistic Hartree-Fock theory

2.1   Relativistic mean field theory

The relativistic mean field (RMF) model is now very popular in describing finite nuclei and nuclear matter as a phenomenological effective field theory. With several (about ten) free parameters fitted once, the RMF theory allows one to study the nuclear matter properties, ground states of finite nuclei, surface vibrations and giant resonances at the quantitative level. The concept of the RMF model was proposed by Duerr already in 1956 [20]. The scalar meson provides large attraction and the vector meson provides large repulsion, which generate an attractive central potential on the order of 50 MeV and at the same time a large spin-orbit interaction in the non-relativistic language for finite nuclei. The RMF model was introduced again by Walecka [21] and then the essential ingredient for quantitative description of nuclei as the non-linear sigma meson terms was introduced by Boguta and Bodmer [22, 35]. Then, more non-linear terms of other mesons were taken into account in the RMF Lagrangian and gave better description about nuclear matter and finite nuclei [23, 36]. The strong foundation of the RMF model was provided by Brockmann and Machleidt in the relativistic Brueckner-Hartree-Fock (RBHF) theory [11]. The RBHF theory gave extremely good saturation properties of symmetric nuclear matter with the use of the bare nucleon-nucleon interaction. The application of the RBHF results in the framework of the RMF model, i.e. density-dependent RMF model, and relativistic Hartree-Fock model, i.e. density-dependent RHF model provided accurate description of finite nuclei in a wide mass range [37, 38, 39, 40].

The parameters for the meson-nucleon coupling constants and the meson masses were obtained as the first time by performing a systematic study of finite nuclei with non-linear terms in a wide mass range by Reinhard *et al.* [41]. These parameter sets were called NL1 and NL2 [41, 42]. Motivated by the dawn of unstable nuclear physics, Sugahara and Toki proposed new parameter sets by adjusting the parameters to finite nuclei and the RBHF

results which are used not only for finite nuclei but also for neutron star and supernova [23]. These parameter sets are called TM1, TM2 and TMA. There are so far many parameter sets to be adopted to study finite nuclei including unstable nuclei in the RMF framework [36, 43, 44]. We know further details about the RMF theory and its applications through the review articles [45, 46, 47, 48].

As the popular example of the RMF model, Walecka model, contains only two mesons, scalar meson, σ and vector meson, ω. The isovector meson, ρ was introduced later to improve the asymmetry energy of nuclear matter and isovector properties of finite nuclei. While the π and η fields in the Bonn potential are not considered due to the unnatural parity, whose expectation values vanish in the mean field approximation. The δ meson usually is also excluded because it does not improve this model so much for its heavy mass. Therefore, to show the main point of the RMF theory, we would like to use the TM1 Lagrangian in nuclear matter, which contains the nucleon field ψ, the scalar field σ, the vector field ω and the isovector field ρ:

$$
\begin{aligned}
\mathcal{L}_{\text{TM1}} = {} & \bar{\psi}(i\gamma_\mu\partial^\mu - M_N - g_\sigma\sigma - g_\omega\gamma_\mu\omega^\mu - g_\rho\tau^a\gamma_\mu\rho^{a\mu})\psi \\
& + \frac{1}{2}\partial_\mu\sigma\partial^\mu\sigma - \frac{1}{2}m_\sigma{}^2\sigma^2 - \frac{1}{3}g_2\sigma^3 - \frac{1}{4}g_3\sigma^4 \\
& - \frac{1}{4}W_{\mu\nu}W^{\mu\nu} + \frac{1}{2}m_\omega{}^2\omega_\mu\omega^\mu + \frac{1}{4}c_3(\omega_\mu\omega^\mu)^2 \\
& - \frac{1}{4}R^a_{\mu\nu}R^{a\mu\nu} + \frac{1}{2}m_\rho{}^2\rho^a_\mu\rho^{a\mu},
\end{aligned}
\tag{2.1}
$$

where

$$
W_{\mu\nu} = \partial_\mu\omega_\nu - \partial_\nu\omega_\mu,
\tag{2.2}
$$
$$
R^a_{\mu\nu} = \partial_\mu\rho^a_\nu - \partial_\nu\rho^a_\mu.
$$

We have ignored the tensor coupling of ρ meson in this Lagrangian. The photon field A^μ is also dropped for the charge neutrality hypothesis of nuclear matter.

With the Euler-Lagrange equation,

$$
\frac{\partial\mathcal{L}}{\partial\phi} - \partial^\mu\left[\frac{\partial\mathcal{L}}{\partial(\partial^\mu\phi)}\right] = 0,
\tag{2.3}
$$

where ϕ represents any field, we can give the equations of motion for various mesons,

$$
(\partial^\mu\partial_\mu + m_\sigma^2)\sigma + g_2\sigma^2 + g_3\sigma^3 = -g_\sigma\bar{\psi}\psi,
\tag{2.4}
$$
$$
\partial^\mu W_{\mu\nu} + m_\omega^2\omega_\nu + c_3(\omega_\mu\omega^\mu)\omega_\nu = g_\omega\bar{\psi}\gamma_\nu\psi,
$$
$$
\partial^\mu R^a_{\mu\nu} + m_\rho^2\rho^a_\nu = g_\rho\bar{\psi}\gamma_\nu\tau^a\psi.
$$

The last two equations are the Proca equations with source terms. They will be expressed in the Klein-Gordon equation, when we consider the nucleon current continuity condition,

$\partial^\nu(\bar{\psi}\gamma_\nu\psi) = 0$, and corresponding isovector currents.

$$(\partial^\mu\partial_\mu + m_\omega^2)\omega_\nu + c_3(\omega_\mu\omega^\mu)\omega_\nu = g_\omega\bar{\psi}\gamma_\nu\psi, \tag{2.5}$$
$$(\partial^\mu\partial_\mu + m_\rho^2)\rho_\nu^a = g_\rho\bar{\psi}\gamma_\nu\tau^a\psi.$$

For later convenience, we should write the Hamiltonian density $\mathcal{H}$ through the general Legendre transformation [49, 50]:

$$\mathcal{H} = \sum_{\substack{i=N,\sigma \\ \omega,\pi,\rho}} \Pi_i(\vec{x}, t)\frac{\partial\phi_i(\vec{x}, t)}{\partial t} - \mathcal{L}, \tag{2.6}$$

where $\Pi_i(\vec{x}, t)$ is the conjugate momentum of various meson fields and nucleon field:

$$\Pi_i(\vec{x}, t) = \frac{\partial\mathcal{L}}{\partial(\partial\phi_i/\partial t)}. \tag{2.7}$$

After we insert the Lagrangian (2.1) into Eq. (2.6), the Hamiltonian including the nucleon field and meson fields is written as,

$$\begin{aligned}
\mathcal{H}_{\text{TM1}} =& \bar{\psi}[-i\vec{\gamma}\cdot\vec{\nabla} + M^*(\sigma) + g_\omega\gamma_\mu\omega^\mu + g_\rho\tau^a\gamma_\mu\rho^{a\mu}]\psi \\
&+ \frac{1}{2}(\vec{\nabla}\sigma)^2 + \frac{1}{2}m_\sigma^2\sigma^2 + \frac{1}{3}g_2\sigma^3 + \frac{1}{4}g_3\sigma^4 \\
&- \frac{1}{2}\left[\vec{\nabla}\omega_\mu\vec{\nabla}\omega^\mu + (\vec{\nabla}\cdot\vec{\omega})^2 + m_\omega^2\omega_\mu\omega^\mu\right] - \frac{1}{4}c_3(\omega_\mu\omega^\mu)^2 \\
&- \frac{1}{2}\left[\vec{\nabla}\rho_\mu^a\vec{\nabla}\rho^{a\mu} + (\vec{\nabla}\cdot\vec{\rho}^a)^2 + m_\rho^2\rho_\mu^a\rho^{a\mu}\right],
\end{aligned} \tag{2.8}$$

with the nucleon effective mass,

$$M^*(\sigma) = M_N + g_\sigma\sigma. \tag{2.9}$$

Here, we have already taken a static approximation for nuclear matter. It means that all time-dependent terms are dropped in the above Hamiltonian density. In this step, the meson parts are still the field operators. The standard method in RMF is to remove all quantum fluctuations of the meson fields and to use their expectation values instead of the field operators. This means that all meson fields are treated as classical $c-$number fields. It can be symbolized by

$$\phi_i \to \langle\phi_i\rangle. \tag{2.10}$$

The mean-field treatment also simplifies the treatment of nucleons. They move as independent particles in the meson fields. Therefore the nucleon field operator can be expanded on a complete set of single-particle states as

$$\psi(\boldsymbol{x}) = \sum_a \varphi_a(\boldsymbol{x})\hat{c}_a, \tag{2.11}$$

where $\hat{c}_a$ is an annihilation operator for a nucleon in a state a and $\varphi_a(\boldsymbol{x})$ is the corresponding single-particle wave function which is assumed as the plane wave function of the free Dirac equation in nuclear matter,

$$\varphi_a(\boldsymbol{x}) = u(\boldsymbol{p}, s)e^{i\boldsymbol{p}\cdot\boldsymbol{x}}. \tag{2.12}$$

The spinor $u(\boldsymbol{p}, s)$ satisfies the following Dirac equation,

$$\begin{aligned}
(\boldsymbol{\alpha} \cdot \boldsymbol{k} + \beta M_N + g_\sigma\sigma)u(\boldsymbol{k}, s) &= [\varepsilon(\boldsymbol{k}) - g_\omega\omega^0]u(\boldsymbol{k}, s) \\
&= E^*(k)u(\boldsymbol{k}, s),
\end{aligned} \tag{2.13}$$

where

$$u(\boldsymbol{k}, s) = \left(\frac{M_N^* + E^*(k)}{2E^*(k)}\right)^{1/2}
\begin{bmatrix}
1 \\
\dfrac{\boldsymbol{\sigma} \cdot \boldsymbol{k}}{M_N^* + E^*(k)}
\end{bmatrix}
\chi(s). \tag{2.14}$$

The Pauli spinor $\chi(s)$ is the spin wave function.

Confined to the single-particle state i with positive energies, i.e., the no-sea approximation, the ground state of the nuclear matter can be constructed as,

$$|\Psi\rangle = \prod_{i=1}^{A} \hat{c}_i^\dagger|0\rangle, \tag{2.15}$$

where $|0\rangle$ is the physical vacuum state. With this ground state and the mean field approximation, the expectation value for the Hamiltonian (2.8) is obtained as,

$$\begin{aligned}
E_{\text{TM1}} &= \langle\Psi|\mathcal{H}_{\text{TM1}}|\Psi\rangle \tag{2.16} \\
&= \sum_{i=n,p} \frac{2}{(2\pi)^3} \int_{|\boldsymbol{k}|<k_F^i} d^3\boldsymbol{k}\sqrt{k^2 + M^{*2}} + g_\omega\omega\sum_{i=n,p}\rho_B^i + g_\rho\rho(\rho_B^p - \rho_B^n) \\
&\quad + \frac{1}{2}m_\sigma^2\sigma^2 + \frac{1}{3}g_2\sigma^3 + \frac{1}{4}g_3\sigma^4 - \frac{1}{2}m_\omega^2\omega^2 - \frac{1}{4}c_3\omega^4 - \frac{1}{2}m_\rho^2\rho^2,
\end{aligned}$$

where the derivative terms of mesons in Hamiltonian vanishes for the uniform structure of nuclear matter. For a static uniform system, the rotational invariance implies the expectation values of spatial components of ω and ρ mesons to be zero. We just need to take their time components, ω_0 and ρ_0. Here, their subscripts are neglected for convenience and the superscript represents different isospin states of nucleon, neutron and proton. k_F is the Fermi momentum and ρ_B is the baryon density,

$$\rho_B = \langle\Psi|\bar{\psi}\psi|\Psi\rangle = \sum_{i=n,p}\rho_B^i = \sum_{i=n,p}\frac{2}{(2\pi)^3}\int_0^{k_F^i} d^3\boldsymbol{k} = \sum_{i=n,p}\frac{1}{3\pi^2}k_F^{i3}. \tag{2.17}$$

These meson fields can be obtained by solving their equations of motion,

$$m_\sigma^2\sigma + g_2\sigma^2 + g_3\sigma^3 = -g_\sigma\rho_S, \tag{2.18}$$

$$m_\omega^2 \omega + c_3 \omega^3 = g_\omega \rho_B,$$
$$m_\rho^2 \rho = g_\rho (\rho_B^p - \rho_B^n).$$

The scalar density ρ_S is defined as

$$\rho_S = \langle \Psi | \psi^\dagger \psi | \Psi \rangle = \sum_{i=n,p} \rho_S^i = \sum_{i=n,p} \frac{2}{(2\pi)^3} \int_0^{k_F^i} d^3\boldsymbol{k} \, \frac{M_N^*}{E^*(k)}. \tag{2.19}$$

Furthermore, in continuum the energy-momentum tensor is given by

$$T_{\mu\nu} = -g_{\mu\nu} \mathcal{L} + \frac{\partial \phi_i}{\partial x^\nu} \frac{\partial \mathcal{L}}{\partial (\partial \phi_i / \partial x_\mu)}, \tag{2.20}$$

where the repeated index i is summed over all generalized coordinates. Therefore, we can insert the TM1 Lagrangian to this expression and obtain the energy-momentum tensor of TM1 model in nuclear matter system,

$$T_{\mu\nu} = i\bar{\psi}\gamma_\mu \partial_\nu \psi + \left[\frac{1}{2}m_\sigma^2 \sigma^2 + \frac{1}{3}g_2 \sigma^3 + \frac{1}{4}g_3 \sigma^4 - \frac{1}{2}m_\omega^2 \omega^2 - \frac{1}{4}c_3 \omega^4 - \frac{1}{2}m_\rho^2 \rho^2 \right] g_{\mu\nu}. \tag{2.21}$$

The pressure p has the following relation with energy-momentum tensor in a uniform system,

$$p = \frac{1}{3} \langle T_{ii} \rangle, \tag{2.22}$$

which gives the pressure of TM1 model as,

$$\begin{aligned} p_{\text{TM1}} &= \sum_{i=n,p} \frac{2}{3(2\pi)^3} \int_{|\boldsymbol{k}|<k_F^i} d^3\boldsymbol{k} \frac{k^2}{\sqrt{k^2 + M^{*2}}} - \frac{1}{2}m_\sigma^2 \sigma^2 - \frac{1}{3}g_2 \sigma^3 - \frac{1}{4}g_3 \sigma^4 \\ &\quad + \frac{1}{2}m_\omega^2 \omega^2 + \frac{1}{4}c_3 \omega^4 + \frac{1}{2}m_\rho^2 \rho^2 \end{aligned} \tag{2.23}$$

We tabulate the parameters of TM1 and Walecka models in Table 2.1. The unit of all masses about nucleon and mesons is MeV. There are only two mesons in Walecka model, σ and ω fields [45].

	M_N	m_σ	m_ω	m_ρ	g_σ	g_ω	g_ρ	g_2 (fm^{-1})	g_3	c_3
TM1	939.0	511.198	783.0	770.0	10.0289	12.6139	4.6322	-7.2325	0.6183	71.3075
Walecka	939.0	550.0	783.0	$-$	9.5726	11.6711	$-$	$-$	$-$	$-$

Table 2.1: The parameters of TM1 [23] and Walecka model [45].

With these parameters, in Fig.2.1 we plot the EOSs of the TM1 Lagrangian and the Walecka model with different asymmetric parameters, $\delta = (\rho_B^n - \rho_B^p)/(\rho_B^n + \rho_B^p)$, which
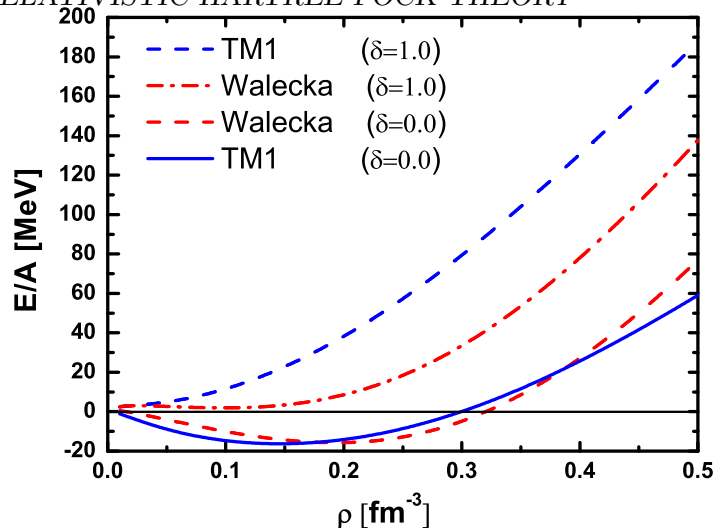
Figure 2.1: The equations of states of TM1 parameter set and Walecka model for symmetric nuclear matter ($\delta = 0.0$) and pure neutron matter ($\delta = 1.0$)

	ρ (fm^{-3})	E/A (MeV)	K (MeV)	a_{asy} (MeV)	M_N^*/M_N
TM1	0.145	-16.26	279.6	37.82	0.635
Walecka	0.193	-15.75	543.5	23.33	0.556

Table 2.2: The saturation properties of TM1 [23] and Walecka model [45].

means that $\delta = 0$ and $\delta = 1$ represent symmetric nuclear matter and pure neutron matter, respectively.

We also show the corresponding saturation properties in Table 2.2. From this table, we can find that the saturation properties of symmetric nuclear matter are largely improved by including the nonlinear terms of σ and ω mesons in the TM1 parameters as compared to Walecka model. The EOS of symmetric nuclear matter becomes softer and asymmetric energy is consistent with the experiment value.

2.2 Relativistic Hartree-Fock theory

So far, the pion does not provide any energy contribution to the binding energy in the RMF model due to its spin and isospin properties. Hence, we would like to extend the phenomenological RMF model to the relativistic Hartree-Fock model by explicitly introducing a part of the pion exchange interaction through the Fock term. In this respect, there are many studies of relativistic Hartree-Fock model from 1970's. These works include the pioneering work of Brockmann [51], a systematic study of Bouyssy and the studies of several groups [52, 53, 54, 55, 56]. There is a recent work on the role of Fock terms on the spin-orbit

splitting and in particular the problem of a magic structure at Z= 58 and Z= 92 by Long *et al.* [57]. This work claims that the ρ meson is more important than pion. However, there are two questions concerning the contribution of the ρ meson exchange interaction. One is the effect of the meson-nucleon form factor due to finite nucleon size and the other is the role of the delta function term in the pion and ρ meson exchange potential. The delta function term in the spin-spin interaction, which is simply removed in their calculations, seems to be the source of the large contribution of the ρ meson exchange interaction.

We would like to start with the Lagrangian which includes two isoscalar mesons (σ and ω) and two isovector ones (π and ρ) [52],

$$
\begin{aligned}
\mathcal{L} \;=\; & \bar{\psi}(i\gamma_\mu\partial^\mu - M_N - g_\sigma\sigma - \frac{f_\pi}{m_\pi}\gamma_5\gamma_\mu\tau^a\partial^\mu\pi^a - g_\omega\gamma_\mu\omega^\mu \\
& -g_\rho\tau^a\gamma_\mu\rho^{a\mu} + \frac{f_\rho}{2M_N}\sigma_{\mu\nu}\partial^\nu\rho^{a\mu}\tau^a)\psi \\
& +\frac{1}{2}\partial_\mu\sigma\partial^\mu\sigma - \frac{1}{2}m_\sigma{}^2\sigma^2 + \frac{1}{2}\partial_\mu\pi^a\partial^\mu\pi^a - \frac{1}{2}m_\pi{}^2\pi^{a2} \\
& -\frac{1}{4}\omega_{\mu\nu}\omega^{\mu\nu} + \frac{1}{2}m_\omega{}^2\omega_\mu\omega^\mu - \frac{1}{4}R^a_{\mu\nu}R^{a\mu\nu} + \frac{1}{2}m_\rho{}^2\rho^a_\mu\rho^{a\mu},
\end{aligned}
\tag{2.24}
$$

where

$$
\begin{aligned}
\omega_{\mu\nu} &= \partial_\mu\omega_\nu - \partial_\nu\omega_\mu, \\
R^a_{\mu\nu} &= \partial_\mu\rho^a_\nu - \partial_\nu\rho^a_\mu.
\end{aligned}
\tag{2.25}
$$

The fields ψ, σ, π^a, ω and $\rho^{a\mu}$ are the nucleon, sigma, pion, omega and rho fields, respectively. It is more reasonable to adopt the pseudovector coupling in πNN interaction. We also take into account the tensor coupling term of the ρ meson which is usually dropped in the relativistic mean field model. Here, we temporarily do not include self-interaction terms for mesons in order to understand the role of the form factor and the short range correlation.

With the Euler-Lagrange equation

$$
\frac{\partial\mathcal{L}}{\partial\phi} - \partial^\mu\left[\frac{\partial\mathcal{L}}{\partial(\partial^\mu\phi)}\right] = 0,
\tag{2.26}
$$

where ϕ represents any field, we can give the equations of motion for various mesons,

$$
(\partial^\mu\partial_\mu + m_\sigma^2)\sigma = -g_\sigma\bar{\psi}\psi,
\tag{2.27}
$$

$$
(\partial^\mu\partial_\mu + m_\pi^2)\pi^a = \frac{f_\pi}{m_\pi}\partial^\mu(\bar{\psi}\gamma_\mu\tau^a\psi),
$$

$$
\partial^\mu\omega_{\mu\nu} + m_\omega^2\omega_\nu = g_\omega\bar{\psi}\gamma_\nu\psi,
$$

$$
\partial^\mu R^a_{\mu\nu} + m_\rho^2\rho^a_\nu = g_\rho\bar{\psi}\gamma_\nu\tau^a\psi + \frac{f_\rho}{2M_N}\partial^\mu(\bar{\psi}\sigma_{\nu\mu}\tau^a\psi).
$$

The last two equations are the Proca equations with source terms. They will be expressed in the Klein-Gordon equation, when we consider the nucleon current continuity condition, $\partial^\nu(\bar{\psi}\gamma_\nu\psi) = 0$, and corresponding isovector currents,

$$(\partial^\mu\partial_\mu + m_\omega^2)\omega_\nu = g_\omega\bar{\psi}\gamma_\nu\psi, \tag{2.28}$$

$$(\partial^\mu\partial_\mu + m_\rho^2)\rho_\nu^a = g_\rho\bar{\psi}\gamma_\nu\tau^a\psi + \frac{f_\rho}{2M_N}\partial^\mu(\bar{\psi}\sigma_{\nu\mu}\tau^a\psi). \tag{2.29}$$

This step is very useful to simplify the Lorentz structure of propagators for the vector mesons.

For later convenience, we should write the Hamiltonian density $\mathcal{H}$ through the general Legendre transformation: After we insert the Lagrangian (2.24) into Eq. (2.6), the Hamiltonian including the nucleon field and meson fields is written as,

$$\begin{aligned}
\mathcal{H} &= \bar{\psi}[-i\vec{\gamma}\cdot\vec{\nabla} + M^*(\sigma) + g_\omega\gamma_\mu\omega^\mu + \frac{f_\pi}{m_\pi}\gamma_5\vec{\gamma}\tau^a\vec{\nabla}\pi^a \\
&\quad + g_\rho\tau^a\gamma_\mu\rho^{a\mu} - \frac{f_\rho}{2M_N}\sigma_{\mu i}\partial^i\rho^{a\mu}\tau^a]\psi \\
&\quad + \frac{1}{2}(\vec{\nabla}\sigma)^2 + \frac{1}{2}m_\sigma^2\sigma^2 + \frac{1}{2}(\vec{\nabla}\pi^a)^2 + \frac{1}{2}m_\pi^2(\pi^a)^2 \\
&\quad - \frac{1}{2}\left[\vec{\nabla}\omega_\mu\vec{\nabla}\omega^\mu + (\vec{\nabla}\cdot\vec{\omega})^2 + m_\omega^2\omega_\mu\omega^\mu\right] \\
&\quad - \frac{1}{2}\left[\vec{\nabla}\rho_\mu^a\vec{\nabla}\rho^{a\mu} + (\vec{\nabla}\cdot\vec{\rho}^a)^2 + m_\rho^2\rho_\mu^a\rho^{a\mu}\right],
\end{aligned} \tag{2.29}$$

with the nucleon effective mass,

$$M^*(\sigma) = M_N + g_\sigma\sigma. \tag{2.30}$$

Here, we have already taken a static approximation for nuclear matter. It means that all the terms having time-dependence disappear in the above Hamiltonian density. In this step, the meson parts are still the field operators. The standard method is to use the expectation value instead of the field operator in the RMF model,

$$\phi_i \to \langle\phi_i\rangle. \tag{2.31}$$

However, we would like to introduce the fluctuation part besides the mean field part for mesons following the method in Refs. [58, 59]. The expectation values of σ and ω meson fields are dominant as compared with the fluctuation parts, while the fluctuation terms become important for the pion and ρ meson whose mean fields are zero in symmetric and spin-saturated nuclear matter. Now, the meson fields are constructed by two parts:

$$\phi_i = \langle\phi_i\rangle + \delta\phi_i, \tag{2.32}$$

where $\langle\phi_i\rangle$ is the expectation value of meson which is c-number, while $\delta\phi_i$ is the meson fluctuation part which usually represents a small quantity compared with the classical filed.

Now, the fluctuation terms also will appear in the total Hamiltonian. We show the σ meson part as an example,

$$
\begin{aligned}
\mathcal{H}_\sigma = \quad & \bar{\psi}[g_\sigma\bar{\sigma} + g_\sigma\delta\sigma]\psi + \vec{\nabla}\bar{\sigma}\cdot\vec{\nabla}\delta\sigma + m_\sigma^2\bar{\sigma}\delta\sigma \\
& +\frac{1}{2}(\vec{\nabla}\bar{\sigma})^2 + \frac{1}{2}m_\sigma^2\bar{\sigma}^2 + \frac{1}{2}(\vec{\nabla}\delta\sigma)^2 + \frac{1}{2}m_\sigma^2\delta\sigma^2
\end{aligned}
\tag{2.33}
$$

Then, we obtain equations of motion about the expectation value and fluctuation part by variational principle from the above Hamiltonian,

$$
\begin{aligned}
(-\vec{\nabla}^2 + m_\sigma^2)\bar{\sigma} &= -g_\sigma\langle\bar{\psi}\psi\rangle, \\
(-\vec{\nabla}^2 + m_\omega^2)\bar{\omega}^0 &= g_\omega\langle\psi^\dagger\psi\rangle, \\
(-\vec{\nabla}^2 + m_\rho^2)\bar{\rho}^{a0} &= g_\rho\langle\psi^\dagger\tau^a\psi\rangle + \frac{f_\rho}{2M_N}\partial_i\langle\bar{\psi}\sigma^{0i}\tau^a\psi\rangle
\end{aligned}
\tag{2.34}
$$

and

$$
\begin{aligned}
(-\vec{\nabla}^2 + m_\sigma^2)\delta\sigma &= -g_\sigma(\bar{\psi}\psi - \langle\bar{\psi}\psi\rangle), \\
(-\vec{\nabla}^2 + m_\pi^2)\delta\pi^a &= \frac{f_\pi}{m_\pi}\vec{\nabla}\cdot\bar{\psi}\gamma^5\vec{\gamma}\tau^a\psi, \\
(-\vec{\nabla}^2 + m_\omega^2)\delta\omega^\mu &= g_\omega(\bar{\psi}\gamma^\mu\psi - \langle\bar{\psi}\gamma^\mu\psi\rangle), \\
(-\vec{\nabla}^2 + m_\rho^2)\delta\rho^{a\mu} &= g_\rho[\bar{\psi}\gamma^\mu\tau^a\psi - \langle\bar{\psi}\gamma^\mu\tau^a\psi\rangle] + \frac{f_\rho}{2M_N}\left[\partial_i(\bar{\psi}\sigma^{\mu i}\tau^a\psi) - \partial_i\langle\bar{\psi}\sigma^{\mu i}\tau^a\psi\rangle\right],
\end{aligned}
\tag{2.35}
$$

where there is no equation of motion for pion classical part due to the parity conservation. The nucleon currents in these equations of motion are separated into two parts. One is the mean field part and the other is the fluctuation part corresponding to meson fluctuations.

$$
\begin{aligned}
\bar{\psi}\Gamma_i\psi &= \langle\bar{\psi}\Gamma_i\psi\rangle + (\bar{\psi}\Gamma_i\psi - \langle\bar{\psi}\Gamma_i\psi\rangle) \\
&= \langle\bar{\psi}\Gamma_i\psi\rangle + \delta\bar{\psi}\Gamma_i\psi.
\end{aligned}
\tag{2.36}
$$

Here, Γ_i represent different spin structures in meson-nucleon interaction.

The introduction of meson fluctuations leads to some new terms in the Hamiltonian density in nuclear matter where the expectation values of mesons are independent of position.

$$
\begin{aligned}
\mathcal{H}_N &= \bar{\psi}(-i\vec{\gamma}\cdot\vec{\nabla} + M_N^*(\sigma) + g_\omega\gamma_0\omega + g_\rho\tau^3\gamma_0\rho^3)\psi \\
&\quad +\frac{1}{2}m_\sigma^2\sigma^2 - \frac{1}{2}m_\omega^2\omega^2 - \frac{1}{2}m_\rho^2(\rho^3)^2 + \frac{1}{2}g_\sigma\delta\sigma(\bar{\psi}\psi - \langle\bar{\psi}\psi\rangle) + \frac{f_\pi}{2m_\pi}\delta\pi^a\vec{\nabla}\cdot\bar{\psi}\gamma_5\vec{\gamma}\tau^a\psi \\
&\quad +\frac{1}{2}g_\omega\delta\omega_\mu(\bar{\psi}\gamma^\mu\psi - \langle\bar{\psi}\gamma^\mu\psi\rangle) + \frac{1}{2}\delta\rho_\mu^a\big[g_\rho(\bar{\psi}\gamma^\mu\tau^a\psi - \langle\bar{\psi}\gamma^\mu\tau^a\psi\rangle) \\
&\quad +\frac{f_\rho}{2M_N}(\partial_i(\bar{\psi}\sigma^{\mu i}\tau^a\psi) - \partial_i\langle\bar{\psi}\sigma^{\mu i}\tau^a\psi\rangle)\big],
\end{aligned}
\tag{2.37}
$$

where we have used σ and ω instead of $\bar{\sigma}$ and $\bar{\omega}^0$ for convenience and choose the isospin third component, ρ^3, for ρ meson. We find that the first and second lines in the above Hamiltonian comes from the mean filed approach, while the rest lines are the contributions of fluctuation.

The meson fluctuations are treated by the Green function. For the Klein-Gordon equation, we have,

$$(-\vec{\nabla}_{\vec{x}}^2 + m_i^2)G_i(\vec{x} - \vec{x}') = \delta^{(3)}(\vec{x} - \vec{x}'), i = \sigma, \pi, \omega, \rho \tag{2.38}$$

where $G(\vec{x} - \vec{x}')$ is the meson propagator. Therefore, for instance, the σ fluctuation can be written as,

$$\delta\sigma(\vec{x}) = -g_\sigma \int d^3x' G_\sigma(\vec{x} - \vec{x}')(\bar{\psi}\psi - \langle\bar{\psi}\psi\rangle)(\vec{x}'). \tag{2.39}$$

Finally, the Hamiltonian density is related with the nucleon current fluctuations.

$$
\begin{aligned}
\mathcal{H}_N &= \bar{\psi}(-i\vec{\gamma}\cdot\vec{\nabla} + M_N^* + g_\omega\gamma_0\omega + g_\rho\tau^3\gamma_0\rho^3)\psi + \frac{1}{2}m_\sigma^2\sigma^2 - \frac{1}{2}m_\omega^2\omega^2 - \frac{1}{2}m_\rho^2(\rho^3)^2 \\
&\quad + \frac{1}{2}\int d^3x_2\Big[-g_\sigma^2\delta\bar{\psi}\psi(\vec{x}_1)G_\sigma(\vec{x}_1 - \vec{x}_2)\delta\bar{\psi}\psi(\vec{x}_2) \\
&\quad + g_\omega^2\delta\bar{\psi}\gamma^\mu\psi(\vec{x}_1)G_\omega(\vec{x}_1 - \vec{x}_2)\delta\bar{\psi}\gamma_\mu\psi(\vec{x}_2) \\
&\quad - \left(\frac{f_\pi}{m_\pi}\right)^2\bar{\psi}\gamma_5\vec{\gamma}\cdot\vec{q}\tau^a\psi(\vec{x}_1)G_\pi(\vec{x}_1 - \vec{x}_2) \times \bar{\psi}\gamma_5\vec{\gamma}\cdot\vec{q}\tau^a\psi(\vec{x}_2) \\
&\quad + g_\rho^2\delta\bar{\psi}\gamma^\mu\tau^a\psi(\vec{x}_1)G_\rho(\vec{x}_1 - \vec{x}_2)\delta\bar{\psi}\gamma_\mu\tau^a\psi(\vec{x}_2) \\
&\quad - i\frac{g_\rho f_\rho}{M_N}(q^i\delta\bar{\psi}\sigma^{\mu i}\tau^a\psi(\vec{x}_1))G_\rho(\vec{x}_1 - \vec{x}_2)\delta\bar{\psi}\gamma_\mu\tau^a\psi(\vec{x}_2) \\
&\quad + \left(\frac{f_\rho}{2M_N}\right)^2 q^i\delta\bar{\psi}\sigma^{\mu i}\tau^a\psi(\vec{x}_1)G_\rho(\vec{x}_1 - \vec{x}_2) \times q_j\delta\bar{\psi}\sigma_{\mu j}\tau^a\psi(\vec{x}_2))\Big],
\end{aligned} \tag{2.40}
$$

where $\vec{q}$ represents momentum transfer between two nucleons. Now, the total energy per unit volume E is given by,

$$E = \langle\Psi|\int d^3x_1 \mathcal{H}_N|\Psi\rangle/V \tag{2.41}$$

with $|\Psi\rangle$ is the ground state for nucleon. The expectation value of the nucleon current fluctuations can be related with the density correlation function [60],

$$
\begin{aligned}
iD(\vec{x}_1, \vec{x}_2) &\tag{2.42} \\
&= \langle\Psi|[\bar{\psi}\Gamma_i\psi - \langle\bar{\psi}\Gamma_i\psi\rangle](\vec{x}_1)[\bar{\psi}\Gamma_i\psi - \langle\bar{\psi}\Gamma_i\psi\rangle](\vec{x}_2)|\Psi\rangle \\
&= \langle\Psi|\bar{\psi}(\vec{x}_1)\Gamma_i\psi(\vec{x}_1)\bar{\psi}(\vec{x}_2)\Gamma_i\psi(\vec{x}_2)|\Psi\rangle - \langle\Psi|\bar{\psi}(\vec{x}_1)\Gamma_i\psi(\vec{x}_1)|\Psi\rangle\langle\Psi|\bar{\psi}(\vec{x}_2)\Gamma_i\psi(\vec{x}_2)|\Psi\rangle \\
&= -\text{Tr}\{G_N(\vec{x}_1 - \vec{x}_2)\Gamma_i G_N(\vec{x}_2 - \vec{x}_1)\Gamma_i\},
\end{aligned}
$$

where $G_N(\vec{x}_1 - \vec{x}_2)$ is the nucleon propagator,

$$G_N(\vec{x}_1 - \vec{x}_2)_{\alpha\beta} = \langle \Psi | \psi_\alpha(\vec{x}_1) \bar{\psi}_\beta(\vec{x}_2) | \Psi \rangle \tag{2.43}$$

and the trace is over the nucleon spin and isospin. For infinite nuclear matter, it is more convenient to work out the total energy in momentum space. Therefore, the total energy per unit volume E in symmetry nuclear matter is,

$$
\begin{aligned}
E &= \int \frac{4d^3k}{(2\pi)^3} \bar{\psi}(k)(\vec{\gamma} \cdot \vec{k} + (M_N + g_\sigma \sigma) + g_\omega \gamma_0 \omega)\psi(k) + \frac{1}{2}m_\sigma^2 \sigma^2 - \frac{1}{2}m_\omega^2 \omega^2 \\
&+ \frac{1}{2} \int \frac{2d^3k d^3k'}{(2\pi)^6} \Big[g_\sigma^2 G_\sigma(\vec{k} - \vec{k}')\mathrm{Tr}\{G_N(k)G_N(k')\} \\
&- g_\omega^2 G_\omega(\vec{k} - \vec{k}')\mathrm{Tr}\{G_N(k)\gamma^\mu G_N(k')\gamma_\mu\} - 3g_\rho^2 G_\rho(\vec{k} - \vec{k}')\mathrm{Tr}\{G_N(k)\gamma^\mu G_N(k')\gamma_\mu\} \\
&+ 3\left(\frac{f_\pi}{m_\pi}\right)^2 G_\pi(\vec{k} - \vec{k}')\mathrm{Tr}\{G_N(k)\gamma_5 \vec{\gamma} \cdot \vec{q} G_N(k')\gamma_5 \vec{\gamma} \cdot \vec{q}\} \\
&+ \frac{i3g_\rho f_\rho}{M_N} G_\rho(\vec{k} - \vec{k}')\mathrm{Tr}\{G_N(k)\sigma^{\mu i} q^i G_N(k')\gamma_\mu\} - \\
&3\left(\frac{f_\rho}{2M_N}\right)^2 G_\rho(\vec{k} - \vec{k}')\mathrm{Tr}\{G_N(k)\sigma^{\mu i} q^i G_N(k')\sigma_{\mu j} q^j\}\Big] \theta(|\vec{k}| < k_F)\theta(|\vec{k}'| < k_F).
\end{aligned}
\tag{2.44}
$$

However, we do not know the exact expression of the single particle wave function, $\psi(k)$, until now. It will be obtained by the variational principle of the total energy,

$$\delta[E - \varepsilon(k)\int \frac{d^3k}{(2\pi)^3}\psi^\dagger(k)\psi(k)] = 0, \tag{2.45}$$

where the Lagrange multiplier ε is defined as the single particle energy. By the variational equation, the wave function satisfies the Dirac function,

$$(\vec{\gamma} \cdot \vec{k} + M_N + \Sigma)u(k,s) = \gamma^0 \varepsilon(k)u(k,s), \tag{2.46}$$

where we have used the Dirac spinor $u(k,s)$ to replace the $\psi(k)$ for consistency with other works. Because of the translational and rotational invariance in the rest frame of infinite nuclear matter and the assumed invariance under parity and time reversal, the nucleon self-energy Σ has the quite general form[45, 52] as

$$\Sigma(\vec{k}) = \Sigma_S(k) + \gamma^0 \Sigma_0(k) + \vec{\gamma} \cdot \hat{\vec{k}} \Sigma_V(k). \tag{2.47}$$

Here, $\hat{\vec{k}}$ is the unit vector of $\vec{k}$. The self-energy also depends on momenta besides the density. When we take the normalization condition for the spinor $u(\vec{k},s)$ as,

$$u^\dagger(\vec{k},s)u(\vec{k},s) = 1, \tag{2.48}$$

the Dirac Eq. (2.46) in nuclear matter can be solved formally,

$$u(\vec{k}, s) = \left(\frac{M_N^* + E^*}{2E^*} \right)^{1/2} \begin{bmatrix} 1 \\ \dfrac{\vec{\sigma} \cdot \vec{k}^*}{M_N^* + E^*} \end{bmatrix} \chi(s), \tag{2.49}$$

with

$$\vec{k}^*(k) = \vec{k} + \hat{\vec{k}}\Sigma_V(k), \tag{2.50}$$

$$M_N^*(k) = M_N + \Sigma_S(k),$$

$$E^*(k) = \sqrt{M_N^{*2} + \vec{k}^{*2}},$$

where $M_N^*(k)$ is defined as the effective mass of nucleon. In RMF, the effective mass of the nucleon is just a function of density like Eq. (2.30), while it is now also related with the momentum. Here, $\chi(s)$ is the spin wave function. With this solution, the nucleon propagator with Pauli principle has the following explicit expression,

$$G_N(k) = \frac{\slashed{k}^* + M_N^*(k)}{2E^*(k)}. \tag{2.51}$$

We can substitute the propagator into Eq.(2.44) to calculate the trace in total energy. It is found that this energy has completely the same form as the one in Ref. [52], where the retardation effect in meson propagator is neglected. The total energy is given by,

$$\begin{aligned}
E &= \sum_{i=n,p} \frac{1}{\pi^2} \int^{k_F^i} k^2 dk (k\hat{K} + M_N\hat{M}) - \frac{g_\sigma^2}{2m_\sigma^2}\rho_S^2 + \frac{g_\omega^2}{2m_\omega^2}\rho_B^2 + \frac{g_\rho^2}{2m_\rho^2}\rho_{B3}^2 \\
&+ \sum_{i=n,p} \frac{1}{2(2\pi)^4} \int kk' dk dk' \Bigg[\sum_i A_i(k,k') + \hat{M}(k)\hat{M}(k') \sum_i B_i(k,k') \\
&+ \hat{K}(k)\hat{K}(k') \sum_i C_i(k,k') + \hat{K}(k)\hat{M}(k')D(k,k') \Bigg] \theta(k_F^i - k)\theta(k_F^i - k') \\
&+ \frac{2}{(2\pi)^4} \int kk' dk dk' \Bigg[\sum_i A_i(k,k') + \hat{M}(k)\hat{M}(k') \sum_i B_i(k,k') \\
&+ \hat{K}(k)\hat{K}(k') \sum_i C_i(k,k') + \hat{K}(k)\hat{M}(k')D(k,k') \Bigg] \theta(k_F^i - k)\theta(k_F^n - k'),
\end{aligned} \tag{2.52}$$

where the scalar density ρ_S, baryon density ρ_B and the third component ρ_{B3} are defined as,

$$\rho_S = \sum_{i=n,p} \frac{1}{\pi^2} \int^{k_F^i} k^2 \hat{M}(k) dk, \tag{2.53}$$

$$\rho_B = \sum_{i=n,p} \frac{(k_F^i)^3}{3\pi^2},$$

$$\rho_{B3} = \frac{(k_F^n)^3}{3\pi^2} - \frac{(k_F^p)^3}{3\pi^2},$$

with the Fermi momentum k_F^i and

$$\hat{K}(k) = \frac{k^*(k)}{E^*(k)} \tag{2.54}$$

$$\hat{M}(k) = \frac{M_N^*(k)}{E^*(k)}.$$

The self-energy of proton changes as,

$$\Sigma_S^p(k) = -\frac{g_\sigma^2}{m_\sigma^2}\rho_S + \int^{k_F^p} \frac{k'dk'}{(4\pi)^2 k} \left[\hat{M}(k') \sum_{i=\sigma,\omega,\pi,\rho} B_i(k,k') + \frac{1}{2}\hat{K}(k')D(k',k) \right] \tag{2.55}$$

$$+ \frac{2}{(4\pi)^2 k} \int^{k_F^n} k'dk' \left[\hat{M}(k') \sum_{i=\pi,\rho} B_i(k,k') + \frac{1}{2}\hat{K}(k')D(k',k) \right],$$

$$\Sigma_0^p(k) = \frac{g_\omega^2}{m_\omega^2}\rho_B + \frac{1}{(4\pi)^2 k} \left[\int^{k_F^p} k'dk' \sum_{i=\sigma,\omega,\pi,\rho} A_i(k,k') + 2\int^{k_F^n} k'dk' \sum_{i=\pi,\rho} A_i(k,k') \right],$$

$$\Sigma_V^p(k) = \frac{1}{(4\pi)^2 k} \int^{k_F^p} k'dk' \left[\hat{K}(k') \sum_{i=\sigma,\omega,\pi,\rho} C_i(k,k') + \frac{1}{2}\hat{M}(k')D(k,k') \right]$$

$$+ \frac{2}{(4\pi)^2 k} \int^{k_F^n} k'dk' \left[\hat{K}(k') \sum_{i=\pi,\rho} C_i(k,k') + \frac{1}{2}\hat{M}(k')D(k,k') \right].$$

The neutron also obeys the similar expression to the exchange of the position of k_F^p and k_F^n. The functions A_i, B_i, C_i and D are listed in the Table.2.3, where the θ_i and ϕ_i functions are coming from the angular integration,

$$\theta(m,k,k') = \ln\left[\frac{m^2 + (k+k')^2}{m^2 + (k-k')^2} \right], \tag{2.56}$$

$$\phi(m,k,k') = \frac{k^2 + k'^2 + m^2}{4kk'}\theta(m,k,k') - 1.$$

We should notice that for the symmetry nuclear matter, these functions should have an additional factor 3 for the π and ρ meson in the energy (4.52).

However, we want to emphasize that we keep the contact terms in pion and the tensor coupling term of ρ meson exchange interactions where the exchange interaction of spin-spin central part can be written as

$$V_C(\vec{q}) = \frac{\vec{q}^2}{\vec{q}^2 + m^2} = 1 - \frac{m^2}{\vec{q}^2 + m^2}, \tag{2.57}$$

i	A_i	B_i	C_i
σ	$g_\sigma^2 \theta_\sigma$	$g_\sigma^2 \theta_\sigma$	$-2g_\sigma^2 \phi_\sigma$
ω	$2g_\omega^2 \theta_\omega$	$-4g_\omega^2 \theta_\omega$	$-4g_\omega^2 \phi_\omega$
ρ_V	$2g_\rho^2 \theta_\rho$	$-4g_\rho^2 \theta_\rho$	$-4g_\rho^2 \phi_\rho$
π	$\left[\frac{f_\pi}{m_\pi}\right]^2 (m_\pi^2 \theta_\pi - 4kk')$	$\left[\frac{f_\pi}{m_\pi}\right]^2 (m_\pi^2 \theta_\pi - 4kk')$	$2\left[\frac{f_\pi}{m_\pi}\right]^2 [(k^2+k'^2)\phi_\pi - kk'\theta_\pi]$
ρ_T	$\left[\frac{f_\rho}{2M_N}\right]^2 (m_\rho^2 \theta_\rho - 4kk')$	$3\left[\frac{f_\rho}{2M_N}\right]^2 (m_\rho^2 \theta_\rho - 4kk')$	$4\left[\frac{f_\rho}{2M_N}\right]^2 [(k^2+k'^2-m_\rho^2/2)\phi_\rho - kk'\theta_\rho]$
ρ_{VT}		$D = 12\frac{f_\rho g_\rho}{2M_N}(k\theta_\rho - 2k'\phi_\rho)$	

Table 2.3: The function A_i, B_i, C_i and D in the Eq. (2.52).

where, the factor 1 will be transformed to the δ function in the configuration space which is called as contact term. The δ function term is often removed due to the short range correlation. This is very important when discussing which one is more important between the pion and ρ meson in Fock terms. We should not remove the contact terms of the pion and ρ meson exchange interactions simply. Therefore there is slight difference about the expression for pion and tensor coupling part of ρ meson in this work as compared with Ref. [52]. We should take the following replacement for pion and tensor coupling term of ρ meson in Fock energies,

$$-m^2\theta(m,k,k') \to 4kk' - m^2\theta(m,k,k'). \tag{2.58}$$

By minimizing the total energy E with respect to the $\hat{M}(k)$, we obtain a self-consistent equation for the self-energy. Because for the other variational parameter, $\hat{K}(k)$, there is $\hat{M}^2(k) + \hat{K}^2(k) = 1$ This equation can be solved numerically by the iterative method.

In Lagrangian (2.24), there are six free parameters, i.e., five coupling constants $(g_\sigma, g_\omega, g_\rho, f_\pi, f_\rho)$ and σ meson mass, m_σ. As for the coupling constants, we fix the π-N and ρ-N coupling constants as in Ref.[52], i.e., $f_\pi^2/4\pi = 0.08$ and $g_\rho^2/4\pi = 0.55$. The tensor ρ-N coupling constant is related to the ratio $f_\rho/g_\rho = \kappa$. This ratio usually has two values, $\kappa = 3.7$ or $\kappa = 6.6$. We use these two values to study the effect of the tensor coupling term of the ρ meson. Therefore, there are just three parameters which need to be adjusted in this work, ω and σ coupling constants, g_ω and g_σ, and σ meson mass m_σ. As for the σ meson mass, we choose $m_\sigma = 550$ MeV. Then, we fit g_σ and g_ω according to the saturation properties of nuclear matter, $E/A = -15.75$ MeV and $\rho_0 = 0.1484$ fm^{-3}.

Here, we take two cases, with and without the delta-function piece (contact term) in the pion and ρ meson exchange interactions. We tabulate these parameter sets in Table 2.4. Other properties of nuclear matter such as the incompressibility K and the effective nucleon mass of Fermi surface M_N^* at the saturation density are also given in Table 2.4. We find the EOS with the Fock energy is softer than the Walecka model which contains only

the Hartree energy. The contributions of pion and ρ meson are completely different for the cases with and without the delta-function pieces (contact terms). The contact terms are removed in the cases I and II, while they are kept in the cases III and IV. The Fock energy contributions have opposite signs for the cases with and without the contact terms. The ρ meson contribution is very large when we remove the contact term, while it become rather small when we keep the contact term.

	Parameters						$\langle V_{Fock}\rangle/\rho_B$		
Case	g_σ	g_ω	κ	M_N^*/M_N	K (MeV)	σ	ω	π	ρ
I	9.031	11.697	3.7	0.568	441	28.93	-21.49	-6.56	-18.81
II	6.740	11.202	6.6	0.633	384	16.26	-20.50	-6.49	-58.20
III	10.28	11.091	3.7	0.555	472	37.40	-19.10	14.45	1.970
IV	9.980	10.175	6.6	0.602	395	35.46	-16.53	14.62	8.902

Table 2.4: The parameter sets of the EOS of nuclear matter in RHF model. We remove the contact terms of pion and ρ meson in cases I and II, while we keep them in cases III and IV. In addition to the coupling constants, we show the contributions of Fock energies from various mesons and the incompressibility K and the effective nucleon mass M_N^*.
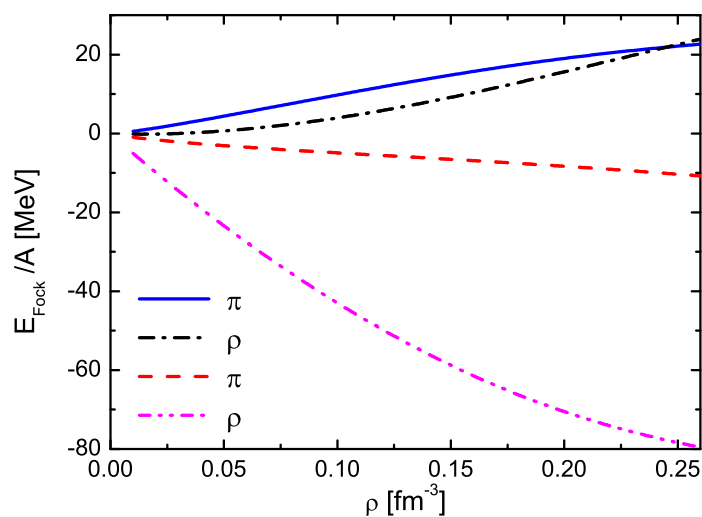
Figure 2.2: The pion and ρ meson contributions in the Fock term. The solid and dash-dotted curves are the pion and ρ meson contributions to the Fock term, respectively, for the case IV in Table 2.4, while the dashed and dash-dot-dotted curves correspond the pion and ρ meson contributions to the Fock term for case II.

We elucidate the roles of the contact terms by showing the Fock energies from the pion

and ρ meson with and without the contact terms in Fig.2.2. The signs of the two cases are opposite. We find, in particular, that the contribution of the ρ meson is quite different. As for the σ and ω mesons, their Fock energies are shown in Table 2.4 at the saturation density. The Fock term reduces only the contribution of the Hartree term for each meson.

2.3 The form factor in RHF theory

The nucleon form factor appears in the relativistic mean field (RMF) model as a simple modification of the coupling constants, because the momentum transfer is zero. On the other hand, it is essential to take into account the form factor in the calculation of the Fock energies, because the meson fields are virtually excited (quantum effect). We have to consider the finite size effect of the nucleon which is to be treated in terms of form factor. Although it seems simple to introduce the form factor in the relativistic Hartree-Fock framework, the form factor effect is often dropped for quantitative studies of finite nuclei and nuclear matter.

We employ the dipole form factor in which we replace the meson-nucleon interactions in the momentum space by

$$\frac{1}{\vec{q}^2 + m^2} \rightarrow \frac{1}{\vec{q}^2 + m^2}\left(\frac{\Lambda^2 - m^2}{\Lambda^2 + \vec{q}^2}\right)^2 ,$$ (2.59)

$$\frac{\vec{q}^2}{\vec{q}^2 + m^2} \rightarrow \frac{\vec{q}^2}{\vec{q}^2 + m^2}\left(\frac{\Lambda^2 - m^2}{\Lambda^2 + \vec{q}^2}\right)^2 .$$

These two interactions are the typical interactions appearing in the Fock term in this work. We can then manipulate these replacement as,

$$\frac{1}{\vec{q}^2 + m^2}\left(\frac{\Lambda^2 - m^2}{\Lambda^2 + \vec{q}^2}\right)^2 = \frac{1}{\vec{q}^2 + m^2} - \frac{1}{\vec{q}^2 + \Lambda^2} + (\Lambda^2 - m^2)\frac{d}{d\Lambda^2}\frac{1}{\vec{q}^2 + \Lambda^2}$$ (2.60)

and

$$\frac{\vec{q}^2}{\vec{q}^2 + m^2}\left(\frac{\Lambda^2 - m^2}{\Lambda^2 + \vec{q}^2}\right)^2 = \frac{\Lambda^2}{\vec{q}^2 + \Lambda^2} - \frac{m^2}{\vec{q}^2 + m^2} - (\Lambda^2 - m^2)\frac{d}{d\Lambda^2}\frac{\Lambda^2}{\vec{q}^2 + \Lambda^2} .$$ (2.61)

From the above expressions, we notice that the delta function of pion interaction in configuration space does not appear any more. The delta function piece becomes now momentum dependent.

The energy contribution of σ meson after introducing the form factor is expressed as

$$E_{FF}^\sigma = -\frac{g_\sigma^2}{2m_\sigma^2}\rho_S^2\left(1 - \frac{m_\sigma^2}{\Lambda^2}\right)^2$$ (2.62)

$$+ \frac{g_\sigma^2}{(2\pi)^4}\int_0^{k_F} dk\,dk'\left[\theta_\sigma^{FF} + \theta_\sigma^{FF}\hat{M}(k)\hat{M}(k') - 2\phi_\sigma^{FF}\hat{K}(k)\hat{K}(k')\right],$$

where θ^{FF} and ϕ^{FF} have the following relations with original θ and ϕ as,

$$\theta^{FF}(m, \Lambda, k, k') = \theta(m, k, k') - \theta(\Lambda, k, k') + (\Lambda^2 - m^2)\frac{d}{d\Lambda^2}\theta(\Lambda, k, k'), \qquad (2.63)$$

$$\phi^{FF}(m, \Lambda, k, k') = \phi(m, k, k') - \phi(\Lambda, k, k') + (\Lambda^2 - m^2)\frac{d}{d\Lambda^2}\phi(\Lambda, k, k').$$

These relations are based on the cut off momentum Λ. For the pion and the tensor coupling term of ρ meson, we should use the corresponding expression in Eq. (2.61).

The form factor in the meson-nucleon coupling vertex is particularly important in the RHF lagrangian, since the Fock term needs integration over various meson momenta (virtual process). The form factor effect is simple in the RMF approximation where the momentum transfer is zero. The consideration of the form factor in the bare nucleon-nucleon interaction ($\Lambda \sim 1.0 - 2.0$ GeV) has a large influence on the meson exchange interaction particularly for mesons with large masses.

Hence, we calculate the EOS by introducing the cut-off masses of the form factors in Bonn-A for various mesons. We provide the parameter sets obtained by considering the form factor of $\Lambda_\sigma = 2.0, \Lambda_\omega = 1.5, \Lambda_\pi = 1.05, \Lambda_\rho = 1.3$ GeV [11] in Table 2.5. We list two cases with $\kappa = 3.7$ and $\kappa = 6.6$ for the ρ tensor coupling, which are shown as case V and case VI. The effect of the form factor is large for meson exchange interactions with ρ meson. The ρ meson contribution is largely cut down by nearly half. On the other hand, the σ and ω meson contributions do not change much. The contribution of the ρ meson turns out to be much smaller than the pion contribution, which becomes relatively important now in the total Fock energy.

	Parameters					$\langle V_{Fock}\rangle/\rho_B$			
Case	g_σ	g_ω	κ	M_N^*/M_N	K (MeV)	σ	ω	π	ρ
V	11.594	16.451	3.7	0.519	564	39.19	-20.48	11.92	0.724
VI	11.545	16.164	6.6	0.530	540	38.73	-19.90	11.95	3.348

Table 2.5: The parameter sets of the EOS of nuclear matter with form factor. We introduce the form factor for the meson-nucleon coupling vertices for all the mesons with the cut-off masses in Bonn-A potential, while keeping the contact pieces of pion and the tensor coupling term of ρ meson exchange interactions. The parameters are listed for two κ's in the cases V and VI.

In Fig.2.3, we show the EOS after introducing the form factor. The dotted curve is the EOS of nuclear mater with the inclusion of the form factor effect in RHF theory (HFFF). The solid curve denotes the case IV without considering the form factor, which is shown as the reference of form factor effect. The form factor does not improve the saturation properties of nuclear matter in RHF model.
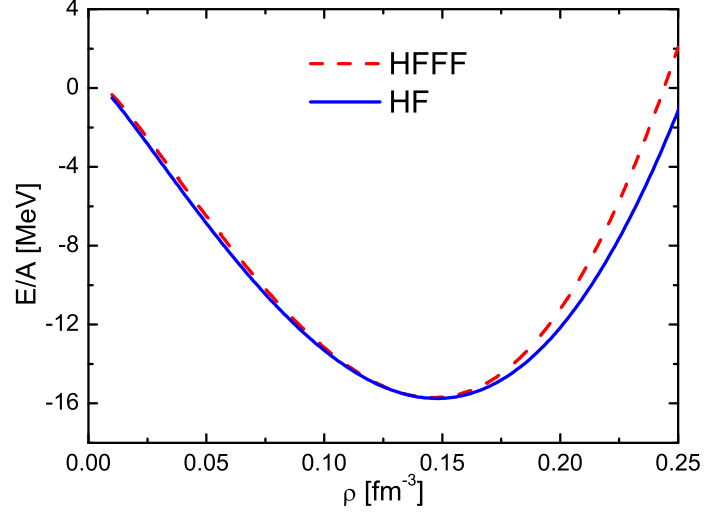
Figure 2.3: The EOS with form factor as a function of the matter density. The dotted curve is the EOS of the case V, which includes the form factor effect; the solid curve corresponds to the EOS without the form factor (Case III in previous subsection).
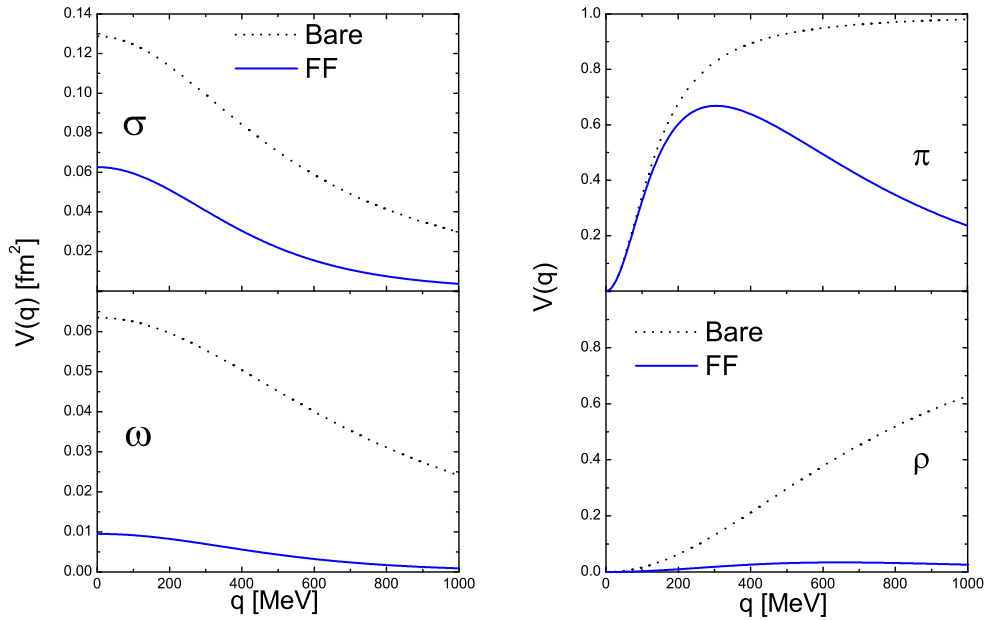
Figure 2.4: The momentum dependence of the meson exchange interactions with the inclusion of the form factor are shown as a function of the momentum. In the left panel, we show the σ and ω meson cases. In the right panel, we show the pion and tensor coupling term of ρ meson.

The σ and ω meson exchange interactions have the momentum dependence, $1/(\vec{q}^2 + m^2)$, which does not have much strength at short distance after taking the form factor effect. The pion and tensor coupling term of ρ meson exchange interactions have the momentum dependence, $\vec{q}^2/(\vec{q}^2 + m^2)$. This form of the interaction increases with the momentum. We

show in Fig.2.4 the momentum dependence of the meson exchange interaction for the σ and ω mesons in the left two panels. To compare the form factor effect conveniently, we choose $\Lambda = 1.0$ GeV for all mesons here. We see that these interactions are quite difference between the result with (FF) and without (bare) form factors. In the right panels, we show the momentum dependence of the pion and tensor coupling term of ρ meson exchange interactions. The high momentum components are largely suppressed by the form factor. In the ρ meson case, the form factor effect is enormous because the mass of the ρ meson, $m_\rho = 780$MeV, is close to the cut-off mass, $\Lambda = 1$GeV. The Fock term has the contribution from momenta below the twice of Fermi momentum, $|q| < 2k_F$. Hence, the ρ meson Fock term changes its sign as can be seen in Fig.2.4.

Now, we vary the cut-off masses of the form factor on the basis of the EOS with parameter set VI. We show in Fig. 2.5 the cases with $\Lambda'_i = \Lambda_i, 1.25\Lambda_i$ and $1.5\Lambda_i$ where Λ_i is the value in Bonn-A. The EOS moves up appreciably with Λ. This is due to the large increase of Hartree part for the ω meson contributions by increasing the cut-off mass.
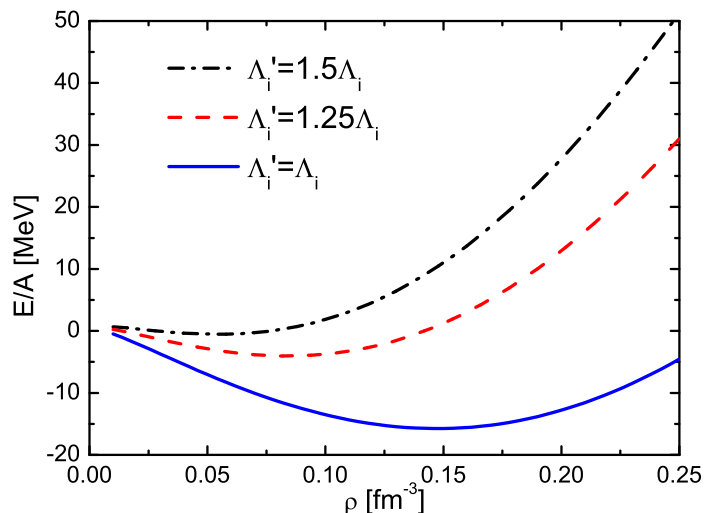
Figure 2.5: We show the EOS of nuclear matter for several cut-off masses of the form factor. The cut-off masses are taken as $\Lambda'_i = 1.0\Lambda_i, \ 1.5\Lambda_i, \ 2.0\Lambda_i$ GeV, respectively and the other parameters are fixed as the case VI.

2.4 The RHF theory with nonlinear Lagrangian

We find the nuclear matter incompressibility stays very large as compared with the experimental data once we introduce the form-factor into the Fock term, because its contribution becomes small. To solve this problem, we would like to introduce the nonlinear terms of the σ and ω mesons following the idea of TM1 [23]. Therefore, we replace the Lagrangian (2.24)

for the σ and ω mesons by including the non-linear self-coupling terms

$$\frac{1}{2}m_\sigma^2\sigma^2 \longrightarrow \frac{1}{2}m_\sigma^2\sigma^2 + \frac{1}{3}g_2\sigma^3 + \frac{1}{4}g_3\sigma^4, \tag{2.64}$$

$$\frac{1}{2}m_\omega^2\omega^2 \longrightarrow \frac{1}{2}m_\omega^2\omega^2 + \frac{1}{4}c_3(\omega_\mu\omega^\mu)^2.$$

With these nonlinear terms, we can make similar HF calculations as formulated in Chapter 2.2 except for the use of modified meson masses for the σ and ω mesons in the meson propagators,

$$m_\sigma^{*2} = m_\sigma^2 + 2g_2\sigma + 3g_3\sigma^2, \tag{2.65}$$

$$m_\omega^{*2} = m_\omega^2 + 3c_3\omega^2.$$

There are now additionally three parameters, g_2, g_3 and c_3. For the present tentative study, we choose the values of the three parameters as those of the TM1 parameter set. It means $g_2 = -7.2325$ fm^{-1}, $g_3 = 0.6183$ and $c_3 = 71.3075$. By reproducing the saturation density and the binding energy, we obtain the parameter sets in Table 2.6. The incompressibility comes out to be about 320 MeV after including the nonlinear terms, and the effective nucleon mass becomes $M_N^* \sim 0.60M_N$ at the saturation density.

	Parameters					$\langle V_{Fock}\rangle/\rho_B$			
Case	g_σ	g_ω	κ	M_N^*/M_N	K (MeV)	σ	ω	π	ρ
VII	11.286	15.172	3.7	0.604	336	30.00	-16.76	12.31	0.541
VIII	11.143	14.680	6.6	0.621	324	29.36	-15.91	12.35	3.150
IX	11.798	18.850	6.1	0.615	387	26.28	-20.70	6.841	-5.444

Table 2.6: The parameter sets for the EOS of nuclear matter with the nonlinear terms of the σ and ω mesons. In cases VII and VIII, we include the form factor effect for all mesons. In case IX, we fix all the parameters, like the cut-off mass of the form factor and the tensor-vector ratio as the Bonn-A potential, except the σ and ω coupling constants [11]. The non-linear terms are included in the calculation where we use the non-linear coupling constants of σ and ω mesons as TM1 [23].

To discuss the ρ meson contribution further, we also calculate the nuclear EOS by fixing its coupling constant as the value in Bonn-A, where the pion and ρ coupling constants are $f_\pi^2/4\pi = 0.0805$, $g_\rho^2/4\pi = 0.99$ and $\kappa = f_\rho/g_\rho = 6.1$ as parameter set IX. Now, we show the contributions of each meson to the Fock energy changing as function of density, ρ, in Fig. 2.6. We find that the ρ meson contribution in the Fock term has increased largely from Table 2.6. The reason is that the vector coupling constant is larger than the previous choice. Finally, the total energy contribution of ρ meson becomes comparable to that of pion.
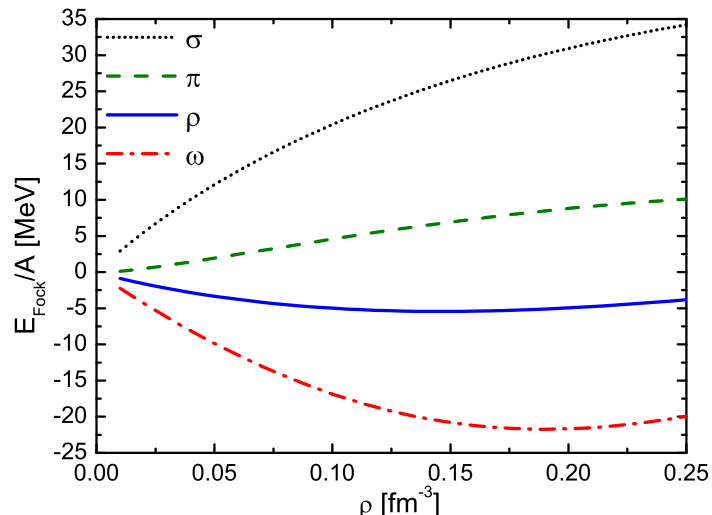
Figure 2.6: The contributions of the Fock energies from various mesons in parameter IX.

2.5   Conclusion

We firstly introduce the RMF model with TM1 Lagrangian. The properties of symmetric nuclear matter are given for TM1 parameter and compared with Walecka model. These properties satisfy the experiment data very well. However, the contribution of pion can not be taken into account in the mean field approximation. Then, we discussed the nuclear matter in RHF model, where pion will contribute to the total energy through the Fock terms.

Explicitly, we formulated the RHF model by taking first the mean field approximation and then use the fluctuation terms to calculate the Fock energies. We consider that the RHF Lagrangian is obtained by integrating out the effect of the tensor correlation and the short range correlation in the bare nucleon-nucleon interaction. Hence, the Lagrangian should reflect the properties of the nucleon-nucleon interaction. This consideration naturally makes us consider the meson-nucleon form factor, which is on the order of $\Lambda \sim 1.0$ GeV.

We have studied first the equation of state (EOS) of nuclear matter without the form factor. We have found large contributions from the ρ meson exchange interaction. Here, there is a problem of the contact term, which is to be or not to be removed in the Fock energy. We have then introduced the form factor in the Fock term on the order of $\Lambda \sim 1.0$ GeV. This introduction of the form factor has a large effect on meson contributions. Particularly, the effect of the ρ meson is largely reduced. Now the contribution of the Fock term due to the ρ meson is smaller than that of the pion. The form factor modifies the delta-function term of the Yukawa interaction within the range of the cut-off mass of the form factor. Hence, there is not a concept of the delta-function piece for the case with form factor.

Once we take into account the form factor, the incompressibility became too large. Hence, we have to additionally include the non-linear terms for a quantitative description of nuclear matter. We took the same nonlinear coupling constants as in the TM1 parameter set. At

last, we obtain the EOS with the incompressibility of about 300 MeV.

Chapter 3

Short range correlation in RHF model

3.1 Unitary Correlation Operator Method

As we showed in Chapter 1.2, there is a very strong repulsion at short distance for the realistic NN interaction. With this repulsion, we could not obtain the bound state of nuclear matter with this realistic NN interaction in the Hartree-Fock space. Therefore, one of the crucial issue in many-body calculation is how to deal with this short-range repulsive correlation. This is investigated with Jastrow correlation functions in the simplest case [12], which was developed as a variational chain summation (VCS) approach, based on hyper-netted chain-summation techniques in nuclear matter system in 1970's by Panharipande *et al.* [13]. However, it is not an unitary transformation for the wave-function in the Jastrow function method.

Recently, there is a very attractive method developed by Feldmeier *et al.* in terms of the unitary correlation operator method (UCOM) [61, 62]. The UCOM was demonstrated extremely efficient to provide binding energies and wave functions for light nuclei with the use of effective NN interaction with only the central interaction including the short range repulsive interaction [61]. The essence of UCOM is to introduce a unitary transformation,

$$\psi = U\phi. \tag{3.1}$$

Here, ψ indicates the full wave function, while ϕ indicates a uncorrelated trivial wave function. Hence, if we know the detailed U, we can obtain the exact wave function in terms of the trivial wave function. The unitary correlation operator U is written as

$$U = \exp\{-iC\}, \quad C = C^\dagger, \tag{3.2}$$

where C is the hermitian generator of the correlations. Hence, we can get a set of new equation of motion for nucleon as

$$\mathcal{H}\psi = E\psi, \tag{3.3}$$

$$U^{\dagger}\mathcal{H}U\psi = E\psi.$$

Furthermore, C should have to be a two-body operator or higher because a one-body operator would only cause a unitary transformation of the single particle states,

$$C = \sum_{i<j}^{A} c(i,j) + \text{three-body} + ... \tag{3.4}$$

However, we just make an approximation of UCOM up to two-body correlation terms [61]. This approximation is justified for the short-range correlation, because the probability that three-body nucleons enter their interaction ranges is small around the normal nuclear matter density. Now, we can use the two-body correlation operator $u(i,j)$ instead of U. For a Hamiltonian in nuclear matter, which consists of a one-body kinetic energy operator and a two-body potential,

$$\mathcal{H} = \sum_{i}^{A} T_i + \sum_{i<j}^{A} V(i,j), \tag{3.5}$$

after the UCOM correlation, it will be changed as

$$\begin{aligned} \widetilde{\mathcal{H}} &= u^{\dagger}(i,j)\mathcal{H}u(i,j) \\ &= \sum_{i}^{A} T_i + \sum_{i<j}^{A} \widetilde{V}(i,j), \end{aligned} \tag{3.6}$$

where the effective two-body interaction $\widetilde{V}(i,j)$ is generated from the short range correlation on two-body kinetic energy and bare interaction,

$$\widetilde{V}(i,j) = u^{\dagger}(i,j)Vu(i,j) + u^{\dagger}(i,j)(T_i + T_j)u(i,j) - (T_i + T_j). \tag{3.7}$$

This effective interaction provides the same effect as the G-matrix.

In actual calculation, the correlation operator is not convenient. This correlator, $u(i,j)$, can be expressed in terms of a coordinate transformation $R_+(r)$ for the radial distance,

$$R_+(r) = r + \alpha \left(\frac{r}{\beta}\right)^{\eta} \exp(-\exp(r/\beta)). \tag{3.8}$$

The parameter α determines the overall amount of the shift and β the length scale. η controls the steepness around $r = 0$. The double-exponential can ensure the correlator just has effect in the short distance. We give some useful transformations as following,

$$\begin{aligned} u^{\dagger}(i,j)ru(i,j) &= R_+(r) \\ u^{\dagger}(i,j)V(r)u(i,j) &= V(R_+(r)) \end{aligned} \tag{3.9}$$

$$u^\dagger(i,j)p_r u(i,j) \;\; = \;\; \frac{1}{\sqrt{R'_+(r)}}\frac{1}{r}p_r\frac{1}{\sqrt{R'_+(r)}},$$

where p_r is the radial momentum, $\langle\vec{r}|p_r|\phi\rangle = -i\frac{\partial}{\partial r}\langle\vec{r}|\phi\rangle$ All the other operators as $\vec{l}$ and $\vec{s}$ are unchanged.

3.2 Relativistic Hartree-Fock UCOM model

The knowledge of neutron-rich matter is very important for the study of compact stars as neutron stars and supernova. As the matter density increases after gravitational collapse of stars, the electron pressure increases due to its small mass and charge neutrality and eventually nuclear matter becomes highly neutron-rich through electron capture by protons. The formation of compact object as hot proton-neutron star and resulting cold neutron star depends completely on the property of neutron-rich matter. In this respect, it is most important to obtain the properties of neutron-rich matter reliably in nuclear physics for the description of exciting phenomena as supernova and neutron stars [63].

High density neutron-rich matter is far from the standard nuclear physics. Nuclei consist of finite number of neutrons and protons due to repulsive Coulomb interaction among protons. Even we will be fully equipped with radioactive beams, the neutron-proton ratios of neutron-rich nuclei are limited up to about 3 [64, 65, 66]. Although we are able to describe nuclei including unstable ones using some phenomenological models, we need large extrapolation to provide enough information on neutron-rich matter. In fact, phenomenological models as the relativistic mean field model are able to describe finite nuclei very nicely by fitting about 10 parameters, but these phenomenological models provide quite different equations of state (EOS) of neutron-rich matter [23]. Besides, the widely used EOS of the RMF model in nuclear astrophysics differs from those of the RBHF theory for pure neutron matter [67].

Hence, we should rely on nuclear many-body theory for the extraction of the properties of neutron-rich matter. In this sense, we are encouraged by the work of Brockmann and Machleidt on nuclear matter in the RBHF theory [11]. With the use of the coupling constants and the form factors of the one-boson exchange potential (OBEP) fixed by the nucleon-nucleon scattering data, the RBHF theory is able to provide good saturation properties of symmetric nuclear matter. In particular, the parameter set Bonn-A, which has the weakest tensor force among the parameter sets used there, reproduces the saturation properties very well [11]. As a microscopic theory, the RBHF theory excellently deals with the short range correlation and tensor interaction by solving the Bethe-Salpeter equation, which is the standard method of treating the many-body problem.

There are several problems, however, in the RBHF theory to go ahead for the application to astrophysics problems. One is a phenomenological aspect. The direct use of the RBHF

theory to finite nuclei is very difficult and its approximation in terms of the relativistic mean field (RMF) model with density dependent coupling constants provides good results for finite nuclei, but not satisfactory for describing the binding energies of various nuclei in the R-process nuclear synthesis [37]. Another one is a theoretical aspect, where the extraction of the G-matrix (effective interaction) for neutron-rich matter has some ambiguity on the treatment of highly excited intermediate states [11, 68]. Furthermore, the most severe limitation of the RBHF theory for the application to astrophysics is the necessity of solving the G-matrix consistently with nuclear ground states for many situations. Hence, it is desirable to develop a theoretical model to describe finite nuclei and at the same time to handle easily for astrophysical applications in a wide density and temperature regions [67].

There is a big hint on the possibility of using the Hartree-Fock model for this purpose. We are aware of the fact that the G-matrix takes care of high momentum components due to the short range correlation and the tensor interaction. There are several studies on the role of the tensor interaction, which is extremely important to provide large binding energy for symmetric nuclear matter and finite nuclei [69, 70, 71, 72, 73, 74]. The tensor interaction arises from the pion exchange interaction, which is strong in the triplet S channel ($S = 1$, $L = 0$ and $T = 0$) due to involvement of large momentum transfer and hence short distance between the interacting nucleons. For pure neutron matter, the triplet S channel is absent and hence we expect that the effect of the tensor interaction is weakened largely. In fact, it was shown by Kaiser *et al.* that the contribution of the pion exchange interaction is extremely small in pure neutron matter [69]. Hence, we are motivated to look into neutron-rich matter by just considering explicitly the short range correlation.

Hence, the purpose of this section is to apply the relativistic Hartree-Fock model with the UCOM (RHFU) to investigate properties of neutron-rich matter, which can deal with the realistic nucleon-nucleon interaction. To simplify the calculation, we assume that the UCOM operator U is independent on the spin, isospin and Dirac structure of wave function in the RHFU model.

The Lagrangian of Bonn potential can be written as [31],

$$
\begin{aligned}
\mathcal{L}_{\text{int}} \;=\;& \bar{\psi}\bigg[-g_\sigma\sigma - g_\delta\tau_a\delta^a - \frac{f_\eta}{m_\eta}\gamma_5\gamma_\mu\partial^\mu\eta - \frac{f_\pi}{m_\pi}\gamma_5\gamma_\mu\tau_a\partial^\mu\pi^a \\
&- g_\omega\gamma_\mu\omega^\mu + \frac{f_\omega}{2M}\sigma_{\mu\nu}\partial^\nu\omega^\mu - g_\rho\gamma_\mu\tau_a\rho^{a\mu} + \frac{f_\rho}{2M}\sigma_{\mu\nu}\partial^\nu\tau_a\rho^{a\mu}\bigg]\psi \\
&+ \frac{1}{2}\partial_\mu\sigma\partial^\mu\sigma - \frac{1}{2}m_\sigma^2\sigma^2 + \frac{1}{2}\partial_\mu\delta^a\partial^\mu\delta^a - \frac{1}{2}m_\delta^2\delta^{a2} \\
&+ \frac{1}{2}\partial_\mu\eta\partial^\mu\eta - \frac{1}{2}m_\eta^2\eta^2 + \frac{1}{2}\partial_\mu\pi^a\partial^\mu\pi^a - \frac{1}{2}m_\pi^2\pi^{a2} \\
&- \frac{1}{4}W_{\mu\nu}W^{\mu\nu} + \frac{1}{2}m_\omega^2\omega_\mu\omega^\mu - \frac{1}{4}R_{\mu\nu}^aR^{a\mu\nu} + \frac{1}{2}m_\rho^2\rho_\mu^a\rho^{a\mu},
\end{aligned}
\tag{3.10}
$$

where

$$W_{\mu\nu} = \partial_\mu \omega_\nu - \partial_\nu \omega_\mu \, , \tag{3.11}$$

$$R^a_{\mu\nu} = \partial_\mu \rho^a_\nu - \partial_\nu \rho^a_\mu \, .$$

ψ is the nucleon field and M the nucleon mass. Moreover, we use a monopole form factor,

$$F_\alpha(q^2) = \frac{\Lambda_\alpha^2 - m_\alpha^2}{\Lambda_\alpha^2 + q^2} \, , \tag{3.12}$$

for each meson-nucleon vertex denoted by α.

Once we include the form factor into the meson exchange potential, the contact terms in the meson exchange interaction become momentum dependent. Hence, all the meson exchange interactions in Bonn potential can be written in the form of Yukawa functions in coordinate space even after considering the form factor effect,

$$V(m, r) = \frac{e^{-mr}}{r}. \tag{3.13}$$

When the unitary correlation operator U is applied to the two-body NN interaction, we just take the following transformation in the potential $V(r)$ as,

$$c^\dagger(i,j)V(m,r)c(i,j) = V(m, R_+(r)). \tag{3.14}$$

On the other hand, the kinetic energy part after the transformation by UCOM operator is

$$c^\dagger(i,j)T(i,j) - T = \sum_{i<j} (\vec{\alpha}_i - \vec{\alpha}_j) \cdot \frac{\vec{r}}{r} \frac{1}{\sqrt{R'_+(r)}} \frac{1}{r} q_r \frac{r}{\sqrt{R'_+(r)}} \tag{3.15}$$

$$+ (\vec{\alpha}_i - \vec{\alpha}_j) \cdot \frac{\vec{r}}{r} \left(\frac{1}{R'_+(r)} - \frac{r}{R_+(r)} \right) q_r + \left(\frac{r}{R_+(r)} - 1 \right) (\vec{\alpha}_i - \vec{\alpha}_j) \cdot \vec{q}.$$

Here, $q_r = \vec{r} \cdot \vec{q}/r$ is defined as the radial momentum. The Dirac matrix $\vec{\alpha}_i$ is an operator on the Dirac spinor of i-th nucleon and the prime denotes differentiation with respect to the relative coordinate r. The detailed derivations about this equation are given in Appendix B.2.

We show the calculated result for the EOS of pure neutron matter in the RHFU model by using the Bonn-A potential in Fig. 3.1. The meson masses, meson-nucleon coupling constants and cut-off masses in the form factor are taken from Table VI of Ref. [11]. For the parameters of the UCOM, we take $\alpha = 0.8$ fm, $\beta = 0.6$ fm and $\eta = 0.37$ which are obtained from the parameters by fitting the properties of light nuclei [61]. We change β while keeping the behavior of the UCOM function at the origin so as to reproduce the EOS of neutron matter. We will come back to the UCOM function in the discussion of symmetric nuclear matter. The result of our model calculation is shown by the solid curve in Fig.3.1.
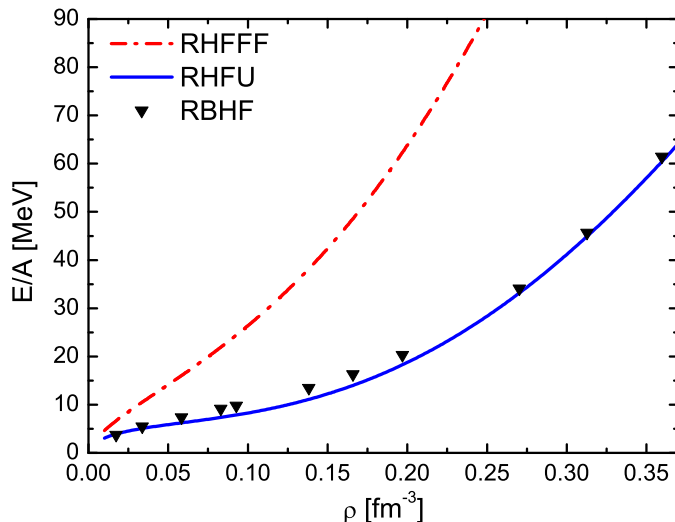
Figure 3.1: The EOS of pure neutron matter calculated with the Bonn-A potential. The solid curve is the result of the RHFU model, which is compared with the result of the RBHF theory shown by triangle dots [68]. The dot-dashed curve does not include the short range correlation.

We reproduce completely the result of the RBHF theory [68]. In order to see the effect of the short range correlation, we remove the UCOM transformation, and plot the EOS by the dot-dashed curve in Fig.3.1. The effect of the short range correlation is very large and increases with density.

We show various components of potential energies for pure neutron matter at $\rho = 0.15$ fm^{-3}, which is close to the saturation density of symmetric nuclear matter in Table 3.1. $E_{H,i}$ are the Hartree contributions from various mesons, while $E_{F,i}$ are those from the Fock contributions. We find that σ and ω mesons provide the main contributions to the total energy. The other components of meson exchange potentials for pion and ρ meson are very small. The pion contribution is larger than the ρ meson contribution.

i	σ	ω	π	ρ	δ	η
$E_{H,i}$ (MeV)	-109.2	75.3	0.0	3.1	-1.4	0.0
$E_{F,i}$ (MeV)	42.5	-26.8	4.7	-1.9	0.8	-0.6
$E_{HF,i}$ (MeV)	-66.7	48.5	4.7	1.2	-0.6	-0.6

Table 3.1: Various energy components of meson exchange potentials to the EOS of pure neutron matter at $\rho = 0.15$ fm^{-3}. The kinetic energy is 25.7 MeV and the total energy is 12.2 MeV.

The Dirac nucleon mass in nuclear matter is defined as $M_{D,i}^* = M_N + \Sigma_{S,i}$, where $\Sigma_{S,i}$ is the scalar components of nucleon self-energy for protons and neutrons. There are striking

differences found in the literatures between the Dirac proton and neutron masses due to their calculation methods in the relativistic Brueckner-Hartree-Fock theory. In Ref. [11], the neutron Dirac mass is larger than the proton mass, while the situation is completely opposite in the RBHF calculation by Dalen *et al.* who used the projection techniques [68]. In our RHFU model, the proton and neutron Dirac masses are $M_{D,p}^*$=703 MeV and $M_{D,n}^*$=612 MeV respectively at $\rho = 0.15$ fm^{-3}. These values are close to the results of Dalen *et al.* [68], where $M_{D,p}^*$=724 MeV and $M_{D,n}^*$=606 MeV.
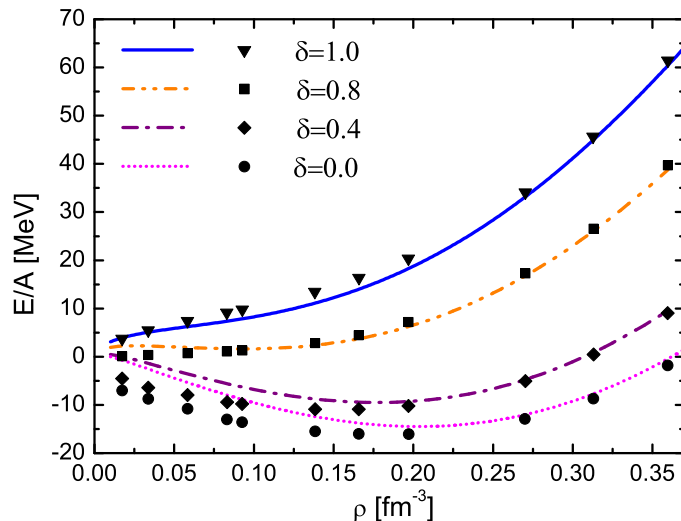
Figure 3.2: The EOS's of asymmetric nuclear matter with the Bonn-A potential for various proton-to-neutron ratios δ, where $\delta = (\rho_n - \rho_p)/(\rho_n + \rho_p)$. The continuous curves are the results of the RHFU model for various δ. The corresponding results of the RBHF theory are shown by various symbols, which are taken from Ref. [68].

The successful result for pure neutron matter encourages us to consider the EOS's of other ratios of neutrons and protons in asymmetric nuclear matter. Therefore, we plot the EOS's of asymmetric nuclear matter for various values of the asymmetry parameter $\delta = (\rho_n - \rho_p)/(\rho_n + \rho_p)$ with Bonn-A potential in Fig. 3.2. Here, $\delta = 1$ corresponds to pure neutron matter and $\delta = 0$ corresponds to symmetric nuclear matter. The results for neutron-rich matter are satisfactory until $\delta = 0.8$. We start to see small deviation of the RHFU results from the RBHF ones in the low density region. As the δ decreases further the deviation of the two results becomes significant. For the symmetric nuclear matter $\delta = 0$, we are not able to reproduce the RBHF results in the low density regions $\rho \leq 0.2$ fm^{-3}. We have expected large deviation of the RHFU results from those of the RBHF theory for $\delta = 0$. In this case, the binding energy per nucleon is -14.48 MeV at saturation Fermi momentum, $k_F = 1.44$ fm^{-1} and the symmetry energy is 33.56 MeV. The incompressibility K is about 400 MeV which means the EOS in the RHFU model is stiffer than the one of the RBHF theory. Now, we discuss here the properties of the UCOM parameters. As mentioned in the introduction, the tensor interaction has a significant role on symmetric nuclear matter

by providing a large attraction, which is large at the low density and decreases with density due to the Pauli blocking effect. With the choice of the UCOM parameters to reproduce the EOS of pure neutron matter, we find the RHFU model provides the EOS deviating to the under binding direction. If we use a larger β, the EOS will be more bound than that of the RBHF theory in the high density region.
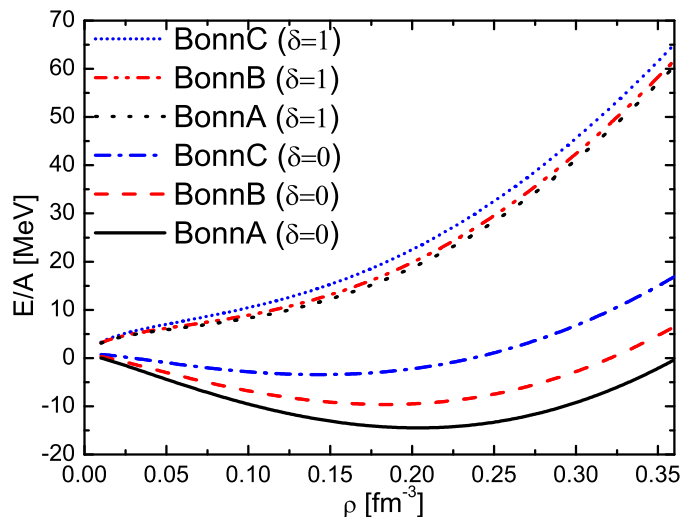
Figure 3.3: The EOS of symmetric nuclear matter and pure neutron matter with the NN interaction of Bonn-A, Bonn-B and Bonn-C.

We discuss the EOS for different potentials now. Here, we take the three potentials of the Bonn group, Bonn-A, Bonn-B and Bonn-C, where the large difference among these three potentials lies on the strength of the tensor interaction. The Bonn-A has the weakest tensor strength [11]. We show the results of the EOS's of pure neutron and symmetric nuclear matter in Fig. 3. The EOS's of the three cases almost agree each other for pure neutron matter. Again, this fact indicates that the tensor interaction does not contribute much for pure neutron matter. Actually, this situation also has been proved in Fig.1 of Ref. [75] with RBHF theory. On the other hand, the EOS's of symmetric nuclear matter differ with each other to a large extent. For the case of Bonn A potential, the resulting EOS is not so bad, but other cases are quite different from the RBHF results and the saturation properties. In this case, the tensor interaction plays an important role to provide a large binding effect as demonstrated by Kaiser *et al.* [69].

It is very important to find that the RHF model with the UCOM is able to reproduce the EOS's of neutron-rich matter of the sophisticate RBHF theory by using the bare nucleon-nucleon interaction. It is then straightforward to calculate EOS's in various situations at finite temperature and higher densities within the RHFU model for neutron-rich matter. We are also able to calculate the neutrino reaction rates in neutron-rich matter, which are necessary for formation of hot neutron star in the course of supernova explosion. In the region where experimental data are available for smaller asymmetry parameter $\delta < 0.5$, we

may introduce several parameters for the coupling constants of the Lagrangian in the RHFU model to be fixed by experimental data.

3.3 Non-relativistic Hartree-Fock UCOM model

We have discussed the properties of neutron-rich matter in the framework of relativistic Hartree-Fock model with UCOM (RHFU) by using the realistic NN interaction, Bonn potential in section 3.2. We found that the EOS in our calculation can completely reproduce the one of pure neutron matter in RBHF model with Bonn-A potential. This achievement drives us to consider whether we can also obtain the similar results as the variational method in a simpler theory like the Hartree-Fock UCOM model.

It is necessary to introduce the three-body interaction to provide enough repulsive contribution in the high density region in the framework of a non-relativistic microscopic calculation. Li *et al.* obtained reasonable saturation properties of symmetric nuclear matter by including the microscopic meson-exchange three-body interaction in Brueckner-Hartree-Fock approach [77]. However, Akmal used a phenomenological three-body interaction, Urbana model IX (UIX) to improve the EOS of nuclear matter, especially in high density region [14]. Therefore, it is very interesting to study the effect of a three-body interaction in the Hartree-Fock framework for neutron matter.

Furthermore, the realistic NN potential is obtained from the center of mass framework where the total momentum $\mathbf{P}_{ij}$ is zero. To take the effect of non-zero $\mathbf{P}_{ij}$ into account, the relativistic boost correction was applied in the variational method with the AV18 potential. However, Forest *et al.* [76] pointed out that the meson-exchange potential has contained the relativistic boost correction. Hence, we will discuss the properties of nuclear matter with the Bonn potential, which is constructed by using the meson exchange model without introducing the relativistic boost correction term.

Hence, we would like to develop the Hartree-Fock theory with UCOM and three-body interaction (HFUT), which can deal with a bare NN interaction, to investigate the properties of neutron matter. We want to find a simpler way to discuss neutron matter in the many-body framework.

Firstly, we would like to estimate the contributions of the tensor interaction both for neutron matter and symmetric nuclear matter in the perturbation theory with non-relativistic pion interaction. In the one-boson-exchange model of the NN interaction, the tensor contribution mainly comes from the one-pion exchange potential (OPEP). For the pseudo-vector coupling between pion and nucleon, the OPEP in momentum space is given by

$$V_\pi(\mathbf{q}) = -\frac{f_{\pi NN}^2}{m_\pi^2} \frac{\boldsymbol{\sigma}_1 \cdot \mathbf{q}\boldsymbol{\sigma}_2 \cdot \mathbf{q}}{q^2 + m_\pi^2}\boldsymbol{\tau}_1 \cdot \boldsymbol{\tau}_2 \ , \tag{3.16}$$

where $f_{\pi NN}$ is the pion-nucleon coupling constant and $\mathbf{q}$ is the exchanged momentum between

two nucleons. The operators, $\boldsymbol{\sigma}$ and $\boldsymbol{\tau}$, represent the spin and isospin operators, respectively. This interaction can be separated into the spin-spin central and tensor parts

$$V_\pi(\mathbf{q}) = -\frac{1}{3}\frac{f_{\pi NN}^2}{m_\pi^2}\left(\frac{\boldsymbol{\sigma}_1 \cdot \boldsymbol{\sigma}_2 q^2}{q^2 + m_\pi^2} + \frac{S_{12}(\hat{\mathbf{q}})q^2}{q^2 + m_\pi^2}\right)\boldsymbol{\tau}_1 \cdot \boldsymbol{\tau}_2 \ . \tag{3.17}$$

Here, $S_{12}(\hat{\mathbf{q}})$ is the tensor operator

$$S_{12}(\hat{\mathbf{q}}) = 3\boldsymbol{\sigma}_1 \cdot \hat{\mathbf{q}}\boldsymbol{\sigma}_2 \cdot \hat{\mathbf{q}} - \boldsymbol{\sigma}_1 \cdot \boldsymbol{\sigma}_2 \ . \tag{3.18}$$

As we know, the expectation value of the tensor operator is zero at the Hartree-Fock level for a spin-saturated system. We should discuss the tensor effect of pion in the higher-order terms of the perturbation theory. They are called as the iterated one-pion-exchange Hartree and Fock terms in Ref. [69], which can be expressed in the following Feynman diagrams.
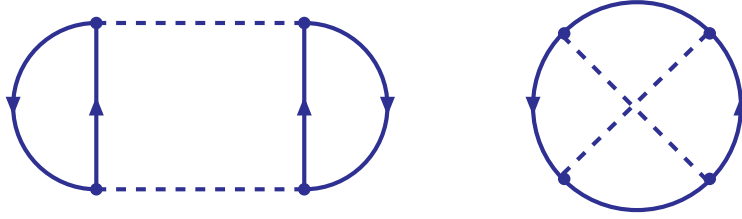
Figure 3.4: The iterated one-pion-exchange Hartree and Fock diagrams. The left-hand figure is the Hartree diagram and the right hand one is the Fock diagram.

To evaluate the energy contribution from the iterated one-pion-exchange term, we would like to write the matrix elements of OPEP as,

$$\begin{aligned}V_{\mathbf{k}_1,\mathbf{k}_2,\mathbf{k}_1',\mathbf{k}_2'}^\pi &= \frac{1}{(2\pi)^3}\delta^{(3)}(\mathbf{k}_1 + \mathbf{k}_2 - \mathbf{k}_1' - \mathbf{k}_2')V_\pi(\mathbf{q}) \\ &= -\frac{1}{3(2\pi)^3}\frac{f_{\pi NN}^2}{m_\pi^2}\delta^{(3)}(\mathbf{k}_1 + \mathbf{k}_2 - \mathbf{k}_1' - \mathbf{k}_2')[C\boldsymbol{\sigma}_1 \cdot \boldsymbol{\sigma}_2 + TS_{12}(\hat{\mathbf{q}})]\boldsymbol{\tau}_1 \cdot \boldsymbol{\tau}_2 \ ,\end{aligned} \tag{3.19}$$

where $\mathbf{q} = \mathbf{k}_1' - \mathbf{k}_1 = \mathbf{k}_2 - \mathbf{k}_2'$ and

$$C = T = \frac{q^2}{q^2 + m_\pi^2} \ . \tag{3.20}$$

Therefore, the energy per particle arising from the Hartree contribution of iterated one-pion-exchange is,

$$E_H^{[2]} = \frac{1}{2\rho V}\int_\Gamma d^3\mathbf{k}_1 d^3\mathbf{k}_2 d^3\mathbf{k}_1' d^3\mathbf{k}_2'\frac{\sum_{\text{spin, isospin}}|V_{\mathbf{k}_1,\mathbf{k}_2,\mathbf{k}_1',\mathbf{k}_2'}^\pi|^2}{\varepsilon_{\mathbf{k}_1} + \varepsilon_{\mathbf{k}_2} - \varepsilon_{\mathbf{k}_1'} - \varepsilon_{\mathbf{k}_2'}} \ , \tag{3.21}$$

where ρ is the baryon density and V the volume of nuclear matter. The single particle energies $\varepsilon_{\mathbf{k}}$ occurring in the energy denominator are simple kinetic energies $k^2/2M$. M is the

nucleon mass, while the integration region Γ is limited by the Pauli principle, $|\mathbf{k}_1|, |\mathbf{k}_2| < k_F$ and $|\mathbf{k}'_1|, |\mathbf{k}'_2| > k_F$, which means that two states are above the Fermi surface and the other two states are below the Fermi surface. After taking the summation of spin and isospin operators with plane wave functions in Eq. (3.21), the energy $E_H^{[2]}$ can be rewritten as,

$$E_H^{[2]} = \frac{4MT_H f_{\pi NN}^4}{3(2\pi)^8 m_\pi^4 \rho} \int_0^\infty (C^2 + 2T^2) I_H(q) q^2 dq \ . \tag{3.22}$$

Here, T_H is the result of summation of the isospin operator. Its value depends on the isospin channel:

$$T_H = \begin{cases} 12 & \text{for symmetric nuclear matter,} \\ 1 & \text{for pure neutron matter} \end{cases} \tag{3.23}$$

and $I_H(q)$ is the integration related with the Pauli principle,

$$I_H(q) = \int_\Gamma \frac{d^3\mathbf{k}_1 d^3\mathbf{k}_2}{\mathbf{q} \cdot (\mathbf{q} + \mathbf{k}_1 - \mathbf{k}_2)} \ , \tag{3.24}$$

where the region of integration Γ is given by

$$\Gamma = \begin{cases} |\mathbf{k}_i \pm \mathbf{q}| > k_F \\ |\mathbf{k}_i| < k_F \end{cases} \quad i = 1, 2 \ , \tag{3.25}$$

where k_F is the Fermi momentum. The integration about $I_H(q)$ can be expressed in the analytical form,

$$I_H(q) = \begin{cases} \dfrac{\pi^2 k_F^4}{x} \left[\dfrac{(58 - 80\ln 2)x^2}{15} - \dfrac{2x^4}{5} + \dfrac{8}{15}\ln\left(1 - x^2\right) \right. \\ \left. + \left(x - \dfrac{2x^3}{3} + \dfrac{x^5}{5}\right)\ln\left(\dfrac{1+x}{1-x}\right) \right], \quad \text{if} \quad x \le 1, \\[3mm] \dfrac{\pi^2 k_F^4}{x} \left[\dfrac{44x}{15} + \dfrac{8x^3}{15} + \left(-\dfrac{8x^3}{3} + \dfrac{8x^5}{15}\right)\ln\left(1 - \dfrac{1}{x^2}\right) \right. \\ \left. + \left(\dfrac{8}{15} - \dfrac{8x^2}{3}\right)\ln\left(\dfrac{x+1}{x-1}\right) \right] \quad \text{if} \quad x > 1 \ . \end{cases}$$

Here we have defined $x = q/2k_F$.

The energy per particle in Eq. (3.22) is divergent when the integral upper limit q is taken to the infinite. Therefore it is necessary to introduce a form factor for the OPEP to regularize this integration. We choose a monopole form factor for the vertex between the pion and nucleon,

$$F_\pi(q) = \frac{\Lambda^2 - m_\pi^2}{\Lambda^2 + q^2} \ , \tag{3.26}$$

where Λ is the cut off momentum. From Eq. (3.22), we find that in nuclear matter for the Hartree diagram of iterated one-pion-exchange term, the tensor contribution of pion (related with T) is twice of spin-spin central force (related with C). Furthermore, the tensor effect is much smaller in neutron matter than in symmetric nuclear matter due to the isospin factor.

In a similar way, we can discuss the Fock energy contribution per particle from the diagram at the right in Fig. 3.4. It is written as,

$$E_F^{[2]} = \frac{1}{2\rho V} \int_\Gamma d^3\mathbf{k}_1 d^3\mathbf{k}_2 d^3\mathbf{k}_1' d^3\mathbf{k}_2' \frac{\sum_{\text{spin, isospin}} V_{\mathbf{k}_1,\mathbf{k}_2,\mathbf{k}_1',\mathbf{k}_2'}^\pi V_{\mathbf{k}_2',\mathbf{k}_1',\mathbf{k}_1,\mathbf{k}_2}^\pi}{\varepsilon_{\mathbf{k}_1} + \varepsilon_{\mathbf{k}_2} - \varepsilon_{\mathbf{k}_1'} - \varepsilon_{\mathbf{k}_2'}} \ , \tag{3.27}$$

where the exchange momentum for $V_{\mathbf{k}_2',\mathbf{k}_1',\mathbf{k}_1,\mathbf{k}_2}^\pi$, is changed as $\mathbf{q}' = \mathbf{q} + \mathbf{k}_1' - \mathbf{k}_2'$. After taking the spin and isospin sum in Eq. (3.27) and using the momentum conservation in intermediate states, we obtain

$$E_F^{[2]} = \frac{MT_F f_{\pi NN}^4}{2(2\pi)^9 m_\pi^4 \rho} \int d^3\mathbf{q} \int_\Gamma \frac{d^3\mathbf{k}_1 d^3\mathbf{k}_2}{\mathbf{q} \cdot (\mathbf{q} + \mathbf{k}_1 - \mathbf{k}_2)} \left[4TT'(\hat{\mathbf{q}} \cdot \hat{\mathbf{q}}')^2 - \frac{2}{3}(CC' + 2TT') \right] . \tag{3.28}$$

Here, C', T' have the same expressions as C, T but with $\mathbf{q}$ replaced by $\mathbf{q}' = \mathbf{q} + \mathbf{k}_1 - \mathbf{k}_2$ and the isospin factor T_F is,

$$T_F = \begin{cases} -6 & \text{for symmetric nuclear matter,} \\ 1 & \text{for pure neutron matter.} \end{cases} \tag{3.29}$$

$\hat{\mathbf{q}} \cdot \hat{\mathbf{q}}'$ represents the cosine of the angle between $\mathbf{q}$ and $\mathbf{q}'$. The second integration of the Fock term over the region Γ in Eq. (3.28) can not be written in an analytical form like the Hartree term anymore in the case with the Pauli principle on the exchanged momentum $\mathbf{q}'$. Hence, we obtained it by numerical calculation in the cylindrical coordinates which reduces to a 6-dimensional integration over the radius, height and angles. We reproduce the results of the analytical expression for the case of an abrupt momentum cutoff [69] with the above method. Now the relation between the tensor contribution and the spin-spin central contribution is not so obvious. We can only discuss them based on the numerical results.

We show the total tensor contributions from the iterated one-pion-exchange Hartree and Fock diagrams for neutron matter and symmetric nuclear matter in Fig. 3.5. The pion coupling constant is fixed as $f_{\pi NN}^2/4\pi = 0.08$ and $\Lambda = 1000$ MeV in the form factor of the pion-nucleon vertex. We find that the tensor contribution in neutron matter is much smaller than the one in symmetric nuclear matter. There are two reasons which cause this large difference. The first one is the isospin factor T_H, which for neutron matter is $1/12$ of symmetric nuclear matter value for Hartree diagram. The second one is that the tensor contribution to Fock term is repulsive which is opposite to the Hartree term in neutron matter, while this contribution to Hartree and Fock term are both attractive in symmetric nuclear matter. Therefore, we may drop the tensor effect in the discussion of neutron matter and treat the many body system in a simple framework as the Hartree-Fock theory.
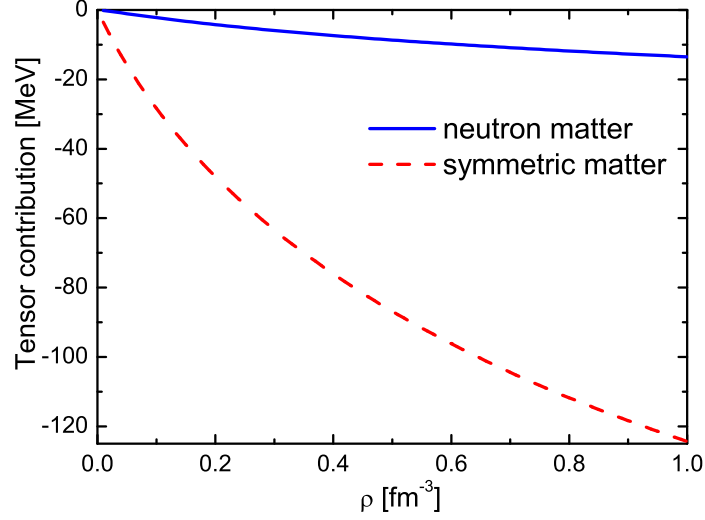
Figure 3.5: The tensor contribution of iterated one-pion-exchange terms. The solid curve denotes the tensor contribution for neutron matter, while the dashed curve denotes the one for symmetric nuclear matter. We take $\Lambda = 1000$ MeV in the form factor.

Next, we construct the Hartree-Fock theory in the unitary correlation operator method (UCOM) with the non-relativistic framework. We still adopt the Lagrangian of Bonn potential, Eq.3.10. The correlation in the potential part is similar to that in RHFU model.

However, the short range correlation does not have a simple form for the kinetic energy part in non-relativistic framework. Because the unitary operator $u(i,j)$ has an effect for the relative momentum, we need to separate the kinetic energy of two particles into relative and center of mass energy,

$$T_i + T_j = \frac{\mathbf{q}^2}{M} + \frac{(\mathbf{p}_i + \mathbf{p}_j)^2}{4M} \ . \tag{3.30}$$

The UCOM operator just correlates the part which is related with the relative momentum, $\mathbf{q} = (\mathbf{p}_i - \mathbf{p}_j)/2$. More details can be found in section 2 of Ref. [61]. Here, we directly give the kinetic energy operator modified by the correlation operator:

$$
\begin{aligned}
T^{[2]} &= u^\dagger(i,j)(T_i + T_j)u(i,j) - (T_i + T_j) \tag{3.31} \\
&= q_r^\dagger \frac{1}{M}\left[\frac{1}{R_+'^2}(r) - 1\right]q_r + \frac{1}{M}\left[\frac{1}{R_+^2(r)} - \frac{1}{r^2}\right]\mathbf{L}^2 + w(r) \ ,
\end{aligned}
$$

where q_r is the radial component of relative momentum, $q_r = \frac{1}{r}\mathbf{r}\cdot\mathbf{q}$, $\mathbf{L} = \mathbf{r}\times\mathbf{q}$ the angular momentum and $r = |\mathbf{r}_1 - \mathbf{r}_2|$ the relative distance. The function $w(r)$ comes from the commutation between the momentum operator and $R_+(r)$,

$$w(r) = \frac{1}{MR_+'^2(r)}\left(2\frac{R_+''(r)}{rR_+'(r)} - \frac{5}{4}\left(\frac{R_+''(r)}{R_+'(r)}\right)^2 + \frac{1}{2}\frac{R_+'''(r)}{R_+'(r)}\right) \ . \tag{3.32}$$

Now, we can obtain the ground-state energy per particle in Hartree-Fock approximation with UCOM correlation,

$$\frac{\mathcal{E}_{HFU}}{A} = \frac{3}{10}\frac{k_F^2}{M} + \frac{1}{A}\sum_{i<j}^{A}\langle ij|\widetilde{V}_{ij}|ij\rangle_A. \tag{3.33}$$

Here, $\langle ij|\widetilde{V}_{ij}|ij\rangle_A$ means the anti-symmetrized two-body matrix element of operator $\widetilde{V}_{ij}$ taken with the single particle plane wave functions,

$$|i\rangle = \frac{1}{\sqrt{V}}\exp(i\mathbf{k}_i \cdot \mathbf{r}) \otimes |\chi_s\rangle \otimes |\chi_t\rangle, \tag{3.34}$$

where $|\chi_s\rangle$ and $|\chi_t\rangle$ represent the eigenstates of spin and isospin.

As defined in Eq. (3.8), there are three parameters, α, β and η, when we consider the short range correlation of realistic NN interaction. We determine them by minimizing the energy per particle of whole system with variational principle,

$$\frac{\partial^3(\mathcal{E}_{HFU}/A)}{\partial\alpha\partial\beta\partial\eta} = 0. \tag{3.35}$$

In this way, we have constructed the non-relativistic Hartree-Fock model with UCOM (HFU), where we do not have any free parameters.

The three-body interaction is very important to provide the saturation properties in a microscopic calculation in the non-relativistic framework [14, 77]. We shall introduce the Urbana three nucleon interaction (TNI) [78], which contains two terms: the two-pion exchange part $V_{ijk}^{2\pi}$ from the Fujita-Miyazawa model [79], and the repulsive part V_{ijk}^{R} due to the relativistic effect,

$$V_{ijk} = V_{ijk}^{2\pi} + V_{ijk}^{R} . \tag{3.36}$$

Now, the Hamiltonian of the whole system is given by,

$$\mathcal{H} = \sum_{i=1}^{A} T_i + \sum_{i<j}^{A} V_{ij} + \sum_{i<j<k}^{A} V_{ijk}^{2\pi} + \sum_{i<j<k}^{A} V_{ijk}^{R} . \tag{3.37}$$

The three nucleon interaction part can be written explicitly as,

$$V_{ijk}^{2\pi} = A_{2\pi} \sum_{cyclic} \left[\{\mathbf{X}_{ij}, \mathbf{X}_{ik}\}\{\boldsymbol{\tau}_i \cdot \boldsymbol{\tau}_j, \boldsymbol{\tau}_i \cdot \boldsymbol{\tau}_k\} + \frac{1}{4}[\mathbf{X}_{ij}, \mathbf{X}_{ik}][\boldsymbol{\tau}_i \cdot \boldsymbol{\tau}_j, \boldsymbol{\tau}_i \cdot \boldsymbol{\tau}_k] \right], \tag{3.38}$$

$$V_{ijk}^{R} = A_R \sum_{cyclic} [T(r_{ij})]^2[T(r_{ik})]^2$$

with

$$\mathbf{X}_{ij} = Y(r_{ij})\boldsymbol{\sigma}_i \cdot \boldsymbol{\sigma}_j + T(r_{ij})S_{ij} . \tag{3.39}$$

Here, $\{,\}$ and $[,]$ denote the anti-commutator and commutator, respectively. The functions $Y(r)$ and $T(r)$ are radial functions related with the Yukawa and tensor part of the one-pion exchange interaction including a form factor,

$$Y(r) = \frac{e^{-m_\pi r}}{m_\pi r}[1 - \exp(-br^2)] , \tag{3.40}$$

$$T(r) = \left(1 + \frac{3}{m_\pi r} + \frac{3}{m_\pi^2 r^2}\right) \frac{e^{-m_\pi r}}{m_\pi r}[1 - \exp(-br^2)]^2 , $$

where $b = 2.0$ fm^{-2}.

Now, the correlated potential after short range correlation is written as,

$$\widetilde{V} = C^\dagger V_{ij} C + C^\dagger V_{ijk} C + C^\dagger (T_i + T_j) C - (T_i + T_j) . \tag{3.41}$$

For the three-body interaction, we take the two-body correlation in UCOM part. The Urbana TNI V_{ijk} can be separated as the product of two two-body interactions, $V_{ij}^{[3]}$ and $V_{ik}^{[3]}$. Therefore, the short range correlation on the TNI yields,

$$\widetilde{V}_{ijk} = C^\dagger V_{ijk} C = C^\dagger V_{ij}^{[3]} C C^\dagger V_{ik}^{[3]} C = \widetilde{V}_{ij}^{[3]} \widetilde{V}_{ik}^{[3]} , \tag{3.42}$$

where, we have used the unitary property of the short range operator C.

Finally, the energy per particle in the HFU model with three-body interaction is obtained:

$$\frac{\mathcal{E}_{HFUT}}{A} = \frac{3}{10} \frac{k_F^2}{M} + \frac{1}{A} \sum_{i<j}^{A} \langle ij|\widetilde{V}_{ij}|ij\rangle_A + \frac{1}{A} \sum_{i<j<k}^{A} \langle ijk|\widetilde{V}_{ijk}|ijk\rangle_A . \tag{3.43}$$

Because there is a cyclic symmetry in the interaction of $V_{ijk}^{2\pi}$ and V_{ijk}^R, the expectation value of the three-body interaction in Eq. (3.43) can be simplified,

$$\sum_{i<j<k}^{A} \langle ijk|\widetilde{V}_{ijk}|ijk\rangle_A = \sum_{i,j,k}^{A} \left[\frac{1}{6}\langle ijk|\widetilde{V}_{ijk}|ijk\rangle - \frac{1}{2}\langle ijk|\widetilde{V}_{ijk}|ikj\rangle + \frac{1}{3}\langle ijk|\widetilde{V}_{ijk}|kij\rangle\right] . \tag{3.44}$$

More detailed expression for the energy contribution of the Urbana TNI in nuclear matter with plane wave function is described in detail in Ref. [80]. The only difference with this work appears in the treatment of the short range correlation on the three-body interaction.

The tensor effect is very small in neutron matter. It should be a good approximation to consider only the short range correlation. We adopt the Bonn-A potential as a realistic NN interaction which is constructed by exchanging six non-strange mesons with masses below 1 GeV. The meson masses, meson-nucleon coupling constants and cut-off masses in the form factor are taken from Table VI of Ref. [11]. We plot the EOS of pure neutron matter from the HFU model in Fig. 3.6. We find that it compares very well with the calculation of the variational method with the AV18 potential including the relativistic boost correction (δv) [14]. This success is based on the following two points. The first one is that the

UCOM takes the reasonable short range correlation into account for the Bonn-A potential and the contribution of the tensor interaction can be neglected for neutron matter. The other one is that the HFU model with the Bonn potential includes the relativistic boost effect automatically. Actually, we have the similar framework to the relativistic mean field approximation in the HFU model except for the kinetic energy part. Forest *et al.* have proved that the boost corrections for the meson-exchange potential, obtained from the relativistic mean field model are in agreement with the results of δv [76]. The relativistic boost correction coming from the NN interaction is described in the framework where the total momentum $\mathbf{P}_{ij} = \mathbf{p}_i + \mathbf{p}_j$ is zero. However, there is no such constraint when we calculate the energy in the framework of the relativistic mean field approximation. Furthermore, the meson-exchange potentials contain the Dirac spinors which take care of the relativistic effect.
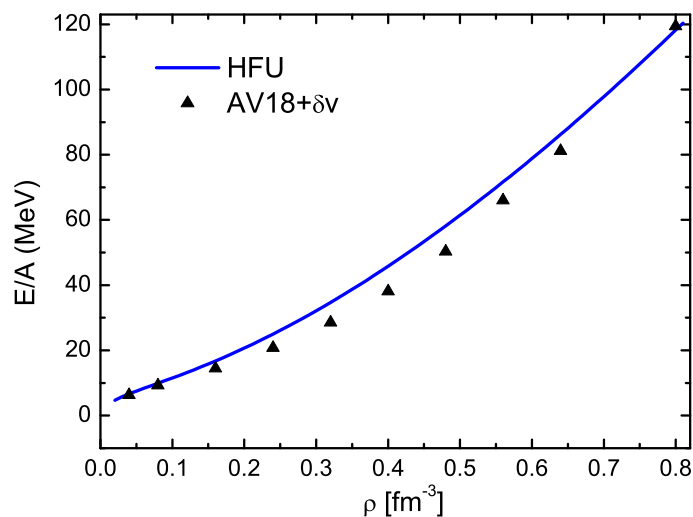
Figure 3.6: The EOS of neutron matter with the HFU model as a function of density. The solid curve is the result of the HFU model with the Bonn-A potential. The triangles are the EOS from the variational method with the AV18 potential.

Although we reproduce the results of the variational calculation for neutron matter with the two-body realistic NN interaction, Bonn Potential, this EOS is still too soft in the high density region. An additional repulsive contribution should be introduced. It can be obtained from the Z graph of the σ meson exchange through nucleon-antinucleon excitation in the RBHF theory. However, we would like to adopt a phenomenological three-body interaction, Urbana three-nucleon interaction (TNI), following the variational method. The EOS of pure neutron matter in the HFU model with a three-body interaction (HFUT) is given in the (a) panel of Fig. 3.7. The strengths of the Urbana TNI, $A_{2\pi}$ and A_R, are chosen as the same values as the UIX* in Ref. [14], which have values $A_{2\pi} = -0.0293$ MeV and $A_R = 0.63 \times 0.048$ MeV.

In beginning of this section, we have shown that the tensor contribution and even the
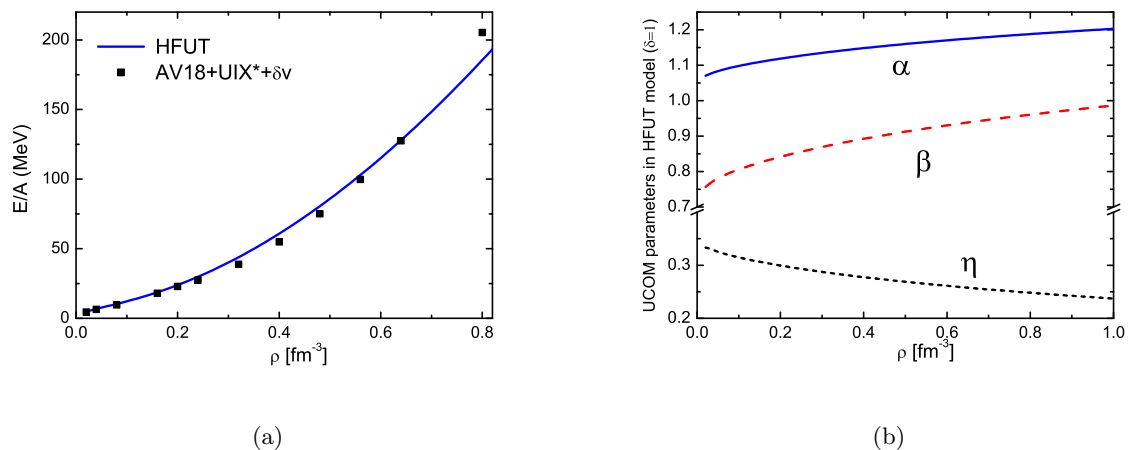
(a)   (b)

Figure 3.7: The EOS of neutron matter with the HFUT model and the UCOM parameters. In panel (a), the solid curve is the results of the HFUT model. The square points are the EOS in the variational method with the AV18 potential and three-body interaction. In panel (b), the UCOM parameters are shown with the HFUT model for neutron matter.

central spin-spin interaction of the pion in neutron matter are both suppressed by the isospin factor. For the 2π exchange part of the Urbana three-body interaction, a similar suppression effect of the pion matrix elements is present. Its effect can be neglected compared with the contribution from the repulsive term. Therefore, for consistency with the two-body interaction, we also drop the 2π term of the three-body interaction. The solid curve in the (a) panel of Fig. 3.7 represents the EOS of neutron matter in the HFUT model without the term $V_{ijk}^{2\pi}$, which is 20 times smaller than that of the repulsive three-body interaction in the present calculation. We find that our results almost reproduce those of the variational method with the AV18 potential and the Urbana three-body interaction [14].

In the (b) panel of Fig. 3.7, we show the UCOM parameters, α, β and η, as a function of density in the HFUT model for neutron matter. These parameters are obtained by minimizing the ground state energy with variational principle. The minimization of the binding energy is obtained by the competition between the short range correlation on the kinetic energy and the potential energy. The short range correlation effect on the kinetic energy is repulsive, while it is attractive for the NN interaction energy. Finally, they cancel each other and minimize the binding energy. In the high density region, these parameters change gradually with the density and are not stabilized. This is because the three-body interaction is influenced largely by the short range correlation. In the high density region, the repulsive contribution of the three-body interaction, for which the UCOM plays a very important role, becomes large.

Although we know that the present model should not work for symmetric nuclear matter, we would like to see how far the properties of nuclear matter differ from the full model. In

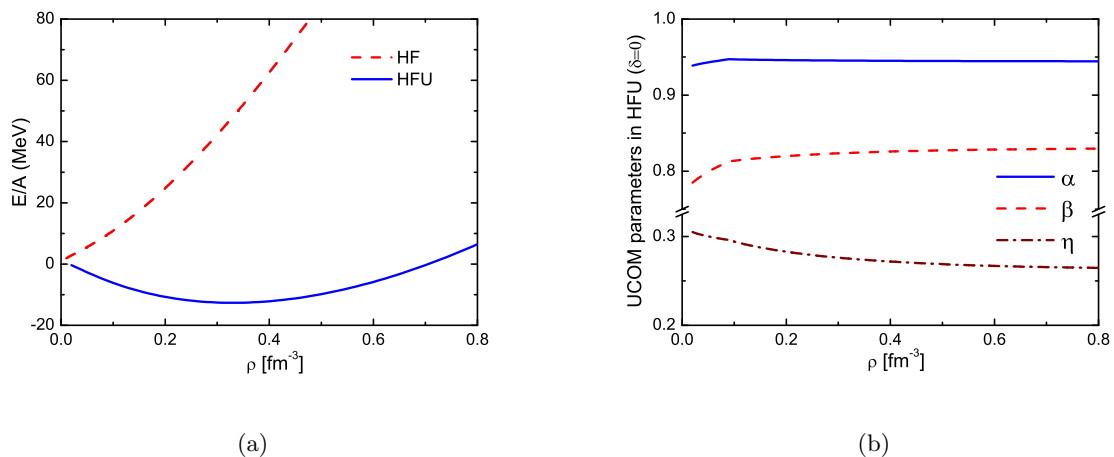(a)   (b)

Figure 3.8: The EOS of nuclear matter with the HFU model and the UCOM parameters for symmetric nuclear matter. In panel (a), the dashed curve is the EOS of symmetric nuclear matter without the short range correlation in the Hartree-Fock approximation, while the solid curve is the result of the HFU model. Shown in panel (b) are the UCOM parameters as functions of density.

Fig. 3.8, we show the EOS of symmetric nuclear matter with the Bonn-A potential for HFU model. In the (a) panel, we compare the results of symmetric nuclear matter with and without the short range correlation in the Hartree-Fock theory. The realistic NN interaction cannot bind the system of symmetric nuclear matter due to the strong repulsive effect at short distance. The UCOM effect can largely cut down the repulsive effect at short distance and make the symmetric nuclear matter bound. This correlation effect becomes larger with the density. However, the saturation properties of symmetric nuclear matter in the HFU model, $E/A = -12.66$ MeV and $\rho_0 = 0.33$ fm^{-3}, are far from the empirical values. This is caused by the omission of the tensor effect in the Hartree-Fock model, which is very important as shown in the beginning part of this section for symmetric nuclear matter. We also give the corresponding UCOM parameters, α, β and η, as functions of density in the (b) panel. They change slightly in the low density region and become more stable in the high density region comparing with the case of three-body interaction.

We also apply the HFUT model for symmetric nuclear matter in Fig. 3.9. The solid curve shows the EOS of symmetric nuclear matter with UIX* three-body interaction. Its strong repulsive effect makes the binding energy of nuclear matter very small. The binding energy is -3.38 MeV at saturation density, $\rho_0 = 0.1$ fm^{-3}, which is not the reasonable saturation properties. While, the saturation properties are $E/A = -16.0$ MeV at $\rho_0 = 0.16$ fm^{-3}, which are consistent with the experiment data, as being shown as the symbol of squares for variational method [14] in Fig. 3.9. This difference is caused by the tensor force. Therefore, in symmetric nuclear matter, the tensor effect is very important for the saturation mechanism; however, it can not be included in the Hartree-Fock framework for nuclear matter.
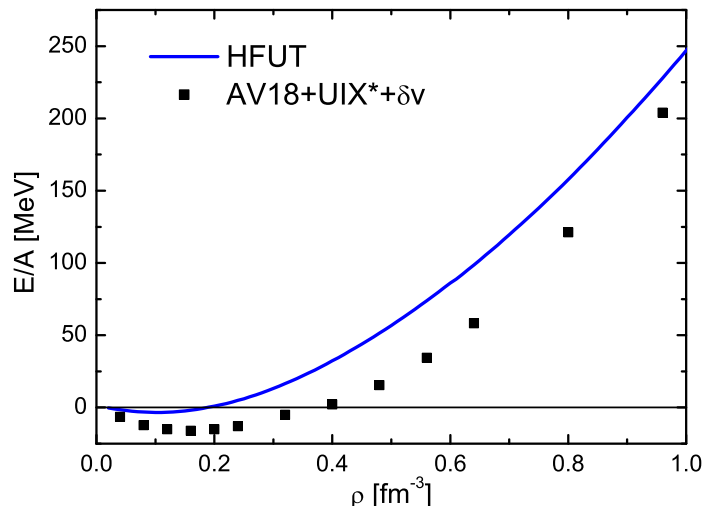
Figure 3.9: The EOS of nuclear matter with the HFUT model for symmetric nuclear matter. The solid curve is the results of HFUT model with the Urbana TNI, UIX*. The symbols of squares are the EOS from the variational method with the AV18 potential and three-body interaction.

3.4 Relativistic Hartree-Fock model with Jastrow correlation function method

In RHFU model, the energy contribution from the short range correlation on the kinetic energy is found negligibly small comparing with the one in the non-relativistic calculation as shown in chapter 3.3 . A few years ago, Panda *et al.* extended the Jastrow correlation function method into the relativistic case with a phenomenological Lagrangian, Walecka model, in relativistic Hartree-Fock (RHF) framework [81, 82, 83]. In these works, the meson coupling constants and the short range effect are determined by reproducing the reasonable saturation properties of nuclear matter. The effect of short range correlation on kinetic energy is significant in such studies which has the similar magnitude as the one from the UCOM in the non-relativistic case.

Hence, the intention of this section is to study the properties of nuclear matter with the Jastrow correlation function method in the RHF model where the realistic NN interaction, boson exchange potential can be treated.

In the variational method, one introduces a correlation function on the wave function [14] to treat this short range effect,

$$|\Psi\rangle = F|\Phi\rangle, \tag{3.45}$$

where the correlation factor F is, in general, an $n-$body operator which can be separated into a two-body, a three-body part, etc. Now the energy density is ,

$$\mathcal{E}_c = \frac{\langle\Phi|F^\dagger\mathcal{H}F|\Phi\rangle}{\langle\Phi|F^\dagger F|\Phi\rangle}. \tag{3.46}$$

However, we restrict our study to the two-body correlated problem. Therefore, the correlation factor F is chosen to be the production of two-body correlation functions $f(r_{ij})$

$$F = \prod_{i<j}^{A} f(r_{ij}), \tag{3.47}$$

The $f(r_{ij})$ is also called as Jastrow correlation function [12]. In usual case, it has some parameterized form and should go to zero for small r_{ij}, because of the repulsive core. Meanwhile, $f(r_{ij})$ is required to approach unity at large r_{ij}. Furthermore, a natural choice from the unitary property of correlation factor is a normalization constraint on $f(r_{ij})$,

$$\int d^3\mathbf{r}_{ij}[f^2(r_{ij}) - 1] = 0. \tag{3.48}$$

With this constraint, the correlated energy density becomes,

$$\mathcal{E}_c = \frac{1}{V}\langle\Phi|\widetilde{\mathcal{H}}|\Phi\rangle. \tag{3.49}$$

where, the explicit form of correlated Hamiltonian, $\widetilde{\mathcal{H}}$, is

$$
\begin{aligned}
\widetilde{\mathcal{H}} &= \sum_i^A T_i + \frac{1}{2}\sum_{i,j}^A \widetilde{V}_{ij} \\
&= \sum_i^A T_i + \frac{1}{2}\sum_{i,j}^A \{f^\dagger(r_{ij})[T_i + T_j + V_{ij}]f(r_{ij}) - (T_i + T_j)\}.
\end{aligned}
\tag{3.50}
$$

Now, the correlated energy density can be decomposed into the kinetic energy part and potential energy part, $\langle V\rangle$. The kinetic energy part is related with the one-body kinetic operator $\langle T\rangle$ and the two-body operator with correlation function $\langle T_c\rangle$,

$$
\begin{aligned}
\langle T\rangle + \langle T_c\rangle &= \frac{\lambda}{\pi^2}\int_0^{k_F} p^2 dp[p\hat{P} + M_N\hat{M}] + C\rho_B\frac{\lambda}{\pi^2}\int_0^{k_F} p^2 dp[p\hat{P} + M_N\hat{M}] \\
&\quad - \frac{2\lambda}{(2\pi)^4}\int_0^{k_F} p^2 dp\, p'^2 dp'\{[p\hat{P}(p) + 2M_N\hat{M}(p)]I(p,p') + p'\hat{P}(p)J(p',p)\},
\end{aligned}
\tag{3.51}
$$

where the last two terms are generated by the Hartree and Fock approximation of T_c and $C = \int d^3\mathbf{x}[f^2(r) - 1]$. λ is the isospin degeneracy. For symmetric nuclear matter, $\lambda = 2$ and for pure neutron matter, $\lambda = 1$. $\hat{P}$ and $\hat{M}$ are defined as

$$\hat{P}(p) = \frac{p^*(p)}{E^*(p)}, \qquad\qquad \hat{M}(p) = \frac{M_N^*(p)}{E^*(p)}. \tag{3.52}$$

The potential energy $\langle V\rangle$ can be split into its Hartree contribution, $\langle V_H\rangle$, and Fock contribution, $\langle V_F\rangle$. The pseudo-vector mesons do not contribute in the Hartree approximation.

We therefore have the result for $\langle V_H \rangle$ as,

$$
\langle V_H \rangle = -\frac{\widetilde{F}_\sigma(0,0)}{2}(\rho_S^p + \rho_S^p)^2 - \frac{\widetilde{F}_\delta(0,0)}{2}(\rho_S^p - \rho_S^n)^2 \tag{3.53}
$$

$$
+\frac{\widetilde{F}_\omega(0,0)}{2}(\rho_B^p + \rho_B^n)^2 + \frac{\widetilde{F}_\rho(0,0)}{2}(\rho_B^p - \rho_B^n)^2.
$$

The proton and neutron cases are distinguished by the superscript, p and n. For instance, the Fock contribution from σ meson, $\langle V_F^\sigma \rangle$, is given by,

$$
\langle V_F^\sigma \rangle = \frac{\lambda}{2(2\pi)^4} \int_0^{k_F} pdpp'dp \left[\tilde{A}_\sigma(p,p') + \hat{M}(p)\hat{M}(p')\tilde{B}_\sigma(p,p') + \hat{P}(p)\hat{P}(p')\tilde{C}_\sigma(p,p') \right] \tag{3.54}
$$

Here, the $\tilde{A}_i, \tilde{B}_i, \tilde{C}_i, I, J$ and F_i are exchange integral related with potential which are listed as following,

$$
\widetilde{F}_i(k,k') = \int f(r)V_i(r)f(r)e^{i(\mathbf{k}-\mathbf{k'})\cdot\mathbf{r}}d^3\mathbf{r}, \tag{3.55}
$$

$$
I(k,k') = \int 16\pi r^2 dr[f^2(r) - 1]j_0(kr)j_0(k'r),
$$

$$
J(k,k') = \int 16\pi r^2 dr[f^2(r) - 1]j_1(kr)j_1(k'r),
$$

$$
\tilde{A}_i(k,k') = \tilde{B}_i(k,k') = \int 16\pi r^2 dr[f(r)V_i(r)f(r)]j_0(kr)j_0(k'r),
$$

$$
\tilde{C}_i(k,k') = \int 16\pi r^2 dr[f(r)V_i(r)f(r)]j_1(kr)j_1(k'r).
$$

Here $j_0(r) = \sin(r)/r$ and $j_1(r) = \sin(r)/r^2 - \cos(r)/r$ are the zeroth-order and first-order spherical Bessel functions, respectively. $V_i(r)$ is the representation in the coordinate space of corresponding meson exchange interaction.

There are also similar structures for the contribution from other mesons. Finally, the total energy density is obtained as,

$$
\mathcal{E}_c = \langle T \rangle + \langle T_c \rangle + \langle V_H \rangle + \sum_i \langle V_F^i \rangle. \tag{3.56}
$$

Usually, several free parameters, $c_1, c_2, \ldots, c_i$, still appear in the correlation function $f(r)$ after we consider the constraints which are mentioned before. We would like to determine these parameters by variational principle with the energy density,

$$
\frac{\partial \mathcal{E}_c}{\partial c_i} = 0. \tag{3.57}
$$

The coupling constants between the nucleon and meson and corresponding cut-off momenta in our model have been fixed by the NN scattering data of Bonn-A potential [31].

There are only the variable parameters left in the Jastrow correlation function $f(r)$. We would like to assume that it can be written in the following form,

$$f(r) = 1 - (c_0 + c_1 r + c_2 r^2 + c_3 r^3)e^{-c_4 r}, \tag{3.58}$$

where the exponential term makes $f(r)$ unity at large distance. With the constraint as mentioned above, $c_0 = 1$ is taken to deal with the strong repulsion at $r = 0$. Furthermore, we also should ensure the monotonously increasing property of this function at short distance,

$$f'(0) \geq 0. \tag{3.59}$$

Then, we can calculate the binding energy of nuclear matter after determining the remaining parameters with variational principle. The minimal value of the total energy should appear at $f'(0) = 0$ and $f''(0) = 0$ with the constraint (3.59) to keep the Jastrow correlation function increasing at short range. Therefore, we can obtain the relations between c_1, c_2 and c_4 as following,

$$c_1 = c_4, \qquad c_2 = \frac{c_4^2}{2}. \tag{3.60}$$

Now, there is only one parameter, c_4, in the actual calculation. Because, the parameter c_3 will be fixed by the normalization condition of Jastrow correlation function as Eq. (3.48). The EOSs of asymmetric nuclear matter are showed in Fig. 3.10 at different asymmetry parameters $\delta = (\rho_n - \rho_p)/(\rho_n + \rho_p)$ for the relativistic Hartree-Fock model with Jastrow correlation function (RHFJ). It means that $\delta = 0$ and $\delta = 1$ correspond to symmetric nuclear matter and pure neutron matter, respectively. The saturation properties of symmetric nuclear matter in RHFJ model are not consistent with the empirical data. Other microscopic calculations also have the similar problem [14, 11]. It is well known that the tensor interaction can not provide any contribution for the spin-saturation matter at the Hartree-Fock level. Because of losing the attractive effect from the tensor force, the binding energy per particle of symmetric nuclear matter at saturation density in RHFJ model, $E/A = -11.65$ MeV, is smaller than the experimental value, $E/A \sim -16$ MeV. In Table 3.2, we give the parameter, c_4, and the saturation properties of symmetric nuclear matter calculated by the RHFJ model.

c_4 [fm^{-1}]	ρ [fm^{-3}]	E/A [MeV]	K [MeV]	a_4 [MeV]	T_c/A [MeV]
6.701	0.192	-11.66	264	37.88	6.57

Table 3.2: Parameter and ground state properties of nuclear matter at saturation density.

The energy contribution from the short range correlation on the kinetic energy is 6.57 MeV at the saturation density in RHFJ model, which is much larger than the one, 0.5 MeV, in the RHFU model. The larger repulsive contribution from the short range correlation on

kinetic energy is in favor of canceling with the strong attractive effect through the Jastrow correlation function cutting down the strong repulsion between the NN interaction at short distance, so that we can obtain the minimal value of binding energy by the variational principle.
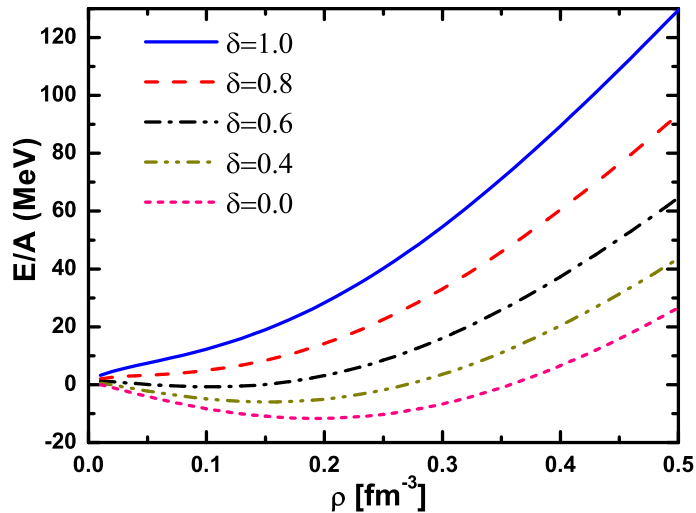

Figure 3.10: The binding energies per particle as a function of density for asymmetric nuclear matter.

To study the characters of different short range correlation methods, we plot the EOSs of pure neutron matter for the RHFJ model, RHFU model and RBHF model [68] by using the Bonn-A potential in Fig. 3.11. We obtained almost the same results for the RHFU and RBHF models. However, the binding energy of pure neutron matter in RHFJ model contains more repulsive effect than the ones in the other two methods. We have noticed that the short range correlation on the kinetic energy is much stronger in the RHFJ model than the RHFU model. Therefore, we believe that the extra contribution in the RHFJ model is generated by the short range correlation on the kinetic energy. We will discuss particularly on this point later.

We also give the only parameter, c_4, in the Jastrow correlation function as a function of the density for pure neutron matter in the (a) panel of Fig. 3.12. However, we fix the effect of the short range correlation with density in the RHFU model, because the short range correlation effect on the kinetic energy is so small that there does not exist a minimum value of binding energy by variation with UCOM parameters. It is obvious that the effect of the short range correlation is stronger for the smaller c_4 in the form of Eq. (3.58) for the Jastrow correlation function. Therefore, the short range correlation becomes stronger at high density. The correlated wave functions are shown for the RHFJ and RHFU models in the (b) panel of Fig. 3.12, where the uncorrelated wave function is assumed to be a constant, $\phi = 1$. Here, the weakest short range correlation is chosen as $c_4 = 7.867$ in RHFJ model, while its effect is still stronger than the one in UCOM. Their mechanisms on the short range correlation are
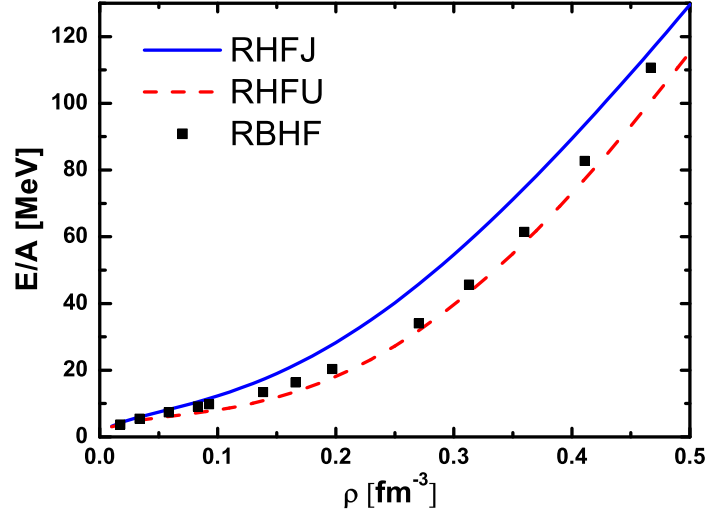
Figure 3.11: The EOSs of pure neutron matter. The solid curve represents the results of the RHF model with Jastrow function (RHFJ). The dashed curve is for the RHFU model and the full-squares are for RBHF.

not exactly the same.

(a)   (b)
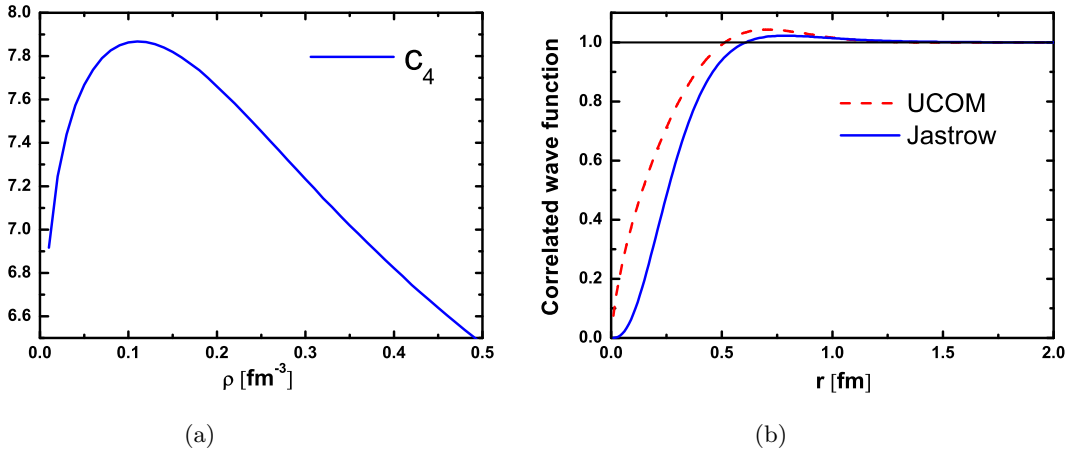
Figure 3.12: The parameter c_4 as a function of the density and correlated wave function. In the (a) panel, the solid curve denotes the parameter c_4 in the Jastrow factor. In the (b) panel, the solid curve and dashed one correspond the Jastrow correlated wave function and UCOM correlated wave function for unity wave function, respectively.

The short range correlation on the kinetic energy in RHFJ model is removed to find the relation between the RHFJ model and the RHFU model, because this correlation is very small in the RHFU model. Now, we can not determine the parameter, c_4, in the Jastrow correlation function by the variational principle anymore. There is no competition between the short range correlation on the kinetic energy and the NN interaction. The binding energy of a nuclear system keeps decreasing as the short range correlation becomes stronger.

Therefore, we would like to fix c_4 at the value where the short range correlation is the weakest in the previous complete calculation, namely $c_4 = 7.867$. The detailed results are given in Fig. 3.13. We find that the EOSs in the RHFJ model after removing the short range correlation on the kinetic energy are almost identical with the ones in the RHFU model. It demonstrates that the short range correlations on the NN interaction are identical between the Jastrow correlation function method and the UCOM. The difference of them in Fig. 3.11 is due to their effects on the kinetic energy.

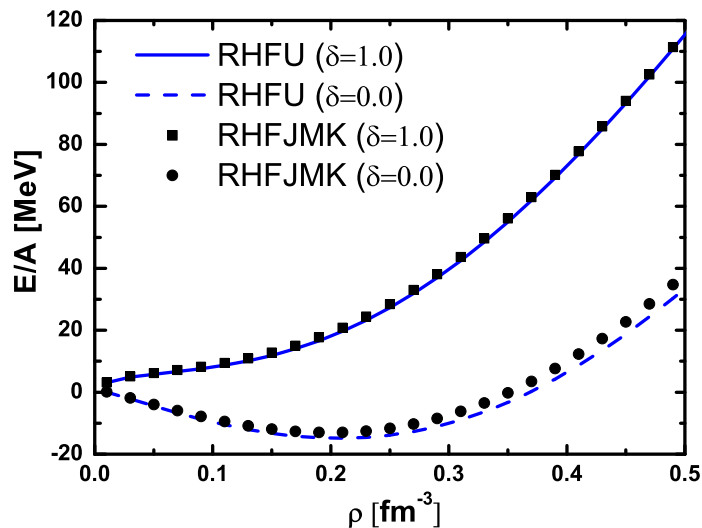Figure 3.13: The relation between the RHFJ and RHFU models. The EOSs of symmetric nuclear matter and pure neutron matter in the RHFJ model after removing the short range correlation on the kinetic energy (RHFJMK) are shown by the circle and square symbols, while the ones in the RHFU model are denoted by the dashed and solid curves, respectively.

Furthermore, in the RBHF model, there is no obvious term about the short range correlation on the kinetic energy. All the effect of the short range correlation is concentrated in the G-matrix of the Bethe-Goldstone equation. But this equation is just used in the P space in the Feshbach representation, while the correlation of Q space on the kinetic energy is not included in the RBHF model. Therefore, its result can be completely compared with the one in RHFU model where the short range correlation on the kinetic energy is very weak.

Although the UCOM correlation on the kinetic energy is not so obvious in the relativistic case, its effect in the non-relativistic kinetic energy becomes not negligible, because there are no spin operators in the non-relativistic kinetic operator as we showed in last section. We show the energies per particle from the short range correlation on kinetic energy as a function of density in the RHFJ and NHFU models in Fig. 3.14. Their values are very similar below $\rho = 0.25$ fm^{-3}. Then, the difference of $\langle T_c \rangle / A$ between the relativistic and non-relativistic cases increases with the density. The contribution in the non-relativistic case is only about 70% of the relativistic case at $\rho = 0.5$ fm^{-3}. This relativistic effect, which
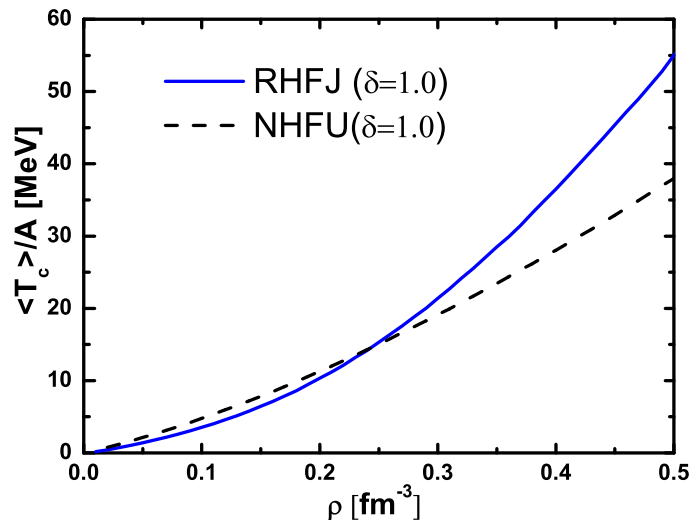
Figure 3.14: The energy per particle from the short range correlation on the kinetic energy. The solid curve denotes the short range correlation contribution in the RHFJ model. The dashed curve corresponds the correlation energy in the non-relativistic HFU case.

provides more repulsive contribution, can be interpreted as coming from virtual nucleon-antinucleon excitations in the many-body Z graph process.

3.5   Conclusion

In summary, we have successfully built a framework to deal with neutron rich matter with a realistic nucleon-nucleon interaction. For this, it was essential to include the short range correlation in terms of the unitary correlation operator method (UCOM) in the RHF model. With the form factor of the nucleon-nucleon interaction, we have completely reproduced the EOS of pure neutron matter in RBHF model with Bonn-A potential. The RHFU model turned out to be good until the asymmetry parameter $\delta \sim 0.8$ compared with the calculation of RBHF theory. As the asymmetry parameter δ is decreases and the system approaches symmetric nuclear matter, we have found that the deviations of the EOS's become larger and larger in particular in the low density region. The RHFU model works well for neutron-rich matter with the asymmetry parameters δ above 0.8. This is related with the construction of the RHFU model, which does not include the tensor interaction. The tensor interaction is indispensable for symmetric nuclear matter. We have studied the EOS's dependence on the interaction. As for the neutron matter, the results are not much different among Bonn-A, Bonn-B and Bonn-C potentials. On the other hand, for the symmetric nuclear matter these three potentials provide quite different EOS's. This is related with the fact that the tensor interactions are different among the three potentials.

It is very important to find that the RHF model with the UCOM is able to reproduce the

EOS's of neutron-rich matter of the sophisticate RBHF theory by using the bare nucleon-nucleon interaction. It is then straightforward to calculate EOS's in various situations as finite temperature and higher densities within the RHFU model for neutron-rich matter. We are able also to calculate the neutrino reaction rates in neutron-rich matter, which are necessary for formation of hot neutron star in the course of supernova explosion. In the region where experimental data are available for smaller asymmetry parameter $\delta < 0.5$, we may introduce several parameters for the coupling constants of the Lagrangian in the RHFU model to be fixed by experimental data.

We also have studied the properties of nuclear matter, especially pure neutron matter in the non-relativistic Hartree-Fock theory with three-body interaction. We explain the role of tensor force in the different isospin channels of nuclear matter by evaluating the iterated one-pion-exchange diagram. The tensor force makes a very large attractive contribution to symmetric nuclear matter, while its effect becomes very weak in neutron matter which has only $T = 1$ nucleon pairs. Therefore, it is sufficient to treat only the short range correlation induced by the strong repulsive interaction of a realistic NN interaction in neutron matter.

The unitary correlation operator method (UCOM) has been adopted to treat the short range correlation. We constructed the Hartree-Fock theory with UCOM (HFU) by using the two-body meson-exchange potential, Bonn-A potential, which is a realistic NN interaction fitted to the phase shifts of NN scattering. It is necessary to introduce a three-body interaction to improve the properties of nuclear matter in the microscopic calculation of nuclear matter within a non-relativistic framework. We choose a phenomenological one, Urbana three-nucleon interaction. The HFU model with three-body interaction was called the HFUT model.

We have studied first the EOS of nuclear matter with the Bonn-A potential in the HFU model. For pure neutron matter, we have obtained a similar EOS to the variational method using the AV18 potential with the relativistic boost effect. This success is based on the facts that the tensor effect is very weak in neutron matter, as we have shown before, and that the Bonn-A potential contains the relativistic boost effect in the framework of the HFU model.

To make the EOS of pure neutron matter harder, we also have performed calculations in the HFU model by including a three-body interaction, UIX*, for neutron matter. In this calculation, we include only the V_{ijk}^{R} three-body interaction and do not include the $V_{ijk}^{2\pi}$ three-body interaction for consistency with the treatment of the two-body interaction without inclusion of the tensor interaction for neutron matter. The HFUT calculation compares nicely with the one in the variational method for neutron matter.

Although the present model is not sufficient to discuss the symmetric nuclear matter, we still want to find how far the properties of symmetric nuclear matter in our model differ from the full model. It indicates that the UCOM can largely cut down the strong repulsive contribution of a realistic NN interaction for symmetric nuclear matter, making it bound

in HFU model. However, the saturation properties are still a bit far from the empirical values due to the lack of the tensor effect. The parameters, α, β and η in the UCOM are obtained by minimizing the ground energy of the total system with the variational principle. They changed somewhat at the low density region and become very stable in the high density region. We also do not obtain good saturation properties for symmetric nuclear matter within the HFUT model. We can not include the strong attraction from the tensor interaction in the HFUT model. The binding energy of symmetric nuclear matter becomes very small at the saturation point.

Furthermore, the Jastrow correlation function was applied to consider the short range correlation induced by the strong repulsive interaction of a realistic NN interaction. We formulated the relativistic Hartree-Fock model with Jastrow correlation function (RHFJ) with the two-body meson-exchange potential, Bonn-A potential.

We have calculated the EOSs of asymmetric nuclear matter at different asymmetric parameters. The strength of Jastrow correlation function was determined by the variational principle through the binding energy per particle is minimized with the parameters in the Jastrow correlation function. The saturation properties were not exactly in accordance with the empirical values. There was not enough attractive contribution to the binding energy in the RHFJ model due to the lack of the tensor force contribution, which cannot be treated at the Hartree-Fock level in a spin-saturated system. However, the short range correlation on the kinetic energy becomes remarkable. This conclusion is quite different from another short range correlation model for nuclear matter, RHFU model, where the contribution from the short range correlation on the kinetic energy is very small, just about $1/10$ of the one in RHFJ model at the saturation density.

As we said before, the tensor effect is very weak in neutron matter, which has only $T = 1$ nucleon pairs. It is sufficient to consider only the short range correlation of a realistic NN interaction in neutron matter. To discuss the characters between different short range correlation methods, we have compared the EOS of pure neutron matter in the RHFJ, RHFU and RBHF models. We found that the EOS of the RHFJ model had a more repulsive effect as compared with the ones of the RHFU and RBHF models. This extra contribution is generated by the short range correlation on the kinetic energy. Actually, the different short correlation methods, the Jastrow correlation function method and the UCOM, on the potential energy are completely the same, which can provide essentially an identical EOS without the short range correlation on the kinetic energy in neutron matter.

The relativistic effect in the short range correlation on the kinetic energy was also discussed. The effects of the short range correlation on the relativistic kinetic operator is very similar to the one on the non-relativistic kinetic energy operator at low density. Their difference becomes larger with the density. This relativistic effect, which provides more repulsive effect, can be interpreted, as coming from virtual nucleon-antinucleon excitations in the

many-body Z graph process.

According to these studies, we are aware that the tensor interaction is an essential ingredient for the nuclear matter saturation. Usually, the pion is the most important component in the realistic NN interaction. Thus, we try to include the tensor contribution of pion in a chiral Lagrangian, which contains the Nambu-Goldstone particle, pion, through introducing the 2 particle-2 hole (2p-2h) states in the nucleon ground state. Because this discussion is just within the mean field approximation, not in the RHF framework, it has been shown in the Appendix C.

Chapter 4

Extended Brueckner-Hartree-Fock theory

4.1 Brueckner-Hartree-Fock theory

As mentioned in the introduction, in the Brueckner theory the realistic NN interaction is replaced by the reaction matrix G which sums over all the possible scattering processes of two interacting nucleons into unoccupied stats, because of the strong repulsion and tensor interaction between nucleons at short distance. This infinite sum of ladder diagrams is evaluated by solving the Bethe-Goldstone integral equation,

$$G(w) = V + V \frac{Q}{w - H_0} G(w), \tag{4.1}$$

where the Pauli operator Q projects intermediate states onto unoccupied states, i.e. particle states and V is a realistic NN interaction. If we define the correlated wave function ψ in terms of the uncorrelated wave function ϕ,

$$G\phi = V\psi, \tag{4.2}$$

then, we can obtain

$$\psi = \phi + \frac{Q}{w - H_0} G\phi. \tag{4.3}$$

The ladder sum takes ψ with short-range correlations induced by the repulsive core. In free space ($Q = 1$), G matrix reduces to the familiar scattering T matrix and ψ simply corresponds to the exact scattering wave function.

In the lowest order many-body theory (Hartree-Fock approximation), the energy per particle in nuclear matter at a Fermi momentum k_F is written as,

$$\frac{E}{A} = \frac{1}{A} \sum_{i < k_F} \langle i|T|i \rangle + \frac{1}{2A} \sum_{i,j < k_F} \langle ij|G(w)|ij - ji \rangle \tag{4.4}$$

with starting energy

$$w = \varepsilon(i) + \varepsilon(j) \tag{4.5}$$

and $\varepsilon(i)$ is the single particle energy of hole occupied states (hole states),

$$\varepsilon(i) = T(i) + U(i). \tag{4.6}$$

The $U(i)$ is the single particle potential which is calculated by,

$$U(i) = \begin{cases} \displaystyle\sum_{j<k_F} \langle ij|G(w)|ij - ji\rangle, & i < k_F \\[3ex] 0, & i > k_F \end{cases}$$

This choice produces a gap at Fermi surface (standard choice)[84]. Alternatively, a continuous choice for U can be made[85],

$$U(i) = \Re \sum_{j<k_F} \langle ij|G(w)|ij - ji\rangle \tag{4.7}$$

for all states i below and above the Fermi surface.

The formulae involved in the Brueckner Hartree-Fock (BHF) theory in a more explicit form and methods for their numerical calculation can be found in Refs.[86, 87, 88]. Some results of BHF theory for nuclear matter will be shown later to compare with the one in our model.

4.2 Extended Brueckner-Hartree-Fock theory

In the previous chapters, we have considered the short range correlation of realistic NN interaction in pure neutron matter. We have also discussed the tensor effect for the symmetric nuclear matter with an effective chiral Lagrangian in appendix C. These works can demonstrate that the tensor effect is very important for the mechanism of symmetric nuclear matter, while it becomes very week in pure neutron matter. In this chapter, we will try to consider both of these effects in symmetric nuclear matter and pure neutron matter to construct a new microscopic framework to deal with nuclear matter with realistic NN interaction.

The pion contribution was taken care of through 2p-2h excited states in appendix C. This idea comes from the tensor optimized shell model (TOSM). In the TOSM, the strong tensor correlation can be treated in the shell model framework by introducing 2p-2h states up to high excitations with compact configurations for finite nuclei. It is shown that there is a good convergence of the tensor correlation with full tensor strength by taking enough partial waves in 2p-2h states. Therefore, it is very interesting to extend the Hartree-Fock

model space to include 2p-2h states with spatially compact configurations to treat the tensor correlation in the many-body theory.

Based on this point, recently Ogawa *et al.* [89] formulated a method to treat the tensor correlation in a consistent manner to the nuclear many-body framework, where an extended variational model space up to 2p-2h configurations plus Hartree-Fock model space is regarded as the nuclear ground state. This extended ground state is determined by the variational principle for an expectation value of the total Hamiltonian. It means that the present HF single particle states are also self-consistently obtained under the minimization of the total energy, namely in the model space including all the possible 2p-2h states. A new term between 2p-2h states with the Hartree-Fock space is very similar to the one of the G-matrix theory in an infinite system as shown in chapter 1.3. Hence, this framework is named as an extended Brueckner-Hartree-Fock (EBHF) theory. We would like to apply this theory on the study of nuclear matter with a realistic NN interaction.

We start this section with the particle-hole picture. In the single-particle model, the nuclear ground state is given by A nucleons occupying the lowest-available single-particle states. If we arrange the indices in the order of increasing single-particle energy[60, 90],

$$\varepsilon_1 < \varepsilon_2 < \ldots \varepsilon_A < \varepsilon_{A+1} < \ldots, \tag{4.8}$$

the lowest state of the A-nucleon system is

$$|\Psi_0\rangle = \prod_{i=1}^{A} c_i^\dagger |0\rangle, \tag{4.9}$$

where $c^\dagger$ is the creation operator in second quantization. The highest occupied state with energy ε_A is the Fermi level. The expectation value of an operator $\hat{O}$ in the ground state may then be written as

$$\langle \Psi_0 | \hat{O} | \Psi_0 \rangle = \langle 0 | c_A \ldots c_1 \hat{O} c_1^\dagger \ldots c_A^\dagger | 0 \rangle. \tag{4.10}$$

To avoid a complicated expression, we can redefine the ground state as the 'Fermi vacuum'. The following relations are used for this vacuum,

$$c_i | \Psi_0 \rangle = 0, \quad i > A \tag{4.11}$$

$$c_i^\dagger | \Psi_0 \rangle = 0, \quad i \leq A. \tag{4.12}$$

The simplest excited states will have one particle lifted from an occupied state into an unoccupied one. They can be written as

$$|\Psi_{mi}\rangle = c_m^\dagger c_i | \Psi_0 \rangle, \quad m > A, \quad i \leq A. \tag{4.13}$$

The state $|\Psi_{mi}\rangle$ has an unoccupied level i, a hole below the Fermi energy, and a particle in state m above the Fermi energy. For that reason, it is called a one-particle-one-hole (1p1h)

state. The next more complicated type of excitation is a two-particle-two-hole (2p-2h) state
like,

$$|\Psi_{klij}\rangle = c_k^\dagger c_l^\dagger c_i c_j |\Psi_0\rangle, \quad k, l > A, \quad i, j \leq A. \tag{4.14}$$

We introduce new particle and hole operators a_i and b_i related to the usual one via,

$$
\begin{aligned}
c_i &= \theta(i - A)a_i + \theta(A - i)b_i^\dagger, \\
c_i^\dagger &= \theta(i - A)a_i^\dagger + \theta(A - i)b_i,
\end{aligned}
\tag{4.15}
$$

where the θ function is the step function defined by

$$\theta(A - i) = \begin{cases} 1, & \text{if } i \leq A, \\ 0, & \text{if } i > A \end{cases}. \tag{4.16}$$

Therefore, we can obtain the following relations about the particle and hole operators acting
on the Fermi vacuum $|\Psi_0\rangle$,

$$
\begin{aligned}
a_i|\Psi_0\rangle &= b_i|\Psi_0\rangle = 0, \\
a_i^\dagger|\Psi_0\rangle &= |i\rangle_p, \quad b_i^\dagger|\Psi_0\rangle = |i\rangle_h.
\end{aligned}
\tag{4.17}
$$

In this new notation, 1p-1h state and 2p-2h state are written as,

$$
\begin{aligned}
|\Psi_{mi}\rangle &= a_m^\dagger b_i^\dagger |\Psi_0\rangle, \quad m > A, \quad i \leq A \\
|\Psi_{klij}\rangle &= a_k^\dagger a_l^\dagger b_i^\dagger b_j^\dagger |\Psi_0\rangle, \quad k, l > A, \quad i, j \leq A.
\end{aligned}
\tag{4.18}
$$

The Hamiltonian of many-body system in the second quantization with the usual representation has the form,

$$
\begin{aligned}
\mathcal{H} &= T + V \tag{4.19} \\
&= \sum_{\alpha\beta}\langle\alpha|T|\beta\rangle c_\alpha^\dagger c_\beta + \frac{1}{2}\sum_{\alpha\beta\gamma\delta}\langle\alpha\beta|V|\gamma\delta\rangle c_\alpha^\dagger c_\beta^\dagger c_\delta c_\gamma,
\end{aligned}
$$

where the indices, $\alpha, \ldots$, include the quantum numbers of momentum, spin and isospin.
This Hamiltonian may be expressed in the particle-hole formalism as,

$$
\begin{aligned}
\mathcal{H} &= \sum_{\alpha,\beta>F}\langle\alpha|T|\beta\rangle a_\alpha^\dagger a_\beta + \sum_{\alpha,\beta<F}\langle\alpha|T|\beta\rangle b_\alpha b_\beta^\dagger \tag{4.20} \\
&+ \frac{1}{2}\sum_{\substack{\alpha\beta>F \\ \gamma\delta<F}}\langle\alpha\beta|V|\gamma\delta\rangle a_\alpha^\dagger a_\beta^\dagger b_\delta^\dagger b_\gamma^\dagger + \frac{1}{2}\sum_{\alpha\beta\gamma\delta>F}\langle\alpha\beta|V|\gamma\delta\rangle a_\alpha^\dagger a_\beta^\dagger a_\delta a_\gamma \\
&+ \frac{1}{2}\sum_{\substack{\beta\gamma>F \\ \alpha\delta<F}}\langle\alpha\beta|V|\gamma\delta\rangle b_\alpha a_\beta^\dagger b_\delta^\dagger a_\gamma + \frac{1}{2}\sum_{\substack{\beta\delta>F \\ \alpha\gamma<F}}\langle\alpha\beta|V|\gamma\delta\rangle b_\alpha a_\beta^\dagger a_\delta b_\gamma^\dagger \\
&+ \frac{1}{2}\sum_{\substack{\alpha\gamma>F \\ \beta\delta<F}}\langle\alpha\beta|V|\gamma\delta\rangle a_\alpha^\dagger b_\beta b_\delta^\dagger a_\gamma + \frac{1}{2}\sum_{\substack{\alpha\delta>F \\ \beta\gamma<F}}\langle\alpha\beta|V|\gamma\delta\rangle a_\alpha^\dagger b_\beta a_\delta b_\gamma^\dagger
\end{aligned}
$$

$$+\frac{1}{2}\sum_{\substack{\gamma\delta>F \\ \alpha\beta<F}}\langle\alpha\beta|V|\gamma\delta\rangle b_\alpha b_\beta a_\delta a_\gamma + \frac{1}{2}\sum_{\alpha\beta\gamma\delta<F}\langle\alpha\beta|V|\gamma\delta\rangle b_\alpha b_\beta b_\delta^\dagger b_\gamma^\dagger.$$

Here, F is the quantum number which corresponds the Fermi energy ε_A and we have already neglected those terms which only contain one particle or one hole operator. Because, it is very obvious to find that these terms do not have contribution on the expectation value.

We construct a new nucleon ground state as a linear combination of Fermi vacuum (0p-0h) and 2p-2p states in order to take care of the contribution of high momentum component, above the Fermi momentum, in the nucleon-nucleon interaction,

$$|\Psi\rangle = C_0|\Psi_0\rangle + \sum_m C_m|2p-2h,m\rangle \tag{4.21}$$

The coefficient, C_0 and C_m, will be determined later and 2p-2h states are written as,

$$|2p-2h,m\rangle = N_m a_k^\dagger a_l^\dagger b_i^\dagger b_j^\dagger|\Psi_0\rangle. \tag{4.22}$$

Here, N_m denotes the normalization constant, and to avoid non-orthogonal basis, we impose the ordering condition, $k < l$ and $i < j$. To facilitate the notation, we also use the following convention:

- The indices i, j and their superscripted forms i', j' et., refer to the hole states.

- The indices k, l and their superscripted forms k', l' et., refer to the particle states.

The quantum number m specifies the 2p-2h states: $m = ijkl$. We consider that the new nucleon ground states should be ortho-normalized. Therefore, the normalization condition about the coefficient has,

$$\langle\Psi|\Psi\rangle = |C_0|^2 + \sum_m |C_m|^2\langle 2p-2h,m|2p-2h,m\rangle = 1. \tag{4.23}$$

Now the expectation value of the Hamiltonian for the whole system becomes,

$$\langle\Psi|\mathcal{H}|\Psi\rangle = |C_0|^2\langle\Psi_0|\mathcal{H}|\Psi_0\rangle + \sum_m C_0^* C_m\langle\Psi_0|\mathcal{H}|2p-2h,m\rangle \tag{4.24}$$

$$+ \sum_n C_0 C_n^*\langle 2p-2h,n|\mathcal{H}|\Psi_0\rangle + \sum_{m,n} C_n^* C_m\langle 2p-2h,n|\mathcal{H}|2p-2h,m\rangle.$$

The next step is evaluating all the matrix elements in the above equation.

To simplify the expression in the following part, we would like to use $|0\rangle$ and $|m\rangle$ instead of $|\Psi_0\rangle$ and $|2p-2h,m\rangle$,

$$|\Psi_0\rangle = |0\rangle \tag{4.25}$$
$$|2p-2h,m\rangle = |m\rangle.$$

We first work out matrix elements of the many-body Hamiltonian between 0p-0h state,

$$\langle 0|\mathcal{H}|0\rangle = \langle 0|T|0\rangle + \langle 0|V|0\rangle. \tag{4.26}$$

For the kinetic term, we have

$$
\begin{aligned}
\langle 0|T|0\rangle &= \sum_{\alpha\beta<F} \langle\alpha|T|\beta\rangle \langle 0|b_\alpha b_\beta^\dagger|0\rangle \tag{4.27}\\
&= \sum_{\alpha<F} \langle\alpha|T|\alpha\rangle,
\end{aligned}
$$

where we have used the property of annihilation operator of particle states, $a_k|0\rangle = 0$, to cancel the term for particle states. For the matrix elements of interaction, the same property is applied so that there is only one term survived which is only formed by the hole operators,

$$
\begin{aligned}
\langle 0|V|0\rangle &= \frac{1}{2} \sum_{\alpha\beta\gamma\delta<F} \langle\alpha\beta|V|\gamma\delta\rangle \langle 0|b_\alpha b_\beta b_\delta^\dagger b_\gamma^\dagger|0\rangle \tag{4.28}\\
&= \frac{1}{2} \sum_{\alpha\beta\gamma\delta<F} \langle\alpha\beta|V|\gamma\delta\rangle (\delta_{\beta\delta}\delta_{\alpha\gamma} - \delta_{\alpha\delta}\delta_{\beta\gamma})\\
&= \frac{1}{2} \sum_{\alpha\beta<F} [\langle\alpha\beta|V|\alpha\beta\rangle - \langle\alpha\beta|V|\beta\alpha\rangle]\\
&= \frac{1}{2} \sum_{\alpha\beta<F} \langle\alpha\beta|V|\alpha\beta\rangle_A.
\end{aligned}
$$

Here, we have defined a new notation,

$$|\alpha\beta\rangle_A = |\alpha\beta\rangle - |\beta\alpha\rangle, \tag{4.29}$$

to simplify the expression of matrix elements.

In the matrix elements of Hamiltonian between 0p-0h and 2p-2h states, the kinetic term vanishes,

$$\langle 0|T|m\rangle = 0, \tag{4.30}$$

which is caused by the fact that there are not enough annihilation operators in kinetic term to make contraction with creation operators in 2p-2h states. Based on the same reason, only one term exists in the matrix element of interaction,

$$
\begin{aligned}
\langle 0|V|m\rangle &= \frac{N_m}{2} \sum_{\substack{\alpha\beta<F\\\delta\gamma>F}} \langle\alpha\beta|V|\gamma\delta\rangle \langle 0|b_\alpha b_\beta a_\delta a_\gamma a_k^\dagger a_l^\dagger b_i^\dagger b_j^\dagger|0\rangle \tag{4.31}\\
&= \frac{N_m}{2} \sum_{\substack{\alpha\beta<F\\\delta\gamma>F}} \langle\alpha\beta|V|\gamma\delta\rangle (\delta_{\gamma k}\delta_{\delta l} - \delta_{\gamma l}\delta_{\delta k})(\delta_{\alpha j}\delta_{\beta i} - \delta_{\alpha i}\delta_{\beta j})
\end{aligned}
$$

$$= \frac{N_m}{2}[\langle ij|V|lk\rangle - \langle ij|V|kl\rangle + \langle ji|V|kl\rangle - \langle ji|V|lk\rangle]$$
$$= -N_m\langle ij|V|kl\rangle_A$$

Now we calculate the matrix elements of Hamiltonian between two 2p-2h states,

$$\langle n|\mathcal{H}|m\rangle = \langle n|T|m\rangle + \langle n|V|m\rangle. \tag{4.32}$$

These terms are more complicated than those matrix elements above. First, we take the kinetic term, which contains two pieces from the particle and hole operators. For the particle part of kinetic term, we have

$$\sum_{\alpha\beta>F}\langle\alpha|T|\beta\rangle\langle n|a_\alpha^\dagger a_\beta|m\rangle \tag{4.33}$$

$$= N_m N_n^* \sum_{\alpha\beta>F}\langle\alpha|T|\beta\rangle\langle 0|b_{j'}b_{i'}a_{l'}a_{k'}a_\alpha^\dagger a_\beta a_k^\dagger a_l^\dagger b_i^\dagger b_j^\dagger|0\rangle$$

$$= N_m N_n^*\delta_{ii'}\delta_{jj'}[\langle k'|T|k\rangle\delta_{ll'} - \langle k'|T|l\rangle\delta_{kl'} + \langle l'|T|l\rangle\delta_{kk'} - \langle l'|T|k\rangle\delta_{lk'}].$$

Because we have defined $i < j, i' < j', k < l$ and $k' < l'$, the contractions of hole operator do not produce those pieces like $\delta_{ij'}$. While for the hole term, it can be written as

$$\sum_{\alpha\beta>F}\langle\alpha|T|\beta\rangle\langle n|b_\alpha b_\beta^\dagger|m\rangle \tag{4.34}$$

$$= N_m N_n^* \sum_{\alpha\beta>F}\langle\alpha|T|\beta\rangle\langle 0|b_{j'}b_{i'}a_{l'}a_{k'}b_\alpha b_\beta^\dagger a_k^\dagger a_l^\dagger b_i^\dagger b_j^\dagger|0\rangle$$

$$= N_m N_n^* \sum_{\alpha<F}\langle\alpha|T|\alpha\rangle\delta_{ii'}\delta_{jj'}\delta_{kk'}\delta_{ll'}$$

$$+ N_m N_n^*\delta_{kk'}\delta_{ll'}[\langle i|T|j'\rangle\delta_{ji'} - \langle i|T|i'\rangle\delta_{jj'} + \langle j|T|i'\rangle\delta_{ij'} - \langle j|T|j'\rangle\delta_{ii'}].$$

Next, we will evaluate the matrix elements of interaction one by one,

$$\frac{1}{2}\sum_{\alpha\beta\gamma\delta>F}\langle\alpha\beta|V|\gamma\delta\rangle\langle 0|b_{j'}b_{i'}a_{l'}a_{k'}a_\alpha^\dagger a_\beta^\dagger a_\delta a_\gamma a_k^\dagger a_l^\dagger b_i^\dagger b_j^\dagger|0\rangle \tag{4.35}$$

$$= \frac{1}{2}\sum_{\alpha\beta\gamma\delta>F}\langle\alpha\beta|V|\gamma\delta\rangle\delta_{ii'}\delta_{jj'}\langle 0|a_{l'}a_{k'}a_\alpha^\dagger a_\beta^\dagger a_\delta a_\gamma a_k^\dagger a_l^\dagger|0\rangle$$

$$= \frac{1}{2}\sum_{\alpha\beta\gamma\delta>F}\langle\alpha\beta|V|\gamma\delta\rangle\delta_{ii'}\delta_{jj'}(\delta_{\alpha k'}\delta_{\beta l'} - \delta_{\alpha l'}\delta_{\beta k'})(\delta_{\gamma k}\delta_{\delta l} - \delta_{\gamma l}\delta_{\delta k})$$

$$= \frac{1}{2}\delta_{ii'}\delta_{jj'}[\langle k'l'|V|kl\rangle - \langle k'l'|V|lk\rangle + \langle l'k'|V|lk\rangle - \langle l'k'|V|kl\rangle]$$

$$= \delta_{ii'}\delta_{jj'}\langle k'l'|V|[kl]_A\rangle,$$

$$\frac{1}{2}\sum_{\alpha\beta\gamma\delta>F}\langle\alpha\beta|V|\gamma\delta\rangle\langle 0|b_{j'}b_{i'}a_{l'}a_{k'}a_\alpha^\dagger a_\beta^\dagger b_\delta^\dagger b_\gamma^\dagger a_k^\dagger a_l^\dagger b_i^\dagger b_j^\dagger|0\rangle = 0, \tag{4.36}$$

which is caused by two extra creation operators and

$$\frac{1}{2}\sum_{\substack{\alpha\delta<F\\\beta\gamma>F}}\langle\alpha\beta|V|\gamma\delta\rangle\langle0|b_{j'}b_{i'}a_{l'}a_{k'}b_{\alpha}a_{\beta}^{\dagger}b_{\delta}^{\dagger}a_{\gamma}a_{k}^{\dagger}a_{l}^{\dagger}b_{i}^{\dagger}b_{j}^{\dagger}|0\rangle \tag{4.37}$$

$$= -\frac{1}{2}\sum_{\substack{\alpha\delta<F\\\beta\gamma>F}}\langle\alpha\beta|V|\gamma\delta\rangle\langle0|b_{j'}b_{i'}b_{\alpha}b_{\delta}^{\dagger}b_{i}^{\dagger}b_{j}^{\dagger}|0\rangle\langle0|a_{l'}a_{k'}a_{\beta}^{\dagger}a_{\gamma}a_{k}^{\dagger}a_{l}^{\dagger}|0\rangle$$

$$= -\frac{1}{2}\sum_{\substack{\alpha\delta<F\\\beta\gamma>F}}\langle\alpha\beta|V|\gamma\delta\rangle(\delta_{\alpha\delta}\delta_{ii'}\delta_{jj'}+\delta_{\alpha i}\delta_{\delta j'}\delta_{ji'}+\delta_{\alpha j}\delta_{\delta i'}\delta_{ij'}-\delta_{\alpha i}\delta_{\delta i'}\delta_{jj'}$$

$$-\delta_{\alpha j}\delta_{\delta j'}\delta_{ii'})(\delta_{\beta k'}\delta_{\gamma k}\delta_{ll'}+\delta_{\beta l'}\delta_{\gamma l}\delta_{kk'}-\delta_{\beta k'}\delta_{\gamma l}\delta_{kl'}-\delta_{\beta l'}\delta_{\gamma k}\delta_{lk'})$$

$$= -\frac{1}{2}\delta_{ii'}\delta_{jj'}\sum_{\alpha<F}[\langle\alpha k'|V|k\alpha\rangle\delta_{ll'}-\langle\alpha k'|V|l\alpha\rangle\delta_{kl'}+\langle\alpha l'|V|l\alpha\rangle\delta_{kk'}-\langle\alpha l'|V|k\alpha\rangle\delta_{lk'}]$$

$$-\delta_{ji'}[\langle ik'|V|kj'\rangle\delta_{ll'}-\langle ik'|V|lj'\rangle\delta_{kl'}+\langle il'|V|lj'\rangle\delta_{kk'}-\langle il'|V|kj'\rangle\delta_{lk'}]$$

$$-\delta_{ij'}[\langle jk'|V|ki'\rangle\delta_{ll'}-\langle jk'|V|li'\rangle\delta_{kl'}+\langle jl'|V|li'\rangle\delta_{kk'}-\langle jl'|V|ki'\rangle\delta_{lk'}]$$

$$+\delta_{ii'}[\langle jk'|V|kj'\rangle\delta_{ll'}-\langle jk'|V|lj'\rangle\delta_{kl'}+\langle jl'|V|lj'\rangle\delta_{kk'}-\langle jl'|V|kj'\rangle\delta_{lk'}]$$

$$+\delta_{jj'}[\langle ik'|V|ki'\rangle\delta_{ll'}-\langle ik'|V|li'\rangle\delta_{kl'}+\langle il'|V|li'\rangle\delta_{kk'}-\langle il'|V|ki'\rangle\delta_{lk'}].$$

For the following three terms, they also have similar results to Eq. (4.37). The difference appears just by changing the places of α, β, γ and δ.

$$\frac{1}{2}\sum_{\substack{\alpha\gamma<F\\\beta\delta>F}}\langle\alpha\beta|V|\gamma\delta\rangle\langle0|b_{j'}b_{i'}a_{l'}a_{k'}b_{\alpha}a_{\beta}^{\dagger}a_{\delta}b_{\gamma}^{\dagger}a_{k}^{\dagger}a_{l}^{\dagger}b_{i}^{\dagger}b_{j}^{\dagger}|0\rangle, \tag{4.38}$$

$$\frac{1}{2}\sum_{\substack{\alpha\gamma>F\\\beta\delta<F}}\langle\alpha\beta|V|\gamma\delta\rangle\langle0|b_{j'}b_{i'}a_{l'}a_{k'}a_{\alpha}^{\dagger}b_{\beta}b_{\delta}^{\dagger}a_{\gamma}a_{k}^{\dagger}a_{l}^{\dagger}b_{i}^{\dagger}b_{j}^{\dagger}|0\rangle,$$

$$\frac{1}{2}\sum_{\substack{\alpha\delta>F\\\beta\gamma<F}}\langle\alpha\beta|V|\gamma\delta\rangle\langle0|b_{j'}b_{i'}a_{l'}a_{k'}a_{\alpha}^{\dagger}b_{\beta}a_{\delta}b_{\gamma}^{\dagger}a_{k}^{\dagger}a_{l}^{\dagger}b_{i}^{\dagger}b_{j}^{\dagger}|0\rangle\ .$$

Then

$$\frac{1}{2}\sum_{\substack{\alpha\beta<F\\\delta\gamma>F}}\langle\alpha\beta|V|\gamma\delta\rangle\langle0|b_{j'}b_{i'}a_{l'}a_{k'}b_{\alpha}b_{\beta}a_{\delta}a_{\gamma}a_{k}^{\dagger}a_{l}^{\dagger}b_{i}^{\dagger}b_{j}^{\dagger}|0\rangle = 0 \tag{4.39}$$

and

$$\frac{1}{2}\sum_{\alpha\delta\beta\gamma<F}\langle\alpha\beta|V|\gamma\delta\rangle\langle0|b_{j'}b_{i'}a_{l'}a_{k'}b_{\alpha}b_{\beta}b_{\delta}^{\dagger}b_{\gamma}^{\dagger}a_{k}^{\dagger}a_{l}^{\dagger}b_{i}^{\dagger}b_{j}^{\dagger}|0\rangle \tag{4.40}$$

$$= \frac{1}{2}\sum_{\alpha\delta\beta\gamma<F}\langle\alpha\beta|V|\gamma\delta\rangle\delta_{kk'}\delta_{ll'}\langle0|b_{j'}b_{i'}b_{\alpha}b_{\beta}b_{\delta}^{\dagger}b_{\gamma}^{\dagger}b_{i}^{\dagger}b_{j}^{\dagger}|0\rangle$$

$$
= \frac{1}{2} \sum_{\alpha\beta<F} \langle \alpha\beta|V|\alpha\beta\rangle_A \delta_{ii'}\delta_{jj'}\delta_{kk'}\delta_{ll'} - \langle ij|V|i'j'\rangle_A
$$

$$
-\frac{1}{2}\delta_{kk'}\delta_{ll'} \sum_{\beta<F}[\langle i\beta|V|i'\beta\rangle\delta_{jj'} - \langle i\beta|V|j'\beta\rangle\delta_{ji'} + \langle j\beta|V|j'\beta\rangle\delta_{ii'} - \langle j\beta|V|i'\beta\rangle\delta_{ij'}]
$$

$$
+\frac{1}{2}\delta_{kk'}\delta_{ll'} \sum_{\beta<F}[\langle i\beta|V|\beta i'\rangle\delta_{jj'} - \langle i\beta|V|\beta j'\rangle\delta_{ji'} + \langle j\beta|V|\beta j'\rangle\delta_{ii'} - \langle j\beta|V|\beta i'\rangle\delta_{ij'}]
$$

$$
+\frac{1}{2}\delta_{kk'}\delta_{ll'} \sum_{\alpha<F}[\langle \alpha i|V|i'\alpha\rangle\delta_{jj'} - \langle \alpha i|V|j'\alpha\rangle\delta_{ji'} + \langle \alpha j|V|j'\alpha\rangle\delta_{ii'} - \langle \alpha j|V|i'\alpha\rangle\delta_{ij'}]
$$

$$
-\frac{1}{2}\delta_{kk'}\delta_{ll'} \sum_{\alpha<F}[\langle \alpha i|V|\alpha i'\rangle\delta_{jj'} - \langle \alpha i|V|\alpha j'\rangle\delta_{ji'} + \langle \alpha j|V|\alpha j'\rangle\delta_{ii'} - \langle \alpha j|V|\alpha i'\rangle\delta_{ij'}]
$$

$$
= \frac{1}{2} \sum_{\alpha\beta<F} \langle \alpha\beta|V|\alpha\beta\rangle_A \delta_{ii'}\delta_{jj'}\delta_{kk'}\delta_{ll'} - \langle ij|V|i'j'\rangle_A
$$

$$
-\delta_{kk'}\delta_{ll'} \sum_{\alpha<F}[\langle \alpha i|V|\alpha i'\rangle_A\delta_{jj'} - \langle \alpha i|V|\alpha j'\rangle_A\delta_{ji'} + \langle \alpha j|V|\alpha j'\rangle_A\delta_{ii'}
$$

$$
-\langle \alpha j|V|\alpha i'\rangle_A\delta_{ij'}].
$$

Finally, matrix elements of the total Hamiltonian between two 2p-2h states are written as,

$$
\langle n|\mathcal{H}|m\rangle \tag{4.41}
$$

$$
= N_n^* N_m \delta_{ii'}\delta_{jj'}\delta_{kk'}\delta_{ll'} \left[\sum_{\alpha<F}\langle \alpha|T|\alpha\rangle + \frac{1}{2}\sum_{\alpha\beta<F}\langle \alpha\beta|V|\alpha\beta\rangle_A\right]
$$

$$
+ N_n^* N_m \delta_{ii'}\delta_{jj'}\left\{ \left[\langle k'|T|k\rangle + \sum_{\alpha<F}\langle \alpha k'|V|\alpha k\rangle_A\right]\delta_{ll'}\right.
$$

$$
- \left[\langle k'|T|l\rangle + \sum_{\alpha<F}\langle \alpha k'|V|\alpha l\rangle_A\right]\delta_{kl'} + \left[\langle l'|T|l\rangle + \sum_{\alpha<F}\langle \alpha l'|V|\alpha l\rangle_A\right]\delta_{kk'}
$$

$$
\left. - \left[\langle l'|T|k\rangle + \sum_{\alpha<F}\langle \alpha l'|V|\alpha k\rangle_A\right]\delta_{lk'}\right\}
$$

$$
- N_n^* N_m \delta_{kk'}\delta_{ll'}\left\{ \left[\langle i|T|i'\rangle + \sum_{\alpha<F}\langle \alpha i|V|\alpha i'\rangle_A\right]\delta_{jj'}\right.
$$

$$
- \left[\langle i|T|j'\rangle + \sum_{\alpha<F}\langle \alpha i|V|\alpha j'\rangle_A\right]\delta_{ji'} + \left[\langle j|T|j'\rangle + \sum_{\alpha<F}\langle \alpha j|V|\alpha j'\rangle_A\right]\delta_{ii'}
$$

$$
\left. - \left[\langle j|T|i'\rangle + \sum_{\alpha<F}\langle \alpha j|V|\alpha i'\rangle_A\right]\delta_{ij'}\right\}
$$

$$+N_n N_m \Big\{ \delta_{ii'}\delta_{jj'}\langle k'l'|V|kl\rangle_A - \delta_{kk'}\delta_{ll'}\langle ij|V|i'j'\rangle_A$$

$$+\delta_{ji'}[\langle k'i|V|kj'\rangle_A\delta_{ll'} - \langle k'i|V|lj'\rangle_A\delta_{kl'} + \langle l'i|V|lj'\rangle_A\delta_{kk'} - \langle l'i|V|kj'\rangle_A\delta_{lk'}]$$

$$+\delta_{ij'}[\langle k'j|V|ki'\rangle_A\delta_{ll'} - \langle k'j|V|li'\rangle_A\delta_{kl'} + \langle l'j|V|li'\rangle_A\delta_{kk'} - \langle l'j|V|ki'\rangle_A\delta_{lk'}]$$

$$-\delta_{ii'}[\langle k'j|V|kj'\rangle_A\delta_{ll'} - \langle k'j|V|lj'\rangle_A\delta_{kl'} + \langle l'j|V|lj'\rangle_A\delta_{kk'} - \langle l'j|V|kj'\rangle_A\delta_{lk'}]$$

$$-\delta_{jj'}[\langle k'i|V|ki'\rangle_A\delta_{ll'} - \langle k'i|V|li'\rangle_A\delta_{kl'} + \langle l'i|V|li'\rangle_A\delta_{kk'} - \langle l'i|V|ki'\rangle_A\delta_{lk'}] \Big\}$$

The explicit matrix elements of kinetic energy and interaction have,

$$\langle \alpha|T|\beta\rangle = \int d\mathbf{x}\,\psi_\alpha^*(\mathbf{x})T\psi_\beta(\mathbf{x}) \tag{4.42}$$

$$\langle \alpha\beta|V|\gamma\delta\rangle = \int d\mathbf{x}_1 d\mathbf{x}_2 \psi_\alpha^*(\mathbf{x}_1)\psi_\beta^*(\mathbf{x}_2)V\psi_\delta(\mathbf{x}_2)\psi_\gamma(\mathbf{x}_1). $$

Here, $\psi_\alpha(\mathbf{x})$ is the single particle wave function which has the form of plane wave function in nuclear matter,

$$\psi_\alpha(\mathbf{x}) = \frac{1}{\sqrt{V}}\varphi(p,s,\tau)\exp(i\mathbf{p}\cdot\mathbf{x}), \tag{4.43}$$

where s and τ represent spin and isospin respectively. For the relativistic kinetic energy operator, it is written as,

$$\begin{aligned}
\langle \alpha|T|\beta\rangle &= \frac{1}{V}\int d\mathbf{x}\,\overline{\varphi}(p_\alpha,s_\alpha,\tau_\alpha)e^{-i\mathbf{P}_\alpha\cdot\mathbf{x}}(-i\boldsymbol{\gamma}\cdot\boldsymbol{\nabla}+M)\varphi(p_\beta,s_\beta,\tau_\beta)e^{i\mathbf{P}_\beta\cdot\mathbf{x}} \tag{4.44}\\
&= \overline{\varphi}(p_\alpha,s_\alpha,\tau_\alpha)(\boldsymbol{\gamma}\cdot\mathbf{p}+M)\varphi(p_\beta,s_\beta,\tau_\beta)\delta_{\mathbf{P}_\alpha,\mathbf{P}_\beta}
\end{aligned}$$

and

$$\begin{aligned}
\langle \alpha\beta|V|\gamma\delta\rangle &= \frac{1}{V^2}\int d\mathbf{x}_1 d\mathbf{x}_2 \varphi^*(p_\alpha,s_\alpha,\tau_\alpha)e^{-i\mathbf{P}_\alpha\cdot\mathbf{x}_1}\varphi^*(p_\beta,s_\beta,\tau_\beta)e^{-i\mathbf{P}_\beta\cdot\mathbf{x}_2}V(\mathbf{x}_1-\mathbf{x}_2) \tag{4.45}\\
&\quad \varphi(p_\gamma,s_\gamma,\tau_\gamma)\varphi(p_\delta,s_\delta,\tau_\delta)e^{i\mathbf{P}_\gamma\cdot\mathbf{x}_1}e^{i\mathbf{P}_\delta\cdot\mathbf{x}_2}\\
&= \frac{1}{V^2}\varphi^*(p_\alpha,s_\alpha,\tau_\alpha)\varphi^*(p_\beta,s_\beta,\tau_\beta)\int d\mathbf{x}_1 d\mathbf{x}_2 e^{i(\mathbf{P}_\gamma-\mathbf{P}_\alpha)\cdot\mathbf{x}_1}e^{i(\mathbf{P}_\delta-\mathbf{P}_\beta)\cdot\mathbf{x}_2}V(\mathbf{x}_1-\mathbf{x}_2)\\
&\quad \varphi(p_\gamma,s_\gamma,\tau_\gamma)\varphi(p_\delta,s_\delta,\tau_\delta)\\
&= \frac{1}{V^2}\varphi^*(p_\alpha,s_\alpha,\tau_\alpha)\varphi^*(p_\beta,s_\beta,\tau_\beta)\left[\int d\mathbf{x}_1 d\mathbf{x}_2 e^{i(\mathbf{P}_\gamma-\mathbf{P}_\alpha)\cdot(\mathbf{x}_1-\mathbf{x}_2)}e^{i(\mathbf{P}_\delta+\mathbf{P}_\gamma-\mathbf{P}_\alpha-\mathbf{P}_\beta)\cdot\mathbf{x}_2}\right.\\
&\quad \left. V(\mathbf{x}_1-\mathbf{x}_2)\right]\varphi(p_\gamma,s_\gamma,\tau_\gamma)\varphi(p_\delta,s_\delta,\tau_\delta)\\
&= \frac{1}{V}\delta_{\mathbf{P}_\alpha+\mathbf{P}_\beta,\mathbf{P}_\gamma+\mathbf{P}_\delta}\varphi^*(p_\alpha,s_\alpha,\tau_\alpha)\varphi^*(p_\beta,s_\beta,\tau_\beta)V(\mathbf{P}_\gamma-\mathbf{P}_\alpha)\varphi(p_\gamma,s_\gamma,\tau_\gamma)\varphi(p_\delta,s_\delta,\tau_\delta)
\end{aligned}$$

$$= \frac{1}{V}\delta_{\mathbf{P}_\alpha+\mathbf{P}_\beta,\mathbf{P}_\gamma+\mathbf{P}_\delta}\varphi^*(p_\alpha,s_\alpha,\tau_\alpha)\varphi(p_\gamma,s_\gamma,\tau_\gamma)V(\mathbf{p}_\gamma-\mathbf{p}_\alpha)\varphi^*(p_\beta,s_\beta,\tau_\beta)\varphi(p_\delta,s_\delta,\tau_\delta).$$

With these equations, we can simplify the matrix elements (4.41),

$$\langle n|\mathcal{H}|m\rangle \tag{4.46}$$

$$= \langle 0|\mathcal{H}|0\rangle\delta_{n,m} + \langle n|\widetilde{\mathcal{H}}|m\rangle$$

$$= \delta_{n,m}\left[\sum_{\alpha<F}\langle\alpha|T|\alpha\rangle + \frac{1}{2}\sum_{\alpha\beta<F}\langle\alpha\beta|V|\alpha\beta\rangle\right]$$

$$+N_n^*N_m\Bigg\{\delta_{ii'}\delta_{jj'}\delta_{kk'}\delta_{ll'}(\varepsilon_k+\varepsilon_l-\varepsilon_i-\varepsilon_j) + \delta_{ii'}\delta_{jj'}\langle k'l'|V|kl\rangle_A - \delta_{kk'}\delta_{ll'}\langle ij|V|i'j'\rangle_A$$

$$+\delta_{ji'}[\langle k'i|V|kj'\rangle_A\delta_{ll'} - \langle k'i|V|lj'\rangle_A\delta_{kl'} + \langle l'i|V|lj'\rangle_A\delta_{kk'} - \langle l'i|V|kj'\rangle_A\delta_{lk'}]$$

$$+\delta_{ij'}[\langle k'j|V|ki'\rangle_A\delta_{ll'} - \langle k'j|V|li'\rangle_A\delta_{kl'} + \langle l'j|V|li'\rangle_A\delta_{kk'} - \langle l'j|V|ki'\rangle_A\delta_{lk'}]$$

$$-\delta_{ii'}[\langle k'j|V|kj'\rangle_A\delta_{ll'} - \langle k'j|V|lj'\rangle_A\delta_{kl'} + \langle l'j|V|lj'\rangle_A\delta_{kk'} - \langle l'j|V|kj'\rangle_A\delta_{lk'}]$$

$$-\delta_{jj'}[\langle k'i|V|ki'\rangle_A\delta_{ll'} - \langle k'i|V|li'\rangle_A\delta_{kl'} + \langle l'i|V|li'\rangle_A\delta_{kk'} - \langle l'i|V|ki'\rangle_A\delta_{lk'}]\Bigg\}$$

where the matrix element is split into two terms. The first term is related with the ground state $\langle 0|\mathcal{H}|0\rangle$ and the second term is completely dependent on 2p-2h states $\langle n|\widetilde{\mathcal{H}}|m\rangle$. Furthermore, ε_k is the single-particle energies of the Hartree-Fock equation,

$$\langle k|T|l\rangle + \sum_{\alpha<F}\langle\alpha k|V|\alpha l\rangle_A = \varepsilon_k\delta_{kl}. \tag{4.47}$$

Therefore, the expectation value of many-body Hamiltonian (4.24) is written as,

$$\langle\Psi|\mathcal{H}|\Psi\rangle \tag{4.48}$$

$$= \sum_{\alpha<F}\langle\alpha|T|\alpha\rangle + \frac{1}{2}\sum_{\alpha\beta<F}\langle\alpha\beta|V|\alpha\beta\rangle_A - \sum_m C_0^*C_m\langle ij|V|kl\rangle_A$$

$$-\sum_n C_0C_n^*\langle k'l'|V|i'j'\rangle_A + \sum_{mn}C_n^*C_m\langle n|\widetilde{\mathcal{H}}|m\rangle.$$

The coefficients in the nucleon ground state, C_0, C_m should be determined by the variational principle,

$$\frac{\delta\left[\langle\Psi|\mathcal{H}|\Psi\rangle - E(C_0^*C_0 + \sum_m C_m^*C_m)\right]}{\delta C_m^*} = 0. \tag{4.49}$$

where, E is the Lagrange multiplier, which corresponds to the total energy of the whole system. Therefore, we can obtain a set of linear equations about C_0 and C_m,

$$C_0\langle m|\mathcal{H}|0\rangle + \sum_n C_n\langle m|\mathcal{H}|n\rangle = EC_m \tag{4.50}$$

Furthermore, the hole state $\varphi_i^*(\mathbf{r})$ also should be obtained from the variational principle,

$$\frac{\delta[\langle\Psi|\mathcal{H}|\Psi\rangle - \sum_i \varepsilon_i \int d^3\mathbf{r}\varphi_i^*(\mathbf{r})\varphi_i(\mathbf{r})]}{\delta\varphi_i^*(\mathbf{r})} = 0, \tag{4.51}$$

where ε_i is a Lagrange multiplier, which corresponds to a single particle energy of $\varphi_i^*(\mathbf{r})$. Finally, we can make the self consistent calculation with Eq. (4.50) and (4.51) to obtain the total energy of the whole system. We get a more explicit form about a hole state as,

$$\frac{\partial}{\partial\varphi_i^*(\mathbf{r})}\langle 0|\mathcal{H}|0\rangle + \sum_m C_0^* C_m \frac{\partial}{\partial\varphi_i^*(\mathbf{r})}\langle 0|\mathcal{H}|m\rangle + \sum_{m,n} C_n^* C_m \frac{\partial}{\partial\varphi_i^*(\mathbf{r})}\langle n|\widetilde{\mathcal{H}}|m\rangle \tag{4.52}$$

$$= \varepsilon_i\varphi_i(\mathbf{r}).$$

The first term of Eq. (4.52) is the ordinary Hartree-Fock equation of single particle state,

$$\frac{\partial}{\partial\varphi_i^*(\mathbf{r})}\langle 0|\mathcal{H}|0\rangle = T|i\rangle + \sum_j \langle\cdot j|V|ij\rangle_A, \tag{4.53}$$

where, the term $\langle\cdot j|V|ij\rangle_A$ denotes the interaction matrix without the i state indicated by a dot in the bra-state with the anti-symmetrization indicated by the suffix A in the ket side. While the non-diagonal matrix elements between the 0p-0 state and 2p-2h states are expressed as before,

$$\langle 0|\mathcal{H}|m\rangle = -N_m\langle ij|V|kl\rangle_A. \tag{4.54}$$

The variation for this non-diagonal term with single particle state is

$$\frac{\partial}{\partial\varphi_i^*(\mathbf{r})}\langle 0|\mathcal{H}|m\rangle = -N_m\langle\cdot j|V|kl\rangle_A. \tag{4.55}$$

Now, the equation of motion for the single particle state is written as,

$$T|i\rangle + \sum_j \langle\cdot j|V|ij\rangle_A - C_0^* \sum_m N_m C_m \langle\cdot j|V|kl\rangle_A + \sum_{m,n} C_n^* C_m \frac{\partial\mathcal{H}_{nm}^{2p-2h}}{\partial\varphi_i^*(\mathbf{r})} = \varepsilon_i|i\rangle. \tag{4.56}$$

This equation has the similar structure to that of the Brueckner-Hartree-Fock model and we have abbreviated the matrix elements $\langle n|\widetilde{\mathcal{H}}|m\rangle$ as $\mathcal{H}_{nm}^{2p-2h}$. To continue calculations , we need solve Eq.(4.50) for C_n,

$$C_n = \sum_m [E\delta_{n,m} - \langle n|\mathcal{H}|m\rangle]^{-1}\langle m|\mathcal{H}|0\rangle C_0. \tag{4.57}$$

We substitute this expression in Eq. (4.56) and find the following equation, which does not contain the coefficients C_m,

$$T|i\rangle + \sum_j \langle\cdot j|V|ij\rangle_A + |C_0|^2 \sum_{m,n} \frac{\partial}{\partial\varphi_i^*(\mathbf{r})}\langle 0|\mathcal{H}|m\rangle \frac{1}{E\delta_{n,m} - \langle n|\mathcal{H}|m\rangle}\langle n|\mathcal{H}|0\rangle \tag{4.58}$$

$$+|C_0|^2 \sum_{m,n} \langle 0|\mathcal{H}|m\rangle \frac{1}{E\delta_{n,m} - \langle n|\mathcal{H}|m\rangle} \frac{\partial \mathcal{H}_{nm}^{2p-2h}}{\partial \varphi_i^*(\mathbf{r})} \frac{1}{E\delta_{n,m} - \langle n|\mathcal{H}|m\rangle} \langle n|\mathcal{H}|0\rangle = \varepsilon_i|i\rangle.$$

This equation can be expressed in a simpler way to compare with the ordinary Hartree-Fock equation,

$$T|i\rangle + \frac{\partial \sum_{ij} \langle ij|\tilde{V}|ij\rangle_A}{\partial \varphi_i^*} = \varepsilon_i|i\rangle, \tag{4.59}$$

where we have defined a new effective potential $\tilde{V}$ to replace the bare NN interaction V as,

$$\tilde{V} = |C_0|^2 V + |C_0|^2 \sum_{m,n} \langle 0|\mathcal{H}|m\rangle \frac{1}{E\delta_{n,m} - \langle n|\mathcal{H}|m\rangle} \langle n|\mathcal{H}|0\rangle. \tag{4.60}$$

When we derive this effective potential from Eq. (4.58), we should take care of a partial derivative on the denominator part of the second term in Eq. 4.60.

Matrix elements between 2p-2h states are very complicated as we showed before. We should take some approximation to simplify the numerical calculation when we apply this framework to nuclear matter. The non-diagonal terms in 2p-2h matrix elements are removed and we just keep the diagonal terms,

$$\begin{aligned}
\langle n|\mathcal{H}|m\rangle &= (\langle 0|\mathcal{H}|0\rangle + \varepsilon_k + \varepsilon_l - \varepsilon_i - \varepsilon_j)\delta_{n,m} \\
&= (\langle 0|\mathcal{H}|0\rangle + E_{2p-2h})\delta_{n,m}.
\end{aligned} \tag{4.61}$$

And the coefficient C_n is now expressed as,

$$C_n = [E - (\langle 0|\mathcal{H}|0\rangle + E_{2p-2h})]^{-1} \langle n|\mathcal{H}|0\rangle C_0. \tag{4.62}$$

With this approximation, the equation of motion for single particle state and the effective interaction becomes,

$$T|i\rangle + \sum_j \langle \cdot j|V|ij\rangle_A + |C_0|^2 \sum_m \frac{\partial}{\partial \varphi_i^*(\mathbf{r})} \langle 0|\mathcal{H}|m\rangle \frac{1}{E - \langle 0|\mathcal{H}|0\rangle - E_{2p-2h}} \langle m|\mathcal{H}|0\rangle \tag{4.63}$$

$$+|C_0|^2 \sum_m \langle 0|\mathcal{H}|m\rangle \frac{1}{E - \langle 0|\mathcal{H}|0\rangle - E_{2p-2h}} \frac{\partial E_{2p-2h}}{\partial \varphi_i^*(\mathbf{r})} \frac{1}{E - \langle 0|\mathcal{H}|0\rangle - E_{2p-2h}} \langle m|\mathcal{H}|0\rangle = \varepsilon_i|i\rangle$$

and

$$\tilde{V} = |C_0|^2 V + |C_0|^2 \sum_m \frac{|\langle 0|\mathcal{H}|m\rangle|^2}{E - \langle 0|\mathcal{H}|0\rangle - E_{2p-2h}}. \tag{4.64}$$

Now the total energy can be written as,

$$E = \langle 0|\mathcal{H}|0\rangle + 2|C_0|^2 \sum_m \frac{|\langle 0|\mathcal{H}|m\rangle|^2}{E - \langle 0|\mathcal{H}|0\rangle - E_{2p-2h}} \tag{4.65}$$

$$+|C_0|^2 \sum_m \frac{|\langle 0|\mathcal{H}|m\rangle|^2 E_{2p-2h}}{(E - \langle 0|\mathcal{H}|0\rangle - E_{2p-2h})^2}$$

The normalization condition of coefficient C_m has,

$$|C_0|^2 + |C_0|^2 \sum_m \frac{|\langle 0|\mathcal{H}|m\rangle|^2}{(E - \langle 0|\mathcal{H}|0\rangle - E_{2p-2h})^2} = 1. \tag{4.66}$$

We can solve the many-body problem in nuclear matter though Eqs.(4.63)-(4.66) with numerical calculation. To make this process more clear, we would like to make another approximation,

$$E - \langle 0|\mathcal{H}|0\rangle \sim 0 \quad \text{and} \quad \frac{\partial E_{2p-2h}}{\partial \varphi_i^*(\mathbf{r})} \tag{4.67}$$

which is taken by the perturbation theory. This approximation makes Eqs.(4.63)-(4.66) as,

$$T|i\rangle + \sum_j \langle \cdot j|V|ij\rangle_A - |C_0|^2 \sum_m \frac{\partial}{\partial \varphi_i^*(\mathbf{r})} \langle 0|\mathcal{H}|m\rangle \frac{1}{E_{2p-2h}} \langle m|\mathcal{H}|0\rangle = \varepsilon_i |i\rangle \tag{4.68}$$

$$E = \langle 0|\mathcal{H}|0\rangle - |C_0|^2 \sum_m \frac{|\langle 0|\mathcal{H}|m\rangle|^2}{E_{2p-2h}}$$

$$|C_0|^2 + |C_0|^2 \sum_m \frac{|\langle 0|\mathcal{H}|m\rangle|^2}{E_{2p-2h}^2} = 1.$$

These equations can be solved in the momentum space, where the quantum numbers, k, l, i, j, takes corresponding momenta.

$$T|i\rangle + \sum_j \langle \cdot j|V|ij\rangle_A - |C_0|^2 \sum_{j,k,l} \frac{\langle \cdot j|V|kl\rangle \langle kl|V|ij\rangle_A}{E_{2p-2h}} = \varepsilon_i |i\rangle \tag{4.69}$$

$$E = \sum_i \langle i|T|i\rangle + \frac{1}{2} \sum_{i,j} \langle ij|V|ij\rangle_A - \frac{|C_0|^2}{2} \sum_{i,j,k,l} \frac{\langle ij|V|kl\rangle \langle kl|V|ij\rangle_A}{E_{2p-2h}}$$

$$|C_0|^2 + |C_0|^2 \sum_{i,j,k,l} \frac{\langle ij|V|kl\rangle \langle kl|V|ij\rangle_A}{E_{2p-2h}^2} = 1.$$

Therefore, we can define a new effective potential $\widetilde{V}$, which is related with the bare NN interaction V as,

$$\widetilde{V} = |C_0|^2 V - |C_0|^2 V \frac{Q}{E_{2p-2h}} V, \tag{4.70}$$

where Q, the Pauli principle projection operator, projects out states with two nucleons above the Fermi sea:

$$Q|\alpha\beta\rangle = \begin{cases} 1 & \text{for } \alpha \text{ and } \beta \text{ above the } \varepsilon_F \\ 0 & \text{for } \alpha \text{ and } \beta \text{ at or below the } \varepsilon_F. \end{cases} \tag{4.71}$$

$$\varepsilon_i = \frac{k_i^2}{2M} + U(k_i) \tag{4.72}$$

The single particle potential is determined by the interaction of each nucleon with all others in the Fermi sea; For nucleons below the Fermi level it is defined by

$$\langle i|U|i\rangle = U(k_i) = \sum_{j<F}\langle ij|\widetilde{V}|ij\rangle_A, \quad \text{for } i \le F, \tag{4.73}$$

which includes both direct and exchange terms. For the single particle potential above the Fermi sea, there are two different treatments. One choice is to use a zero single-particle potential above the Fermi sea which produces a gap at the Fermi surface. It is usually called standard choice.

$$\langle l|U|l\rangle = U(k_l) = 0, \quad \text{for } l \ge F. \tag{4.74}$$

Alternatively, a continuous choice for U can be made by defining,

$$\langle i|U|i\rangle = U(k_i) = \text{Re} \sum_{j<F}\langle ij|\widetilde{V}|ij\rangle_A \tag{4.75}$$

for all states i below and above the Fermi surface. In this note, we will mainly discuss with the standard choice. To determine the hole-state potential $U(k_i)$, we use the effective mass approximation for the non-relativistic Hartree-Fock case.

$$U(k_i) = U + \frac{M - M^*}{2MM^*}k_i^2, \tag{4.76}$$

where the potential depth U and effective mass M^* are the self-consistent parameters, while M is the nucleon mass. This single-particle potential is set equal to zero above the Fermi surface. We will discuss the relativistic case in the next section.

When we find the effective interaction $\widetilde{V}$, the binding energy of total system can be evaluated from

$$\begin{aligned} E &= \sum_{i<F}\langle i|T|i\rangle + \frac{1}{2}\sum_{i,j\le F}\langle ij|\widetilde{V}|ij\rangle_A \\ &= \sum_{i<F}(\varepsilon_i - \frac{1}{2}U_i). \end{aligned} \tag{4.77}$$

Here, i (or j) denotes a plane-wave state in the Fermi sea with momentum $\boldsymbol{k}_i$, spin s_i and isospin t_i; T is the kinetic energy operator. It is seen that $\widetilde{V}$ plays the role of an effective two-body interaction in the nuclear medium.

We can now write Eq. (4.70) explicitly in the relative and c.m. momenta,

$$\langle \mathbf{q}'|\widetilde{V}(\mathbf{P})|\mathbf{q}\rangle = \langle \mathbf{q}'|V|\mathbf{q}\rangle - |C_0|^2 \int \frac{d\mathbf{k}}{e(\mathbf{q},\mathbf{k},\mathbf{P})}\langle \mathbf{q}'|V|\mathbf{k}\rangle Q(\mathbf{k},\mathbf{P})\langle \mathbf{k}|V|\mathbf{q}\rangle, \tag{4.78}$$

where $\mathbf{P} = \frac{1}{2}(\mathbf{k}_m + \mathbf{k}_n)$ denotes the c.m. momentum and $\mathbf{q} = \frac{1}{2}(\mathbf{k}_m - \mathbf{k}_n)$, $\mathbf{k}$ the relative momentum of the initial and intermediate states. The Pauli projection operator Q is defined by

$$Q(\mathbf{k}, \mathbf{P}) = \begin{cases} 1 & \text{for}|\mathbf{P} \pm \mathbf{k}| > k_F, \\ 0 & \text{otherwise}, \end{cases} \tag{4.79}$$

and the energy denominate e is

$$e(\mathbf{q}, \mathbf{k}, \mathbf{P}) = E(\mathbf{P} + \mathbf{k}) + E(\mathbf{P} - \mathbf{k}) - W(\mathbf{q}, \mathbf{P}) \tag{4.80}$$

Here, E is the single-particle energy in the intermediate state and W the so-called starting energy. The latter involves the single-hole energies in the initial state and is calculated on the energy shell, i.e.

$$W(\mathbf{q}, \mathbf{P}) = E(\mathbf{P} + \mathbf{q}) + E(\mathbf{P} - \mathbf{q}). \tag{4.81}$$

In the nuclear matter, the single-particle energies are function of $|\mathbf{k}_m|$,

$$E(k_i) = \frac{k_i^2}{2M} + U(|\mathbf{k}_i|). \tag{4.82}$$

With the effective mass approximation (4.76), the resulting energy denominator e is

$$e(q, k, P) = \frac{k^2 + \gamma^2(q, P)}{M}, \tag{4.83}$$

where

$$\gamma^2(q, P) = \left(1 - \frac{M}{M^*}\right)(q^2 + P^2) - 2MA - q^2. \tag{4.84}$$

We can find that the energy denominator e is independent of the angle between $\mathbf{P}$ and $\mathbf{k}$, and between $\mathbf{P}$ and $\mathbf{q}$.

In order to simplify Eq. (4.70), the angle-averaged Pauli projector $\overline{Q}(k, P)$ is used.

$$\overline{Q}(k, P) = \begin{cases} 0 & k \le (k_F^2 - P^2)^{\frac{1}{2}} \\ \frac{k^2 + P^2 - k_F^2}{2kP} & (k_F^2 - P^2)^{\frac{1}{2}} \le k \le k_F + P \\ 1 & k > k_F + P \end{cases} \tag{4.85}$$

The correction to this approximation is very small [11]. Using the angle-averaged $\overline{Q}$ and the effective mass approximation, Eq. (4.70) becomes,

$$\langle \mathbf{q}'|\widetilde{V}(\mathbf{P})|\mathbf{q}\rangle = \langle \mathbf{q}'|V|\mathbf{q}\rangle - |C_0|^2 M \int \frac{d\mathbf{k}}{k^2 + \gamma^2} \overline{Q}(k, P)\langle \mathbf{q}'|V|\mathbf{k}\rangle\langle \mathbf{k}|V|\mathbf{q}\rangle. \tag{4.86}$$

To take advantage of the simple helicity representation of the momentum space potential, we can use the decomposition of the effective interaction $\widetilde{V}$ into helicity states as well. We can apply the partial wave representation of the effective interaction $\widetilde{V}$,

$$\langle \mathbf{q}'\lambda_1'\lambda_2'|\widetilde{V}|\mathbf{q}\lambda_1\lambda_2\rangle = \sum_{JM}\langle \hat{\mathbf{q}}'\lambda_1'\lambda_2'|JM\lambda_1'\lambda_2'\rangle\langle JM\lambda_1\lambda_2|\hat{\mathbf{q}}\lambda_1\lambda_2\rangle\langle\lambda_1'\lambda_2'|\widetilde{V}^J(q',q)|\lambda_1\lambda_2\rangle. \quad (4.87)$$

Finally, we easily find the integral equation for effective interaction $\widetilde{V}$ in the basis of the angular momentum states $|JM\lambda_1\lambda_2\rangle$ as,

$$\langle\lambda_1'\lambda_2'|\widetilde{V}^J(q',q)|\lambda_1\lambda_2\rangle = \langle\lambda_1'\lambda_2'|V^J(q',q)|\lambda_1\lambda_2\rangle \quad (4.88)$$

$$-|C_0|^2 M \sum_{h_1,h_2}\int \frac{k^2 dk}{k^2+\gamma^2}\overline{Q}(k,P)\langle\lambda_1'\lambda_2'|V^J(q',k)|h_1 h_2\rangle\langle h_1 h_2|V^J(k,q)|\lambda_1\lambda_2\rangle$$

After h_1 and h_2 are summed over, Eq. (4.70) in helicity representation can be separated into six coupled integral equations,

$$^0\widetilde{V}^J(q',q) = {}^0V^J(q',q)|C_0|^2 - M|C_0|^2\int \frac{k^2 dk}{k^2+\gamma^2}\overline{Q}(k,P)\, {}^0V^J(q',k)\, {}^0V^J(k,q), \quad (4.89)$$

$$^1\widetilde{V}^J(q',q) = {}^1V^J(q',q)|C_0|^2 - M|C_0|^2\int \frac{k^2 dk}{k^2+\gamma^2}\overline{Q}(k,P)\, {}^1V^J(q',k)\, {}^1V^J(k,q), \quad (4.90)$$

$$^{12}\widetilde{V}^J(q',q) = {}^{12}V^J(q',q)|C_0|^2 - M|C_0|^2\int \frac{k^2 dk}{k^2+\gamma^2}\overline{Q}(k,P)[\, {}^{12}V^J(q',k)\, {}^{12}V^J(k,q) \quad (4.91)$$

$$+ {}^{55}V^J(q',k)\, {}^{66}V^J(k,q)],$$

$$^{34}\widetilde{V}^J(q',q) = {}^{34}V^J(q',q)|C_0|^2 - M|C_0|^2\int \frac{k^2 dk}{k^2+\gamma^2}\overline{Q}(k,P)[\, {}^{34}V^J(q',k)\, {}^{34}V^J(k,q) \quad (4.92)$$

$$+ {}^{66}V^J(q',k)\, {}^{55}V^J(k,q)],$$

$$^{55}\widetilde{V}^J(q',q) = {}^{55}V^J(q',q)|C_0|^2 - M|C_0|^2\int \frac{k^2 dk}{k^2+\gamma^2}\overline{Q}(k,P)[\, {}^{12}V^J(q',k)\, {}^{55}V^J(k,q) \quad (4.93)$$

$$+ {}^{55}V^J(q',k)\, {}^{34}G^J(k,q)],$$

$$^{66}\widetilde{V}^J(q',q) = {}^{66}V^J(q',q)|C_0|^2 - M|C_0|^2\int \frac{k^2 dk}{k^2+\gamma^2}\overline{Q}(k,P)[\, {}^{34}V^J(q',k)\, {}^{66}V^J(k,q) \quad (4.94)$$

$$+ {}^{66}V^J(q',k)\, {}^{12}V^J(k,q)],$$

where the notations of V can be found in appendix D.

Now we can express the nuclear matter ground state energy per particle in terms of the helicity state of $\widetilde{V}$-matrix. Using the continuity condition $\sum_k \to [V/(2\pi)^3]\int d\mathbf{k}$, Eq. (4.77) can be written as

$$\frac{E}{A} = \frac{3}{5}\frac{k_F^2}{2M} + \frac{1}{2\rho}\frac{1}{(2\pi)^3}\int d\mathbf{q}\int_\Gamma d\mathbf{P}\sum_{m_1,m_2}\langle\mathbf{q}m_1 m_2|\widetilde{V}(q,P)(1-P_{12})|\mathbf{q}m_1 m_2\rangle, \quad (4.95)$$

where m denotes the spin and isospin quantum numbers of the nucleon and Γ is the integration region: $|\mathbf{q} \pm \mathbf{P}| < k_F$, P_{12} is an operator which exchanges particle 1 and 2. It should be mentioned that

$$\langle \mathbf{k}_m, \mathbf{k}_n | \widetilde{V} | \mathbf{k}_m, \mathbf{k}_n \rangle = \frac{(2\pi)^3}{V} \langle \mathbf{q} | \widetilde{V} | \mathbf{q} \rangle. \tag{4.96}$$

Therefore, the normalization condition of coefficient can be written as

$$|C_0|^{-2} = 1 + \frac{1}{2\rho} \frac{1}{(2\pi)^3} \int d\mathbf{q} \int_\Gamma d\mathbf{P} \sum_{m_1, m_2} \langle \mathbf{q} m_1 m_2 | C(q, P)(1 - P_{12}) | \mathbf{q} m_1 m_2 \rangle. \tag{4.97}$$

The plane-wave spin states can be transformed into angular momentum states by means of

$$|\mathbf{q} m_1 m_2\rangle = \sum_{JM} \sum_{TT_3} \langle JM\lambda_1\lambda_2 | \mathbf{q}\lambda_1\lambda_2 \rangle \langle \tfrac{1}{2} t_1 \tfrac{1}{2} t_2 | TT_3 \rangle | JM\lambda_1\lambda_2 \rangle | TT_3 \rangle. \tag{4.98}$$

Using the relation

$$\langle \tfrac{1}{2} t_1 \tfrac{1}{2} t_2 | TT_3 \rangle = (-)^{T+1} \langle \tfrac{1}{2} t_2 \tfrac{1}{2} t_2 | TT_3 \rangle, \tag{4.99}$$

and

$$(1 - P_{12}) | JM\lambda_1\lambda_2 \rangle = |JM\lambda_1\lambda_2\rangle + (-)^J |JM\lambda_2\lambda_1\rangle, \tag{4.100}$$

we obtain

$$(1 - P_{12}) | \mathbf{q} m_1 m_2 \rangle = \sum_{JM} \sum_{TT_3} \langle JM\lambda_1\lambda_2 | \mathbf{q}\lambda_1\lambda_2 \rangle \langle \tfrac{1}{2} t_1 \tfrac{1}{2} t_2 | TT_3 \rangle \{ |JM\lambda_1\lambda_2\rangle \tag{4.101}$$

$$- (-)^{J+T} |JM\lambda_2\lambda_1\rangle \} | TT_3 \rangle.$$

Inserting this equation to Eq. (4.95), and using the completeness relation,

$$\int d\Omega_q \langle JM\lambda_1\lambda_2 | \mathbf{q}\lambda_1\lambda_2 \rangle \langle \mathbf{q}\lambda_1\lambda_2 | JM\lambda_1\lambda_2 \rangle = 1, \tag{4.102}$$

the summation about t_1, t_2 gives

$$\frac{E}{A} = \frac{3}{5} \frac{k_F^2}{2M} + \frac{1}{2\rho(2\pi)^3} \sum_{JT} (2J+1)(2T+1) \int dq q^2 \int_\Gamma d\mathbf{P} \tag{4.103}$$

$$\times \sum_{\lambda_1\lambda_2} [\langle \lambda_1\lambda_2 | \widetilde{V}(q, P) | \lambda_1\lambda_2 \rangle - (-)^{T+J} \langle \lambda_1\lambda_2 | \widetilde{V}(q, P) | \lambda_2\lambda_1 \rangle].$$

When the helicity λ_1, λ_2 are summed over, the part of the summation in the above equation becomes

$$\sum_{\lambda_1\lambda_2} [M.E.] = 2 \begin{cases} \widetilde{V}_3^J(q, P) - \widetilde{V}_4^J(q, P) & \begin{cases} \text{for } J \text{ odd and } T = 1 \\ \text{or } J \text{ even and } T = 0 \end{cases} \\ 2\widetilde{V}_1^J(q, P) + \widetilde{V}_3^J(q, P) + \widetilde{V}_4^J(q, P) & \begin{cases} \text{for } J \text{ odd and } T = 0 \\ \text{or } J \text{ even and } T = 1 \end{cases} \end{cases}$$

Because of the Pauli-principle condition $|\mathbf{q} + \mathbf{P}| < \mathbf{k_F}$, the integration over $d\Omega_{\mathbf{P}}$ is given by

$$
\int d\Omega_{\mathbf{P}} =
\begin{cases}
4\pi & P \leq k_F - q \\
4\pi \frac{k_F^2 - q^2 - P^2}{2qP} & k_F - q \leq P \leq (k_F^2 - q^2)^{\frac{1}{2}} \\
0 & (k_F^2 - q^2)^{\frac{1}{2}} \leq P,
\end{cases}
\tag{4.104}
$$

We finally obtain

$$
\frac{E}{A} = \frac{3k_F^2}{10M} + \int \frac{q^2 dq}{2\pi^2 \rho} \left[\int_0^{k_F - q} P^2 dP + \int_{k_F - q}^{(k_F^2 - q^2)^{\frac{1}{2}}} P^2 dP \frac{k_F^2 - q^2 - P^2}{4qP} \right] \widetilde{V}_T(q, P) \tag{4.105}
$$

Here the abbreviation has been introduced for symmetric nuclear matter.

$$
\widetilde{V}_T(q, P) = \sum_{J=\text{even}} (2J + 1)[\, {}^1\widetilde{V}^J + 3(\, {}^0\widetilde{V}^J + \, {}^{12}\widetilde{V}^J + \, {}^{34}\widetilde{V}^J)] \tag{4.106}
$$

$$
+ \sum_{J=\text{odd}} (2J + 1)[3 \, {}^1\widetilde{V}^J + \, {}^0\widetilde{V}^J + \, {}^{12}\widetilde{V}^J + \, {}^{34}\widetilde{V}^J].
$$

Following the same procedure as in the binding-energy case, we obtain the averaged single-particle potential for the occupied states,

$$
U(k_i) = 2 \left[2 \int_0^{\frac{k_F - k_i}{2}} q^2 dq + \int_{\frac{k_F - k_i}{2}}^{\frac{k_F + k_i}{2}} q^2 \frac{k_F^2 - (2q - k_i)^2}{4qk_i} \right] \widetilde{V}_T(q, P). \tag{4.107}
$$

With this equation, we can determine U and M^* in Eq. (4.76) by a self-consistent procedure. In the actual calculation, we use the EBHF equation (4.63), where $E - \langle 0|\mathcal{H}|0\rangle$ and $\frac{\partial E_{2p-2h}}{\partial \varphi_i^*(\mathbf{p})}$ are included. In this case, the total energy E is included in the EBHF equation, and therefore we have to perform iterative calculations to achieve self-consistency.

We first of all present the results of the non-relativistic case in this section. In Fig. 4.1, we plot the EOS of symmetric nuclear matter in the non-relativistic extended Brueckner Hartree-Fock (NREBHF) theory with a realistic NN interaction, Bonn B potential [31]. The binding energy is -14.2 MeV at the saturation density $\rho = 0.228$ fm^{-3}, which is slightly larger than the empirical value $\rho = 0.16$ fm^{-3}. For comparison, the EOS of symmetric nuclear matter given by the non-relativistic BHF (NRBHF) theory is also shown by dashed curve. Its behavior is very similar to the one of the NREBHF theory at low density below 0.25 fm^{-3}. As the density increases, the more repulsive contribution to the binding energy appears in the NREBHF theory, which leads to a smaller saturation density versus the one of the NRBHF theory. This is caused by the correlation energy of 2p-2h states on the kinetic energy. This correlation energy was not considered in the NRBHF theory.
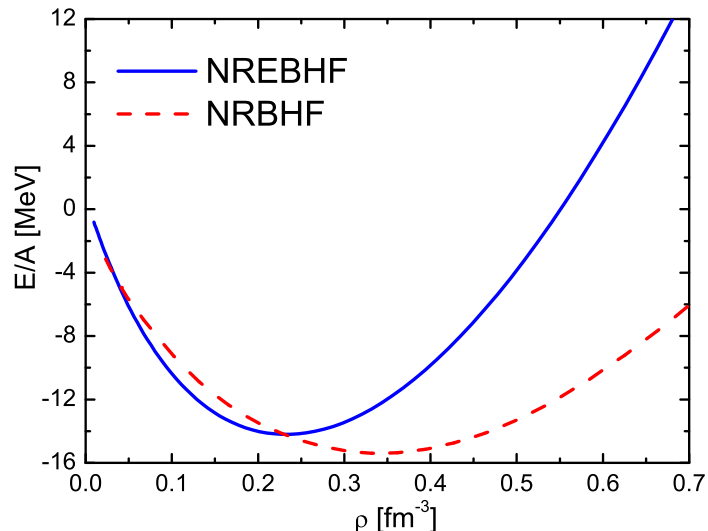
Figure 4.1: The EOS of symmetric nuclear matter in the NREBHF theory with Bonn B potential. The solid curve represents the EOS of NREBHF theory, while the dashed curve is for the NRBHF theory.

The effective nucleon mass as a function of density in the NREBHF theory with the Bonn B potential is displayed in Fig. 4.2. This quantity is extracted from Eq. 4.76 by parameterizing the single particle potential. It indicates medium effects on nucleons; its effective mass M_N^* reduces as density is increased. At the saturation density, the effective nucleon mass is about 66% of the free nucleon mass M_N in the NREBHF theory, which coincides with the result of other calculations, such as TM1 in RMF model shown in Table 2.2 . The effective nucleon masses in the NRBHF theory is denoted with square. We can find that the effective nucleon masses in two different models almost take the same value.

Furthermore, in Fig. 4.3 we also show the potential depth U in Eq. 4.76, when we parameterize the single particle potential as a function of density in the NREBHF theory. This potential depth represents the value of single particle potential at zero momentum. It becomes deeper as the density increases. At low density ($\rho \leq 0.25$ fm^{-3}), their values are very similar to the ones of the NRBHF plotted as shown by dashed curves. The decline of potential depth U in the NREBHF theory slows down with density. This behavior leads to that the binding energy of nuclear matter gets more repulsion in the NREBHF theory as compared to the one in the NRBHF theory.

The coefficient $|C_0|^2$ of the 0p-0h state of symmetric matter as a function of density in the NREBHF theory with the Bonn B potential is given in Fig. 4.4. This coefficient demonstrates the probability of nuclear wave function in the 0p-0h state, which is about 0.78 at the saturation density. This probability decreases as the density increases. The 2p-2h components become important in high density region, because the high momentum correlation of realistic NN interaction such as the tensor interaction and the short range
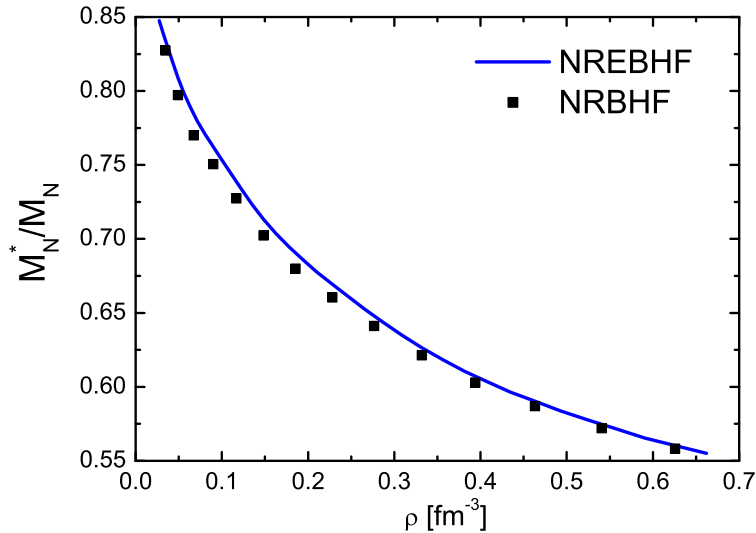
Figure 4.2: The effective nucleon mass of symmetric nuclear matter as a function of density in the NREBHF theory with the Bonn B potential. The solid curve represents the effective nucleon masses of the NREBHF theory, while the square dots denote the results of the NRBHF theory.

Figure 4.3: The depth U of the single particle potential for symmetric nuclear matter in the NREBHF theory with Bonn B potential. The solid curve represents the single particle potential of the NREBHF theory, while the dashed curve corresponds the results of the NRBHF theory.

repulsion is treated by the 2p-2h states.

We study the EOS's for various potentials in the NREBHF theory. We display the EOS's of symmetric nuclear matter with the Bonn A, B, and C potentials in Fig. 4.5. Their differences appear in the tensor interaction [11]. The tensor interaction is the strongest in the Bonn C potential. Their binding energies per particle are very similar to with each other below $\rho = 0.1$ fm $^{-3}$. The EOS of Bonn C is the first to saturate at $\rho = 0.170$ fm^{-3}, while
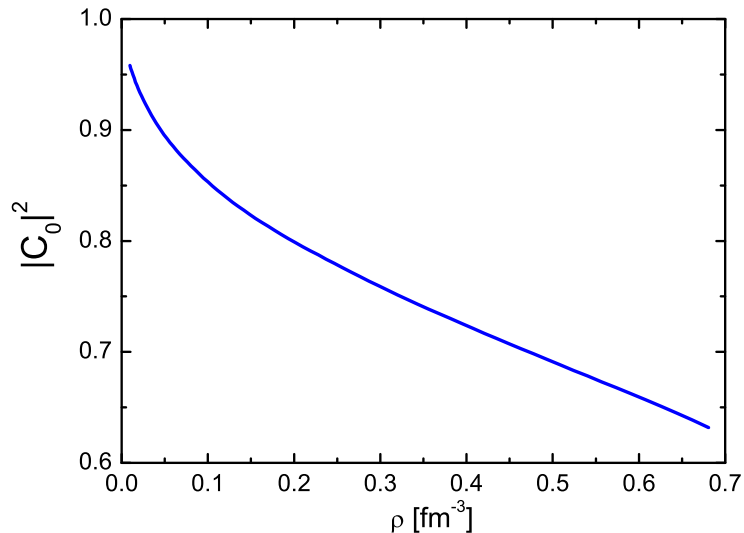
Figure 4.4: The coefficient $|C_0|^2$ of symmetric nuclear matter as a function of density in the NREBHF theory with Bonn B potential.

Figure 4.5: The EOS's of symmetric nuclear matter in the NREBHF theory with the Bonn A, B, C potentials. The solid curve is obtained with Bonn B, while dashed curve for Bonn A and dash-dotted curve for Bonn C.

the EOS of Bonn A has the largest saturation binding energy. These results are consistent with the results in the NRBHF theory in Ref. [11].

The potential depths U of the single particle potentials in the NREBHF theory with Bonn A, B, C potentials are also given in Fig. 4.6. These potential depths have similar trends as the EOS's for its dependence on potentials. At low density, they are the same, while the depth of Bonn C becomes flattened at high density.

Finally, in Fig. 4.7, we plot the coefficient $|C_0|^2$ of the 0p-0h state as a function of density
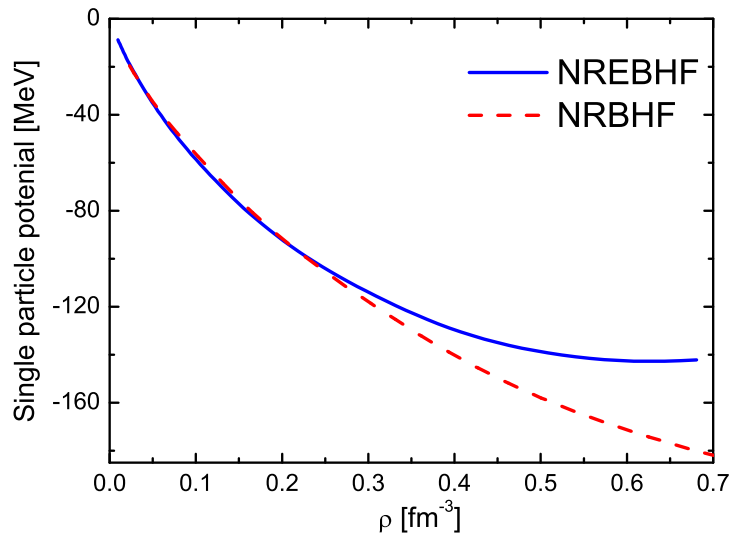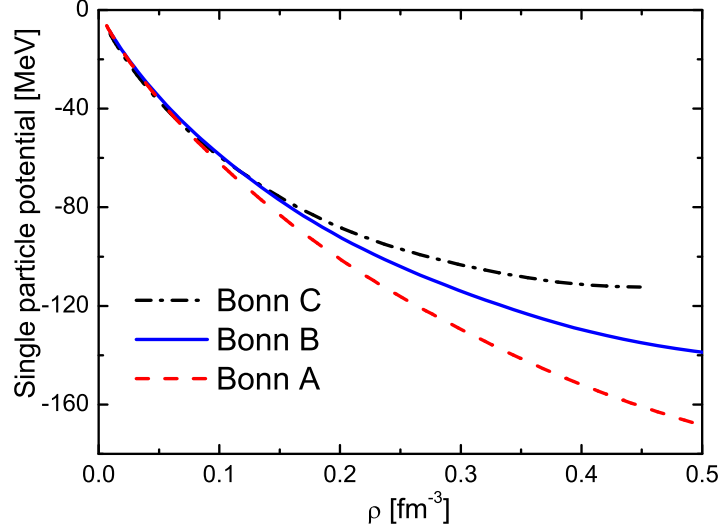
Figure 4.6: The potential depth U of the single particle potential for symmetric nuclear matter in the NREBHF theory with Bonn A, B, C potentials. The solid curve is obtained with Bonn B, while dashed curve for Bonn A and dash-dotted curve for Bonn C
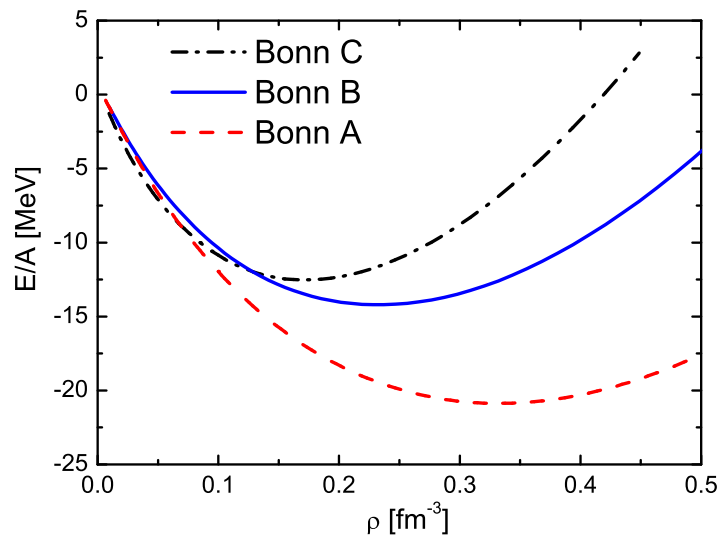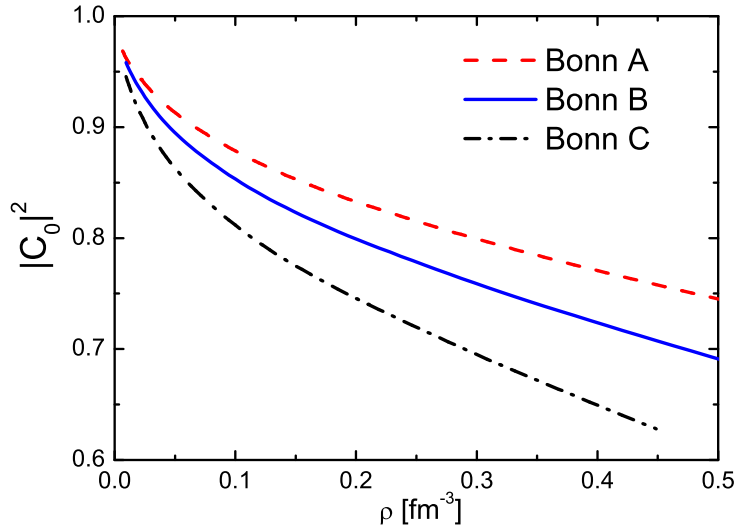

Figure 4.7: The coefficient $|C_0|^2$ as a function of density ρ in the NREBHF theory with Bonn A, B, C potentials. The solid curve is obtained with Bonn B, while dashed curve for Bonn A and dash-dotted curve for Bonn C.

in the EBHF theory with Bonn A, B, C potentials. At each density, the components of the 0p-0h state are the smallest for Bonn C potential, which means that more components of 2p-2h states are required. This is because, as we said before, the tensor interaction is strongest in the Bonn C potential. The motivation of the introduction of 2p-2h states is to properly treat the tensor interaction, and therefore the stronger tensor interaction demands more 2p-2h components.

4.3 Extended Brueckner-Hartree-Fock theory in the relativistic framework

In Chapter 4.2, we have constructed the extended Brueckner Hartree-Fock theory in the non-relativistic framework. The NREBHF theory is applied to calculate the EOS of symmetric nuclear matter with the Bonn potentials. However, the saturation properties are not completely consistent with the empirical data in the non-relativistic case. In this section, we would like to develop the EBHF theory in the relativistic framework. In the relativistic case, the essential point is to use the Dirac equation for the single-particle states in nuclear matter [91, 92, 93, 94],

$$(\boldsymbol{\alpha} \cdot \mathbf{p} + \beta M + \beta U)u(\mathbf{p}, s) = \varepsilon_p u(\mathbf{p}, s) \tag{4.108}$$

with

$$U = U_S + \gamma^0 U_V, \tag{4.109}$$

where U_S is an attractive scalar and U_V a repulsive vector field. They are in the order of several hundred MeV and strongly density dependent. In nuclear matter, they can be determined self-consistently. The solution of Eq. (4.108) is

$$u(\mathbf{p}, s) = \left(\frac{M_N^* + E^*}{2M^*} \right)^{1/2} \left[\begin{array}{c} 1 \\ \frac{\boldsymbol{\sigma} \cdot \mathbf{p}}{M_N^* + E^*} \end{array} \right] \chi(s), \tag{4.110}$$

with

$$M_N^*(p) = M_N + U_S, \tag{4.111}$$

$$E^*(p) = \sqrt{M_N^{*2} + \mathbf{p}^2}$$

and $\chi(s)$ a Pauli spinor. The normalization condition about this solution is

$$\bar{u}(\mathbf{q}, \lambda)u(\mathbf{q}, \lambda) = 1. \tag{4.112}$$

The single-particle potential

$$U(i) = \frac{M_N^*}{E_i^*} \langle i|U|i \rangle = \frac{M_N^*}{E_i^*} \langle i|U_S + \gamma^0 U_V|i \rangle = \frac{M_N^*}{E_i^*} U_S + U_V \tag{4.113}$$

is the many-body self-energy which is defined in terms of the effective interaction $\widetilde{V}$ as in the non-relativistic case,

$$U(i) = \sum_{j<F} \frac{M_N^{*2}}{E_i^* E_j^*} \langle ij|\widetilde{V}|ij \rangle_A \tag{4.114}$$

from which the constants U_S and U_V are determined. This is used for states i below and above the Fermi surface, which corresponds to the continuous choice. Note that the ansatz Eq. (4.109) is an approximation, since the scalar and vector fields are in principle momentum dependent; however, it has been shown that this momentum dependence is very weak [11].

Finally the energy in nuclear matter is obtained by

$$\frac{E}{A} = \frac{1}{A} \sum_{i<F} \frac{M_N M_N^* + \mathbf{p}_i^2}{E_i^*} + \frac{1}{2A} \sum_{i,j<F} \frac{M_N^{*2}}{E_i^* E_j^*} \langle ij|\widetilde{V}|ij\rangle_A - M. \tag{4.115}$$

The single-particle energy is

$$\begin{aligned} \varepsilon_i &= \frac{M_N^*}{E_i^*} \langle i|\boldsymbol{\gamma} \cdot \mathbf{p}_i + M|i\rangle + U(i) \\ &= E_i^* + U_V. \end{aligned} \tag{4.116}$$

Through Eqs. (4.113) and (4.114), we can determine U_S and U_V self-consistently, and obtain the binding energy per particle from Eq. (4.115).

We show first the EOS of symmetric nuclear matter in the relativistic extended Brueckner-Hartree-Fock (REBHF) theory with Bonn B potential in Fig. 4.8. The binding energy is -15.27 MeV at the saturation density 0.148 fm^{-3}. The saturation properties are largely improved comparing with the results of the NREBHF theory. The saturation properties are quite close to the requirement of experiment. We also plot the EOS of the RBHF theory in this figure by dashed curve. This comparison is very similar to the case in non-relativistic version, where the more repulsive effect is obtained in the REBHF theory for the 2p-2h correlation on the kinetic energy. Now we can conclude that the REBHF theory can properly deal with the tensor interaction and the short range repulsion of the realistic NN interaction and obtain more reasonable saturation properties.

The scalar and vector components of single particle potential in the REBHF theory with Bonn B potential are given in Fig. 4.9. They are extracted from the single particle potential by using Eq. 4.113. In finite nuclei, large spin-orbit splittings can be explained with these two components. Furthermore, the nucleon effective mass is also related with the scalar potential, which is defined as $M_N^* = M_N + U_S$. We also compare these two components with the ones given by the RBHF theory. The scalar potentials U_S in REBHF and RBHF, are almost the same. It means that the nucleon effective masses of these two cases should be similar. While the vector potentials U_V in two cases are similar at low density, it becomes more repulsive for the REBHF case as density is increased. This behavior is the same as the potential depth which was discussed in the non-relativistic case.

The density distribution of nuclear matter with Hartree-Fock approximation is usually conveniently described by the step function,

$$n(k) = \begin{cases} 1 & k < k_F \\ 0 & k > k_F \end{cases}$$
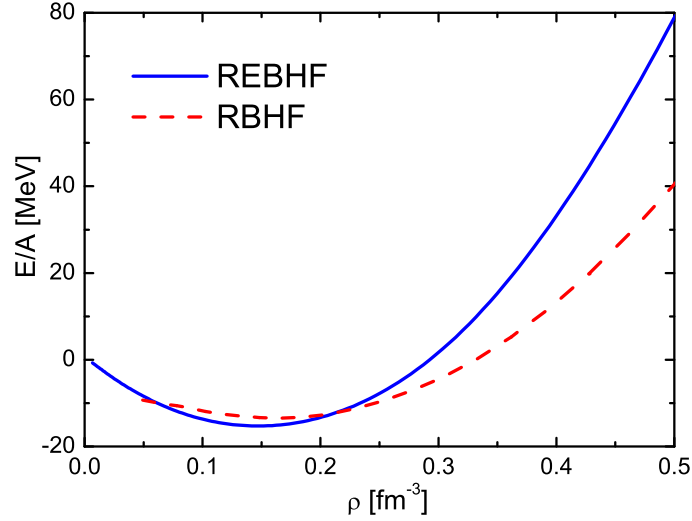
Figure 4.8: The EOS of symmetric nuclear matter in the REBHF theory with the Bonn B potential. The solid curve denotes the EOS of REBHF theory. The dashed curve is the one of the non-relativistic RBHF theory.
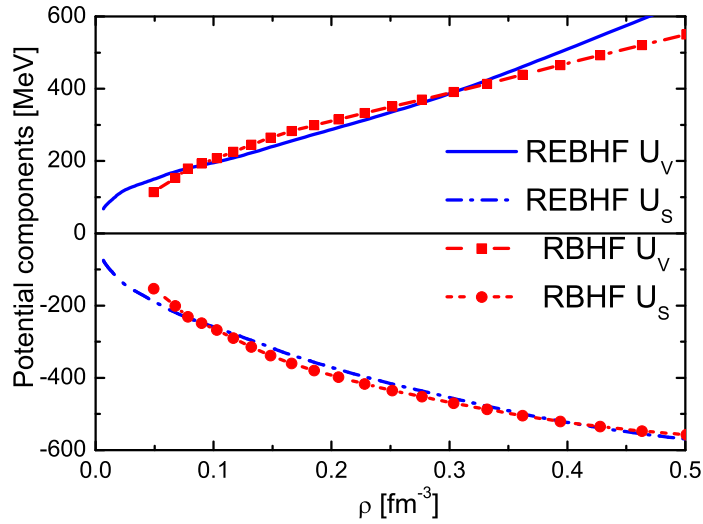
Figure 4.9: The components of the single particle potential for symmetric nuclear matter in the REBHF theory with the Bonn B potential. The solid curves denote the results of the REBHF theory and the circles and squares denote those of the RBHF theory.

It means that all of Hartree-Fock state stay under the Fermi surface. However, after introducing 2p-2h states into the nucleon ground state, the situation is changed. There is some possibility of particle state above the surface. Then density distribution is not the step function. Now we can define the density distribution of hole states, $n(i)$, as,

$$n(i) \ = \ \langle \Psi | b_i b_i^\dagger | \Psi \rangle \tag{4.117}$$

$$= 1 - \sum_{jkl} 2C_m^* C_m$$

and density distribution of particle states, $n(k)$,

$$n(k) = \langle \Psi | a_k^\dagger a_k | \Psi \rangle \qquad (4.118)$$
$$= \sum_{ijl} 2C_m^* C_m,$$

where, the subscript of coefficient, m, represent different i, j, k, l and $i, j < k_F$, $k, l > k_F$. With this definition of density distribution, we calculate the density distribution and plot the density distribution of particle and hole states in the REBHF theory with the Bonn B potential at $k_F = 1.30$ fm^{-1} in Fig. 4.10. We find that the density distribution of the hole state reduces to 0.8 at the Fermi surface. The occupied states above the Fermi momentum contribute about 0.2 close to $k_F = 1.3$ fm^{-1} due to the presence of 2p-2h states. This conclusion is consistent with the result from the self-consistent Green's function method by Dickhoff *et al.* [95].
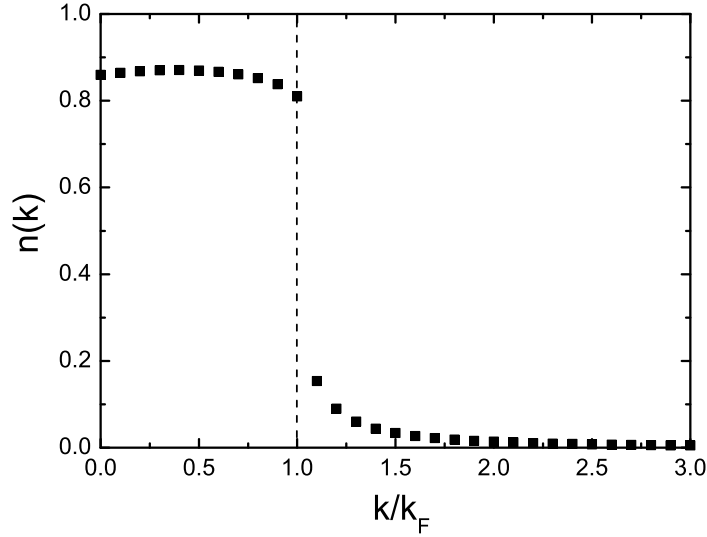
Figure 4.10: The density distributions at $k_F = 1.30$ fm^{-1} for symmetric nuclear matter in the REBHF theory with the Bonn B potential.

As for a further comment about the differences between the REBHF theory and RBHF theory, we compare the on shell matrix elements of effective interaction in the REBHF theory with the G matrix elements in RBHF theory with Bonn A potential in Fig. 4.11-4.13, where the Fermi momentum is $k_F = 1.3$ fm^{-1} ($\rho = 0.148$ fm^{-3}). We can find that large difference appears in $^1S_0$, $^3P_0$ and $^3S_1$ channels which have extra attractive contribution in the REBHF theory. The $^1S_0$ and $^3S_1$ channel usually denote the central and tensor interactions respectively. Therefore, the short range correlation in REBHF theory is stronger than the

G-matrix of RBHF theory. However, the tensor correlation with 2p-2h states in the REBHF theory is smaller than the G matrix in the RBHF theory.

Figure 4.11: The on-shell matrix elements of effective interactions in the REBHF theory and RBHF theory with $k_F = 1.35$ fm^{-1} for $J = 0$.

We also plot these comparisons at high Fermi momentum $k_F = 1.8$ ($\rho = 0.3939$ fm^{-3}) in Fig.4.14-4.16. Now the changes also happen in $^3P_1$ channel besides $^1S_0$, $^3P_0$ and $^3S_1$ channels.

In Fig. 4.17, we plot the EOS's of symmetric nuclear matter in the REBHF theory with the Bonn A, B, C potential. Their differences increase with density. The EOS of Bonn A has the largest binding energy.

The saturation properties of symmetric nuclear matter in the RBHF and REBHF theories with the Bonn potentials have been listed in Table 4.1, respectively. The binding energy of each potential at saturation density in the REBHF theory is larger than the one of the RBHF theory and the corresponding EOS becomes larger. These results can be both explained by the 2p-2h correlation on the kinetic energy. Now, the saturation properties of Bonn B in the REBHF theory have been compared with the empirical data very well.

The coefficients $|C_0|^2$ of 0p-0h states for symmetric nuclear matter in the REBHF theory with the Bonn A, B, C potentials in Fig. 4.18. We see more 2p-2h components due to stronger tensor correlation for the Bonn C potential. Meanwhile, their values are smaller than the ones of non-relativistic case. It is about 0.71 at the saturation density for the
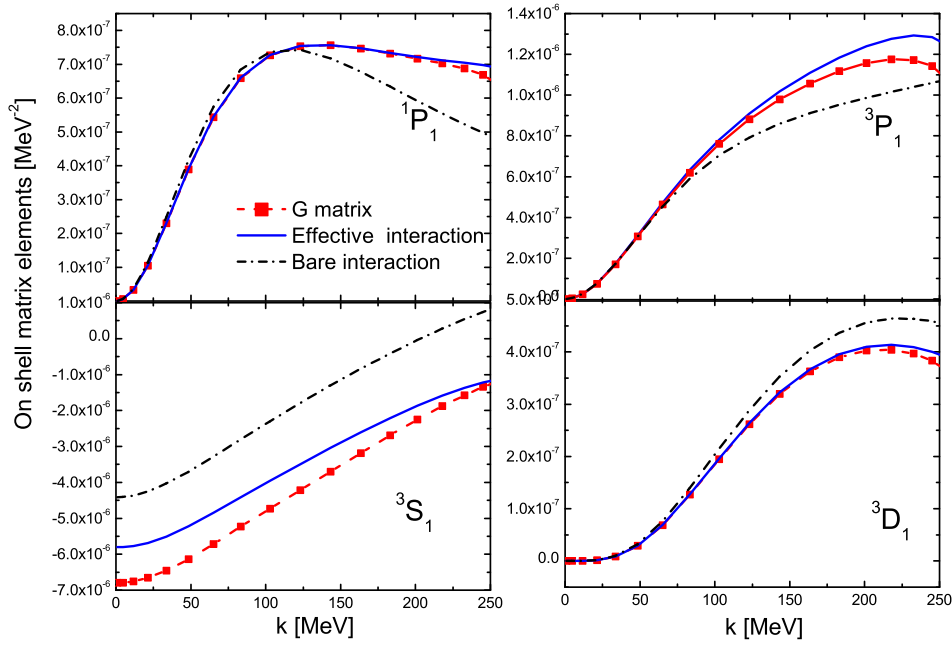
Figure 4.12: The on-shell matrix elements of effective interactions in the REBHF theory and RBHF theory with $k_F = 1.35$ fm^{-1} for $J = 1$
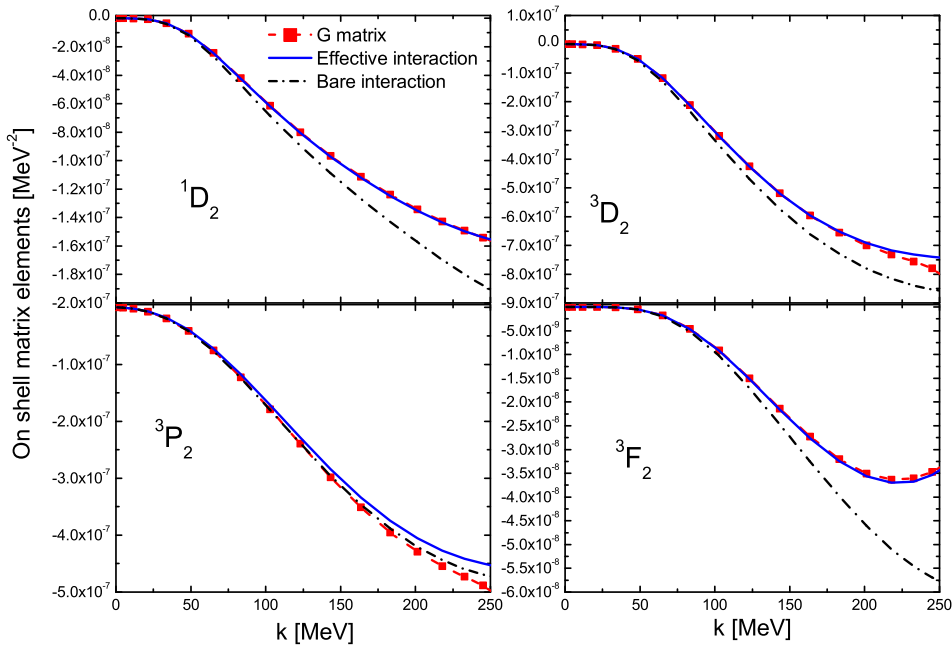
Figure 4.13: The on-shell matrix elements of effective interactions in the REBHF theory and RBHF theory with $k_F = 1.35$ fm^{-1} for $J = 2$

Bonn B potential. This result indicates that 2p-2h states play more important role in the relativistic framework.
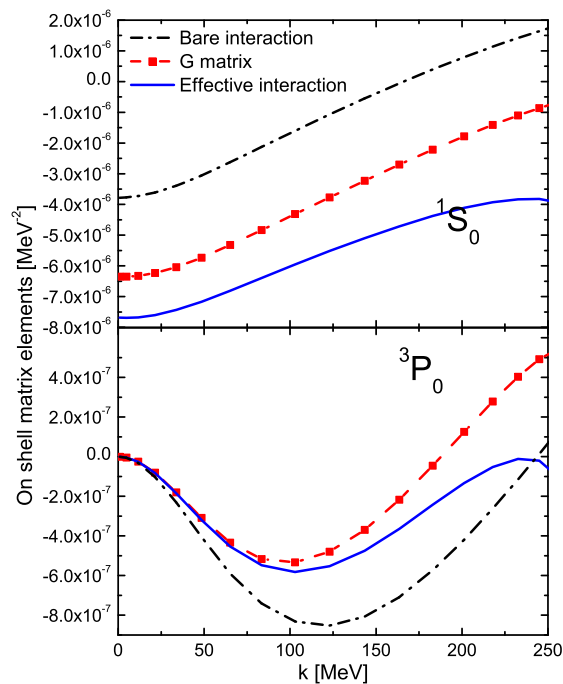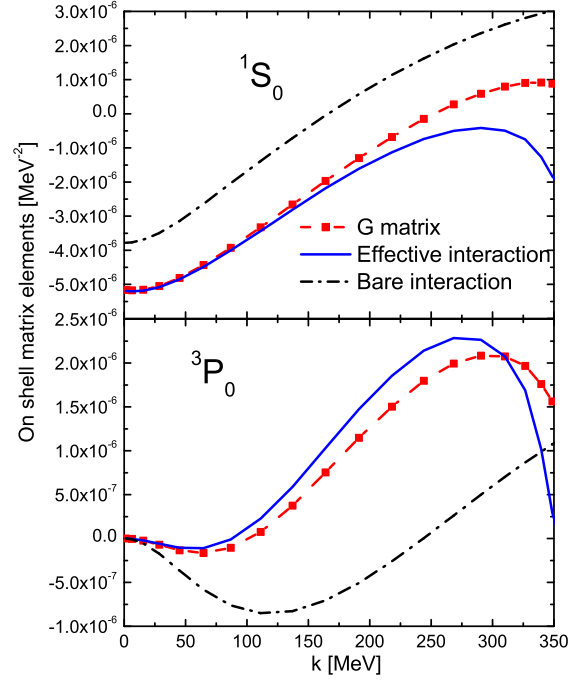
Figure 4.14: The on-shell matrix elements of effective interactions in REBHF theory and RBHF theory with $k_F = 1.8$ fm^{-1} for $J = 0$.
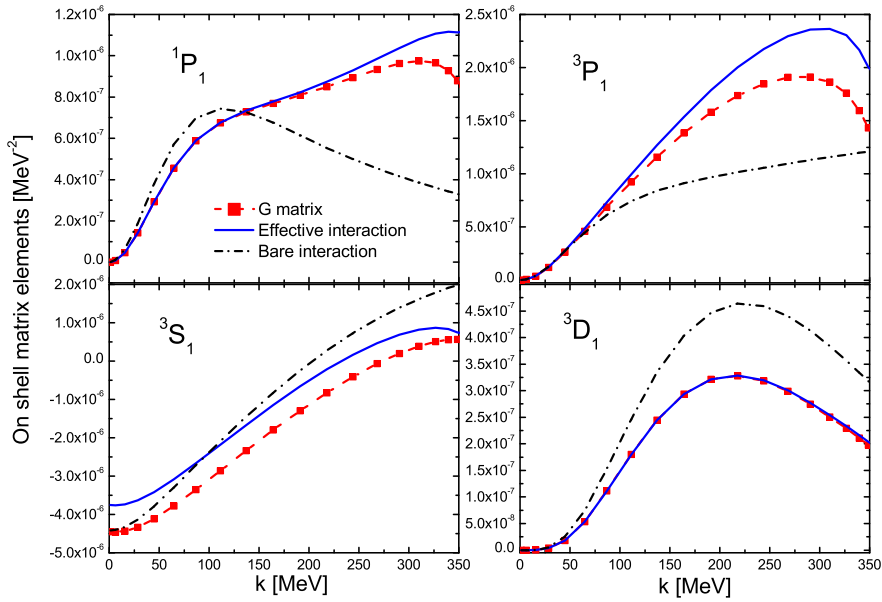
Figure 4.15: The on-shell matrix elements of effective interactions in the REBHF theory and RBHF theory with $k_F = 1.8$ fm^{-1} for $J = 1$

In Fig.4.19-4.21, we also consider the potential dependence of these matrix elements in the REBHF theory. The Bonn A and Bonn C are compared at the Fermi momentum of $k_F = 1.8$
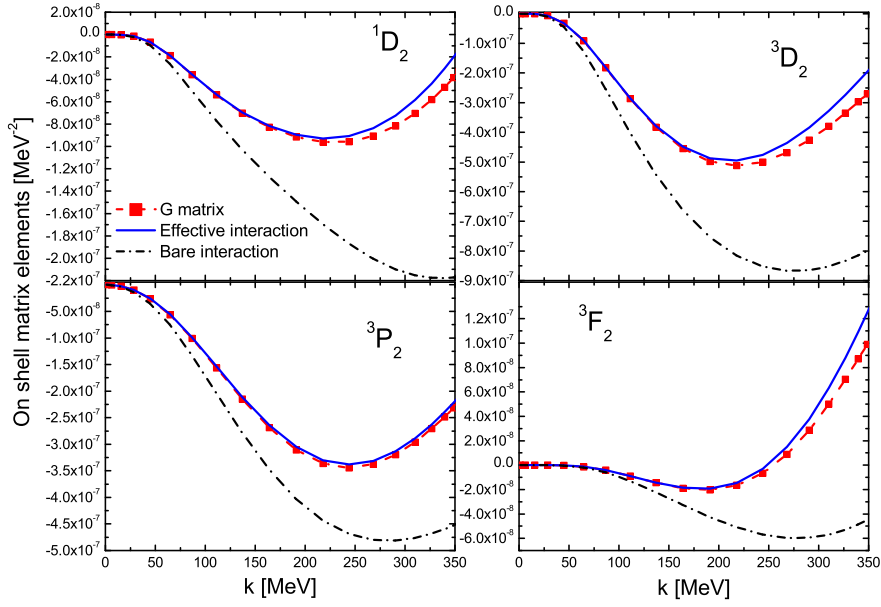
Figure 4.16: The on-shell matrix elements of effective interactions in the REBHF theory and RBHF theory with $k_F = 1.8$ fm^{-1} for $J = 2$.
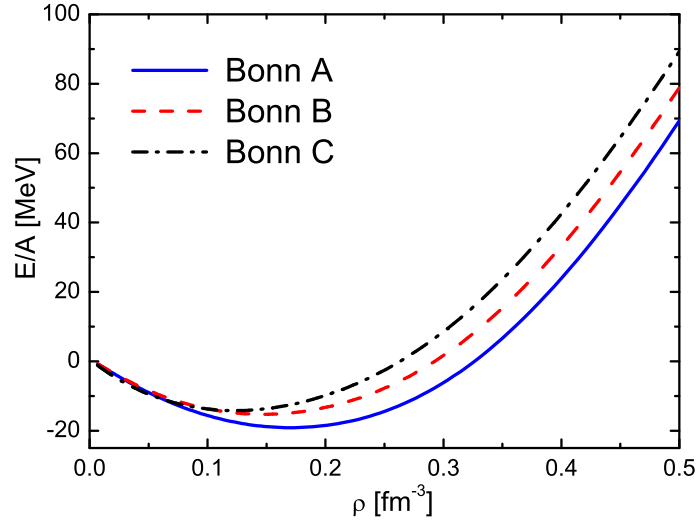
Figure 4.17: The EOS's of symmetric nuclear matter in the REBHF theory with the Bonn A, B, C potential. The solid curve is obtained with Bonn A, while dashed curve for Bonn B and dash-dotted curve for Bonn C.

fm^{-1}. The obvious difference is found in the $^3S_1$ channel, where the tensor component is the strongest in the NN interaction.

We also study the EOS of pure neutron matter in the REBHF theory with the Bonn A, B, C potentials in Fig. 4.22. We see that they are almost identical for different potentials. This conclusion is also found in the framework of the RBHF theory by Krastev and Sammarruca

Methods	Potential	ρ [fm^{-3}]	E/A [MeV]	K [MeV]	M_N^*/M_N	$|C_0|^2$
RBHF	Bonn A	0.1814	-15.38	302.9	0.598	-
	Bonn B	0.1625	-13.44	240.3	0.621	-
	Bonn C	0.1484	-12.12	181.6	0.640	-
REBHF	Bonn A	0.1699	-19.13	374.1	0.632	0.712
	Bonn B	0.1484	-15.28	294.2	0.664	0.710
	Bonn C	0.1227	-14.20	222.1	0.703	0.689

Table 4.1: The saturation properties of symmetric nuclear matter in the REBHF theory and RBHF theory with Bonn potentials.
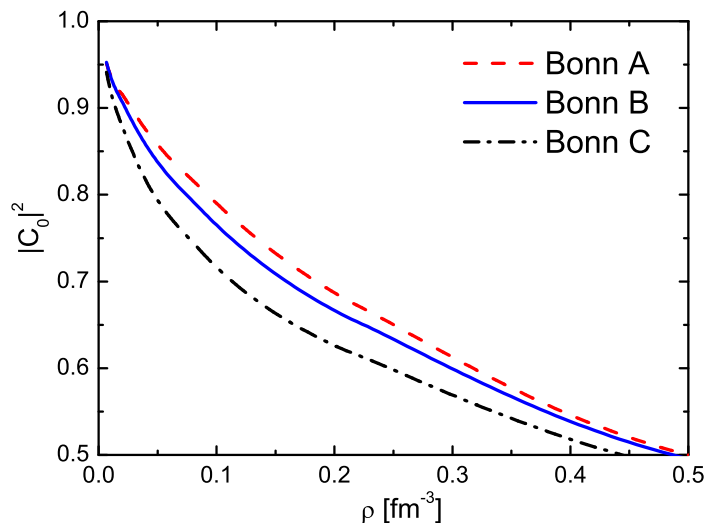
Figure 4.18: $|C_0|^2$ of symmetric nuclear matter in the REBHF theory with the Bonn A, B, C potentials. The solid curve is obtained with Bonn B, while dashed curve for Bonn A and dash-dotted curve for Bonn C

[75]. Actually, the effect of the tensor interaction in neutron matter is largely suppressed due to its isospin channel $T = 1$. The partial wave components about $T = 0$ channels such as $^3S_1$ channel disappear in neutron matter, when we use Eq. 4.106 to calculate the total energy. Therefore, in neutron matter, the short range correlation is enough for the realistic NN interaction. This is the theoretical foundation of our work in Chapter 3.

For pure neutron matter, its properties with three kinds of Bonn potentials are almost the same. Therefore, we will concentrate our discussion with the Bonn B potential in the later part. We first show the coefficient $|C_0|^2$ of pure neutron matter as a function of density in Fig. 4.23. For comparison, we also plot the one of symmetric matter. The coefficient $|C_0|^2$ in pure neutron matter is obviously larger than the one in symmetric nuclear matter.
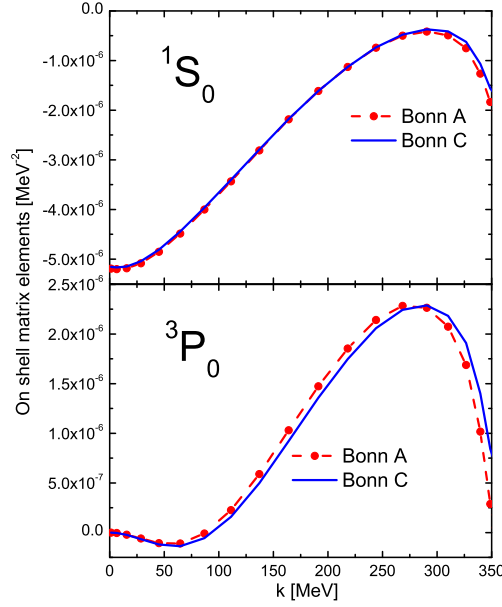
Figure 4.19: The on-shell matrix elements of effective interactions in REBHF theory with the Bonn A and Bonn C potentials at $k_F = 1.8$ fm^{-1} for $J = 0$.
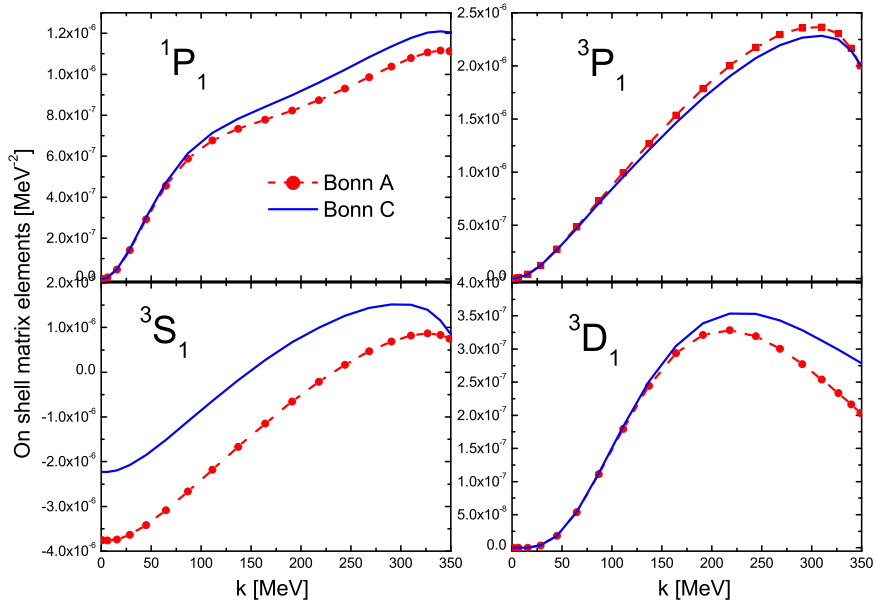
Figure 4.20: The on-shell matrix elements of effective interactions in the REBHF theory with the Bonn A and Bonn C potentials at $k_F = 1.8$ fm^{-1} for $J = 1$

It means 2p-2h components are larger and play more important roles in symmetric nuclear matter. High momentum correlations between two nucleons include both the short range correlation, and also the tensor correlation in symmetric nuclear matter. The effect of tensor interaction is very small in pure neutron matter and therefore 2p-2h states just take care of
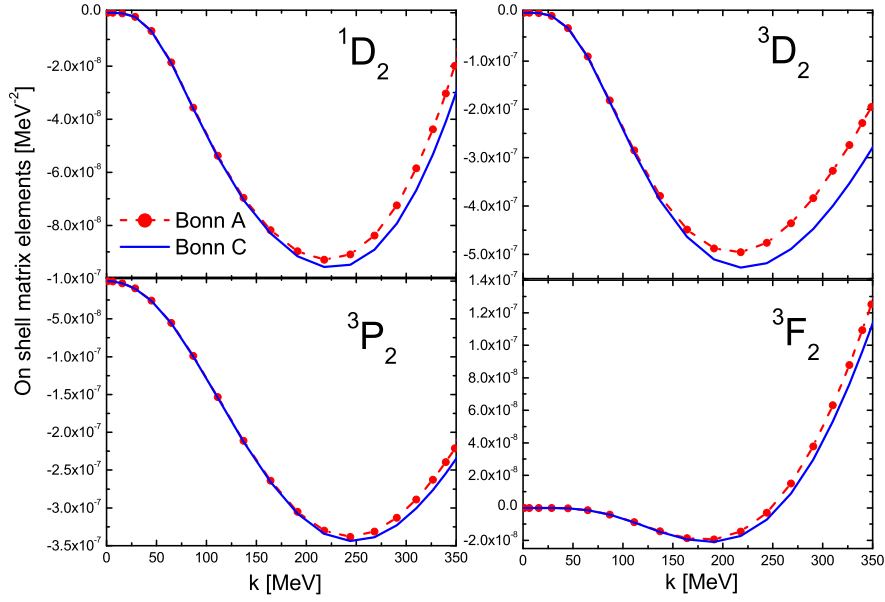
Figure 4.21: The on-shell matrix elements of effective interactions in the REBHF theory with the Bonn A and Bonn C potentials at $k_F = 1.8$ fm^{-1}, where $J = 2$
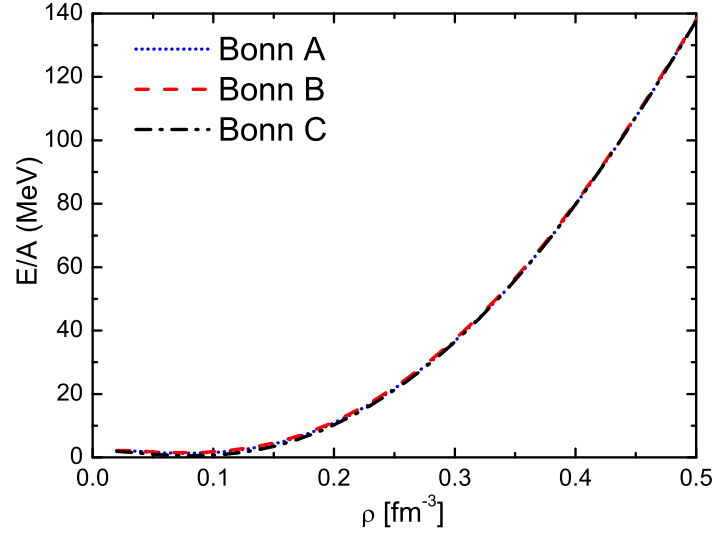
Figure 4.22: The EOS's of pure neutron matter in the REBHF theory with Bonn A, B, C potentials.

the short range correlation.

The scalar potential and vector potential of pure neutron matter in the REBHF theory are given in Fig. 4.24. We also compare them with the ones generated in the RBHF theory. This situation is in accordance with symmetric nuclear matter. The scalar density in the REBHF theory is still very similar to the one in the RBHF theory, while the vector potential in the REBHF theory is stronger than the piece from the RBHF theory at high density, which makes the binding energy more repulsive. However, at low density, the vector potential in the
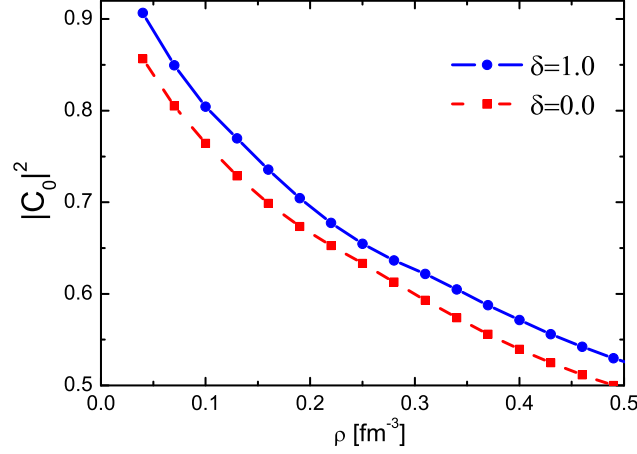
Figure 4.23: The coefficients $|C_0|^2$ for symmetric nuclear matter and pure neutron matter in the REBHF theory with Bonn B potential. The dotted and diamond curves correspond the pure neutron matter ($\delta = 1.0$) and symmetric nuclear matter ($\delta = 0.0$) cases, respectively.
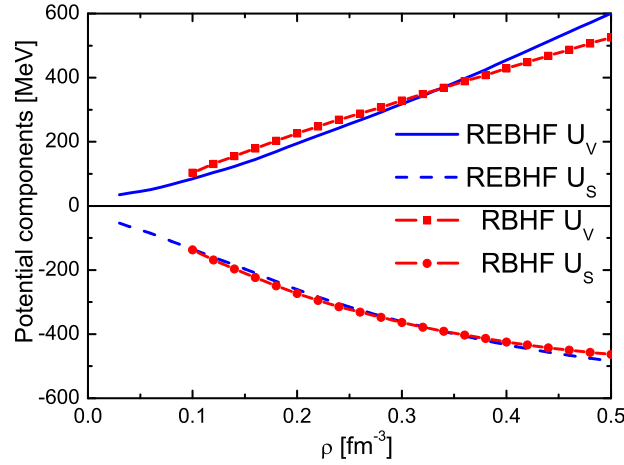
Figure 4.24: The components of single particle potential for pure neutron matter in the REBHF theory with the Bonn B potential.

REBHF theory is smaller than the one in the RBHF theory. This effect causes the smaller binding energy of pure neutron matter at low density. The corresponding asymmetric energy is also very small as shown in Fig. 4.25. At the saturation density, it is just about 20 MeV. We can find approximate linear relation between density and asymmetric energy.

Finally, the effective nucleon masses of pure neutron matter and symmetric nuclear matter as a function of density in REBHF theory are plotted in Fig. 4.26. The effective nucleon mass in neutron matter is larger than the one in symmetric nuclear matter. Their difference is about 100 MeV at the saturation density. This conclusion is consistent with the calculation of the RBHF theory by Krastev *et al.* [75]. However, the effective nucleon mass in symmetric nuclear matter is larger than the one in pure neutron matter in the RBHF theory with a
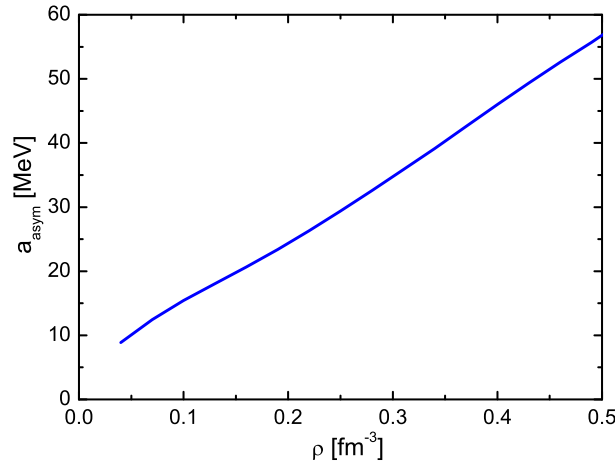
Figure 4.25: The asymmetric energy of nuclear matter as a function of density in the REBHF theory with the Bonn B potential.
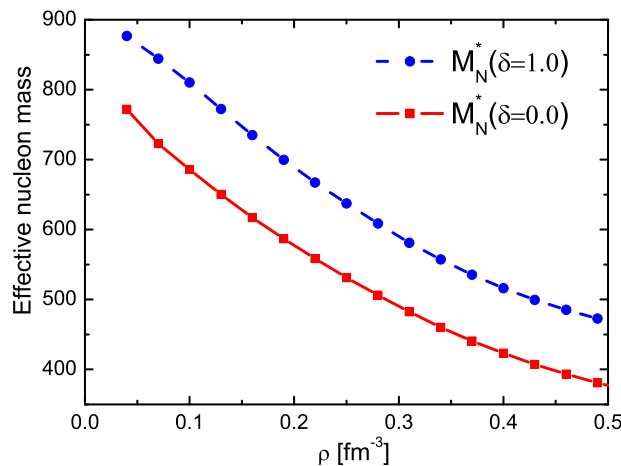
Figure 4.26: The effective nucleon masses of pure neutron matter and symmetric matter in the REBHF theory with the Bonn B potential. The dotted and diamond curves represent the pure neutron matter ($\delta = 1.0$) and symmetric nuclear matter ($\delta = 0.0$), respectively.

projection method [68] and in RHFU model [96]. It is necessary to discuss the mechanism of these opposite conclusions from different models about effective nucleon mass in the future work.

4.4   Conclusion

We have formulated the extended Brueckner-Hartree-Fock (EBHF) theory by properly dealing with the tensor and short range correlations of realistic NN interaction for nuclear matter. These correlations were considered through two-particle-two-hole (2p-2h) states in the configuration space in addition to the Hartree-Fock wave function. The equation of motion

for Hartree-Fock single particle states in the EBHF theory contains the usual Hartree-Fock potential and the coupling term to 2p-2h states. This coupling term can take care of high momentum correlations of realistic NN interaction and modifies the HF equation to provide additional attractions to the HF single particle states. In addition, there is a new term which corresponds to the 2p-2h states correlation on kinetic energy.

In the helicity representation, we have calculated the equation of state (EOS) of symmetric nuclear matter with the NREBHF theory. The Bonn potentials, a kind of realistic NN interaction, were adopted as the two-body NN interaction. We compare these EOS's in NREBHF with the results of the NRBHF model. We found that they are almost the same in the low density region. As the density increases, the nuclear matter contains more repulsive contributions in the NREBHF theory. This contribution is generated by 2p-2h states by including the kinetic energy contribution, which was ignored in the NRBHF theory. The saturation density in the NREBHF theory was closer to the empirical value due to this repulsive effect. There is not much difference between the effective nucleon masses in these two models.

To improve the saturation properties of nuclear matter, we applied the EBHF theory to study nuclear matter in the relativistic framework, where the effective nucleon mass was determined self-consistently. We call this method as relativistic extended Brueckner-Hartree-Fock theory (REBHF). More repulsive effect in the high density region is caused from virtual nucleon-antinucleon excitations in the many-body environment (Z graphs) in the relativistic kinematics. Therefore, we obtain more reasonable saturation properties in the REBHF theory. Especially, the binding energy and saturation density of Bonn B potential are already consistent with the experiment data. We also calculate pure neutron matter in the REBHF framework with the Bonn potentials. Their EOS's were identical from each other due to the fact that tensor interaction is suppressed almost completely in the isospin $T = 1$ channel in pure neutron matter.

Chapter 5

Summary and Outlook

It is a very important problem to properly describe the nuclear matter, as a hypothetical system of a huge number of protons and neutrons, from the realistic nucleon-nucleon (NN) interaction based on the proper many-body theory. We have developed a series of many-body theories to study the properties of nuclear matter with effective NN interaction and realistic NN interaction in this thesis, especially focusing on the pionic effect in nuclear matter. As we know, the density functional theories, such as the Skyrme Hartree-Fock model and the relativistic mean field (RMF) model have a lot of achievements in the description of nuclear many-body systems. However, these effective (phenomenological) theories do not include explicitly the pion, although the pion is the most important particle in nuclear physics. Therefore, we would like to introduce higher order terms of many-body system to take the pion contribution into account.

To start with, we have pointed out the significance of pion with an effective Lagrangian in the relativistic Hartree-Fock (RHF) model by keeping its contact term, which was usually removed simply in the RHF framework before [52]. To regularize the effect of the contact term, the finite-size effect of the nucleon is treated in terms of the form factor. The NN interaction is largely suppressed at high momentum region by the form factor effect. The EOS of nuclear matter was found still very hard in such a treatment. We have included the self interaction terms of σ and ω mesons to decrease the incompressibility. Finally it was about 300 MeV, which is in coincidence with experiment.

We have then discussed the short range correlation of realistic NN interaction in the RHF model for nuclear matter. One feature of the realistic NN interaction is the strong repulsion in the short range distance. A reasonably short range correlation of the realistic NN interaction is necessary for nuclear many body theory. We have tried to employ the unitary correlation operator method and the Jastrow function method to treat this strong repulsive correlation. The EOS of the pure neutron matter from a microscopic theory, relativistic Brueckner-Hartree-Fock model, was explained nicely with these two methods, because the other feature of realistic NN interaction, tensor interaction, is very weak in the isospin $T = 1$

channel. The saturation properties of symmetric nuclear matter were not good due to the lack of the tensor correlation in such an approximation for symmetric nuclear matter.

We have developed a new framework to handle the pion to treat the strong tensor correlation in nuclear matter. To this end, we include 2-particle-2-hole states to treat the tensor correlation in addition to the short range correlation of the realistic NN interaction following the idea of tensor optimized shell-model (TOSM) of finite nuclei. We have successfully constructed the extended Brueckner-Hartree-Fock (EBHF) theory with the Hartree-Fock variational model space together with 2p-2h states. The tensor and short range correlations were contained in the extended Brueckner-Hartree-Fock theory, where the effective potential consists of the Hartree-Fock potential and a coupling term of HF particle states with 2p-2h states. In addition, there was a new term corresponding the 2p-2h correlation on kinetic energy. We have obtained the EOS's of nuclear matter with EBHF in both the non-relativistic and relativistic frameworks. The saturation properties of nuclear matter in relativistic version were largely improved, which are consistent with the empirical data. We have also calculated pure neutron matter. We found that their EOS's were identical for different Bonn potentials, in which differences were mostly in the strength of the tensor interaction. This result demonstrates that the effect of the tensor interaction is very weak in the $T = 1$ channel.

So far, a new many-body framework, extended Brueckner-Hartree-Fock model, which can deal with the high momentum correlations of the realistic NN interaction has been constructed. We have demonstrated that the method works very well by calculating the properties of nuclear matter. It would be very important to apply the EBHF theory to finite nuclei, where we have more experimental data to compare.

The nuclear physics was born about 80 years ago. For a human being, 80 years are about the duration to take him from the cradle to the grave yard. However, we just have arrived at a foot of nuclear physics. There are still many puzzles about nuclear matter systems, although many studies are performed everyday. Such puzzles inspire us every time to continue to go forward and to get more achievement for understand this universe better.

Appendix A

Matrix elements of nucleon-nucleon interaction

The Bonn-A potential is constructed by considering six non-strange bosons with masses below 1 GeV with π and η pseudoscalar, σ and δ scalar, and ρ and ω vector mesons. The contributions from the isovector boson π,δ and ρ are to be multiplied by a factor of $\vec{\tau}_1 \cdot \vec{\tau}_2$. Now, the potential can be written in the following form,

$$V(r) = \sum_{S,T} V_{ST}^c(r) + \sum_{T} V_{1T}^t(r)\hat{S}_{12}(\hat{r}) + \sum_{T} V_{T}^b(r)\vec{L} \cdot \vec{S} + \sum_{S,T} \frac{1}{2} \left(\vec{p}^2 V_{ST}^{\vec{p}^2}(r) + V_{ST}^{\vec{p}^2}(r)\vec{p}^2 \right) \quad (A.1)$$

with

$$
\begin{aligned}
V^c(r) &= -\frac{g_\sigma^2}{4\pi} \left[1 - \frac{1}{4}\left(\frac{m_\sigma}{M}\right)^2 \right] \frac{e^{-m_\sigma r}}{r} + \frac{g_\omega^2}{4\pi} \left[1 + \frac{1}{2}\left(\frac{m_\omega}{M}\right)^2 \right] \frac{e^{-m_\omega r}}{r} \qquad (A.2)\\[2mm]
&\quad + \left[\frac{g_\eta^2}{48\pi}\left(\frac{m_\eta}{M}\right)^2 \frac{e^{-m_\eta r}}{r} + \frac{g_\omega^2}{24\pi}\left(\frac{m_\omega}{M}\right)^2 \frac{e^{-m_\omega r}}{r} \right] \vec{\sigma}_1 \cdot \vec{\sigma}_2 \\[2mm]
&\quad + \left\{ -\frac{g_\delta^2}{4\pi}\left[1 - \frac{1}{4}\left(\frac{m_\delta}{M}\right)^2 \right] \frac{e^{-m_\delta r}}{r} + \frac{g_\rho^2}{4\pi}\left[1 + \frac{1 + f_\rho/g_\rho}{2}\left(\frac{m_\rho}{M}\right)^2 \right] \frac{e^{-m_\rho r}}{r} \right\} \vec{\tau}_1 \cdot \vec{\tau}_2 \\[2mm]
&\quad + \left[\frac{g_\pi^2}{48\pi}\left(\frac{m_\pi}{M}\right)^2 \frac{e^{-m_\pi r}}{r} + \frac{(g_\rho + f_\rho)^2}{24\pi}\left(\frac{m_\rho}{M}\right)^2 \frac{e^{-m_\rho r}}{r} \right] \vec{\sigma}_1 \cdot \vec{\sigma}_2 \vec{\tau}_1 \cdot \vec{\tau}_2,
\end{aligned}
$$

$$
\begin{aligned}
V^t(r) &= \frac{g_\eta^2}{48\pi}\left(\frac{m_\eta}{M}\right)^2 \left[1 + \frac{3}{m_\eta r} + \frac{3}{(m_\eta r)^2} \right] \frac{e^{-m_\eta r}}{r} \qquad (A.3)\\[2mm]
&\quad - \frac{g_\omega^2}{48\pi}\left(\frac{m_\omega}{M}\right)^2 \left[1 + \frac{3}{m_\omega r} + \frac{3}{(m_\omega r)^2} \right] \frac{e^{-m_\omega r}}{r} \\[2mm]
&\quad + \left\{ \frac{g_\pi^2}{48\pi}\left(\frac{m_\pi}{M}\right)^2 \left[1 + \frac{3}{m_\pi r} + \frac{3}{(m_\pi r)^2} \right] \frac{e^{-m_\pi r}}{r} \right.
\end{aligned}
$$

$$-\frac{(g_\rho + f_\rho)^2}{48\pi} \left(\frac{m_\rho}{M}\right)^2 \left[1 + \frac{3}{m_\rho r} + \frac{3}{(m_\rho r)^2}\right] \frac{e^{-m_\rho r}}{r} \bigg\} \vec{\tau}_1 \cdot \vec{\tau}_2,$$

$$V^b(r) = -\frac{g_\sigma^2}{8\pi} \left(\frac{m_\sigma}{M}\right)^2 \left[\frac{1}{m_\sigma r} + \frac{1}{(m_\sigma r)^2}\right] \frac{e^{-m_\sigma r}}{r} - \frac{3g_\omega^2}{8\pi} \left(\frac{m_\omega}{M}\right)^2 \left[\frac{1}{m_\omega r} + \frac{1}{(m_\omega r)^2}\right] \frac{e^{-m_\omega r}}{r} \quad (A.4)$$

$$\bigg\{ -\frac{g_\delta^2}{8\pi} \left(\frac{m_\delta}{M}\right)^2 \left[\frac{1}{m_\delta r} + \frac{1}{(m_\delta r)^2}\right] \frac{e^{-m_\sigma r}}{r}$$

$$-\frac{g_\rho(3g_\rho + 4f_\rho)}{8\pi} \left(\frac{m_\rho}{M}\right)^2 \left[\frac{1}{m_\rho r} + \frac{1}{(m_\rho r)^2}\right] \frac{e^{-m_\rho r}}{r} \bigg\} \vec{\tau}_1 \cdot \vec{\tau}_2$$

$$V^{\vec{p}^2}(r) = -\frac{1}{M^2} \left[\frac{g_\sigma^2}{8\pi} \frac{e^{-m_\sigma r}}{r} + \frac{3g_\omega^2}{8\pi} \frac{e^{-m_\omega r}}{r} + \left(\frac{g_\delta^2}{8\pi} \frac{e^{-m_\delta r}}{r} + \frac{3g_\rho^2}{8\pi} \frac{e^{-m_\rho r}}{r}\right) \vec{\tau}_1 \cdot \vec{\tau}_2\right], \quad (A.5)$$

where we have omitted the $\delta^{(3)}(\vec{r})$ term in the above expressions.

Let us consider the matrix elements of the difference spin operator in $|LSJ\rangle$ basis. For the spin operator this is rather straightforward.

$$\sigma_1 \cdot \sigma_2 = \frac{1}{2}(4\mathbf{S}^2 - \sigma_1^2 - \sigma_2^2) = 2\mathbf{S}^2 - 3 \quad (A.6)$$

and therefore

$$\sigma_1 \cdot \sigma_2 |LSJ\rangle = (2S(S+1) - 3)|LSJ\rangle \quad (A.7)$$
$$= |LSJ\rangle\delta_{S,1} - 3|LSJ\rangle\delta_{S,0},$$

where $\mathbf{S} = \frac{\sigma_1 + \sigma_2}{2}$ and is the quantum number of the total spin.

The spin-orbit operator can be treated analogously,

$$\mathbf{l} \cdot \mathbf{S}|LSJ\rangle = \frac{1}{2}[\mathbf{J}^2 - \mathbf{L}^2 - \mathbf{S}^2]|LSJ\rangle \quad (A.8)$$

$$= \frac{1}{2}[J(J+1) - l(l+1) - S(S+1)]|LSJ\rangle.$$

The tensor operator requires a slightly more elaborated procedure. It is the only operator which mixes different partial waves L. Because of parity conservation, the two coupled partial waves L and L' must be both even or both odd. Furthermore, they can differ at most of two units, since the total spin is at most $S = 1$. Therefore, in conclusion $L' = L, L \pm 2$. The explicit form of the matrix elements can be obtained by writing the tensor operator S_{12} in the following form

$$S_{12} = \sqrt{\frac{24\pi}{5}}(\mathbf{S}_2 \cdot \mathbf{Y}_2) = \sqrt{\frac{24\pi}{5}} \sum_M \hat{S}_{2-M} Y_{2M}(-1)^M, \quad (A.9)$$

where Y_{2M} are the spherical harmonics of order two and $\hat{S}_{2M}$ the irreducible tensor operator of rank two, given by

$$\hat{S}_{2M} = \sum_{mm'} \langle 1m1m'|2M \rangle \tilde{\sigma}_{1m} \tilde{\sigma}_{2m'}, \tag{A.10}$$

where the operator $\tilde{\sigma}$ are the spin operator in the spherical basis

$$\tilde{\sigma}_1 = -\frac{\sigma_x + i\sigma_y}{\sqrt{2}}, \quad \tilde{\sigma}_0 = \sigma_z, \quad \tilde{\sigma}_{-1} = \frac{\sigma_x - i\sigma_y}{\sqrt{2}}. \tag{A.11}$$

This relation shows that the tensor operator S_{12} is the scalar product of two rank-2 irreducible tensors. Now, we can get,

$$\langle LSJ|\hat{S}_{12}|L'SJ \rangle = \sqrt{\frac{24\pi}{5}} (-1)^{L+S+J} \begin{Bmatrix} S & 2 & S \\ L & J & L' \end{Bmatrix} \langle L||Y_2||L' \rangle \langle S||S_2||S \rangle, \tag{A.12}$$

where the symbol in curly brackets is the 6-j angular momentum re-coupling coefficient, and we have introduced the so-called reduced matrix elements of the spherical harmonics and of the operators $\hat{S}_{12}$. The form of Eq. (A.12) establishes the main selection rules for the tensor operator. First of all the 6-j symbol vanishes if $S = 0$, and therefore the tensor operator $\hat{S}_{12}$ has non vanishing matrix elements only for the $S = 1$ two-nucleon channels. One can easily find the value of the reduced matrix elements

$$\langle L||Y_2||L' \rangle = (-1)^{L'}[(2L+1)(2L'+1)]^{\frac{1}{2}} \sqrt{\frac{5}{4\pi}} \begin{pmatrix} L & 2 & L' \\ 0 & 0 & 0 \end{pmatrix} \tag{A.13}$$

$$\langle S||S_2||S \rangle = 2\sqrt{5}.$$

For $S = 1$, there are only three choices for J, $J = L-1, \ L, \ L+1$. Using explicit expressions for the 3-j and 6-j symbols, we can find a very simple form for the matrix elements of the tensor operator $(S = 1)$

$$\langle JSJ|\hat{S}_{12}|JSJ \rangle = 2 \tag{A.14}$$

$$\langle J-1SJ|\hat{S}_{12}|J-1SJ \rangle = -\frac{2(J-1)}{2J+1}$$

$$\langle J+1SJ|\hat{S}_{12}|J-1SJ \rangle = \langle J-1SJ|\hat{S}_{12}|J+1SJ \rangle = 6\frac{\sqrt{J(J+1)}}{2J+1}$$

$$\langle J+1SJ|\hat{S}_{12}|J+1SJ \rangle = -\frac{2(J+2)}{2J+1}.$$

Now, it's obvious that these matrix elements are finite when $L = J \pm 1$ and $L' = J \mp 1$. Other terms are canceled with each other. To evaluate these matrix elements, we have used the following formulae about 3-j and 6-j symbols,

$$\begin{pmatrix} J & 2 & J \\ 0 & 0 & 0 \end{pmatrix} = -\frac{(-1)^{-J}\sqrt{J(J+1)}}{\sqrt{(2J-1)(2J+1)(2J+3)}} \tag{A.15}$$

$$\begin{pmatrix} J-1 & 2 & J+1 \\ 0 & 0 & 0 \end{pmatrix} = \begin{pmatrix} J+1 & 2 & J-1 \\ 0 & 0 & 0 \end{pmatrix} = \sqrt{\frac{3}{2}} \frac{(-1)^{-J}\sqrt{J(J+1)}}{\sqrt{(2J-1)(2J+1)(2J+3)}}$$

$$\begin{Bmatrix} 1 & 2 & 1 \\ J & J & J \end{Bmatrix} = \frac{(-1)^{-2J}\sqrt{(2J-1)(2J+3)}}{\sqrt{30J(J+1)(2J+1)}}$$

$$\begin{Bmatrix} 1 & 2 & 1 \\ J+1 & J & J+1 \end{Bmatrix} = \frac{(-1)^{-2J}\sqrt{(J+2)(2J+5)}}{\sqrt{30(J+1)(2J+1)(2J+3)}}$$

$$\begin{Bmatrix} 1 & 2 & 1 \\ J-1 & J & J-1 \end{Bmatrix} = \frac{(-1)^{-2J}\sqrt{(J-1)(2J-3)}}{\sqrt{30J(2J-1)(2J+1)}}$$

$$\begin{Bmatrix} 1 & 2 & 1 \\ J-1 & J & J+1 \end{Bmatrix} = \begin{Bmatrix} 1 & 2 & 1 \\ J+1 & J & J-1 \end{Bmatrix} = \frac{(-1)^{-2J}}{\sqrt{5(2J+1)}}$$

Appendix B

Short range correlation on kinetic energy

B.1 Short range correlation on kinetic energy with UCOM method

For the nuclear many-body system, we can write a nonrelativistic Hamiltonian as:

$$H = T + V = \sum_i^A \frac{p_i^2}{2m_i} + \sum_{i<j}^A V(i,j), \tag{B.1}$$

where A is the particle number. In nuclear matter, it is reasonable to neglect the difference between proton and neutron. The unitary correlator operator C should ensure the unitarity,

$$C = \exp(-iS), \quad S = S^\dagger. \tag{B.2}$$

Here S is a hermitian generator of the correlations. It has to be a two-body operator or higher because a one-body operator would only cause a unitary transformation of the single-particle states and this variational degree of freedom is already present in the product state $|\Phi\rangle$.

$$S = \sum_{i<j}^A g(i,j) + three - body + \dots. \tag{B.3}$$

Now we just assume that the generator is a two-body operator $S = \sum_{i<j}^A g(i,j)$. For the kinetic energy, a one-body operator, transforms as,

$$\hat{K} = C^\dagger K C = \hat{K}^{[1]} + \hat{K}^{[2]} + \hat{K}^{[3]} + \dots, \tag{B.4}$$

where the one-body part is just the regular uncorrelated kinetic energy,

$$\hat{K}^{[1]} = \sum_i^A \frac{p_i^2}{2m}. \tag{B.5}$$

The two-body part $\hat{K}^{[2]}$ is,

$$\hat{K}^{[2]} = \sum_{i<j}^{A} K^{[2]}(i,j), \tag{B.6}$$

with

$$K^{[2]}(i,j) = c^{\dagger}(i,j) \left(\frac{p_i^2}{2m} + \frac{p_j^2}{2m} \right) c(i,j) - \left(\frac{p_i^2}{2m} + \frac{p_j^2}{2m} \right), \tag{B.7}$$

and $c(i,j) = \exp -ig(i,j)$ denotes the correlator between particle i and j. Now we transform a two body operator $V(i,j)$ like the potential,

$$\hat{V} = C^{\dagger} V C = \hat{V}^{[2]} + \hat{V}^{[3]} + \dots, \tag{B.8}$$

which starts with a two-body part,

$$\hat{V}^{[2]} = c^{\dagger}(i,j) V^{[2]}(i,j) c(i,j). \tag{B.9}$$

It means that the bare potential $V^{[2]}$ is in lowest order replaced by the correlated interaction which should be much less repulsive at short distance.

In the unitary correlation operator method (UCOM), a operator which just contains the relative distance can be transformed as,

$$
\begin{aligned}
\langle \phi' | c^{\dagger} f(\vec{r}) c | \phi \rangle &= \int \langle \phi' | \vec{r} \rangle \langle \vec{r} | c^{\dagger} f(\vec{r}) c | \phi \rangle d^3 r \\
&= \int \langle \phi' | \vec{r} \rangle f(\vec{R}_+(\vec{r})) \langle \vec{r} | \phi \rangle d^3 r.
\end{aligned}
\tag{B.10}
$$

We also can make a similar procedure for the radial momentum $q_r = \frac{\vec{r}}{r} \cdot \vec{q}$, where $\vec{q} = \frac{1}{2}(\vec{p}_1 - \vec{p}_2)$ is the relative momentum.

$$
\begin{aligned}
\langle \vec{r} | c^{\dagger} q_r c | \phi \rangle &= -i \frac{1}{r \sqrt{R'_+(r)}} \frac{\partial}{\partial r} \frac{1}{\sqrt{R'_+(r)}} \langle \vec{r} | \phi \rangle \\
&= -i \frac{1}{r \sqrt{R'_+(r)}} \left(\frac{\partial}{\partial r} r - \frac{1}{2} \frac{R''_+(r)}{R'_+(r)} r \right) \langle \vec{r} | \phi \rangle.
\end{aligned}
\tag{B.11}
$$

In the nonrelativistic energy, the square of the radial momentum q_r^2 is more important in calculation process,

$$
\begin{aligned}
\langle \phi' | c^{\dagger} q_r^2 c | \phi \rangle &= \langle \phi' | c^{\dagger} q_r c c^{\dagger} q_r c | \phi \rangle \\
&= \int \langle \phi' | c^{\dagger} q_r c | \vec{r} \rangle \langle \vec{r} | c^{\dagger} q_r c | \phi \rangle \\
&= \int \langle \phi' | \vec{r} \rangle \left(r \frac{\overleftarrow{\partial}}{\partial r} - \frac{1}{2} \frac{r R''_+(r)}{R'_+(r)} \right) \frac{1}{r^2 R'^2_+(r)} \left(\frac{\overrightarrow{\partial}}{\partial r} r - \frac{1}{2} \frac{r R''_+(r)}{R'_+(r)} \right) \langle \vec{r} | \phi \rangle d^3 r
\end{aligned}
\tag{B.12}
$$

$$= \int \langle \phi' | \vec{r} \rangle \left[\overleftarrow{\frac{\partial}{\partial r}} \frac{1}{R_+'^2(r)} \overrightarrow{\frac{\partial}{\partial r}} + \frac{1}{R_+'^2(r)} \left(2\frac{R_+''(r)}{rR_+'(r)} - \frac{5}{4}\left(\frac{R_+''(r)}{R_+'(r)}\right)^2 + \frac{1}{2}\frac{R_+'''(r)}{R_+'(r)} \right) \right] \langle \vec{r} | \phi \rangle d^3r,$$

where we have used some partial integration about r part. It is the key point that the partial integration is just for the linear integration, but not the volume integration.

With the above equation, the two body correlation of kinetic energy can be evaluated by separating it as relative and center of mass energy

$$K(i) + K(j) = \frac{p_i^2 + p_j^2}{2m} = \frac{1}{m}\vec{q}^2 + \frac{1}{4m}(\vec{p}_i + \vec{p}_j)^2 \tag{B.13}$$

$$= \frac{1}{m}\left(q_r^\dagger q_r + \frac{\vec{L}^2}{r^2} \right) + \frac{1}{4m}(\vec{p}_i + \vec{p}_j)^2.$$

Here, $\vec{L} = \vec{r} \times \vec{q}$ is the angular momentum and $r = |\vec{r}_1 - \vec{r}_2|$ is the relative distance. And the correlated relative angular momentum is the same as the uncorrelated one

$$\hat{\vec{L}} = c^\dagger \vec{L} c = \vec{L}. \tag{B.14}$$

Therefore, the two-body part of the correlated kinetic energy can be split into there parts,

$$\hat{K}^{[2]} = q_r^\dagger \frac{1}{m}\left[\frac{1}{R_+'^2(r)} - 1 \right] q_r + \frac{1}{m}\left[\frac{1}{R_+^2(r)} - \frac{1}{r^2} \right] \vec{L}^2 + w(r), \tag{B.15}$$

where $w(r)$ comes from the commutation between momentum operator and $R_+(r)$,

$$w(r) = \frac{1}{mR_+'^2(r)}\left(2\frac{R_+''(r)}{rR_+'(r)} - \frac{5}{4}\left(\frac{R_+''(r)}{R_+'(r)}\right)^2 + \frac{1}{2}\frac{R_+'''(r)}{R_+'(r)} \right). \tag{B.16}$$

It is very convenience to define two effective masses. The first one is the reduced radial mass $\mu_r(r)$,

$$\frac{m}{2\mu_r(r)} \equiv \frac{1}{R_+'^2(r)} - \frac{r^2}{R_+^2(r)} \tag{B.17}$$

and the second one is the reduced angular mass $\mu_\Omega(r)$,

$$\frac{m}{2\mu_\Omega(r)} \equiv \frac{r^2}{R_+^2(r)} - 1. \tag{B.18}$$

Now, we can rewrite the two body correlator of kinetic energy as,

$$\hat{K}^{[2]} = q_r^\dagger \frac{1}{2\mu_r(r)} q_r + \vec{q}\frac{1}{2\mu_\Omega(r)}\vec{q} + w(r) \tag{B.19}$$

$$= t_r + t_\Omega + w(r),$$

where we have used Eq.(B.13) to replace the angular momentum part. In nuclear matter, the expectation value of a two-body operator is,

$$\overline{O} = \frac{1}{2A} \sum_{i,j} \left(\langle ij|\hat{O}|ij\rangle - \langle ij|\hat{O}|ji\rangle \right), \tag{B.20}$$

where

$$|i\rangle = |\vec{k}_i\rangle \otimes |m_i\rangle. \tag{B.21}$$

$|k_i\rangle$ is the momentum related part, which is a plane wave function in nuclear matter,

$$\langle \vec{x}|\vec{k}\rangle = \frac{1}{\sqrt{V}} \exp(i\vec{k}_i \cdot \vec{x}). \tag{B.22}$$

$|m_i\rangle$ is the eigenstate of spin and isospin, whose eigenvalue is $\lambda = 2$ for neutron matter and $\lambda = 4$ for symmetry matter. A is the total particle number,

$$A = \sum_{=1}^{\lambda} \sum^{k_F} 1 = \lambda \frac{V}{(2\pi)^3} \int^{k_F} d^3k 1 = \lambda \frac{V}{6\pi^2} k_F^3. \tag{B.23}$$

There is a simple relation between A and density ρ,

$$\rho = \frac{A}{V} = \frac{\lambda}{6\pi^2} k_F^3. \tag{B.24}$$

Now, we can calculate the expect value of kinetic energy correlation in UCOM,

$$\begin{aligned}
\overline{t_r} &= \frac{1}{2A} \sum_{i,j} \left(\langle ij|q_r \frac{1}{2\mu_r(r)} q_r|ij\rangle - \langle ij|q_r \frac{1}{2\mu_r(r)} q_r|ji\rangle \right) \\
&= \frac{k_F^5}{120\pi^2 m} \int d^3r \left(\frac{1}{R_+'^2(r)} - \frac{r^2}{R_+^2(r)} \right) (\lambda - l_3(k_F r))
\end{aligned} \tag{B.25}$$

$$\begin{aligned}
\overline{t_\Omega} &= \frac{1}{2A} \sum_{i,j} \left(\langle ij|\vec{q} \frac{1}{2\mu_\Omega(r)} \vec{q}|ij\rangle - \langle ij|\vec{q} \frac{1}{2\mu_\Omega(r)} \vec{q}|ji\rangle \right) \\
&= \frac{k_F^5}{40\pi^2 m} \int d^3r \left(\frac{r}{R_+^2(r)} - 1 \right) (\lambda - l_2(k_F r))
\end{aligned} \tag{B.26}$$

$$\begin{aligned}
\overline{w} &= \frac{1}{2A} \sum_{i,j} \left(\langle ij|w(r)|ij\rangle - \langle ij|w(r)|ji\rangle \right) \\
&= \frac{k_F^3}{12\pi^2} \int d^3r w(r)(\lambda - l_1^2(k_F r)),
\end{aligned}$$

where $l_1(x)$, $l_2(x)$, $l_3(x)$ are some functions which are composed of spherical Bessel functions,

$$l_1(x) = 3\frac{j_1(x)}{x} \tag{B.27}$$

$$l_2(x) = 15\left[\frac{j_0^2(x)}{x^2} + \left(\frac{15}{x^4} - \frac{1}{x^2}\right)j_1^2(x) - \frac{8}{x^3}j_0(x)j_1(x)\right]$$

$$l_2(x) = 45\left[\frac{j_0^2(x)}{x^2} + \left(\frac{21}{x^4} - \frac{1}{x^2}\right)j_1^2(x) - \frac{10}{x^3}j_0(x)j_1(x)\right]$$

$$j_0(x) = \frac{\sin(x)}{x}$$

$$j_1(x) = \frac{\sin(x)}{x^2} - \frac{\cos(x)}{x}.$$

B.2 Short range correlation on kinetic energy with Jastrow function method

In this part, we will discuss the short range correlation for the relativistic Hamiltonian. We will use the Walecka model Lagrangian which just includes two kinds of mesons exchange, σ meson and ω meson. The effective Hamiltonian can be written as,

$$H = \int d^3\vec{x}\psi^\dagger(\vec{x})(-i\vec{\alpha}\cdot\vec{\nabla} + \beta M)\psi(\vec{x}) \tag{B.28}$$

$$+\frac{1}{2}\int d^3\vec{x}d^3\vec{y}\overline{\psi}(\vec{x})\overline{\psi}(\vec{y})\left[-\frac{g_\sigma^2}{4\pi}\frac{e^{-m_\sigma|\vec{x}-\vec{y}|}}{|\vec{x}-\vec{y}|} + \frac{g_\omega^2}{4\pi}\frac{e^{-m_\omega|\vec{x}-\vec{y}|}}{|\vec{x}-\vec{y}|}\gamma_\mu(1)\gamma^\mu(2)\right]\psi(\vec{y})\psi(\vec{x}).$$

Here, the field operator is expanded in plane wave functions,

$$\psi(\vec{x}) = \frac{1}{\sqrt{V}}\sum_{k,s}u(\vec{k},s)e^{i\vec{k}\cdot\vec{x}}, \tag{B.29}$$

where $u(\vec{k},s)$ is a Dirac spinor,

$$u(\vec{k},s) = \left(\frac{E^* + M^*}{2E^*}\right)^{1/2}\left(\begin{array}{c}1\\ \frac{\vec{\sigma}\cdot\vec{p}^*}{M_N^*+E_p^*}\end{array}\right)\chi_s. \tag{B.30}$$

In the framework of relativistic Hartree-Fock method, the effective quantities are defined as,

$$\vec{p}^*(p) = \vec{p} + \vec{n}_p\Sigma_V(p) \tag{B.31}$$
$$M^*(p) = M + \Sigma_S(p)$$
$$E^*(p) = \sqrt{p^{*2} + M^{*2}}.$$

If we consider to use the Jastrow method for the short range correlation, the two-body correlated wave function is,

$$\overline{|ij\rangle} = \exp(iS)|ij\rangle \approx f(|\vec{x}_i - \vec{x}_j|)|ij\rangle. \tag{B.32}$$

Therefore, the effective two-body interaction after the short range correlation is given by

$$H^{[2]} = \langle ij|f(r)(t_i + t_j + V(r))f(r)|ij\rangle - \langle ij|(t_i + t_j)|ij\rangle, \tag{B.33}$$

where t_i is the kinetic energy operator of particle i.

Now we can write the two-body correlation interaction of the kinetic energy in the relativistic case,

$$
\begin{aligned}
K^{[2]} &= \int d^3r_1 d^3r_2 \psi^\dagger(\vec{r}_1)\psi^\dagger(\vec{r}_2)f(r)[-i\vec{\alpha}_1 \cdot \vec{\nabla}_1 - i\vec{\alpha}_2 \cdot \vec{\nabla}_2 + 2\beta M]f(r)\psi(\vec{r}_2)\psi(\vec{r}_1) \quad\text{(B.34)} \\
&\quad - \int d^3r_1 d^3r_2 \psi^\dagger(\vec{r}_1)\psi^\dagger(\vec{r}_2)[-i\vec{\alpha}_1 \cdot \vec{\nabla}_1 - i\vec{\alpha}_2 \cdot \vec{\nabla}_2 + 2\beta M]\psi(\vec{r}_2)\psi(\vec{r}_1) \\
&= \int d^3r_1 d^3r_2 \psi^\dagger(\vec{r}_1)\psi^\dagger(\vec{r}_2)f(r)[-i\vec{\alpha}_1 \cdot \vec{\nabla}_1 - i\vec{\alpha}_2 \cdot \vec{\nabla}_2]f(r)\psi(\vec{r}_2)\psi(\vec{r}_1) \\
&\quad - \int d^3r_1 d^3r_2 \psi^\dagger(\vec{r}_1)\psi^\dagger(\vec{r}_2)[-i\vec{\alpha}_1 \cdot \vec{\nabla}_1 - i\vec{\alpha}_2 \cdot \vec{\nabla}_2]\psi(\vec{r}_2)\psi(\vec{r}_1) \\
&\quad + \int d^3r_1 d^3r_2 [f^2(r) - 1]\psi^\dagger(\vec{r}_1)\psi^\dagger(\vec{r}_2)(2\beta M)\psi(\vec{r}_2)\psi(\vec{r}_1) \\
&= \int d^3r_1 d^3r_2 [f^2(r) - 1]\psi^\dagger(\vec{r}_1)\psi^\dagger(\vec{r}_2)(-i\vec{\alpha}_1 \cdot \vec{\nabla}_1 - i\vec{\alpha}_2 \cdot \vec{\nabla}_2 + 2\beta M)\psi(\vec{r}_2)\psi(\vec{r}_1) \\
&\quad + \int d^3r_1 d^3r_2 \psi^\dagger(\vec{r}_1)\psi^\dagger(\vec{r}_2)f(r)[(-i\vec{\alpha}_1 \cdot \vec{\nabla}_1 - i\vec{\alpha}_2 \cdot \vec{\nabla}_2)f(r)]\psi(\vec{r}_2)\psi(\vec{r}_1)
\end{aligned}
$$

.

Here, we first calculate the last line in the above equation.

$$\int d^3r_1 d^3r_2 \psi^\dagger(\vec{r}_1)\psi^\dagger(\vec{r}_2)f(r)[(-i\vec{\alpha}_1 \cdot \vec{\nabla}_1 - i\vec{\alpha}_2 \cdot \vec{\nabla}_2)f(r)]\psi(\vec{r}_2)\psi(\vec{r}_1) \tag{B.35}$$

$$= \int d^3r_1 d^3r_2 \psi^\dagger(\vec{r}_1)\psi^\dagger(\vec{r}_2)(-i)f(r)(\vec{\alpha}_1 - \vec{\alpha}_2) \cdot \frac{\vec{r}}{r}\frac{\partial}{\partial r}f(r)\psi(\vec{r}_2)\psi(\vec{r}_1)$$

$$= \frac{1}{V^2}\int d^3r_1 d^3r_2 \sum_{k,s} e^{i(\vec{k}_1 - \vec{k}_4)\cdot\vec{r}_1} e^{i(\vec{k}_2 - \vec{k}_3)\cdot\vec{r}_2} a^\dagger_{\vec{k}_3,s_3} a^\dagger_{\vec{k}_4,s_4} a_{\vec{k}_1,s_1} a_{\vec{k}_2,s_2}$$

$$u^\dagger(\vec{k}_3, s_3)u^\dagger(\vec{k}_4, s_4)(-i)f(r)(\vec{\alpha}_1 - \vec{\alpha}_2) \cdot \frac{\vec{r}}{r}\frac{\partial}{\partial r}f(r)u(\vec{k}_1, s_1)u(\vec{k}_2, s_2),$$

while, the rest part of the correlated interaction is,

$$\int d^3r_1 d^3r_2 [f^2(r) - 1]\psi^\dagger(\vec{r}_1)\psi^\dagger(\vec{r}_2)(-i\vec{\alpha}_1 \cdot \vec{\nabla}_1 - i\vec{\alpha}_2 \cdot \vec{\nabla}_2 + 2\beta M)\psi(\vec{r}_2)\psi(\vec{r}_1) \tag{B.36}$$

$$= \frac{1}{V^2}\int d^3r_1 d^3r_2 [f^2(r) - 1]\sum_{k,s} e^{i(\vec{k}_1 - \vec{k}_4)\cdot\vec{r}_1} e^{i(\vec{k}_2 - \vec{k}_3)\cdot\vec{r}_2} a^\dagger_{\vec{k}_3,s_3} a^\dagger_{\vec{k}_4,s_4} a_{\vec{k}_1,s_1} a_{\vec{k}_2,s_2}$$

$$u^\dagger(\vec{k}_3, s_3)u^\dagger(\vec{k}_4, s_4)(\vec{\alpha}_1 \cdot \vec{k}_1 + \vec{\alpha}_2 \cdot \vec{k}_2 + 2\beta M)u(\vec{k}_1, s_1)u(\vec{k}_2, s_2).$$

The creation operator and annihilation operator should be simplified by the Hartree-Fock approximation when we evaluated the expect value of the kinetic energy.

$$\langle 0|a^\dagger_{\vec{k}_3,s_3} a^\dagger_{\vec{k}_4,s_4} a_{\vec{k}_1,s_1} a_{\vec{k}_2,s_2}|0\rangle \tag{B.37}$$
$$= \delta_{\vec{k}_1,\vec{k}_4}\delta_{\vec{k}_2,\vec{k}_3}\delta_{s_1,s_4}\delta_{s_2,s_3} - \delta_{\vec{k}_1,\vec{k}_3}\delta_{\vec{k}_2,\vec{k}_4}\delta_{s_1,s_3}\delta_{s_2,s_4}$$

The Hartree piece of the kinetic energy contribution is

$$E^{dir}_{K^{[2]}} = \frac{-iV}{2}\int d^3r f(r)\frac{\partial}{\partial r}f(r)\int\frac{d^3k_1 d^3k_2}{(2\pi)^6}u^\dagger(\vec{k}_2,s_2)u^\dagger(\vec{k}_1,s_1)(\vec{\alpha}_1-\vec{\alpha}_2)\cdot\vec{n}_r u(\vec{k}_1,s_1)u(\vec{k}_2,s_2) \tag{B.38}$$

$$+\frac{V}{2}\int d^3r[f^2(r)-1]\int\frac{d^3k_1 d^3k_2}{(2\pi)^6}u^\dagger(\vec{k}_2,s_2)u^\dagger(\vec{k}_1,s_1)(\vec{\alpha}_1\cdot\vec{k}_1+\vec{\alpha}_2\cdot\vec{k}_2+2\beta M)u(\vec{k}_1,s_1)u(\vec{k}_2,s_2)$$

$$= \frac{-iV}{2}\int d^3r f(r)\frac{\partial}{\partial r}f(r)\int\frac{d^3k_1 d^3k_2}{(2\pi)^6}\left(\frac{\vec{k}_1^*}{E^*(k_1)}-\frac{\vec{k}_2^*}{E^*(k_2)}\right)\cdot\frac{\vec{r}}{r}$$

$$+\frac{V}{2}\int d^3r[f^2(r)-1]\lambda\rho_B\int\frac{d^3k_1}{(2\pi)^3}\left(\vec{k}_1\cdot\frac{\vec{k}_1^*}{E^*(k_1)}+M\frac{M^*(k_1)}{E^*(k_1)}\right)$$

$$= 0,$$

where the first line vanishes due to the angular integration and the second line vanishes by the normalization condition in the Jastrow function,

$$\int[f^2(r)-1]d^3r = 0. \tag{B.39}$$

While the Fock piece of the kinetic energy correlation is

$$E^{Fock}_{K^{[2]}} = \frac{iV}{2}\int\frac{d^3k_1 d^3k_2}{(2\pi)^6}\int d^3r e^{i(\vec{k}_1-\vec{k}_2)\cdot\vec{r}}f(r)\frac{\partial}{\partial r}f(r)u^\dagger(\vec{k}_1,s_1)u^\dagger(\vec{k}_2,s_2)(\vec{\alpha}_1-\vec{\alpha}_2)\cdot\vec{n}_r u(\vec{k}_1,s_1)u(\vec{k}_2,s_2) \tag{B.40}$$

$$-\frac{V}{2}\int\frac{d^3k_1 d^3k_2}{(2\pi)^6}\int d^3r e^{i(\vec{k}_1-\vec{k}_2)\cdot\vec{r}}[f^2(r)-1]$$

$$u^\dagger(\vec{k}_1,s_1)u^\dagger(\vec{k}_2,s_2)(\vec{\alpha}_1\cdot\vec{k}_1+\vec{\alpha}_2\cdot\vec{k}_2+2\beta M)u(\vec{k}_1,s_1)u(\vec{k}_2,s_2)$$

$$= -\frac{V}{2}\int\frac{d^3k_1 d^3k_2}{(2\pi)^6}\int d^3r e^{i(\vec{k}_1-\vec{k}_2)\cdot\vec{r}}[f^2(r)-1]\frac{2\mathrm{Tr}\{(\not{k}_1^*+M_1^*)(\vec{\gamma}\cdot\vec{k}_1+M)(\not{k}_2^*+M_2^*)\gamma^0\}}{4E^*(k_1)E^*(k_2)}$$

$$= V\int\frac{d^3k_1 d^3k_2}{(2\pi)^6}\int d^3r e^{i(\vec{k}_1-\vec{k}_2)\cdot\vec{r}}[f^2(r)-1]\left[\frac{\vec{k}_1\cdot\vec{k}_1^*}{E^*(k_1)}+2\frac{MM^*(k_1)}{E^*(k_1)}+\frac{\vec{k}_1\cdot\vec{k}_2^*}{E^*(k_2)}\right].$$

Here, the first line vanishes due to the spin structure. This contribution of short range correlation for relativistic kinetic energy has the different value with different parameters in Jastrow function. It is about $4\sim27$ MeV in [81]

B.3   Some integration formulas

In this appendix, k_F is the Fermi momentum, r is the relative distant $\vec{r} = \vec{x}_1 - \vec{x}_2$ and $\vec{X} = (\vec{x}_1 + \vec{x}_2)/2$.

$$\int \vec{k}_1 \cdot \vec{k}_2 d^3 k_1 = 0 \tag{B.41}$$

$$\int \sin\theta \exp(-ikr\cos\theta)d\theta = \frac{2\sin(kr)}{kr} = 2j_0(kr) \tag{B.42}$$

$$\int_0^{k_F} k^2 \frac{\sin(kr)}{kr} = \frac{\sin(k_F r) - k_F r \cos(k_F r)}{r^3} = k_F^3 \frac{j_1(k_F r)}{k_F r} \tag{B.43}$$

$$\int_0^{k_F} k^4 \frac{\sin(kr)}{kr} = k_F^5 \left[\frac{2j_0(k_F r)}{(k_F r)^2} + \left(\frac{1}{k_F r} - \frac{6}{(k_F r)^3} \right) j_1(k_F r) \right] \tag{B.44}$$

$$
\begin{aligned}
\langle ij|v(r)|ij\rangle \;&=\; \frac{1}{2} \sum_{\vec{k}_1, \vec{k}_2} \langle \vec{k}_1 \vec{k}_2 | v(r) | \vec{k}_1 \vec{k}_2 \rangle \\
&=\; \frac{1}{2} \int d^3 X d^3 r\, v(r) \sum_{\vec{k}_1, \vec{k}_2} |\langle \vec{x}_1 \vec{x}_2 | \vec{k}_1 \vec{k}_2 \rangle|^2 \\
&=\; \frac{V^3}{2(2\pi)^6} \int d^3 r\, v(r) \int d^3 k_1 d^3 k_2 \frac{1}{V^2} \exp(i\vec{k}_1 \cdot \vec{x}_1 + i\vec{k}_2 \cdot \vec{x}_2 - i\vec{k}_1 \cdot \vec{x}_1 - i\vec{k}_2 \cdot \vec{x}_2) \\
&=\; \frac{V}{2(2\pi)^6} \left(\frac{4\pi}{3} k_F^3 \right)^2 \int d^3 r\, v(r) \\
&=\; \frac{V}{72\pi^4} k_F^6 \int d^3 r\, v(r)
\end{aligned}
\tag{B.45}
$$

$$
\begin{aligned}
\langle ij|v(r)|ji\rangle \;&=\; \frac{1}{2} \sum_{\vec{k}_1, \vec{k}_2} \langle \vec{k}_1 \vec{k}_2 | v(r) | \vec{k}_2 \vec{k}_1 \rangle \\
&=\; \frac{1}{2} \int d^3 X d^3 r\, v(r) \sum_{\vec{k}_1, \vec{k}_2} \langle \vec{k}_1 \vec{k}_2 | \vec{x}_1 \vec{x}_2 \rangle \langle \vec{x}_1 \vec{x}_2 | \vec{k}_2 \vec{k}_1 \rangle \\
&=\; \frac{V^3}{2(2\pi)^6} \int d^3 r\, v(r) \int d^3 k_1 d^3 k_2 \frac{1}{V^2} \exp(i\vec{k}_1 \cdot \vec{x}_2 + i\vec{k}_2 \cdot \vec{x}_1 - i\vec{k}_1 \cdot \vec{x}_1 - i\vec{k}_2 \cdot \vec{x}_2) \\
&=\; \frac{V}{2(2\pi)^6} \int d^3 r\, v(r) \int d^3 k_1 d^3 k_2 \exp(i(\vec{k}_2 - \vec{k}_1) \cdot \vec{r})
\end{aligned}
\tag{B.46}
$$

$$= \frac{V}{2(2\pi)^6} \int d^3 r v(r) [\int 2\pi k_1^3 dk_1 \int \sin\theta d\theta \exp(ik_1 r \cos\theta)]^2$$

$$= \frac{V}{2(2\pi)^6} (4\pi k_F^3)^2 \int d^3 r v(r) \left(\frac{j_1(k_F r)}{k_F r}\right)^2$$

$$= \frac{V}{72\pi^4} k_F^6 \int d^3 r v(r) l_1^2(k_F r)$$

$$\langle ij|\vec{q}v(r)\vec{q}|ij\rangle = \frac{1}{2} \sum_{\vec{k}_1,\vec{k}_2} \langle \vec{k}_1 \vec{k}_2|\vec{q}v(r)\vec{q}|\vec{k}_1 \vec{k}_2\rangle \tag{B.47}$$

$$= \frac{1}{2} \int d^3 X d^3 r v(r) \sum_{\vec{k}_1,\vec{k}_2} |\langle \vec{x}_1 \vec{x}_2|\vec{q}|\vec{k}_1 \vec{k}_2\rangle|^2$$

$$= \frac{V}{2(2\pi)^6} \int d^3 r v(r) \int d^3 k_1 d^3 k_2 \frac{1}{4}(\vec{k}_1 - \vec{k}_2)^2$$

$$= \frac{V}{8(2\pi)^6} \int d^3 r v(r) 2 \int k_1^2 d^3 k_1 d^3 k_2$$

$$= \frac{V}{4(2\pi)^6} \left(\frac{4\pi}{5} k_F^5\right) \left(\frac{4\pi}{3} k_F^3\right) \int d^3 r v(r)$$

$$= \frac{V}{240\pi^4} k_F^8 \int d^3 r v(r)$$

$$\langle ij|\vec{q}v(r)\vec{q}|ji\rangle = \frac{1}{2} \sum_{\vec{k}_1,\vec{k}_2} \langle \vec{k}_1 \vec{k}_2|\vec{q}v(r)\vec{q}|\vec{k}_2 \vec{k}_1\rangle \tag{B.48}$$

$$= \frac{1}{2} \int d^3 X d^3 r v(r) \sum_{\vec{k}_1,\vec{k}_2} \langle \vec{k}_1 \vec{k}_2|\vec{q}|\vec{x}_1 \vec{x}_2\rangle \langle \vec{x}_1 \vec{x}_2|\vec{q}|\vec{k}_1 \vec{k}_2\rangle$$

$$= -\frac{V}{2(2\pi)^6} \int d^3 r v(r) \int d^3 k_1 d^3 k_2 \frac{1}{4}(\vec{k}_1 - \vec{k}_2)^2 \exp(i(\vec{k}_2 - \vec{k}_1) \cdot \vec{r})$$

$$= -\frac{V}{8(2\pi)^6} \int d^3 r v(r) \int d^3 k_1 d^3 k_2 (k_1^2 + k_2^2 - 2\vec{k}_1 \cdot \vec{k}_2) \exp(i(\vec{k}_2 - \vec{k}_1) \cdot \vec{r})$$

$$= -\frac{V}{4(2\pi)^6} \int d^3 r v(r) \left\{ 4\pi k_F^3 \frac{j_1(k_F r)}{k_F r} 4\pi k_F^5 \left[\frac{2j_0(k_F r)}{(k_F r)^2} + \left(\frac{1}{k_F r} - \frac{6}{(k_F r)^3}\right) j_(k_F r) \right] \right.$$

$$\left. - \left[4\pi k_F^4 \left(-\frac{j_0(k_F r)}{k_F r} + \frac{3j_1(k_F r)}{(k_F r)^2} \right) \right]^2 \right\}$$

$$= \frac{15 V k_F^8}{240\pi^4} \int d^3 r v(r) \left[\frac{j_0(k_F r)}{(k_F r)^2} + \left(\frac{15}{(k_F r)^4} - \frac{1}{(k_F r)^2}\right) j_1^2(k_F r) - \frac{8}{(k_F r)^3} j_0(k_F r) j_1(k_F r) \right]$$

$$= \frac{V}{240\pi^4} k_F^8 \int d^3 r v(r) l_2(k_F r)$$

$$
\begin{aligned}
\langle ij|q_r v(r) q_r|ij\rangle &= \frac{1}{2}\sum_{\vec{k}_1,\vec{k}_2}\langle \vec{k}_1\vec{k}_2|q_r v(r) q_r|\vec{k}_1\vec{k}_2\rangle \qquad\qquad\qquad (B.49)\\
&= \frac{1}{2}\int d^3X d^3r\, v(r)\sum_{\vec{k}_1,\vec{k}_2}|\langle \vec{x}_1\vec{x}_2|\vec{q}_r|\vec{k}_1\vec{k}_2\rangle|^2\\
&= \frac{V}{2(2\pi)^6}\int d^3r\, v(r)\int d^3k_1 d^3k_2 \frac{1}{4}\left[\frac{\vec{r}}{r}(\vec{k}_1-\vec{k}_2)\right]^2\\
&= \frac{V}{8(2\pi)^6}\int d^3r\, v(r)2\int \frac{\vec{r}\cdot\vec{k}_1}{r}d^3k_1 d^3k_2\\
&= \frac{V}{4(2\pi)^6}\left(\frac{4\pi}{15}k_F^5\right)\left(\frac{4\pi}{3}k_F^3\right)\int d^3r\, v(r)\\
&= \frac{V}{720\pi^4}k_F^8\int d^3r\, v(r)
\end{aligned}
$$

$$
\begin{aligned}
\langle ij|q_r v(r) q_r|ji\rangle &= \frac{1}{2}\sum_{\vec{k}_1,\vec{k}_2}\langle \vec{k}_1\vec{k}_2|q_r v(r) q_r|\vec{k}_2\vec{k}_1\rangle \qquad\qquad\qquad (B.50)\\
&= \frac{1}{2}\int d^3X d^3r\, v(r)\sum_{\vec{k}_1,\vec{k}_2}\langle \vec{k}_1\vec{k}_2|q_r|\vec{x}_1\vec{x}_2\rangle\langle \vec{x}_1\vec{x}_2|q_r|\vec{k}_1\vec{k}_2\rangle\\
&= -\frac{V}{2(2\pi)^6}\int d^3r\, v(r)\int d^3k_1 d^3k_2\frac{1}{4}\left[\frac{\vec{r}}{r}\cdot(\vec{k}_1-\vec{k}_2)\right]^2\exp(i(\vec{k}_2-\vec{k}_1)\cdot\vec{r})\\
&= -\frac{V}{4(2\pi)^6}\int d^3r\, v(r)\left\{4\pi k_F^3\frac{j_1(k_F r)}{k_F r}4\pi k_F^5\left[\frac{4j_0(k_F r)}{(k_F r)^2}+\left(\frac{1}{k_F r}-\frac{12}{(k_F r)^3}\right)j(k_F r)\right]\right.\\
&\quad\left.-\left[4\pi k_F^4\left(-\frac{j_0(k_F r)}{k_F r}+\frac{3j_1(k_F r)}{(k_F r)^2}\right)\right]^2\right\}\\
&= \frac{45V k_F^8}{720\pi^4}\int d^3r\, v(r)\left[\frac{j_0(k_F r)}{(k_F r)^2}+\left(\frac{21}{(k_F r)^4}-\frac{1}{(k_F r)^2}\right)j_1^2(k_F r)-\frac{10}{(k_F r)^3}j_0(k_F r)j_1(k_F r)\right]\\
&= \frac{V}{720\pi^4}k_F^8\int d^3r\, v(r)l_3(k_F r)
\end{aligned}
$$

When we consider the form factor on the OBEP, the interaction can be changed as,

$$
\frac{1}{\mathbf{q}^2+m_\alpha^2}\left(\frac{\Lambda_\alpha^2-m_\alpha^2}{\mathbf{q}^2+\Lambda_\alpha^2}\right)^2 = \frac{1}{\mathbf{q}^2+m_\alpha^2}-\frac{1}{\mathbf{q}^2+\Lambda_\alpha^2}+(\Lambda_\alpha^2-m_\alpha^2)\frac{d}{d\Lambda_\alpha^2}\frac{1}{\mathbf{q}^2+\Lambda_\alpha^2} \qquad (B.51)
$$

$$
\frac{\mathbf{q}^2}{\mathbf{q}^2+m_\alpha^2}\left(\frac{\Lambda_\alpha^2-m_\alpha^2}{\mathbf{q}^2+\Lambda_\alpha^2}\right)^2 = \frac{\Lambda_\alpha^2}{\mathbf{q}^2+\Lambda_\alpha^2}-\frac{m_\alpha^2}{\mathbf{q}^2+m_\alpha^2}-(\Lambda_\alpha^2-m_\alpha^2)\frac{d}{d\Lambda_\alpha^2}\frac{\Lambda_\alpha^2}{\mathbf{q}^2+\Lambda_\alpha^2} \qquad (B.52)
$$

Appendix C

The extended chiral mean field model

Recently, Kaiser *et al.* have made an interesting work, where they have studied the role of the pion systematically using expansion in the Fermi momentum [69]. They have found that the pion exchange interaction plays the major role for providing the binding energy and the saturation property of nuclear matter. Particularly important in the pion contribution is the direct iterated one-pion exchange diagram, which is far dominant as compared with other terms such as the Fock term and the crossed 2p-2h excitation term. We would like to call the direct iterated pion exchange term as the two-particle-two-hole (2p-2h) excitation diagram in this section.

Another development was made recently by Ericson *et al.* who have studied nuclear matter by using a chiral model Lagrangian [97]. Their treatment of the one-pion exchange interaction is, however, different from that of Kaiser *et al.* [69], and the resulting role of the pion exchange interaction on the property of nuclear matter is very different. The pion contribution is not as large as that of Kaiser *et al.* , while the role of the σ meson exchange is largely attractive to provide sufficient binding energy. They have also studied chiral properties of nuclear matter such as the chiral condensate and the scalar susceptibility which are the first and second order derivatives of the grand potential with respect to the bare quark mass while keeping the chemical potential fixed.

We should find out why completely different conclusions are derived from the work of Kaiser *et al.* [69] and the work of Ericson *et al.* [97]. After clarifying this, we would also like to study chiral properties of nuclear matter, since they are largely influenced by the treatment and the resulting roles of the pion contribution.

In order to work out nuclear matter properly by including pion contributions, we point out that there are important works in recent years on the treatment of the pion exchange potential, especially on the tensor interaction by means of the so called tensor optimized shell model (TOSM) [98, 99]. Myo *et al.* included all 2p-2h configurations with various angular momenta which mix in the ground state by the tensor interaction. The pion exchange interaction has a large tensor term, which should be treated in the TOSM prescription. Fur-

thermore, the short range repulsive interaction, which is caused by quark structure of the nucleon [27], is nicely treated in terms of the unitary correlation operator method (UCOM) by Feldmeier *et al.* [61, 62]. The central spin-spin interaction of the one-pion exchange interaction is subject to the short range correlation, which are treated by the UCOM prescription. In our study we are able to use these two methods for the study of the effect of the pion in nuclear matter. Hence, the second purpose of the present study is to develop a method to treat the pion exchange interaction with the inclusion of the short range effect for the study of nuclear matter.

We write the Hamiltonian density, $\mathcal{H}$ of chiral sigma model, instead of Lagrangian density as follows [100, 101, 102, 103],

$$
\begin{aligned}
\mathcal{H} = {} & \psi^\dagger(-i\vec{\alpha}\cdot\vec{\nabla} + \beta M_N + \beta g_\sigma \sigma + g_\omega \omega)\psi \\
& + \frac{1}{2}m_\sigma^2\sigma^2 + \lambda f_\pi \sigma^3 + \frac{\lambda}{4}\sigma^4 - \frac{1}{2}m_\omega^2\omega^2 - \widetilde{g_\omega}^2 f_\pi \sigma\omega^2 - \frac{1}{2}\widetilde{g_\omega}^2\sigma^2\omega^2 \\
& - \frac{1}{2}\int d^3x' \int \frac{d^3k}{(2\pi)^3}\left(\frac{g_A}{2f_\pi}\right)^2 \bar\psi(x)\gamma_5\gamma_\mu\tau^a k^\mu \psi(x)\frac{e^{i\vec{k}(\vec{x}-\vec{x}')}}{\vec{k}^2 + m_\pi^2}\bar\psi(x')\gamma_5\gamma_\nu\tau^a k^\nu \psi(x').
\end{aligned}
\tag{C.1}
$$

We have written here explicitly only the time component of the omega meson field to anticipate the mean field treatment.

We introduce now a trial wave function for the ground state,

$$
\Psi(\sigma,\omega,\psi) = \Psi(\sigma,\omega)\Psi_N(\{c_i\}).
\tag{C.2}
$$

Here, $\Psi(\sigma,\omega)$ is a coherent state defined by

$$
\begin{aligned}
\langle\Psi(\sigma,\omega)|\sigma|\Psi(\sigma,\omega)\rangle &= \sigma, \\
\langle\Psi(\sigma,\omega)|\omega_\mu|\Psi(\sigma,\omega)\rangle &= \delta_{\mu,0}\omega.
\end{aligned}
\tag{C.3}
$$

We do not need an explicit form of the coherent state wave function for the σ and ω mesons. We need only the mean field values, σ and ω, which are hereafter classical fields. This procedure corresponds to the relativistic mean field (RMF) approximation.

For the nucleon part $\Psi_N(\{c_i\})$, we write a variational wave function by including 2p-2h components for the optimization of pion contributions, following the TOSM prescription for finite nuclei,

$$
\Psi_N(\{c_i\}) = c_0|0\rangle + \sum_i c_i|\text{2p-2h} : i\rangle,
\tag{C.4}
$$

where $|\text{2p-2h} : i\rangle$ is written explicitly as

$$
|\text{2p-2h} : i\rangle = a^\dagger_{\vec{p}_1+\vec{k},s_1,t_1} a_{\vec{p}_1,s_2,t_2} a^\dagger_{\vec{p}_2-\vec{k},s_3,t_3} a_{\vec{p}_2,s_4,t_4}|0\rangle.
\tag{C.5}
$$

Here, $a^\dagger$ and a are creation and annihilation operators of nucleon state, and $|0\rangle$ denotes the ground state in the mean field approximation. This equation shows creation of particle

and hole states of nucleon carrying momenta as indicated by the subscripts of the nucleon creation and annihilation operators. The extra subscripts s and t denote the spin and isospin of the nucleon. For simplicity, these three indices $(\vec{p}, s, t)$ are expressed by a single label i in Eq.(C.5). The corresponding diagram is shown in Fig.C.1.

$$\vec{p}_1 \qquad \vec{p}_1 + \vec{k} \qquad \vec{p}_2 - \vec{k} \qquad \vec{p}_2$$
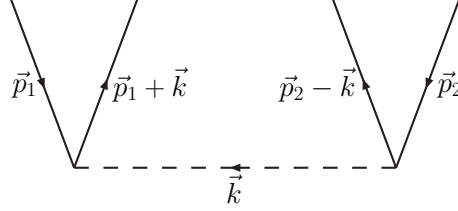
$$\vec{k}$$

Figure C.1: Feynman diagram for 2p-2h state.

The single particle wave function is a product of a plane wave solution, $u(\vec{p}, s)e^{-ipx}$ with a momentum $\vec{p}$ and a spin s, and an isospin wave function, $\chi(t)$, of isospin t,

$$\psi(x) = \frac{1}{\sqrt{V}} u(\vec{p}, s)e^{-ipx}\chi(t). \tag{C.6}$$

Here, V is the volume in which periodic boundary condition is imposed. We take the normalization condition for the spinor $u(\vec{p}, s)$ as $u^\dagger(\vec{p}, s)u(\vec{p}, s) = 1$.

We will now make variation of the total energy with respect to the parameters in the trial wave function; σ, ω and $\{c_i\}$. The total energy per unit volume E is written as

$$E(\sigma, \omega, \{c_i\}) = \langle \Psi | \int d^3x \mathcal{H} | \Psi \rangle / V = \langle \Psi | H | \Psi \rangle / V, \tag{C.7}$$

where H is the Hamiltonian. Then, the minimization of E with respect to σ and ω provides

$$m_\sigma^2 \sigma = -g_\sigma \langle \Psi_N | \bar{\psi}\psi | \Psi_N \rangle + \widetilde{g_\omega}^2 f_\pi \omega^2 + \widetilde{g_\omega}^2 \sigma \omega^2 - 3\lambda f_\pi \sigma^2 - \lambda \sigma^3, \tag{C.8}$$

$$m_\omega^2 \omega = g_\omega \langle \Psi_N | \psi^\dagger \psi | \Psi_N \rangle - 2\widetilde{g_\omega}^2 f_\pi \sigma \omega - \widetilde{g_\omega}^2 \sigma^2 \omega.$$

These two equations determine the mean field values of σ and ω when the scalar density $\langle \Psi_N | \bar{\psi}\psi | \Psi_N \rangle$ and the vector density $\langle \Psi_N | \psi^\dagger \psi | \Psi_N \rangle$ of the ground state are given. For this we need an equation to determine Ψ_N.

We write the total energy as

$$\langle \Psi | H | \Psi \rangle = c_0^* c_0 \langle 0 | H | 0 \rangle + \sum_j c_0^* c_j \langle 0 | H | \text{2p-2h} : j \rangle \tag{C.9}$$

$$+ \sum_i c_i^* c_0 \langle \text{2p-2h} : i | H | 0 \rangle + \sum_{i,j} c_i^* c_j \langle \text{2p-2h} : i | H | \text{2p-2h} : j \rangle.$$

Here, the sigma and omega meson fields take the mean field values in the above matrix element of the Hamiltonian. The energy of the 0p-0h state is given by the expression of the

relativistic mean field (RMF) model,

$$\langle 0|H|0\rangle \;=\; \frac{4}{V}\sum_{|\vec{p}|}^{p_F}\sqrt{\vec{p}^2 + M_N^{*2}} + g_\omega\omega\rho_V \tag{C.10}$$

$$+\;\; \frac{1}{2}m_\sigma^2\sigma^2 + \lambda f_\pi\sigma^3 + \frac{\lambda}{4}\sigma^4 - \frac{1}{2}m_\omega^2\omega^2 - \widetilde{g}_\omega^{\;2}f_\pi\sigma\omega^2 - \frac{1}{2}\widetilde{g}_\omega^{\;2}\sigma^2\omega^2,$$

where the factor 4 of the first term includes spin and isospin degrees of freedom and ρ_V is

$$\rho_V = \frac{4}{V}\sum_{|\vec{p}|}^{p_F}1 = 4\int^{p_F}\frac{d^3p}{(2\pi)^3} = \frac{2}{3\pi^2}p_F^3. \tag{C.11}$$

The nucleon effective mass is written as

$$M_N^* = M_N + g_\sigma\sigma. \tag{C.12}$$

In Eqs.(C.10)-(C.11), $\vec{p}$ is discredited by the quantization in a finite size box. However, we shall replace the summation by integration using the rule, $\frac{1}{V}\sum_i \to \int \frac{d^3p}{(2\pi)^3}$, and write the momentum as a continuous variable.

For the matrix element between $|0\rangle$ and $|2p\text{-}2h\rangle$, we obtain

$$\langle 0| \;\; -\frac{1}{2}\left(\frac{g_A}{2f_\pi}\right)^2\int d^3x_1 d^3x_2\int\frac{d^3k}{(2\pi)^3}\bar{\psi}(x_1)\gamma_5\gamma_\mu\tau^a k^\mu\psi(x_1) \tag{C.13}$$

$$\frac{e^{i\vec{k}(\vec{x_1}-\vec{x_2})}}{\vec{k}^2 + m_\pi^2}\bar{\psi}(x_2)\gamma_5\gamma_\nu\tau^a k^\nu\psi(x_2)|2p\text{-}2h:i\rangle$$

$$=\;\; -\left(\frac{g_A}{2f_\pi}\right)^2\bar{u}(\vec{p_1}+\vec{k},s_1)\gamma_5\vec{\gamma}\cdot\vec{k}u(\vec{p_1},s_2)\langle t_1|\tau^a|t_2\rangle$$

$$\frac{1}{\vec{k}^2 + m_\pi^2}\bar{u}(\vec{p_2}-\vec{k},s_3)\gamma_5\vec{\gamma}\cdot\vec{k}u(\vec{p_2},s_4)\langle t_3|\tau^a|t_4\rangle.$$

As for the 2p-2h matrix elements, we take an approximation of taking only the single particle part and drop the contribution of the pion exchange interaction,

$$\langle 2p\text{-}2h:i|H|2p\text{-}2h:j\rangle \sim \delta_{i,j}\frac{1}{V}\epsilon_{2p\text{-}2h} + \delta_{i,j}\langle 0|H|0\rangle, \tag{C.14}$$

where

$$\epsilon_{2p\text{-}2h} \;=\; \sqrt{(\vec{p_1}+\vec{k})^2 + M_N^{*2}} - \sqrt{\vec{p_1}^2 + M_N^{*2}} \tag{C.15}$$

$$+\;\; \sqrt{(\vec{p_2}-\vec{k})^2 + M_N^{*2}} - \sqrt{\vec{p_2}^2 + M_N^{*2}}.$$

Having all the above ingredients, we can write the total energy as

$$\langle\Psi|H|\Psi\rangle \;=\; \langle 0|H|0\rangle\left(c_0^*c_0 + \sum_i c_i^*c_i\right) + \sum_i c_0^*c_i\langle 0|H|2p\text{-}2h:i\rangle \tag{C.16}$$

$$+ \sum_i c_i^* c_0 \langle \text{2p-2h} : i | H | 0 \rangle + \sum_i c_i^* c_i \frac{1}{V} \epsilon_{\text{2p-2h}}.$$

Using the normalization condition

$$\langle \Psi | \Psi \rangle = c_0^* c_0 + \sum_i c_i^* c_i = 1, \tag{C.17}$$

we get the following equation by variation of $E = \frac{\langle \Psi | H | \Psi \rangle}{\langle \Psi | \Psi \rangle}$ with respect to c_i^* as

$$c_0 \langle \text{2p-2h} : i | H | 0 \rangle + c_i \frac{1}{V} \epsilon_{\text{2p-2h}} + \langle 0 | H | 0 \rangle c_i - E c_i = 0. \tag{C.18}$$

We can then solve for c_i as

$$c_i = \frac{-c_0 \langle \text{2p-2h} : i | H | 0 \rangle}{\frac{1}{V} \epsilon_{\text{2p-2h}} + \langle 0 | H | 0 \rangle - E}, \tag{C.19}$$

where E is the ground state energy. This equation can be solved iteratively. We point out here that the expression for c_i in Eq.(C.19) becomes the one of perturbation if we drop $\langle 0 | H | 0 \rangle - E$ in the denominator. In the actual calculation we make the self-consistent calculation with this term in Eq.(C.19). The self-consistency condition provides important effects in the structure of finite nuclei in the tensor optimized shell model [99].

We get the nucleon wave function, Ψ_N, by solving the above equations for c_i. Hence, we can calculate the vector and scalar densities for the mean field equations,

$$
\begin{aligned}
\rho_V &= \langle \Psi_N | \psi^\dagger \psi | \Psi_N \rangle \tag{C.20} \\
&= \langle 0 | \psi^\dagger \psi | 0 \rangle + \sum_i c_i^* c_i \frac{1}{V} \left(u^\dagger(\vec{p}_1 + \vec{k}, s_1) u(\vec{p}_1 + \vec{k}, s_1) + u^\dagger(\vec{p}_2 - \vec{k}, s_3) u(\vec{p}_2 - \vec{k}, s_3) \right. \\
&\quad \left. - u^\dagger(\vec{p}_1, s_2) u(\vec{p}_1, s_2) - u^\dagger(\vec{p}_2, s_4) u(\vec{p}_2, s_4) \right) \\
&= \frac{2}{3\pi^2} p_F^3, \\
\rho_S &= \langle \Psi_N | \bar{\psi} \psi | \Psi_N \rangle = 4 \int \frac{d^3 p}{(2\pi)^3} \frac{M_N^*}{\sqrt{p^2 + M_N^{*2}}} + \sum_i c_i^* c_i \frac{1}{V} \\
&\quad \left(\frac{M_N^*}{\sqrt{(\vec{p}_1 + \vec{k})^2 + M_N^{*2}}} + \frac{M_N^*}{\sqrt{(\vec{p}_2 - \vec{k})^2 + M_N^{*2}}} - \frac{M_N^*}{\sqrt{p_1^2 + M_N^{*2}}} - \frac{M_N^*}{\sqrt{p_2^2 + M_N^{*2}}} \right),
\end{aligned}
$$

where we have used the spinor normalization condition $u^\dagger(\vec{p}, s) u(\vec{p}, s) = 1$.

We work out now the summation of all the quantum states involving 2p-2h excitations; integration over $\vec{p}_1$, $\vec{p}_2$ and $\vec{k}$ for the case of perturbation. Here, we use the expression of Eq.(C.19) without $\langle 0 | H | 0 \rangle - E$ in the denominator. After tedious calculation, we get the energy for the 2p-2h excitations,

$$E_{\text{2p-2h}} = -\frac{3 M_N^* g_A^4 k_F^7 c_0 c_0^*}{\pi^2 f_\pi^4 (2\pi)^4} \tag{C.21}$$

$$\left\{\left[\int_0^1 dx \frac{x^5}{(x^2 + m_\pi^2/4k_F^2)^2}\left[\frac{(58 - 80\ln 2)x^2}{15} - \frac{2x^4}{5}\right.\right.\right.$$

$$+ \frac{8}{15}\ln\left(1 - x^2\right) + \left(x - \frac{2x^3}{3} + \frac{x^5}{5}\right)\ln\left(\frac{1+x}{1-x}\right)\right]$$

$$+ \int_1^\infty dx \frac{x^5}{(x^2 + m_\pi^2/4k_F^2)^2}\left[\frac{44x}{15} + \frac{8x^3}{15} + \left(-\frac{8x^3}{3} + \frac{8x^5}{15}\right)\ln\left(1 - \frac{1}{x^2}\right)\right.$$

$$\left.\left.\left.+ \left(\frac{8}{15} - \frac{8x^2}{3}\right)\ln\left(\frac{x+1}{x-1}\right)\right]\right]\right\},$$

where we have used $x = p/2k_F$ and $x^2/(x^2 + m_\pi^2/4k_F^2)$ term represents the one-pion exchange interaction. In actual calculation, we use the expression of Eq.(C.19) which include $\langle 0|H|0\rangle - E$ in the denominator for the equation of state and chiral condensate. It will become a self-consistent calculation with total energy E. But the expressions are very complicated and long, we do not write here explicitly. We notice that the second integration in Eq. (C.21) is divergent. We regularize it by introducing the dipole pion-nucleon form factor on the pion exchange interaction, which reflects the finite size effect of the nucleon. Furthermore, for the spin-spin interaction originating from the one-pion exchange interaction, we consider furthermore the effect of the short range correlation in terms of UCOM.

For the use of the central interaction after the UCOM prescription is performed in our formulation, we expand the modified central interaction in terms of gaussian functions and then Fourier transform the coordinate space interaction in the momentum space.

$$\tilde{V}(r) = V(R_+(r)) = \sum_i a_i \exp\left(-(\frac{r}{r_i})^2\right). \tag{C.22}$$

We can then easily perform Fourier transform and the momentum space expression is obtained as

$$\tilde{V}(k) = \sum_i a_i(\pi r_i^2)^{3/2}\exp\left(-\frac{\vec{k}^2 r_i^2}{4}\right). \tag{C.23}$$

Because we just consider the UCOM for the central part of the pion nucleon interaction, we work out now the part which contains spinors in order to separate the matrix element between $|0\rangle$ and $|2\text{p-}2\text{h}\rangle$ into the spin-spin part and the tensor part,

$$M = \bar{u}(\vec{p}_1 + \vec{k}, s_1)\gamma_5\vec{\gamma}\cdot\vec{k}u(\vec{p}_1, s_2)\frac{1}{\vec{k}^2 + m_\pi^2}\bar{u}(\vec{p}_2 - \vec{k}, s_3)\gamma_5\vec{\gamma}\cdot\vec{k}u(\vec{p}_2, s_4) \tag{C.24}$$

$$= u^\dagger(\vec{p}_1 + \vec{k}, s_1)u^\dagger(\vec{p}_2 - \vec{k}, s_3)\begin{pmatrix} 1 & 0 \\ 0 & 1 \end{pmatrix}_1 \frac{\vec{\sigma}_1\cdot\vec{k}\vec{\sigma}_2\cdot\vec{k}}{\vec{k}^2 + m_\pi^2}\begin{pmatrix} 1 & 0 \\ 0 & 1 \end{pmatrix}_2 u(\vec{p}_1, s_2)u(\vec{p}_2, s_4),$$

where the matrices with suffix 1 and 2 are those for particle 1 and 2, respectively. Now we can separate the pion exchange potential into the central and the tensor parts by using the

relation,

$$\frac{\vec{\sigma}_1 \cdot \vec{k}\vec{\sigma}_2 \cdot \vec{k}}{k^2 + m_\pi^2} = \frac{1}{3}\left[\vec{\sigma}_1 \cdot \vec{\sigma}_2 \frac{k^2}{k^2 + m_\pi^2} + \frac{3\vec{\sigma}_1 \cdot \vec{k}\vec{\sigma}_2 \cdot \vec{k} - k^2\vec{\sigma}_1 \cdot \vec{\sigma}_2}{k^2 + m_\pi^2}\right]. \tag{C.25}$$

On the right hand side, the first term is the central part and the second term is the tensor part. By including the short range correlation with the UCOM for the central part, we can express the interaction as

$$\frac{1}{3}\left[\vec{\sigma}_1 \cdot \vec{\sigma}_2\left(\tilde{V}(k) - V(k)\right) + \frac{3\vec{\sigma}_1 \cdot \vec{k}\vec{\sigma}_2 \cdot \vec{k}}{k^2 + m_\pi^2}\right], \tag{C.26}$$

where $V(k) = \vec{k}^2/(\vec{k}^2 + m_\pi^2)$ is the central part of the original interaction and $\tilde{V}(k)$ is the modified one by the UCOM. For simplicity, we shall take the non-relativistic approximation for the evaluation of the spin matrix elements,

$$M = \frac{1}{3}\left(\tilde{V}(k) - V(k)\right)\langle s_1|\sigma_1^a|s_2\rangle\langle s_3|\sigma_2^a|s_4\rangle \tag{C.27}$$

$$+\frac{\langle s_1|\vec{\sigma}_1 \cdot \vec{k}|s_2\rangle\langle s_3|\vec{\sigma}_2 \cdot \vec{k}|s_4\rangle}{k^2 + m_\pi^2}.$$

Here, we have dropped the exchange term contribution, although it is straightforward to work out.

Finally, we have to make a self-consistent calculation in order to get the solution of the whole system by energy minimization. We make the nonrelativistic approximation for the nucleon energy $\sqrt{p_1^2 + m^2}$ and also for the spin matrix elements. Since we solve the above equations step by step, we shall provide the squared quantity for the matrix element between $|0\rangle$ and $|2\text{p-2h}\rangle$. The squared matrix elements are written as

$$|\langle 0|H|2\text{p-2h}:i\rangle|^2$$

$$= \left(\frac{g_A}{2f_\pi}\right)^4 \frac{1}{V^2}\theta(|\vec{p}_1 + \vec{k}| - k_F)\theta(|\vec{p}_2 - \vec{k}| - k_F)\theta(k_F - |\vec{p}_1|)\theta(k_F - |\vec{p}_2|)\left(Tr\{\tau^a\tau^b\}\right)^2$$

$$\left(\frac{1}{9}\left(\tilde{V}(k) - V(k)\right)^2 Tr\{\sigma_1^a\sigma_1^b\}Tr\{\sigma_2^a\sigma_2^b\} + \frac{Tr\{(\vec{\sigma}_1 \cdot \vec{k})^2\}Tr\{(\vec{\sigma}_2 \cdot \vec{k})^2\}}{(k^2 + m_\pi^2)^2}\right.$$

$$\left.+\frac{1}{3}\frac{\tilde{V}(k) - V(k)}{k^2 + m_\pi^2}\left(Tr\{\sigma_1^a\vec{\sigma}_1 \cdot \vec{k}\}Tr\{\sigma_2^a\vec{\sigma}_2 \cdot \vec{k}\} + Tr\{\vec{\sigma}_1 \cdot \vec{k}\sigma_1^b\}Tr\{\vec{\sigma}_2 \cdot \vec{k}\sigma_2^b\}\right)\right)$$

$$= \left(\frac{g_A}{2f_\pi}\right)^4 \frac{1}{V^2}\theta(|\vec{p}_1 + \vec{k}| - k_F)\theta(|\vec{p}_2 - \vec{k}| - k_F)\theta(k_F - |\vec{p}_1|)\theta(k_F - |\vec{p}_2|) \times 12$$

$$\left(\frac{12}{9}\left(\tilde{V}(k) - V(k)\right)^2 + \frac{4k^4}{(k^2 + m_\pi^2)^2} + \frac{8}{3}\frac{k^2\left(\tilde{V}(k) - V(k)\right)}{k^2 + m_\pi^2}\right), \tag{C.28}$$

where we have used $Tr\{\sigma^a\sigma^b\} = 2\delta^{ab}$, $Tr\{\vec{\sigma}\cdot\vec{a}\vec{\sigma}\cdot\vec{b}\} = 2\vec{a}\cdot\vec{b}$ and $Tr\{\sigma^a\vec{\sigma}\cdot\vec{k}\} = 2k^a$, where k^a is the a-th component of $\vec{k}$. Since $V(k) = \frac{\vec{k}^2}{\vec{k}^2+m_\pi^2}$, we get

$$
\begin{aligned}
&|\langle 0|H|\text{2p-2h}:i\rangle|^2 \\
=\quad &\left(\frac{g_A}{2f_\pi}\right)^4 \frac{12}{V^2}\theta(|\vec{p}_1+\vec{k}|-k_F)\theta(|\vec{p}_2-\vec{k}|-k_F)\theta(k_F-|\vec{p}_1|)\theta(k_F-|\vec{p}_2|) \\
&\left(4V^2(k) + \frac{4}{3}\left(\tilde{V}^2(k)-V^2(k)\right)\right).
\end{aligned}
\tag{C.29}
$$

Therefore, when we consider the UCOM effect in our program, we just have to use the modified matrix elements of Eq.(C.29) instead of the corresponding part appearing in Eq.(C.21), which contains $V^2(k)$.

Finally, we consider the nucleon form factor which is associated with the finite size of the nucleon [11]. Here, we employ the dipole form factor in which we replace the one-pion exchange interaction $\frac{\vec{k}^2}{\vec{k}^2+m_\pi^2}$ in the momentum space by

$$
\frac{\vec{k}^2}{\vec{k}^2+m_\pi^2} \rightarrow \frac{\vec{k}^2}{\vec{k}^2+m_\pi^2}\left(\frac{\Lambda^2-m_\pi^2}{\Lambda^2+\vec{k}^2}\right)^2.
\tag{C.30}
$$

We can then manipulate this as

$$
\begin{aligned}
\frac{\vec{k}^2}{\vec{k}^2+m_\pi^2}\left(\frac{\Lambda^2-m_\pi^2}{\Lambda^2+\vec{k}^2}\right)^2 =\quad &\left(\frac{\vec{k}^2}{\vec{k}^2+m_\pi^2}-\frac{\vec{k}^2}{\vec{k}^2+\Lambda^2}\right)\left(\frac{\Lambda^2-m_\pi^2}{\Lambda^2+\vec{k}^2}\right) \\
=\quad &\frac{\Lambda^2}{\vec{k}^2+\Lambda^2}-\frac{m_\pi^2}{\vec{k}^2+m_\pi^2}-\frac{\Lambda^2-m_\pi^2}{2\Lambda}\frac{\partial}{\partial\Lambda}\frac{\Lambda^2}{\Lambda^2+\vec{k}^2}.
\end{aligned}
\tag{C.31}
$$

This form indicates that calculations can be performed with the Yukawa interaction. This is true even for the case $\vec{k}^2$ is included in the numerator.

We would like to start with modification of the pion exchange interaction due to the nucleon form factor and the short range correlation effect. We show first the effect of the form factor in Fig.C.2, where shown is the momentum dependent part of the one-pion exchange interaction, $V(\vec{k}) = \vec{k}^2/(\vec{k}^2+m_\pi^2)$. The pion exchange interaction without the form factor increases with momentum, while that with the form factor decreases in the high momentum region. As the cutoff momentum, Λ, is decreased, the pion exchange interaction decreases particularly in the high momentum region. Due to this behavior, the energy gain associated with the pion is smaller for a smaller Λ by cutting down the contribution from the high momentum region.

Next, the effect of the short range correlation is shown in Fig.C.3. The pion exchange interaction can be separated into the tensor interaction and the spin-spin central interaction.
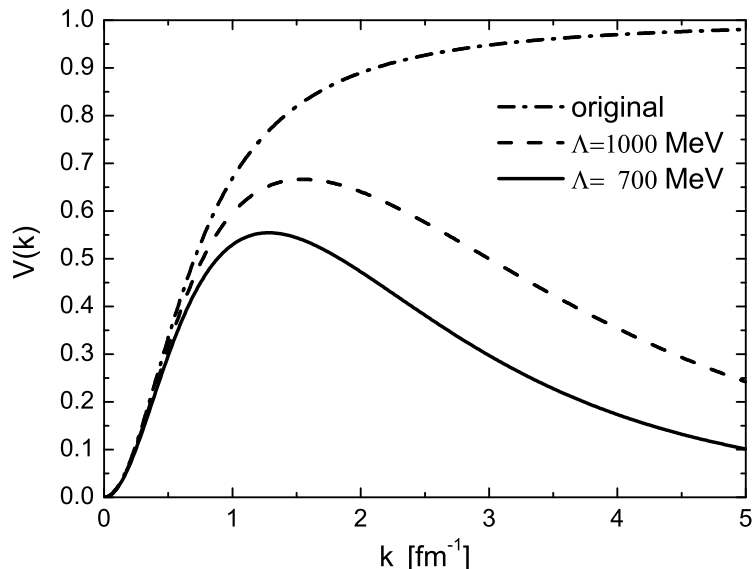
Figure C.2: The momentum dependent part of the pion exchange interaction with and without the form factor as function of momentum. The dot-dashed curve corresponds to the interaction without the form factor, the dashed curve denotes the one with the form factor of $\Lambda = 1000$ MeV and the solid curve with $\Lambda = 700$ MeV.

The tensor interaction requires the change of the quantum number of angular momentum by two, $\Delta l = 2$, because the tensor operator is written as $S_{12}(\hat{r}) = \sqrt{24\pi}[[\sigma_1 \cdot \sigma_2]^{(2)} \times Y_2(\hat{r})]^{(0)}$. Hence, the lowest angular momentum involved in the matrix element of the tensor interaction is between s-state ($l = 0$) and d-state ($l = 2$). The d-state is pushed away from the central region due to the centrifugal potential, $V_c(r = 0.5 \text{ fm}) \sim 1000$ MeV, and hence the effect of the short range correlation is negligible for the tensor interaction. Therefore, in the following discussion, we shall neglect the short range correlation effect for the tensor part of the pion exchange interaction [99].

On the other hand, the effect of the short range correlation is large and essential for the spin-spin central interaction, because it works between s-states. In this case, there is no centrifugal barrier to protect two nucleons to approach into the short range region. We shall take care of the short range correlation effect for the spin-spin central interaction by the UCOM. We choose two sets of parameters. One is the set of Feldmeier and Neff, $\alpha = 0.94$ fm, $\beta = 1$ fm and $\eta = 0.37$ [61], and the other set is $\alpha = 0.8$ fm, $\beta = 0.6$ fm and $\eta = 0.37$. These two sets of UCOM parameters provide the function $R_+(r)$ as function of the relative coordinate of two nucleons, r, as shown in Fig.C.3. They also provide modification of the wave function at $r \lesssim 0.5$ fm as shown in the right panel of Fig.C.3 ($\psi = U\phi$). It is important to express the behavior of the short range part of modified wave functions as closely as possible to the rigorous relative wave function [62].

The spin-spin central part with the UCOM effect, $\tilde{V}(r)$ and $\tilde{V}(k)$ in Eqs. (C.22) and
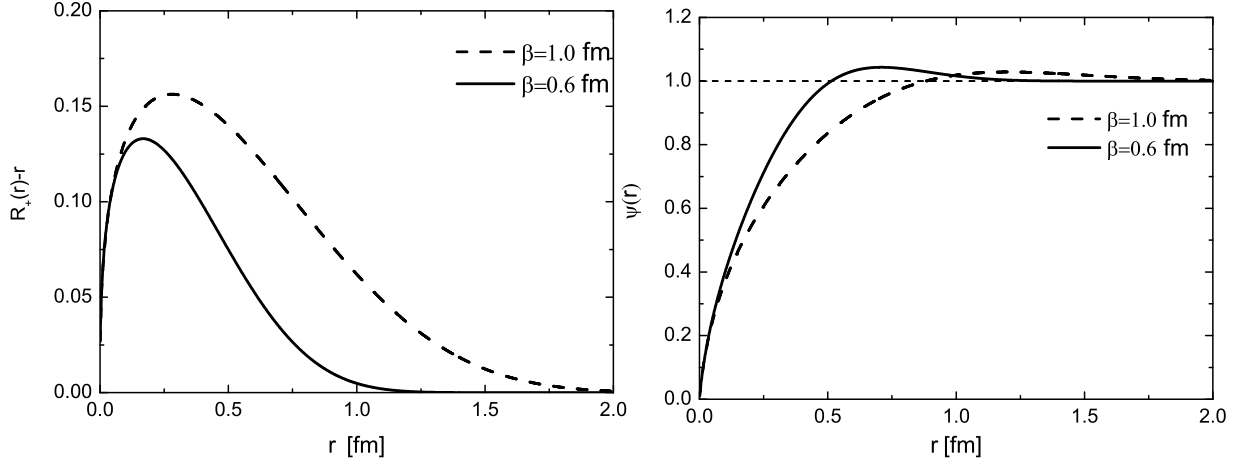
Figure C.3: $R_+(r)$ of the UCOM transformation with a shorter range correlation function ($\beta = 0.6$ fm) shown by the solid curve and the one with longer range correlation function ($\beta = 1$ fm) shown by the dashed curve in the left panel. These transformation functions modify the wave function near the origin as shown in the right panel, respectively. Here, the uncorrelated wave function used for presentation is a constant $\psi = 1$ as shown by the thin dashed line.
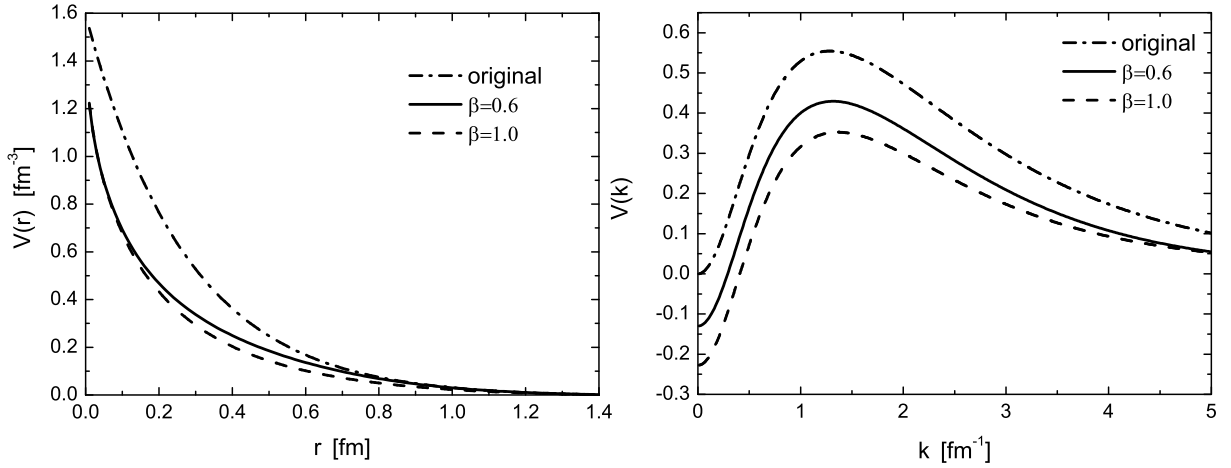
Figure C.4: The spin-spin central part of the pion exchange interaction with and without UCOM for the case Λ=700 MeV in coordinate space in the left panel and one in momentum space in the right panel. The dot-dashed curve corresponds to the interaction without UCOM, the solid curve corresponds to UCOM with $\beta = 0.6$ fm and the dashed curve with $\beta = 1$ fm.

(C.23), are shown in Fig.C.4, where we show the case with $\Lambda = 700$ MeV. We compare the spin-spin central part of the pion exchange interaction in the coordinate- and momentum-space with and without the UCOM effect. We see that the short range part of the central interaction is largely reduced by the UCOM effect. When the parameter β is large, the effect of the short range correlation is large. As we see in the figure, the UCOM effect cuts down the central part of the pion exchange interaction by about 20~40%.

We present now numerical results of equation of state (EOS) for nuclear matter as function of nuclear matter density in Fig.C.5. In the EOS, we choose the parameter set: $\alpha = 0.8$ fm, $\beta = 0.6$ fm and $\eta = 0.37$ for the UCOM effect. We show the EOS for two cases of different Λ's, 635 MeV and 700 MeV. Both cases can reproduce the saturation properties (saturation energy, $E/A = 16.8$ MeV, at density, $\rho_0 = 0.142$ fm^{-3}) by adjusting g_ω and m_σ as tabulated in Table C.1, set A and B, where other properties of the nuclear matter (incompressibility, K, and the nucleon effective mass M^*) are also shown. The dashed curve corresponds to the

set	Λ (MeV)	g_ω	m_σ (MeV)	K (MeV)	$M_N^*(\rho_0)/M_N$
A	635	6.894	867	435	0.837
B	700	6.89	896.5	401	0.850

Table C.1: Two parameter sets used in our numerical calculations. Set A uses a smaller form factor, $\Lambda = 635$ MeV and Set B uses a larger one, $\Lambda = 700$ MeV
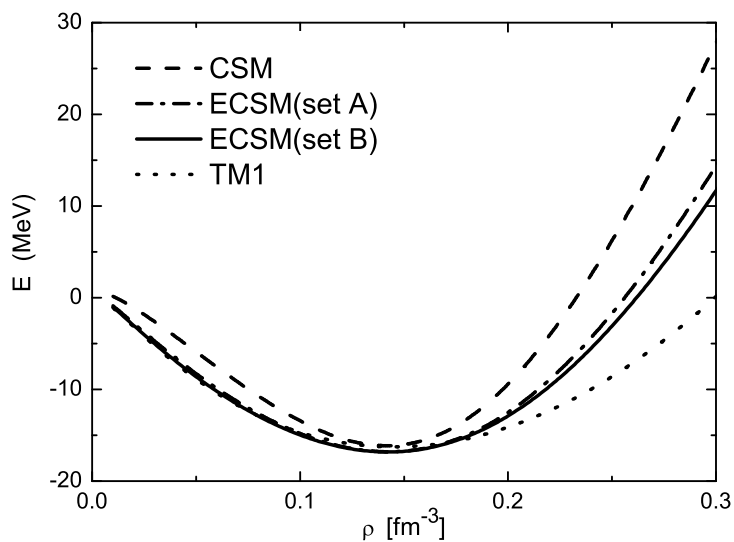
Figure C.5: The equation of state (EOS) of nuclear matter as function of nuclear density. The dashed curve corresponds to the result of chiral sigma model (CSM) without the pionic effect, the dot-dashed curve denotes the result of extended chiral sigma model (ECSM) with the inclusion of the pion exchange effect with the form-factor of $\Lambda = 635$ MeV and the solid curve the ECSM result with $\Lambda = 700$ MeV. The dotted curve is the result of RMF with the parameter set of TM1 for comparison [23].

result of chiral sigma model without the pionic effect, while the dot-dashed and solid curves correspond to the results with the pionic effect (ECSM) with set A and B, respectively. They are compared with a phenomenological EOS, which is calculated by using RMF with the

TM1 parameters [23]. From Fig.C.5, we observe that the nuclear matter of the chiral sigma model ($K \sim 650$ MeV) is stiffer than the phenomenological one of TM1 ($K \sim 280$ MeV). By including the pionic effect in the ECSM, we can obtain a softer nuclear matter, though the incompressibility ($K \sim 400$MeV) is still larger than the phenomenological one. We can reduce further the incompressibility, K, by increasing Λ to have more contribution from the pion. The σ meson mass, m_σ, however, has to increase for larger pionic contribution in order to reduce the sigma meson contribution. In order to keep the σ mass in a reasonable range, we choose $\Lambda = 700$ MeV, which is close to the one of Kaiser *et al.* [69].
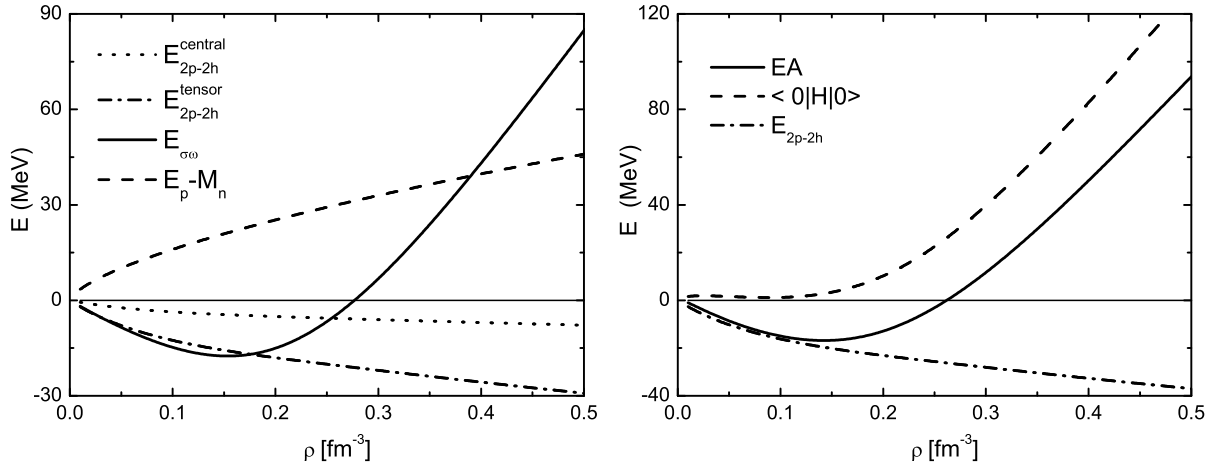
Figure C.6: Energy contributions from various terms for EOS as functions of nuclear density in ECSM

Energy contributions from various terms for EOS as functions of nuclear density. In the left panel, the pion contribution due to the tensor part is shown by dot-dashed curve, while that of the spin-spin part by dotted curve. The interaction energy due to the σ and ω meson contributions is shown by solid curve. The kinetic energy is shown by dashed curve. In the right panel, the dashed curve corresponds to the energy of mean field ground state. The dot-dashed curve corresponds to the pionic contribution, $E_{2p\text{-}2h}$. The whole energy is shown by the solid curve.

We show now various components for EOS in Fig. C.6. For this calculation we take the parameter set B. In the left panel, the dotted curve shows the contribution of the central part of the pion exchange interaction. The tensor part shown by the dot-dashed curve provides a large contribution as it reproduces the binding energy of 15 MeV per nucleon at the saturation density. The contribution of the other interaction, due to σ and ω exchanges, is shown by the solid curve. At low density the $\sigma + \omega$ contribution provides large attraction as the tensor contribution, while it rapidly becomes repulsive at higher density due to the repulsion of ω. At the saturation density, the tensor part of the pion exchange interaction provides the attraction as large as the $\sigma + \omega$ interaction at the saturation density. The kinetic energy is shown here by the dashed curve. We neglect here modification of the kinetic energy

due to the UCOM effect. In the right panel, the dashed curve denotes the contribution of the mean field part of the Hamiltonian, $\langle 0|H|0 \rangle$. Unlike the standard RMF calculation, this 0p-0h part does not provide enough attraction for the binding of nuclear matter. The dot-dashed curve denotes the contribution coming from the pion exchange interaction, $E_{2p\text{-}2h}$. The total energy is shown by the solid curve, where the pion exchange contribution turns out to almost coincide with the whole energy until the saturation density.

We should compare our results with other studies. First, we compare with the results of the variational calculations for light nuclei by Argonne group [70]. They conclude that the contribution of the pion exchange interaction to the entire two-body interaction energy is about $70 \sim 80\%$. If we see the contribution due to the tensor part for ^{4}He, it is about a half of the entire attraction. This feature is consistent with our present result as seen in Fig. C.6. We find here that about 50% of attraction comes from the tensor part of the pion exchange interaction. Additionally we have a contribution from the spin-spin part, which adds the contribution from the tensor part to make the entire contribution of the pion exchange interaction about 60% of the entire two body attraction.

Our result is also qualitatively similar to the one of Kaiser *et al.* [69]. A large amount of attraction is caused by the pion exchange interaction. They calculated the pion 2p-2h contributions without consideration of the short range correlation effect. The Pauli blocking effect, calculated separately in their study, is quite large to reduce the 2p-2h contribution by about one third. In addition, the short range correlation effect further cuts down the 2p-2h contribution. They have calculated the Fock term contribution of pion exchange interaction and the crossed diagram of 2p-2h excitations, which are much smaller than the dominant 2p-2h direct contribution. In our case, the Fock contribution from the pion exchange interaction is estimated to be about 7 MeV repulsive at the saturation density. However, in the present study, we have not included this contribution to be consistent with the RMF approximation used for σ and ω mesons. In fact, the inclusion of the Fock term contributions due to σ and ω exchanges provides slightly attractive energy, which overcomes the repulsive contribution from the pion exchange Fock term, resulting slightly a attractive result[97]. If we were to include the pion Fock contribution, we reduce somewhat the coupling strength of the omega meson exchange interaction in order to get a similar energy of nuclear matter.

We also make comment on the study of Ericson *et al.* [97]. When we calculate the contribution of the pion, we have to include explicitly all the strength coming from the one-pion exchange interaction. This is achieved in our study in terms of the TOSM prescription [99], since the tensor component of the one-pion exchange interaction needs large 2p-2h excitations, which are taken care by Kaiser *et al.* [69]. On the other hand, Ericson and her collaborators treated this effect in terms of the G-matrix by using the Landau-Migdal parameter, g'. Therefore, the tensor contribution is effectively included in the scalar part, $\sigma + \omega$, in their prescription. The binding energy can be calculated by choosing the coupling constants

of the meson-nucleon couplings, and therefore the $\sigma + \omega$ contribution is overestimated.

Appendix D

Partial wave and helicity states for OBE potential

The matrix element of a local potential in coordinate space with plane wave function can be expressed as,

$$
\langle \mathbf{q}'|V|\mathbf{q}\rangle = \frac{1}{(2\pi)^3} \int d^3 r e^{-i\mathbf{q}'\cdot\mathbf{r}} V(r) e^{i\mathbf{q}\cdot\mathbf{r}} \tag{D.1}
$$

$$
= \frac{1}{(2\pi)^3} \int d^3 r \sum_{L'} i^{-L'}(2L'+1) P_{L'}(\hat{\mathbf{q}}'\cdot\hat{\mathbf{r}}) j_{L'}(q'r) V(r) \sum_L i^L (2l+1) P_L(\hat{\mathbf{q}}\cdot\hat{\mathbf{r}}) j_L(kr),
$$

where $j_l(r)$ is the spherical Bessel function of the first kind. Using the addition theorem for spherical harmonics function,

$$
P_{L'}(\hat{\mathbf{q}}'\cdot\hat{\mathbf{r}}) = \frac{4\pi}{2L'+1} \sum_m Y^*_{L'm}(\hat{\mathbf{q}}\cdot\hat{\mathbf{r}}) Y_{L'm}(\hat{\mathbf{q}}'\cdot\hat{\mathbf{q}}), \tag{D.2}
$$

we can carry out the angular integral to give

$$
\langle \mathbf{q}'|V|\mathbf{q}\rangle = \frac{1}{(2\pi)^3} \sum_l 4\pi(2L+1) P_L(\hat{\mathbf{q}}'\cdot\hat{\mathbf{q}}) \int r^2 dr j_L(q'r) V(r) j_L(qr) \tag{D.3}
$$

$$
= \sum_{Lm} Y^*_{Lm}(\hat{\mathbf{q}}') Y_{Lm}(\hat{\mathbf{q}}) \langle q'|V_L|q\rangle.
$$

We called the $\langle q'|V_L|q\rangle$ as the partial wave matrix for potential $V(r)$. Let us, for example, find the lowest partial of Yukawa potential,

$$
V(r) = V_0 \frac{e^{-\mu r}}{r}. \tag{D.4}
$$

This term can be written as,

$$
\langle q'|V_{L=0}|q\rangle = \frac{2}{\pi} \int r^2 dr j_0(q'r) V_0 \frac{e^{-\mu r}}{r} j_0(qr) \tag{D.5}
$$

$$= \frac{2}{\pi} \frac{V_0}{4qq'} \ln \frac{(q'+q)^2 + \mu^2}{(q'-q)^2 + \mu^2}$$

$$= \frac{2}{\pi} \frac{V_0}{2qq'} Q_0 \left(\frac{q'^2 + q^2 + \mu^2}{2q'q} \right).$$

The quantity, Q_0, on the right-hand side is the Legendre function of the second kind. Actually, we can obtain the case of general L,

$$\langle q'|V_L|q \rangle = \frac{2}{\pi} \frac{V_0}{2qq'} Q_L \left(\frac{q'^2 + q^2 + \mu^2}{2q'q} \right). \tag{D.6}$$

When the spin and isospin are considered, the two-body momentum states are written as $|\mathbf{k_1 k_2}\sigma\tau\rangle$. It's convenient to introduce the relative momentum $\mathbf{q} = (\mathbf{k_1} - \mathbf{k_2})/2$, and the c.m momentum $\mathbf{P} = (\mathbf{k_1} + \mathbf{k_2})/2$ of the two particles. Now the states in the coupled basis with quantum numbers is given by the total spin and total isospin

$$|\mathbf{P q}, SS_z TT_z \rangle = \sum_{\sigma\tau} |\mathbf{k_1 k_2}\sigma_{1z}\sigma_{2z}\tau_{1z}\tau_{2z}\rangle (\frac{1}{2}\sigma_{1z}\frac{1}{2}\sigma_{2z}|SS_z)(\frac{1}{2}\tau_{1z}\frac{1}{2}\tau_{2z}|TT_z), \tag{D.7}$$

where the angular momentum coupling coefficients are the usual Clebsh-Gordan coefficients. It's also convenient to introduce the relative angular momentum L and couple it to the total spin S to obtain the total angular momentum J

$$|\mathbf{P} q, (LSJ)MTT_z \rangle = \sum_{mS_z} (LmSS_z|JM) \int d\Omega_q Y^*_{Lm}(\Omega_q)|\mathbf{P q}, SS_z TT_z \rangle. \tag{D.8}$$

The matrix elements of the NN potential between two-body states, which are usually employed in many-body calculation, can be written as

$$\langle \mathbf{P'} q', (L'S'J')M'T'T'_z|V|\mathbf{P} q, (LSJ)MTT_z \rangle \tag{D.9}$$

$$= \delta(\mathbf{P'} - \mathbf{P}) \sum_i V_i^{LL'}(q, q') \langle (LSJ)T|\hat{O}_i|(L'SJ)T \rangle \delta_{JJ'}\delta_{SS'}\delta_{TT'}\delta_{MM'}\delta_{J_z J'_z}.$$

In this equation, we have used, in order, the conservation of total momentum, the Galilei invariance (no explicit dependence on total momentum), the conservation of total angular momentum J and the rotational invariance (no explicit dependence on M), the charge independence of nuclear force (conservation of T) and finally the fact that for two particles of spin $\frac{1}{2}$ the operators $\hat{O}_i$ must also conserve the total spin S. The potentials $V_i(q, q')$ are the Fourier transform of the corresponding potentials in coordinate space,

$$V_i^{LL'}(q, q') = \frac{2}{\pi} i^{L-L'} \int r^2 dr r'^2 dr' j_L(qr) V_i(r, r') j_{L'}(qr'). \tag{D.10}$$

However, the $|LSJM\rangle$ partial-wave states are not eigenfunction of the spin-momentum space operators used in the general momentum space potential whereas all the experimental

data are analyzed in this representation. The most appropriate decomposition of a momentum space potential is the that into helicity states $|\lambda\rangle$. Note that the helicity state function $|\lambda\rangle$ is an eigenfunction of the operator $\frac{1}{2}\boldsymbol{\sigma}\cdot\hat{\mathbf{q}}$ ($\boldsymbol{\sigma}$ the spin operator and $\hat{q}$ the unit c.m. momentum of the nucleon) appearing in the potential. In such a basis the states are classified by the momentum of the two nucleon ($\mathbf{k_1}$ and $\mathbf{k_2}$) and by the helicities λ_1 and λ_2 which describe the projection of the spin of particles one and two along their respective direction of motion. Having the matrix elements of V in the $|JM\lambda_1\lambda_2\rangle$ representation (J the total angular momentum of the two nucleons, M its z-component) it very simple to transform it by means of Clebsch-Gordan coefficients into the $|LSJM\rangle$ representation.

The expansion of $\langle\mathbf{q}'|V|\mathbf{q}\rangle$ into the angular states $|JM\lambda_1\lambda_2\rangle$ is given by [104],

$$\langle\mathbf{q}'\lambda_1'\lambda_2'|V|\mathbf{q}\lambda_1\lambda_2\rangle = \sum_{JM}\langle\hat{\mathbf{q}}'\lambda_1'\lambda_2'|JM\lambda_1'\lambda_2'\rangle\langle JM\lambda_1\lambda_2|\hat{\mathbf{q}}\lambda_1\lambda_2\rangle\langle\lambda_1'\lambda_2'|V^J(q',q)|\lambda_1\lambda_2\rangle, \text{(D.11)}$$

where $\langle JM\lambda_1\lambda_2|\hat{\mathbf{q}}\lambda_1\lambda_2\rangle$ is the transform matrix from the two plane wave state into the angular momentum state. If we choose the incident direction along the z-axis and the outcoming momentum $\mathbf{q}'$ into the x-z plane, it is

$$\langle\mathbf{q}'\lambda_1'\lambda_2'|V|\mathbf{q}\lambda_1\lambda_2\rangle = \sum_J \frac{2J+1}{4\pi}d_{\lambda\lambda'}^J(\vartheta)\langle\lambda_1'\lambda_2'|V^J(q',q)|\lambda_1\lambda_2\rangle, \tag{D.12}$$

where ϑ is the c.m. scattering angle between $\mathbf{q}'$ and $\mathbf{q}$; $\lambda = \lambda_1 - \lambda_2$ and $\lambda' = \lambda_1' - \lambda_2'$. The $d_{\lambda\lambda'}^J(\vartheta)$ are the reduced rotation matrices. In particular

$$d_{\lambda\lambda'}^J(\vartheta) = d_{-\lambda',-\lambda}^J(\vartheta) = (-)^{\lambda-\lambda'}d_{\lambda'\lambda}^J(\vartheta). \tag{D.13}$$

There is an orthogonality relation for these matrices,

$$\int d(\cos\vartheta)d_{\lambda\lambda'}^J(\vartheta)d_{\lambda\lambda'}^{J'}(\vartheta) = \frac{2}{2J+1}\delta_{JJ'}. \tag{D.14}$$

The Eq.(D.12) can be inverted and we can obtain

$$\langle\lambda_1'\lambda_2'|V^J(q',q)|\lambda_1\lambda_2\rangle = 2\pi\int_{-1}^{1}d(\cos\vartheta)d_{\lambda\lambda'}^J(\vartheta)\langle\mathbf{q}'\lambda_1'\lambda_2'|V|\mathbf{q}\lambda_1\lambda_2\rangle. \tag{D.15}$$

This is the basic formula for the representation of the potential in partial wave helicity states. For the V^J matrix elements, the invariance properties of the NN scattering imply the following relations

i) Parity conservation

$$\langle\lambda_1'\lambda_2'|V^J(q',q)|\lambda_1\lambda_2\rangle = \langle-\lambda_1',-\lambda_2'|V^J(q',q)|-\lambda_1,-\lambda_2\rangle. \tag{D.16}$$

ii) Conservation of total spin

$$\langle\lambda_1'\lambda_2'|V^J(q',q)|\lambda_1\lambda_2\rangle = \langle\lambda_2'\lambda_1'|V^J(q',q)|\lambda_2\lambda_1\rangle. \tag{D.17}$$

iii) Time-reversal invariance

$$\langle \lambda_1' \lambda_2' | V^J(q', q) | \lambda_1 \lambda_2 \rangle = \langle \lambda_1 \lambda_2 | V^J(q, q') | \lambda_1' \lambda_3' \rangle. \tag{D.18}$$

Thus, parity and spin conservation alone reduce the total number of sixteen V^J amplitudes to six independent amplitudes. We choose the set,

$$
\begin{aligned}
V_1^J &= \langle + + | V^J(q', q) | + + \rangle & V_2^J &= \langle + + | V^J(q', q) | - - \rangle \\
V_3^J &= \langle + - | V^J(q', q) | + - \rangle & V_4^J &= \langle + - | V^J(q', q) | - + \rangle \\
V_5^J &= \langle + + | V^J(q', q) | + - \rangle & V_6^J &= \langle + - | V^J(q', q) | + + \rangle,
\end{aligned}
\tag{D.19}
$$

where $\lambda = \pm \frac{1}{2}$ is denoted by $\pm$, and $V_i^J = V_i^J(q', q)$. The off-shell scattering of two nucleons, hence, is determined by six amplitudes which in the on-shell case reduce to five only. Because of time-reversal invariance we have,

$$V_6^J(q', q) = V_5^J(q, q') \tag{D.20}$$

and thus $V_6^J(q^2) = V_5^J(q^2)$. However, the amplitudes, actually needed to treat the two-nucleon and infinite nuclear matter system, are the linear combinations,

$$
\begin{aligned}
{}^0V^J &= V_1^J - V_2^J & {}^1V^J &= V_3^J - V_4^J \\
{}^{12}V^J &= V_1^J + V_2^J & {}^{34}V^J &= V_3^J + V_4^J \\
{}^{55}V^J &= 2V_5^J & {}^{66}V^J &= 2V_6^J
\end{aligned}
\tag{D.21}
$$

There is the following transformation to take the potential matrices from the representation $|JM\lambda_1\lambda_2\rangle$ into customarily employed state $|LSJM\rangle$[104],

$$\langle L'SJM | V(q', q) | LSJM \rangle = \sum_{\lambda_1 \lambda_2 \lambda_1' \lambda_2'} \langle L'SJM | JM\lambda_1'\lambda_2' \rangle \langle \lambda_1'\lambda_2' | V^J(q', q) | \lambda_1\lambda_2 \rangle \langle JM\lambda_1\lambda_2 | LSJM \rangle \tag{D.22}$$

The transformation matrix is given as

$$\langle LSJM | JM\lambda_1\lambda_2 \rangle = \left(\frac{2L+1}{2J+1} \right)^{\frac{1}{2}} \langle LS0\lambda | J\lambda \rangle \langle \frac{1}{2}\frac{1}{2}, \lambda_1, -\lambda_2 | S\lambda \rangle \tag{D.23}$$

where $\langle LS0\lambda | J\lambda \rangle$ is the Clebsch-Gordan coefficients.

Specifying L, L' and S for a give J the six off-shell partial-wave amplitudes are:

i) Spin singlet state ($S = 0$, $L' = J = L$)

$$
{}^0V^J(q', q) = V_1^J(q', q) - V_2^J(q', q). \tag{D.24}
$$

ii) Spin triplet states ($S = 1$)
$L' = J = L$:

$$
{}^1V^J(q', q) = V_3^J(q', q) - V_4^J(q', q) \tag{D.25}
$$

$L' = J - 1 = L$:

$$^{--}V^J = \frac{1}{2J+1}\left[J\ ^{12}V^J + (J+1)\ ^{34}V^J + \sqrt{J(J+1)}(\ ^{55}V^J +\ ^{66}V^J) \right] \tag{D.26}$$

$L' = J + 1 = L$:

$$^{++}V^J = \frac{1}{2J+1}\left[(J+1)\ ^{12}V^J + J\ ^{34}V^J - \sqrt{J(J+1)}(\ ^{55}V^J +\ ^{66}V^J) \right] \tag{D.27}$$

$L' = J - 1, L = J + 1$:

$$^{-+}V^J = \frac{1}{2J+1}\left[\sqrt{J(J+1)}(\ ^{12}V^J -\ ^{34}V^J) - J\ ^{55}V^J + (J+1)\ ^{66}V^J \right] \tag{D.28}$$

$L' = J + 1, L = J - 1$:

$$^{+-}V^J = \frac{1}{2J+1}\left[\sqrt{J(J+1)}(\ ^{12}V^J -\ ^{34}V^J) + (J+1)\ ^{55}V^J - J\ ^{66}V^J \right] \tag{D.29}$$

We use the following Lagrangians for meson-nucleon coupling in one-boson-exchange-potential (OBEP)

$$
\begin{aligned}
\mathcal{L}_{\mathrm{ps}} &= -g_{ps}\bar{\psi}i\gamma^5\psi\varphi^{(\mathrm{ps})}, \\
\mathcal{L}_{\mathrm{pv}} &= -\frac{f_{\mathrm{ps}}}{m_{\mathrm{ps}}}\bar{\psi}\gamma^5\gamma^\mu\psi\partial_\mu\varphi^{(\mathrm{ps})}, \\
\mathcal{L}_{\mathrm{s}} &= +g_s\bar{\psi}\psi\varphi^{(\mathrm{s})}, \\
\mathcal{L}_{\mathrm{v}} &= -g_v\bar{\psi}\gamma^\mu\psi\varphi^{(\mathrm{v})}_\mu - \frac{f_{\mathrm{v}}}{4M}\bar{\psi}\sigma^{\mu\nu}\psi(\partial_\mu\varphi^{(\mathrm{v})}_\nu - \partial_\nu\varphi^{(\mathrm{v})}_\mu),
\end{aligned}
\tag{D.30}
$$

with ψ the nucleon and $\varphi^{(\alpha)}_{(\mu)}$ the meson fields. For isospin 1 mesons, $\varphi^{(\alpha)}$ is to be replaced by $\boldsymbol{\tau}\cdot\boldsymbol{\varphi}^{(\alpha)}$ with τ^l ($l = 1, 2, 3$) the usual Pauli matrices. ps, pv, s and v denote pseudo-scalar, pseudo-vector, scalar and vector coupling/fields, respectively.

The above Lagrangians imply the following OBE amplitudes:

$$\langle \mathbf{q}'\lambda_1'\lambda_2'|V_{\mathrm{ps}}^{\mathrm{OBE}}|\mathbf{q}\lambda_1\lambda_2\rangle = -\frac{g_{\mathrm{ps}}^2}{(2\pi)^3}\frac{\bar{u}(\mathbf{q}',\lambda_1')i\gamma^5 u(\mathbf{q},\lambda_1)\bar{u}(-\mathbf{q}',\lambda_2')i\gamma^5 u(-\mathbf{q},\lambda_2)}{(\mathbf{q}'-\mathbf{q})^2 + m_{\mathrm{ps}}^2} \tag{D.31}$$

$$\langle \mathbf{q}'\lambda_1'\lambda_2'|V_{\mathrm{pv}}^{\mathrm{OBE}}|\mathbf{q}\lambda_1\lambda_2\rangle = \frac{1}{(2\pi)^3}\frac{f_{\mathrm{ps}}^2}{m_{\mathrm{ps}}^2}\frac{\bar{u}(\mathbf{q}',\lambda_1')\gamma^5 i(\slashed{q}'-\slashed{q})u(\mathbf{q},\lambda_1)\bar{u}(-\mathbf{q}',\lambda_2')\gamma^5 i(\slashed{q}'-\slashed{q})u(-\mathbf{q},\lambda_2)}{(\mathbf{q}'-\mathbf{q})^2 + m_{\mathrm{ps}}^2}$$

$$\langle \mathbf{q}'\lambda_1'\lambda_2'|V_{\mathrm{s}}^{\mathrm{OBE}}|\mathbf{q}\lambda_1\lambda_2\rangle = -\frac{g_{\mathrm{s}}^2}{(2\pi)^3}\frac{\bar{u}(\mathbf{q}',\lambda_1')u(\mathbf{q},\lambda_1)\bar{u}(-\mathbf{q}',\lambda_2')u(-\mathbf{q},\lambda_2)}{(\mathbf{q}'-\mathbf{q})^2 + m_{\mathrm{s}}^2}$$

$$\langle \mathbf{q}'\lambda_1'\lambda_2'|V_{\mathrm{v}}^{\mathrm{OBE}}|\mathbf{q}\lambda_1\lambda_2\rangle = \frac{1}{(2\pi)^3}\left[g_v\bar{u}(\mathbf{q}',\lambda_1')\gamma_\mu u(\mathbf{q},\lambda_1) + \frac{f_{\mathrm{v}}}{2M}\bar{u}(\mathbf{q}',\lambda_1')\sigma_{\mu\nu}i(q'-q)^\nu u(\mathbf{q},\lambda_1) \right]$$

$$\left[g_v\bar{u}(-\mathbf{q}',\lambda_2')\gamma^\mu u(-\mathbf{q},\lambda_2) - \frac{f_{\mathrm{v}}}{2M}\bar{u}(-\mathbf{q}',\lambda_2')\sigma^{\mu\nu}i(q'-q)_\nu u(-\mathbf{q},\lambda_2) \right] / [(\mathbf{q}'-\mathbf{q})^2 + m_{\mathrm{v}}^2]$$

Working in the two-nucleon c.m. frame, the momenta of two incoming (outgoing) nucleons are $\mathbf{q}$ and $-\mathbf{q}$ ($\mathbf{q}'$ and $-\mathbf{q}'$). The Dirac spinors in helicity representation are given by

$$u(\mathbf{q}, \lambda_1) = \sqrt{\frac{E+M}{2M}} \begin{pmatrix} 1 \\ \frac{2\lambda_1 q}{E+M} \end{pmatrix} |\lambda_1\rangle \tag{D.32}$$

$$u(-\mathbf{q}, \lambda_2) = \sqrt{\frac{E+M}{2M}} \begin{pmatrix} 1 \\ \frac{2\lambda_2 q}{E+M} \end{pmatrix} |\lambda_2\rangle,$$

where $q = |\mathbf{q}|$ and $E = \sqrt{M^2 + \mathbf{q}^2}$. They are normalized covariantly, that is

$$\bar{u}(\mathbf{q}, \lambda) u(\mathbf{q}, \lambda) = 1. \tag{D.33}$$

If we choose $\mathbf{q}$ along the z-axis and $\mathbf{q}'$ in the xz-plane, there is,

$$|\lambda_1\rangle = \chi_{\lambda_1}, \qquad\qquad |\lambda_2\rangle = \chi_{-\lambda_2}, \tag{D.34}$$

$$|\lambda_1'\rangle = \exp\left(-\frac{i}{2}\sigma_y \vartheta\right) \chi_{\lambda_1'}, \qquad |\lambda_2'\rangle = \exp\left(-\frac{i}{2}\sigma_y \vartheta\right) \chi_{-\lambda_2'},$$

with ϑ the angle between $\mathbf{q}$ and $\mathbf{q}'$. $|\lambda_i^{(')}\rangle$ is the eigenstate of the helicity operator for the ith particle with unit momentum $\hat{\mathbf{p}}_i$,

$$\frac{1}{2}\boldsymbol{\sigma}_i \cdot \hat{\boldsymbol{p}}_i |\lambda_i^{(')}\rangle = \lambda_i^{(')} |\lambda_i^{(')}\rangle \tag{D.35}$$

and χ_κ is the conventional Pauli spinor

$$\frac{1}{2}\sigma_z \chi_\kappa = \kappa \chi_\kappa. \tag{D.36}$$

Now we can obtain the OBE amplitudes more explicitly,

$$\langle \mathbf{q}'\lambda_1'\lambda_2' | V_{\text{ps}}^{\text{OBE}} | \mathbf{q}\lambda_1\lambda_2 \rangle = \frac{g_{\text{ps}}^2}{(2\pi)^3} \frac{W'W}{4M^2} \left(\frac{2\lambda_1 q}{W} - \frac{2\lambda_1' q'}{W'}\right) \left(\frac{2\lambda_2 q}{W} - \frac{2\lambda_2' q'}{W'}\right) \tag{D.37}$$

$$\times \frac{\langle \lambda_1'\lambda_2' | \lambda_1\lambda_2 \rangle}{(\mathbf{q}' - \mathbf{q})^2 + m_{\text{ps}}^2},$$

$$\langle \mathbf{q}'\lambda_1'\lambda_2' | V_{\text{pv}}^{\text{OBE}} | \mathbf{q}\lambda_1\lambda_2 \rangle = \frac{1}{(2\pi)^3} \frac{f_{\text{ps}}^2}{m_{\text{ps}}^2} \frac{W'W}{M^2} \frac{\langle \lambda_1'\lambda_2' | \lambda_1\lambda_2 \rangle}{(\mathbf{q}' - \mathbf{q})^2 + m_{\text{ps}}^2}$$

$$\times \left[(E_q - E_{q'}) \left(\frac{\lambda_1 q}{W} + \frac{\lambda_1' q'}{W'}\right) - (\lambda_1 q - \lambda_1' q') \left(1 + \frac{4\lambda_1 \lambda_1' q q'}{WW'}\right) \right]$$

$$\times \left[(E_q - E_{q'}) \left(\frac{\lambda_2 q}{W} + \frac{\lambda_2' q'}{W'}\right) - (\lambda_2 q - \lambda_2' q') \left(1 + \frac{4\lambda_2 \lambda_2' q q'}{WW'}\right) \right],$$

$$\langle \mathbf{q}'\lambda_1'\lambda_2' | V_{\text{s}}^{\text{OBE}} | \mathbf{q}\lambda_1\lambda_2 \rangle = -\frac{g_{\text{s}}^2}{(2\pi)^3} \frac{W'W}{4M^2} \left(1 - \frac{4\lambda_1 \lambda_1' q q'}{WW'}\right) \left(1 - \frac{4\lambda_2 \lambda_2' q q'}{WW'}\right)$$

$$\times \frac{\langle \lambda_1' \lambda_2' | \lambda_1 \lambda_2 \rangle}{(\mathbf{q}' - \mathbf{q})^2 + m_{\mathrm{s}}^2}.$$

For vector boson exchange, the potential is the sum of three term ($V_{\mathrm{v}}^{\mathrm{OBE}} = V_{\mathrm{vv}}^{\mathrm{OBE}} + V_{\mathrm{tt}}^{\mathrm{OBE}} + V_{\mathrm{vt}}^{\mathrm{OBE}}$),

$$
\begin{aligned}
\langle \mathbf{q}' \lambda_1' \lambda_2' | V_{\mathrm{vv}}^{\mathrm{OBE}} | \mathbf{q} \lambda_1 \lambda_2 \rangle &= \frac{g_{\mathrm{v}}^2}{(2\pi)^3} \frac{W'W}{4M^2} \left[\left(1 + \frac{4\lambda_1 \lambda_1' q q'}{WW'} \right) \left(1 + \frac{4\lambda_2 \lambda_2' q q'}{WW'} \right) \langle \lambda_1' \lambda_2' | \lambda_1 \lambda_2 \rangle \right. \\
&\quad \left. - 4 \left(\frac{\lambda_1 q}{W} + \frac{\lambda_1' q'}{W'} \right) \left(\frac{\lambda_2 q}{W} + \frac{\lambda_2' q'}{W'} \right) \langle \lambda_1' \lambda_2' | \boldsymbol{\sigma}_1 \cdot \boldsymbol{\sigma}_2 | \lambda_1 \lambda_2 \rangle \right] \\
&\quad \times \frac{1}{(\mathbf{q}' - \mathbf{q})^2 + m_{\mathrm{v}}^2}
\end{aligned}
$$
(D.38)

$$
\begin{aligned}
\langle \mathbf{q}' \lambda_1' \lambda_2' | V_{\mathrm{tt}}^{\mathrm{OBE}} | \mathbf{q} \lambda_1 \lambda_2 \rangle &= \frac{f_{\mathrm{v}}^2}{(2\pi)^3} \frac{W'W}{4M^2} \left\{ \left[\left(1 + \frac{4\lambda_1 \lambda_1' q q'}{WW'} \right) \left(1 + \frac{4\lambda_2 \lambda_2' q q'}{WW'} \right) \right. \right. \\
&\quad - 2 \frac{E_q + E_{q'}}{M} \left(1 - \frac{16\lambda_1 \lambda_1' \lambda_2 \lambda_2' q^2 q'^2}{W^2 W'^2} \right) + \left(1 - \frac{4\lambda_1 \lambda_1' q q'}{WW'} \right) \\
&\quad \times \left(1 + \frac{4\lambda_2 \lambda_2' q q'}{WW'} \right) \frac{3(E_q E_{q'} + M^2) + q q' \cos \vartheta}{2M^2} \bigg] \langle \lambda_1' \lambda_2' | \lambda_1 \lambda_2 \rangle \\
&\quad - \left[\left(\frac{2\lambda_1 q}{W} + \frac{2\lambda_1' q'}{W'} \right) \left(\frac{2\lambda_2 q}{W} + \frac{2\lambda_2' q'}{W'} \right) + \frac{E_{q'} - E_q}{M} \left(\frac{4q'^2 \lambda_1' \lambda_2'}{W'^2} - \frac{4q^2 \lambda_1 \lambda_2}{W^2} \right) \right. \\
&\quad \left. + \frac{(E_{q'} - E_q)^2}{M^2} \left(\frac{\lambda_1 q}{W} - \frac{\lambda_1' q'}{W'} \right) \left(\frac{\lambda_2 q}{W} - \frac{\lambda_2' q'}{W'} \right) \right] \langle \lambda_1' \lambda_2' | \boldsymbol{\sigma}_1 \cdot \boldsymbol{\sigma}_2 | \lambda_1 \lambda_2 \rangle \bigg\} \\
&\quad \times \frac{1}{(\mathbf{q}' - \mathbf{q})^2 + m_{\mathrm{v}}^2}
\end{aligned}
$$
(D.39)

$$
\begin{aligned}
\langle \mathbf{q}' \lambda_1' \lambda_2' | V_{\mathrm{vt}}^{\mathrm{OBE}} | \mathbf{q} \lambda_1 \lambda_2 \rangle &= \frac{2 g_{\mathrm{v}} f_{\mathrm{v}}}{(2\pi)^3} \frac{W'W}{4M^2} \left\{ \left[\frac{W' + W}{M} \frac{16\lambda_1 \lambda_1' \lambda_2 \lambda_2' q^2 q'^2}{W^2 W'^2} - \frac{E_{q'} - E_q}{M} + 2 \right] \langle \lambda_1' \lambda_2' | \lambda_1 \lambda_2 \rangle \right. \\
&\quad - \left[\left(\frac{2\lambda_1 q}{W} + \frac{2\lambda_1' q'}{W'} \right) \left(\frac{2\lambda_2 q}{W} + \frac{2\lambda_2' q'}{W'} \right) + \frac{E_{q'} - E_q}{2M} \left(\frac{4q'^2 \lambda_1' \lambda_2'}{W'^2} - \frac{4q^2 \lambda_1 \lambda_2}{W^2} \right) \right] \\
&\quad \times \langle \lambda_1' \lambda_2' | \boldsymbol{\sigma}_1 \cdot \boldsymbol{\sigma}_2 | \lambda_1 \lambda_2 \rangle \bigg\} \frac{1}{(\mathbf{q}' - \mathbf{q})^2 + m_{\mathrm{v}}^2}.
\end{aligned}
$$

In above equations, the abbreviations $W = E_q + M$, $W' = E_{q'} + M$ are used. Denoting the angle between $\mathbf{q}$ and $\mathbf{q}'$ by the ϑ, the helicity state matrix elements needed are:

$$
\begin{aligned}
&\langle \lambda_1' \lambda_2' | \lambda_1 \lambda_2 \rangle \\
&= \{ |\lambda_1' + \lambda_1| \cos \tfrac{1}{2} \vartheta + (\lambda_1' - \lambda_1) \sin \tfrac{1}{2} \vartheta \} \{ |\lambda_2' + \lambda_2| \cos \tfrac{1}{2} \vartheta - (\lambda_2' - \lambda_2) \sin \tfrac{1}{2} \vartheta \} \\
&\quad \langle \lambda_1' \lambda_2' | \boldsymbol{\sigma}_1 \cdot \boldsymbol{\sigma}_2 | \lambda_1 \lambda_2 \rangle,
\end{aligned}
$$
(D.40)

$$
\begin{aligned}
= \ & +\{|\lambda_1' - \lambda_1| \cos \tfrac{1}{2}\vartheta + (\lambda_1' + \lambda_1) \sin \tfrac{1}{2}\vartheta\}\{|\lambda_2' - \lambda_2| \cos \tfrac{1}{2}\vartheta - (\lambda_2' + \lambda_2) \sin \tfrac{1}{2}\vartheta\} \\
& -\{|\lambda_1' + \lambda_1| \sin \tfrac{1}{2}\vartheta - (\lambda_1' - \lambda_1) \cos \tfrac{1}{2}\vartheta\}\{|\lambda_2' + \lambda_2| \sin \tfrac{1}{2}\vartheta + (\lambda_2' - \lambda_2) \cos \tfrac{1}{2}\vartheta\} \\
& +\{|\lambda_1' - \lambda_1| \sin \tfrac{1}{2}\vartheta - (\lambda_1' + \lambda_1) \cos \tfrac{1}{2}\vartheta\}\{|\lambda_2' - \lambda_2| \sin \tfrac{1}{2}\vartheta + (\lambda_2' + \lambda_2) \cos \tfrac{1}{2}\vartheta\},
\end{aligned}
$$

where we have used the Eq.(D.34). Now we can use the Eq.(D.15) to evaluate the matrix element of OBE in helicity partial wave state. For convenience, the reduced rotation matrices $d^J_{\lambda\lambda'}(\vartheta)$ in Eq.(D.15) will be expressed in terms of the usual Legendre polynomials $P_J(\cos \vartheta)$. It is

$$
d^J_{00}(\vartheta) = P_J(\cos \vartheta) \tag{D.41}
$$

$$
(1 + \cos \vartheta)d^J_{11}(\vartheta) = P_J + \frac{J+1}{2J+1}P_{J-1} + \frac{J}{2J+1}P_{J+1}
$$

$$
(1 - \cos \vartheta)d^J_{-11}(\vartheta) = -P_J + \frac{J+1}{2J+1}P_{J-1} + \frac{J}{2J+1}P_{J+1}
$$

$$
\sin \vartheta d^J_{10}(\vartheta) = -\sin \vartheta d^J_{01}(\vartheta) = \frac{\sqrt{J(J+1)}}{2J+1}(P_{J+1} - P_{J-1})
$$

Therefore, the basic integral is,

$$
I^{(0)}_J(m_\alpha) = \int_{-1}^{+1} dt \frac{P_J(t)}{(\mathbf{q}' - \mathbf{q})^2 + m_\alpha^2} = \frac{1}{qq'}Q_J(z_\alpha), \tag{D.42}
$$

with $t = \cos \vartheta$, $z_\alpha = (\mathbf{q}'^2 + \mathbf{q}^2 + m_\alpha^2)/2qq'$ and $Q_J(z_\alpha)$ the Legendre function of the second kind. And furthermore,

$$
I^{(1)}_J(m_\alpha) = \int_{-1}^{+1} dt \frac{tP_J(t)}{(\mathbf{q}' - \mathbf{q})^2 + m_\alpha^2} = \frac{1}{qq'}Q^{(1)}_J(z_\alpha), \tag{D.43}
$$

$$
I^{(2)}_J(m_\alpha) = \frac{1}{J+1} \int_{-1}^{+1} dt \frac{JtP_J(t) + P_{J-1}(t)}{(\mathbf{q}' - \mathbf{q})^2 + m_\alpha^2} = \frac{1}{qq'}Q^{(2)}_J(z_\alpha),
$$

$$
I^{(3)}_J(m_\alpha) = \sqrt{\frac{J}{J+1}} \int_{-1}^{+1} dt \frac{tP_J(t) - P_{J-1}(t)}{(\mathbf{q}' - \mathbf{q})^2 + m_\alpha^2} = \frac{1}{qq'}Q^{(3)}_J(z_\alpha),
$$

$$
I^{(4)}_J(m_\alpha) = \int_{-1}^{+1} dt \frac{t^2 P_J(t)}{(\mathbf{q}' - \mathbf{q})^2 + m_\alpha^2} = \frac{1}{qq'}Q^{(4)}_J(z_\alpha),
$$

$$
I^{(5)}_J(m_\alpha) = \frac{1}{J+1} \int_{-1}^{+1} dt \frac{Jt^2 P_J(t) + tP_{J-1}(t)}{(\mathbf{q}' - \mathbf{q})^2 + m_\alpha^2} = \frac{1}{qq'}Q^{(5)}_J(z_\alpha),
$$

$$
I^{(6)}_J(m_\alpha) = \sqrt{\frac{J}{J+1}} \int_{-1}^{+1} dt \frac{t^2 P_J(t) - tP_{J-1}(t)}{(\mathbf{q}' - \mathbf{q})^2 + m_\alpha^2} = \frac{1}{qq'}Q^{(6)}_J(z_\alpha),
$$

with

$$Q^{(1)}(z_\alpha) = z_\alpha Q_J(z_\alpha) - \delta_{J0}, \qquad Q^{(2)}(z_\alpha) = \frac{1}{J+1}(J z_\alpha Q_J(z_\alpha) + Q_{J-1}(z_\alpha)), \quad \text{(D.44)}$$

$$Q^{(3)}(z_\alpha) = \sqrt{\frac{J}{J+1}}(z_\alpha Q_J(z_\alpha) - Q_{J-1}(z_\alpha)), \quad Q^{(4)}(z_\alpha) = z_\alpha Q_J^{(1)}(z_\alpha) - \frac{1}{3}\delta_{J1}$$

$$Q^{(5)}(z_\alpha) = z_\alpha Q_J^{(2)}(z_\alpha) - \frac{2}{3}\delta_{J1}, \quad Q^{(6)}(z_\alpha) = z_\alpha Q_J^{(3)}(z_\alpha) + \frac{\sqrt{2}}{3}\delta_{J1}.$$

Here, these equations are verified with the help of the recurrence relations

$$t P_J(t) = \frac{J+1}{2J+1} P_{J+1}(t) + \frac{J}{2J+1} P_{J-1}(t), \tag{D.45}$$

$$z_\alpha Q_J(z_\alpha) = \frac{J+1}{2J+1} Q_{J+1}(z_\alpha) + \frac{1}{2J+1} Q_{J-1}(z_\alpha) + \delta_{J0}.$$

We state the final expressions for the partial-wave OBE amplitudes in terms of the combinations of helicity amplitudes.

Pseudo-scalar boson (η and π mesons; for π apply an additional factor $\boldsymbol{\tau}_1 \cdot \boldsymbol{\tau}_2$):

$$^0V_{\mathrm{ps}}^J = C_{\mathrm{ps}}(F_{\mathrm{ps}}^{(0)} I_J^{(0)} + F_{\mathrm{ps}}^{(1)} I_J^{(1)}), \tag{D.46}$$

$$^1V_{\mathrm{ps}}^J = C_{\mathrm{ps}}(-F_{\mathrm{ps}}^{(0)} I_J^{(0)} - F_{\mathrm{ps}}^{(1)} I_J^{(2)}),$$

$$^{12}V_{\mathrm{ps}}^J = C_{\mathrm{ps}}(F_{\mathrm{ps}}^{(1)} I_J^{(0)} + F_{\mathrm{ps}}^{(0)} I_J^{(1)}),$$

$$^{34}V_{\mathrm{ps}}^J = C_{\mathrm{ps}}(-F_{\mathrm{ps}}^{(1)} I_J^{(0)} - F_{\mathrm{ps}}^{(0)} I_J^{(2)}),$$

$$^{55}V_{\mathrm{ps}}^J = C_{\mathrm{ps}} F_{\mathrm{ps}}^{(2)} I_J^{(3)},$$

$$^{66}V_{\mathrm{ps}}^J = -C_{\mathrm{ps}} F_{\mathrm{ps}}^{(2)} I_J^{(3)},$$

with

$$C_{\mathrm{ps}} = \frac{g_{\mathrm{ps}}^2}{4\pi} \frac{1}{2\pi M^2} \tag{D.47}$$

and

$$F_{\mathrm{ps}}^{(0)} = EE' - M^2, \qquad F_{\mathrm{ps}}^{(1)} = -qq', \qquad F_{\mathrm{ps}}^{(3)} = -M(E' - E). \tag{D.48}$$

Here, $E = E_q$ and $E' = E_{q'}$. Alternatively, the pseudo-vector (pv) coupling can be used for pseudo-scalar mesons. The basic scheme is the same as above; just replace the subscript ps by pv and use

$$F_{\mathrm{pv}}^{(0)} = EE' - M^2 + (E' - E)^2(EE' + 3M^2)/(4M^2), \tag{D.49}$$

$$F_{\mathrm{pv}}^{(1)} = -qq' + qq'(E' - E)^2/(4M^2),$$

$$F_{\mathrm{pv}}^{(2)} = -(E' - E)[\frac{1}{4}(E' - E)^2 + EE']/M$$

and

$$C_{\mathrm{pv}} = \frac{f_{\mathrm{ps}}^2}{4\pi} \frac{4M^2}{m_\alpha^2} \frac{1}{2\pi M^2}. \tag{D.50}$$

Defining,

$$g_{\text{ps}} = f_{\text{ps}} \frac{2M}{m_{\text{ps}}}, \tag{D.51}$$

we can obtain that $C_{\text{pv}} = C_{\text{ps}}$.

Scalar coupling (s) (σ and δ mesons; for δ apply an additional factor of $\boldsymbol{\tau}_1 \cdot \boldsymbol{\tau}_2$):

$$
\begin{aligned}
{}^{0}V_{\text{s}}^{J} &= C_{\text{s}}(F_{\text{s}}^{(0)}I_{J}^{(0)} + F_{\text{s}}^{(1)}I_{J}^{(1)}), \\
{}^{1}V_{\text{s}}^{J} &= C_{\text{s}}(F_{\text{s}}^{(0)}I_{J}^{(0)} + F_{\text{s}}^{(1)}I_{J}^{(2)}), \\
{}^{12}V_{\text{s}}^{J} &= C_{\text{s}}(F_{\text{s}}^{(1)}I_{J}^{(0)} + F_{\text{s}}^{(0)}I_{J}^{(1)}), \\
{}^{34}V_{\text{s}}^{J} &= C_{\text{s}}(F_{\text{s}}^{(1)}I_{J}^{(0)} + F_{\text{s}}^{(0)}I_{J}^{(2)}), \\
{}^{55}V_{\text{s}}^{J} &= C_{\text{s}}F_{\text{s}}^{(2)}I_{J}^{(3)}, \\
{}^{66}V_{\text{s}}^{J} &= C_{\text{s}}F_{\text{s}}^{(2)}I_{J}^{(3)},
\end{aligned}
\tag{D.52}
$$

with

$$C_{\text{s}} = \frac{g_s^2}{4\pi} \frac{1}{2\pi M^2} \tag{D.53}$$

and

$$F_{\text{s}}^{(0)} = -(EE' + M^2), \quad F_{\text{s}}^{(1)} = qq', \quad F_{\text{s}}^{(3)} = M(E' + E). \tag{D.54}$$

Vector bosons (v) (ω and ρ mesons; for ρ apply an additional factor $\boldsymbol{\tau}_1 \cdot \boldsymbol{\tau}_2$):

Vector-vector coupling

$$
\begin{aligned}
{}^{0}V_{\text{vv}}^{J} &= C_{\text{vv}}(2EE' - M^2)I_{J}^{(0)}, \\
{}^{1}V_{\text{vv}}^{J} &= C_{\text{vv}}(EE'I_{J}^{(0)} + qq'I_{J}^{(2)}), \\
{}^{12}V_{\text{vv}}^{J} &= C_{\text{vv}}(2qq'I_{J}^{(0)} + M^2 I_{J}^{(1)}), \\
{}^{34}V_{\text{vv}}^{J} &= C_{\text{vv}}(qq'I_{J}^{(0)} + EE'I_{J}^{(2)}), \\
{}^{55}V_{\text{vv}}^{J} &= -C_{\text{vv}}MEI_{J}^{(3)}, \\
{}^{66}V_{\text{vv}}^{J} &= -C_{\text{vv}}ME'I_{J}^{(3)},
\end{aligned}
\tag{D.55}
$$

with

$$C_{\text{vv}} = \frac{g_v^2}{4\pi} \frac{1}{\pi M^2} \tag{D.56}$$

Tensor-tensor coupling

$$
\begin{aligned}
{}^{0}V_{\text{tt}}^{J} = \quad & C_{\text{tt}}\{(q'^2 + q^2)(3EE' + M^2)I_{J}^{(0)} \\
& + [q'^2 + q^2 - 2(3EE' + M^2)]qq'I_{J}^{(1)} - 2q^2 q'^2 I_{J}^{(4)}\}, \\
{}^{1}V_{\text{tt}}^{J} = \quad & C_{\text{tt}}\{[4q^2 q'^2 + (q^2 + q'^2)(EE' - M^2)]I_{J}^{(0)} + 2(EE' + M^2)qq'I_{J}^{(1)} \\
& - (q'^2 + q^2 + 4EE')qq'I_{J}^{(2)} - 2q'^2 q^2 I_{J}^{(5)}\},
\end{aligned}
\tag{D.57}
$$

$$
\begin{aligned}
{}^{12}V_{\mathrm{tt}}^{J} =\ & C_{\mathrm{tt}}\{[4M^{2}-3(q'^{2}+q^{2})]qq'I_{J}^{(0)} \\
& +[6q'^{2}q^{2}-(q'^{2}+q^{2})(EE'+3M^{2})]I_{J}^{(1)}+2(EE'+M^{2})qq'I_{J}^{(4)}\}, \\
{}^{34}V_{\mathrm{tt}}^{J} =\ & C_{\mathrm{tt}}\{-(q'^{2}+q^{2}+4EE')qq'I_{J}^{(0)}-2q'^{2}q^{2}I_{J}^{(1)} \\
& +[4q'^{2}q^{2}+(q'^{2}+q^{2})(EE'-M^{2})]I_{J}^{(2)}+2(EE'+M^{2})qq'I_{J}^{(5)}\}, \\
{}^{55}V_{\mathrm{tt}}^{J} =\ & C_{\mathrm{tt}}M\{E'(q'^{2}+q^{2})+E(3q'^{2}-q^{2})]I_{J}^{(3)}-2(E+E')qq'I_{J}^{(6)}\}, \\
{}^{66}V_{\mathrm{tt}}^{J} =\ & C_{\mathrm{tt}}M\{E'(q'^{2}+q^{2})+E(3q'^{2}-q^{2})]I_{J}^{(3)}-2(E+E')qq'I_{J}^{(6)}\},
\end{aligned}
$$

with

$$
C_{\mathrm{tt}} = \frac{f_{\mathrm{v}}^{2}}{4\pi}\frac{1}{8\pi M^{4}} \tag{D.58}
$$

Vector-tensor coupling

$$
\begin{aligned}
{}^{0}V_{\mathrm{vt}}^{J} &= C_{\mathrm{vt}}M[(q^{2}+q'^{2})I_{J}^{(0)}-2qq'I_{J}^{(1)}], \\
{}^{1}V_{\mathrm{vt}}^{J} &= C_{\mathrm{vt}}M[-(q'^{2}+q^{2})I_{J}^{(0)}+2qq'I_{J}^{(2)}], \\
{}^{12}V_{\mathrm{vt}}^{J} &= C_{\mathrm{vt}}M[6qq'I_{J}^{(0)}-3(q'^{2}+q^{2})I_{J}^{(1)}], \\
{}^{34}V_{\mathrm{vt}}^{J} &= C_{\mathrm{vt}}M[2qq'I_{J}^{(0)}-(q'^{2}+q^{2})I_{J}^{(2)}], \\
{}^{55}V_{\mathrm{vt}}^{J} &= C_{\mathrm{vt}}(E'q^{2}+3Eq'^{2})I_{J}^{(3)}, \\
{}^{66}V_{\mathrm{vt}}^{J} &= C_{\mathrm{vt}}(E'q^{2}+3Eq'^{2})I_{J}^{(3)},
\end{aligned} \tag{D.59}
$$

with

$$
C_{\mathrm{vt}} = \frac{g_{\mathrm{v}}f_{\mathrm{v}}}{4\pi}\frac{1}{2\pi M^{3}}. \tag{D.60}
$$

In actually calculation, we should consider the form factor at each meson-nucleon vertex,

$$
\mathcal{F}_{\alpha}[(\mathbf{q}'-\mathbf{q})^{2}] = \left[\frac{\Lambda_{\alpha}^{2}-m_{\alpha}^{2}}{\Lambda_{\alpha}^{2}+(\mathbf{q}'-\mathbf{q})^{2}}\right]^{n_{\alpha}} \tag{D.61}
$$

with m_{α} the mass of the meson involved, Λ_{α} the so-called cutoff mass ,and n_{α} exponent. Thus, the OBE amplitudes should be multiplied by $\mathcal{F}_{\alpha}^{2}$, which means,

$$
\frac{1}{(\mathbf{q}'-\mathbf{q})^{2}+m_{\alpha}^{2}} \longrightarrow \frac{1}{(\mathbf{q}'-\mathbf{q})^{2}+m_{\alpha}^{2}}\left[\frac{\Lambda_{\alpha}^{2}-m_{\alpha}^{2}}{\Lambda_{\alpha}^{2}+(\mathbf{q}'-\mathbf{q})^{2}}\right]^{2n_{\alpha}}. \tag{D.62}
$$

This equation can be decomposed in numerical calculation as ($n_{\alpha}=1$),

$$
\frac{1}{(\mathbf{q}'-\mathbf{q})^{2}+m_{\alpha}^{2}} - \frac{\Lambda_{\alpha,2}^{2}-m_{\alpha}^{2}}{\Lambda_{\alpha,2}^{2}-\Lambda_{\alpha,1}^{2}}\frac{1}{(\mathbf{q}'-\mathbf{q})^{2}+\Lambda_{\alpha,1}^{2}} + \frac{\Lambda_{\alpha,1}^{2}-m_{\alpha}^{2}}{\Lambda_{\alpha,2}^{2}-\Lambda_{\alpha,1}^{2}}\frac{1}{(\mathbf{q}'-\mathbf{q})^{2}+\Lambda_{\alpha,2}^{2}}, \tag{D.63}
$$

with

$$
\Lambda_{\alpha,1}=\Lambda_{\alpha}+\varepsilon, \quad \Lambda_{\alpha,2}=\Lambda_{\alpha}-\varepsilon \quad \text{and} \quad \varepsilon\ll\Lambda_{\alpha} \tag{D.64}
$$

($\varepsilon\approx 10$ MeV is an appropriate choice) before the analytic integration over $\cos\vartheta$ is done.

Bibliography

[1] H. A. Bethe and R. F. Bacher, Rev. Mod. Phys. **8** (1936) 82.

[2] C. S. Wang, K. C. Chung and A. J. Santiago, Phys. Rev. C **60** (1999) 034310.

[3] P. Danielewicz and J. Lee, Nucl. Phys. A **818** (2009) 36.

[4] J. P. Blaizot, Phys. Rep. **64** (1980) 171.

[5] G. Colo and N. Van Giai, Phys. Atom. Nucl. **67** (2004) 1731.

[6] Z. Ma, N. Van Giai, A. Wandelt. *et al.* , Nucl. Phys. A **686** (2001) 173.

[7] P. Möller, J. R. Nix, W. D. Myers and W. J. Swiatecki, At. Data and Nucl. Data Tables **59** (1995) 31.

[8] H. Euler, Z. Phys. **105** (1937) 553.

[9] R. Jastrow, Phys. Rev. **81** (1951) 165.

[10] K. Brueckner, C. Levinson and H. Mahmoud, Phys. Rev. **95** (1954) 217.

[11] R. Brockmann and R. Machleidt, Phys. Rev. C **42** (1990) 1965.

[12] R. Jastrow, Phys. Rev. **98** (1955) 1479.

[13] V. R. Pandharipande and R. B. Wiringa, Rev. Mod. Phys. **51** (1979) 821.

[14] A. Akmal, V. R. Pandharipande and D. G. Ravenhall, Phys. Rev. C **58** (1998) 1804.

[15] P. Danielewicz, R. Lacey, W. G. Lynch, Science **637**, 1592 (2002).

[16] D. Vautherin and D. M. Brink, Phys. Rev. C **5** (1972) 626.

[17] E. Chabanat, P. Bonche, P. Haensel, J. Meyer and R. Schaeffer, Nucl. Phys. A **635** (1998) 231.

[18] J. N. Ginocchio, Rep. Prog. Phys. **414** (2005) 165.

[19] M. H. Johnson and E. Teller, Phys. Rev. **98** (1955) 783.

[20] H. P. Duerr, Phys. Rev. **103** (1956) 469.

[21] J. D. Walecka, Ann. of Phys. **83** (1974) 491.

[22] J. Boguta and A. R. Bodmer, Nucl. Phys. A **292** (1977) 413.

[23] Y. Sugahara and H. Toki, Nucl. Phys. A **579** (1994) 557.

[24] L. W. Chen, C. M. Ko and B. A. Li, Phys. Rev. C **72** (2005) 064309.

[25] H. Yukawa, Proc. Phys. Math. Soc. Jpn **17** (1935) 48.

[26] M. Taketani, S. Nakamura and M. Sasaki, Prog. Theor. Phys. **6** (1951) 581.

[27] H. Toki, Z. Physik A **294** (1980) 173.

[28] M. Oka and K. Yazaki, Prog. Theor. Phys. **66** (1981) 556.; Prog. Theor. Phys. **66** (1981) 572.

[29] N. Hoshizaki and S. Machida, Prog. Theor. Phys. **27** (1962) 288.

[30] K. Erkelenz, Phys. Rep. **13C** (1974) 191.

[31] R. Machleidt, Adv. Nul. Phys. **19** (1989) 189.

[32] V. Stoks, R. Klomps, C. Terhegen and J. Swart, Phys. Rev. C **49** (1994) 2950.

[33] R. B. Wiringa, V. Stoks and R. Schiavilla, Phys. Rev. C **51** (1995) 38.

[34] R. Machleidt, Phys. Rev. C **63** (2001) 024001.

[35] A. R. Bodmer, Nucl. Phys. A **562** (1991) 703.

[36] W. H. Long, J. Meng, N. Van Giai, S. G. Zhou, Phys. Rev. C **69** (2004) 034319.

[37] R. Brockmann and H. Toki, Phys. Rev. Lett. **68** (1992) 3408.

[38] R. Fritz and H. Müther, Phys. Rev. C **49** (1994) 633.

[39] H. Shi, B. Chen and Z. Ma, Phys. Rev. C **52** (1995) 144.

[40] C. Fuchs, H. Lenske and H. H. Wolter, Phys. Rev. C **52** (1995) 3043.

[41] P. G. Reinhard, M. Rufa, J. maruhn, W. Greiner and J. Friedrich, Z. Physik A **323** (1986) 323.

[42] Lee Suk-Joon, J. Fink, A. B. Balantekin, M. R. Strayer, A. S. Umar, P. G. Reinhard, J. A. Maruhn, and W. Greiner, Phys. Rev. Lett. **57** (1986) 2916.

[43] L. Geng, Ph.D. Thesis from Osaka University (2006) 1.

[44] G. A. Lalazissis, J. König and P. Ring, Phys. Rev. C **55** (1997) 540.

[45] B. D. Serot and J. D. Walecka, Adv. Nul. Phys. **16** (1986) 1.

[46] P. G. Reinhard, Rep. Prog. Phys. **52** (1989) 439.

[47] R. Ring, Prog. Part. Nul. Phys. **37** (1996) 193.

[48] J. Meng, H. Toki, S. G. Zhou, S. Q. Zhang, W. H. Long and L. S. Geng, Prog. Part. Nul. Phys. **57** (2006) 470.

[49] P. Ring and P. Schuck, *The Nuclear Many-Body Problem* (Springer-Verlag, Berlin, 1980).

[50] L. Savushkin and H. Toki, *The Atomic Nucleus As A Relativistic System* (Springer-Verlag, Berlin, 2004).

[51] R. Brockmann, Phys. Rev. C **18** (1978) 1510.

[52] A. Bouyssy, J. F. Mathiot N. V. Giai and S. Marcos, Phys. Rev. C **36** (1987) 380.

[53] C. J. Horowitz and B. D. Serot, Nucl. Phys. A **399** (1983) 529.

[54] H. Uechi, Nucl. Phys. A **501** (1989) 813.

[55] A. Bouyssy, S. Marcos, J. F. Mathiot and N. V. Giai, Phys. Rev. C **55** (1985) 1731.

[56] P. Bernardos *et al.*, Phys. Rev. C **48** (1993) 2665.

[57] W. H. Long, H. Sagawa, N. V. Giai, J. Meng, Phys. Rev. C **76** (2007) 034314.

[58] P. A. M. Guichon, H. H. Matevosyan, N. Sandulescu and A. W. Thomas, Nucl. Phys. A **772** (2006) 1.

[59] E. Massot and G. Chanfray , Phys. Rev. C **78** (2008) 015204.

[60] A. L. Fetter and J. D. Walecka, *Quantum Theory of Many-Particle Systems* (McGraw-Hill, San Francisco, 1971).

[61] H. Feldmeier, T. Neff, R. Roth and J. Schnack, Nucl. Phys. A **632** (1998) 61.

[62] T. Neff and H. Feldmeier, Nucl. Phys. A **713** (2003) 311.

[63] K. Sumiyoshi, S. Yamada, H. Suzuki, H. Shen and H. Toki, Astrophys. J. **629** (2005) 922.

[64] G. Audi, A.H. Wapstra and Thibault, Nucl. Phys. A **729** (2003) 3.

[65] L. Geng, H. Toki and J. Meng, Prog. Theor. Phys. **113** (2005) 785.

[66] L. Geng, J. Meng, H. Toki, W. Long and G. Shen, Chin. Phys. Lett. **23** (2006) 1139.

[67] H. Shen, H. Toki, K. Oyamatsu and K. Sumiyoshi, Nucl. Phys. A **637** (1998) 435.

[68] E. N. E. van Dalen, C. Fuchs and A. Faessler, Eur. Phys. J. A **31** (2007) 29.

[69] N. Kaiser, S. Frisch and W. Weise, Nucl. Phys. A **697** (2002) 255.

[70] S. C. Pieper and R. B. Wiringa, Annu. Rev. Nucl. Part. Sci. **51** (2001) 53.

[71] T. Otsuka, T. Suzuki, R. Fujimoto, H. Grawe and Y. Akaishi, Phys. Rev. C **95** (2005) 232502.

[72] J. Hu, Y. Ogawa, H. Toki, A. Hosaka and H. Shen, Phys. Rev. C **79** (2009) 024305.

[73] T. Myo, H. Toki and K. Ikeda, Prog. Theor. Phys. **121** (2009) 511.

[74] Y. Ogawa, H. Toki, S. Tamenaga and A. Haga, Prog. Theor. Phys. **122** (2009) 477.

[75] P. G. Krastev and F. Sammarruca, Phys. Rev. C **74** (2006) 025808.

[76] J. L. Forest, V. R. Pandharipande and J. L. Friar, Phys. Rev. C **52** (1995) 568.

[77] Z. H. Li, U. Lombardo, H, -J. Schulze, W. Zuo, L. W. Chen, and H. R. Ma, Phys. Rev. C **74** (2006) 047304.

[78] J. Carlson and V. R. Pandharipande, Nucl. Phys. A **401** (1983) 59.

[79] J. Fujita and H. Miyazawa, Prog. Theor. Phys. **17** (1957) 360.

[80] H. Kanzawa, K. Oyamatsu, K. Sumiyoshi and M. Takano, Nucl. Phys. A **791** (2007) 232.

[81] P. K. Panda, D. P. Menezes, C. Providência and J. da Providência, Phys. Rev. C **71** (2005) 015801.

[82] P. K. Panda, J. da Providência and C. Providência, Phys. Rev. C **73** (2005) 035805.

[83] P. K. Panda, C. Providência and J. Providência , Phys. Rev. C **75** (2007) 065806.

[84] B. H. Brandow, Phys. Rev. **152** (1966) 863.

[85] J. P. Jeukenne, A. Lejeune and C. Mahaux, Phys. Rep. **25** (1976) 83.

[86] M. Haftel and F. Tabakin, Nucl. Phys. A **158** (1970) 1.

[87] K. Holinde, K. Erkelenz and R. Alzetta, Nucl. Phys. A **198** (1972) 598.

[88] K. Erkelenz, R. Alzetta and K. Holinde, Nucl. Phys. A **176** (1971) 413.

[89] Y. Ogawa and H. Toki, Ann. of Phys. **326** (2011) 2039.

[90] W. Greiner and J. A. Maruhn, *Nuclear model* (Springer, Tokyo, 1996).

[91] M. R. Ansatasio, L. S. Celenza, W. S. Pong and C. M. Shakin, Phys. Rep. **100** (1983) 327.

[92] C. J. Horowitz and B. D. Serot, Phys. Lett. B **137** (1984) 287.

[93] R. Brockmann and R. Machleidt, Phys. Lett. B **149** (1984) 283.

[94] C. J. Horowitz and B. D. Serot, Nucl. Phys. A **464** (1987) 613.

[95] W. H. Dickhoff and C. Barbieri, Prog. Part. Nul. Phys. **52** (2004) 377.

[96] J. Hu, H. Toki, W. Wen and H. Shen, Phys. Lett. B **687** (2010) 271.

[97] G. Chanfray and M. Ericson, Phys. Rev. C **75** (2007) 015206.

[98] T. Myo, K. Kato and K. Ikeda, Prog. Theor. Phys. **113** (2005) 763.

[99] T. Myo, S. Sugimoto, K. Kato, H. Toki and K. Ikeda, Prog. Theor. Phys. **117** (2006) 257.

[100] J. Boguta, Phys. Lett. B **120** (1983) 34.

[101] Y. Ogawa, H. Toki, S. Tamenaga, H. Shen, A. Hosaka, S. Sugimoto and K. Ikeda, Prog. Theor. Phys. **111** (2004) 75.

[102] Y. Ogawa, H. Toki, S. Tamenaga, S. Sugimoto and K. Ikeda, Phys. Rev. C **73** (2006) 034301.

[103] Y. Ogawa, H. Toki and S. Tamenaga, Phys. Rev. C **76** (2007) 014305.

[104] M. Jacob and G. Wick, Ann. of Phys. **7** (1959) 404.